UNIVERSITY OF SALFORD

Department of Mechanical Engineering

# AN OPTIMAL COST APPROACH TO AIRCRAFT STRUCTURAL DESIGN

by

DAVID MODEN

1971

A thesis submitted for the Degree
of Doctor of Philosophy of the
University of Salford

# SUMMARY

The efficiency of the structure of a civil aircraft may be gauged by the financial performance of the aircraft over its life span.

In this thesis a method of structural design is proposed with the object of maximising the life-cycle profit for the airline operating the aircraft. In the formulation of the design process original contributions have been made in various aspects of optimal cost design theory.

The design process is applied to the optimisation of a specimen structure, which is representative of an idealised aircraft wing. The results of the analysis are of importance, since they indicate the manner in which the optimal configuration of a practical structure will vary with the individual characteristics of the aircraft design in which the structure is to be incorporated.

The degree to which the optimisation process is degraded by those errors encountered in a practical environment is ascertained by means of sensitivity analyses.

# ACKNOWLEDGEMENTS

The author wishes to thank Mr S Walmsley, the project supervisor, for the guidance and encouragement he gave in the course of the research work. Thanks are also due to Professor A. W. J. Chisholm, Chairman of the Department of Mechanical Engineering, University of Salford, for allowing the work to be carried out in his department.

The author is indebted to the Manchester Division of Hawker Siddeley Aviation Limited and the Science Research Council for sponsoring the research program.

Of the many people at Hawker Siddeley Aviation who assisted the author, Mr A J Troughton, Chief Designer - Development, who kindly acted as the industrial supervisor, and Mr F. Howarth, Value Engineering Manager, who made available the resources of the Value Engineering Department, merit special thanks.

Finally the author expresses his gratitude to Miss L. Pitts for the efficient manner in which she has typed the manuscript.

C O N T E N T S

# NOTATION

The following notation is employed throughout the thesis. Other notation, applied locally, is introduced when appropriate.

| Symbol | Definition | Units |
|---|---|---|
| a | rib pitch | in. |
| b | stringer pitch | in. |
| C | unit cost | £ |
| d | wing depth | in. |
| D.O.C. | direct operating cost | £ |
| E | modulus of elasticity | $lb./in.^2$ |
| F | Farrar efficiency factor | |
| I.O.C. | indirect operating cost | £ |
| L | life cycle cost per aircraft | £ |
| M | merit function | lb. |
| Nx | end loading | lb./in. |
| p | material density | $lb./in.^3$ |
| P | airline profit per aircraft | £ |
| R | airline revenue per aircraft | £ |
| t | skin thickness | in. |
| $t_c$ | cover thickness | in. |
| $t_R$ | rib thickness | in. |
| $t_s$ | stringer thickness | in. |
| T | aircraft service life | hr. |
| V | exchange rate | £/lb. |
| W | component structural weight | lb. |
| $W_s$ | aircraft structural weight | lb. |

| Symbol | Definition | Units |
|---|---|---|
| $\sigma_c$ | 0.1% proof stress | lb./in.$^2$ |
| $\sigma_t$ | ultimate tensile stress | lb./in.$^2$ |

Subscripts

| | |
|---|---|
| B | break-even value |
| C | compression cover |
| D | detail value |
| G | global value |
| L | lower bound value |
| min | minimum gauge |
| N | normalised value |
| O | operative value |
| R | rib |
| ST | standard value |
| T | tension cover |
| U | upper bound value |

# INTRODUCTION

The expenditure of enormous sums of money is required by airframe and engine manufacturing companies alike, in the areas of design, research and development, tooling and manufacture, for a modern aircraft project to reach the production stage.

The capital investment involved in a new aircraft program is often so great as to exceed the capital resources of the aircraft companies involved, necessitating large government subsidies to sustain the project. The Anglo-French supersonic transport program has required the investment of £885m by the British and French governments for research and development funding alone.(1)

The large expenditure involved in the Tri-star Airbus program caused the Rolls-Royce and Lockheed companies to experience extreme financial crises, and other aircraft companies have been in similar difficulties.

The very large program costs of modern aircraft, when coupled with relatively short production runs, means that the cost of purchasing new aircraft has placed an enormous financial strain on the operating airline, giving rise to a depression in the airline industry at the present time. The manner in which the first cost of long haul civil aircraft has increased with time is presented in fig I.1, emphasising the growing financial burden re-equipment places on the operator.

In the light of the depressed financial state of the aircraft and the airline industries, it is essential that

new projects are developed which permit economic benefits to be gained by both the manufacturer and the operator.

This thesis proposes a method of structural design which takes full account of the cost of manufacture and operation of an aircraft, enabling an aircraft possessing a good economic performance to be developed.

## I.1 Design Philosophy

The philosophy of aircraft structural design has shown a distinct evolutionary pattern, as follows:

i) The fundamental method of aircraft structural design consisted of arranging a structure capable of carrying the predicted aerodynamic loads. In general, the structural arrangement chosen was not the minimum weight configuration for the applied loading system.

ii) In a search for better aircraft performance, attempts were made to reduce aircraft structural weight. Minimum weight analyses were conducted in order to determine the arrangement of internal geometry required for the lightest structure. However, minimum weight structures tend to be very expensive to produce, leading to increases in aircraft first cost.

iii) A worsening economic climate forced aircraft manufacturers to endeavour to reduce aircraft first cost by minimising the production cost involved. The application of value engineering techniques to aircraft designs gave significant reductions in both cost and weight of many structural components.

iv) Generally the optimal aircraft structure is neither the minimum weight structure nor the minimum first

cost structure. Alvey and Emero[2] proposed a method of aircraft structural design which sought to minimise the aircraft first cost and the operating cost of the aircraft over its lifetime.

v) The design philosophy presented in this thesis proposes a method of aircraft structural design which enables the aircraft, in which the structure is incorporated, to yield the maximum profit to the operating airline, for the capital invested. This design objective takes full account of the first cost of the aircraft, the operating costs incurred and the passenger and freight revenue generated over its lifetime.

The optimisation procedure was developed for civil aircraft, since the optimal structure may be readily defined in terms of maximised airline profit. The monetary value used to define the optimal structure for a military aircraft is a less tangible quantity. However, the same design process may be applied to military aircraft, once this value has been specified.

## I.2 A Review of Recent Progress in the Field of Optimal Cost Structural Design

The introduction of cost as an important parameter in the process of aircraft structural design would appear to be a desirable aim, especially in the light of the economic conditions mentioned earlier. However, a review of recent literature indicates that this aspect of structural design has been sadly neglected.

Recently, considerable emphasis has been placed on the application of statistical techniques to data accumulated on

completed aircraft programs. In this way Levenson and Barro,[3] Carrier and Smith,[4] Yates[5] and Sanchez[6] derived equations relating airframe costs to various aircraft parameter, including airframe weight, gross thrust, maximum cruise speed, and number of aircraft produced.

The equations, termed cost-estimating relationships, were developed for the prediction of costs at the project stage. However, these cost-estimating relationships may be used for the improvement of an aircraft design by allowing the manipulation of the parametric values to achieve a specified cost. The cost-estimating relationships developed to date are of little use in the process of structural design, since the main structural parameters influencing costs were not included in the structural analyses.

Any technique of structural design which attempts to optimise the cost performance of the aircraft in which the structure is incorporated, is dependent upon savings in structural weight being assigned an economic value.

Dykes[7] presented the criteria which influence the economic value assiged to reductions in weight.

The lower bound of the economic value of weight reductions was derived mathematically by Gerard,[8] who assumed that the economic value was given by the incremental reduction in the fuel cost of operating a lighter aircraft. This value has been utilised in the derivation of the lower bound value of the break-even exchange rate presented in section 2.3.

The outstanding contribution in the field of the optimal cost design of aircraft structures has been made by Alvey and

Emero.[2] As mentioned in section I.1, they proposed a method of structural design with the aim of minimising the life-cycle cost of the aircraft in whichthe structure is incorporated.

The merit function value proposed by Alvey and Emero[2] allows the comparison of different structures on a cost-weight basis. This concept represents an advance in structural design techniques, and has been employed in the design process presented in this thesis.

However, although the paper represents an important milestone along the path towards the introduction of cost as a major consideration in the process of structural design, its accuracy must be questioned in several areas, as follows:

i) The validity of the design objective, requiring the minimisation of aircraft life-cycle cost, is challenged in Chapter 2.

ii) In the thesis, optimal configuration curves for the component parts of a box beam are presented. The validity of the results given by the optimisation of structural components is challenged in Chapter 10.

## I.3 Aims of the Research Program

The general lack of evidence of a concerted effort to integrate cost considerations in the structural design process, together with the shortcomings of the best design method available, gave the impetus to the research work described in this thesis.

The aims of the research program were as follows:

i) The formulation of a method of structural design enabling the structure possessing the optimal cost

characteristics, as defined by the design objective stated in section I.1, to be selected from a series of alternative structures.

ii) The examination of the sensitivity of the analytical process to factors present in a practical environment, including the influence of errors in the cost and weight estimation methods.

iii) The examination of a specimen structure to evaluate the performance of the structural design method and to obtain results having practical significance.

iv) The modification of the design process, in the light of the findings of the analysis of the specimen structure, to accommodate practical structures.

In order to achieve the aims stated above, advances were required in the following areas:

i) The definition of each element of the design process.

ii) The mathematical derivation of a suitable exchange rate value for use in the selection process for the location of the optimal cost structure.

iii) The mathematical derivation of a relationship expressing the sensitivity of the selection process to estimation errors.

iv) The specification of alternative structural systems for examination in the specimen analysis.

v) The formulation of suitable models to allow the costs and weights of different structural systems to be equitably compared.

vi) The derivation of suitable design equations, for use

in the structural model of the specimen analysis, defining the internal dimensions of the structure required for structural integrity.

FIG. I.1 THE INCREASE IN THE FIRST COST OF LONG-HAUL CIVIL AIRCRAFT WITH TIME

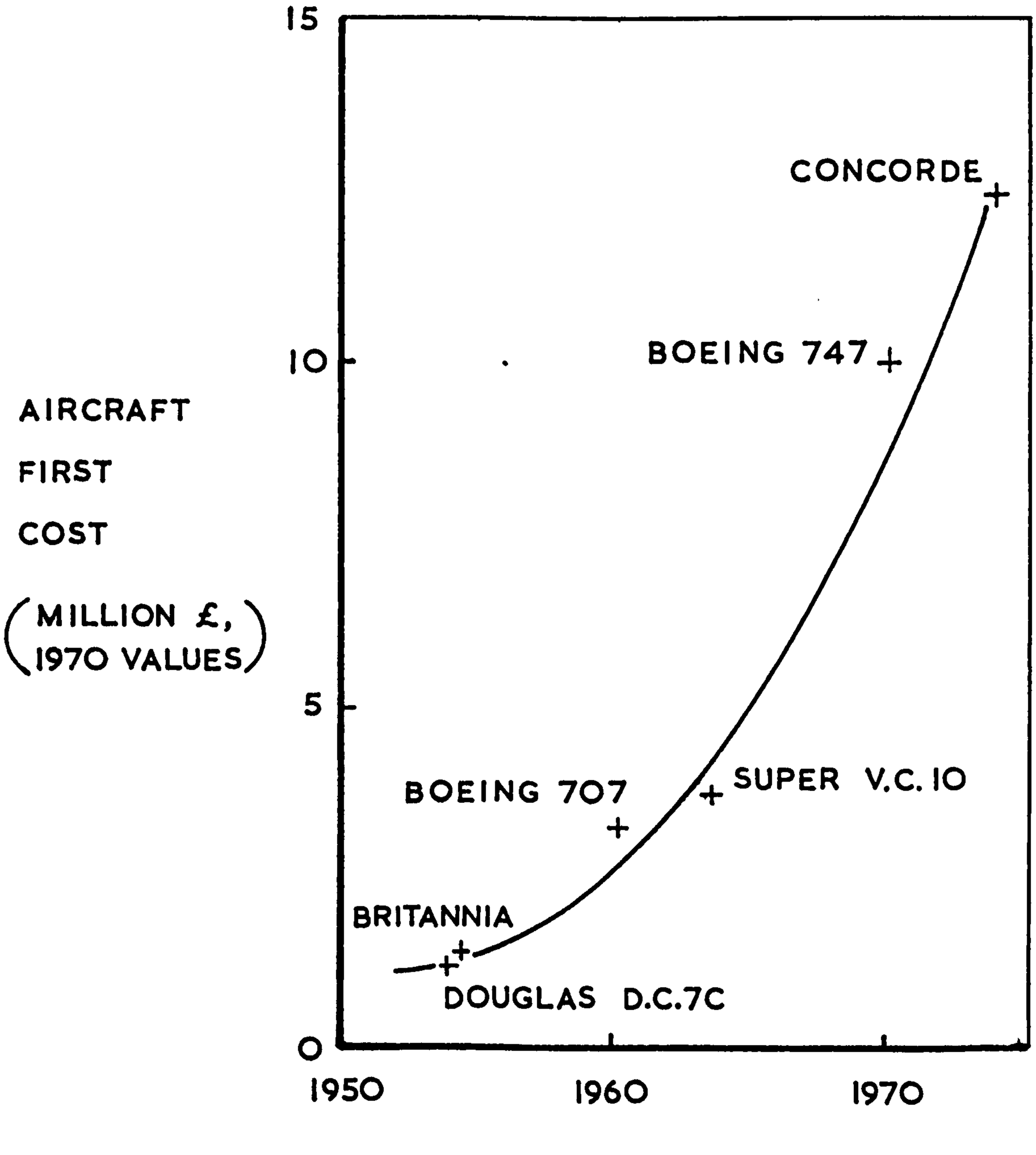

# P A R T  1 :

# GENERAL DESIGN PROCESS

# C H A P T E R  1

# A DESCRIPTION OF THE COMPLETE DESIGN PROCESS

## 1.1 Introduction

The design process proposed in this chapter may be used for the location of the optimal configuration for a given structural system, or for the selection of the optimal system from a range of alternative systems.

The design process consists of certain basic stages which are summarised in block diagram form in fig. 1.1. When the design process is applied to the optimisation of a specific item, each stage must be adapted to suit the characteristicts of the particular application. The optimisation of a specimen structure using the design process is demonstrated in part 2.

Each stage in the design process is now described.

## 1.2 A Statement of the Design Objective

The aims of the design process are stated in the design objective. The design objective used in this thesis, which was presented in section I.1, seeks to maximise the airline profit generated by the aircraft in which the structure is incorporated. The structural system fulfilling the design objective is defined as the optimum.

## 1.3 The Definition of a Design Model

A design model must be formulated to ensure that:

i) the basic design requirements, which are essential for a satisfactory solution, are incorporated in each structural system, and

ii) the alternative structure systems are compared on an equitable basis. Within the overall design model, a structural model must be specified to delimit the extent of the structural item under analysis and to set a series of geometric requirements to be satisfied by all structural systems. Similarly a cost model must be specified to govern the allocation of the cost elements to each system.

## 1.4 The Specification of the Alternative Structural Systems

The alternative structural systems chosen for comparison may vary in material type, production method or type of structural component employed. The arrangement of the components of a given structural system may be varied to change the configuration of the system, enabling the design process to be used to locate the optimal configuration.

It is essential that realistic systems are chosen for analysis, since the validity of the resulting optimal solutions is dependent on the original data. It must be emphasised that structural systems, which are superior to those examined, may exist.

## 1.5 The Selection of the Optimal System

The introduction of a common measure of system merit

makes it possible to compare the relative performances of the alternative structural systems in terms of the achievement of the design objective. The merit function parameter, evolved by Alvey and Emero,[2] is used for this purpose. The merit function value for a particular structural system is dependent on the system values, that is the values of the structural weight and the unit cost, and on the magnitude of the global exchange rate value of the aircraft project for which the structure is intended.

The system values must be evaluated for each structural system in the manner prescribed by the design model.

A mathematical derivation of the break-even exchange rate value, from whichthe global exchange rate value may be determined, is presented in Chapter 2.

A comparative procedure must be employed to locate the system having the minimum value of the merit function. By definition, this is the system, from the alternatives examined, which fulfils the design objective, and hence is termed the optimum.

FIG. 1.1 A DIAGRAMMATIC REPRESENTATION OF THE DESIGN PROCESS

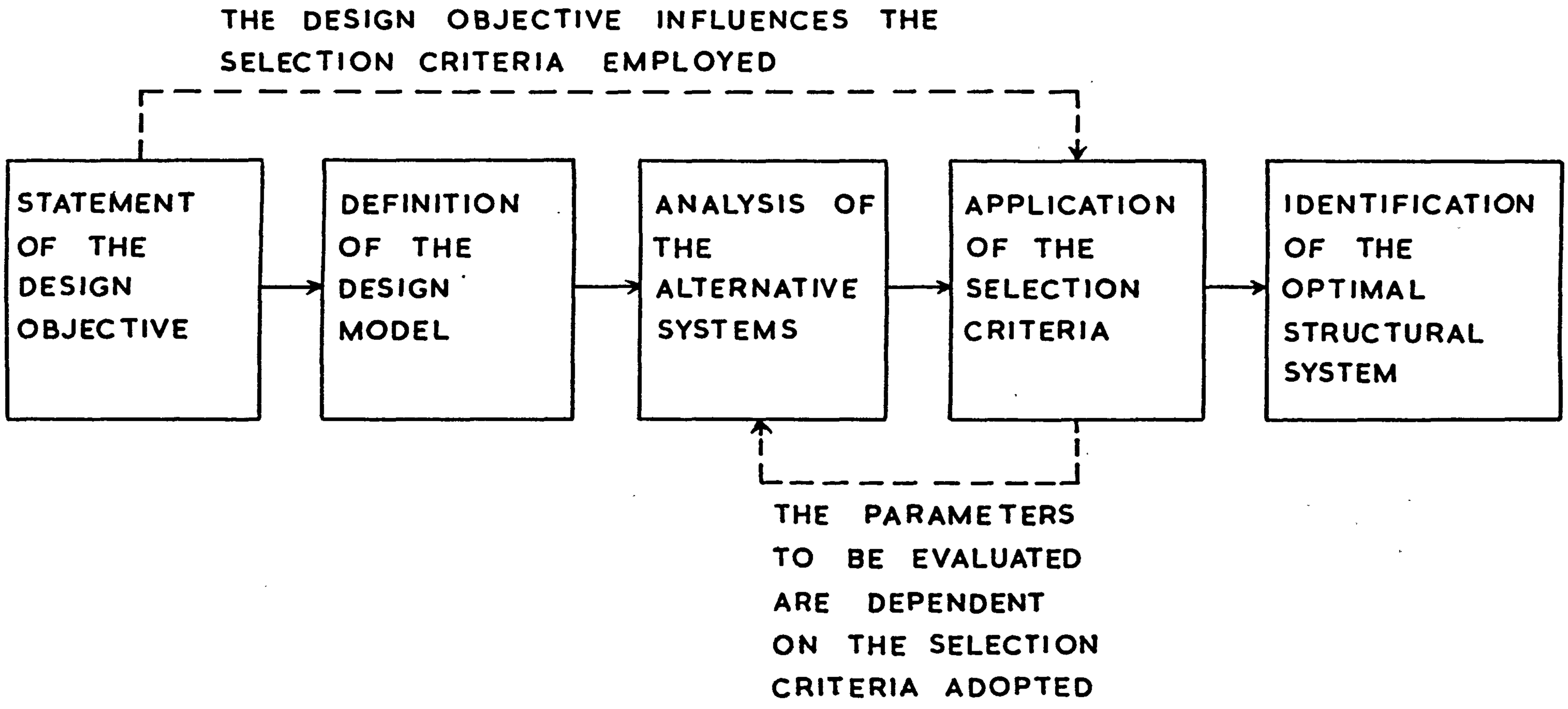

# C H A P T E R  2

# THE DEFINITION OF THE SELECTION CRITERIA

## 2.1 Introduction

The design objective, stated in section I.1, proposed that the optimal structure shall enable the aircraft, in which the structure is incorporated, to yield the maximum profit to the operating airline, for the capital invested in the aircraft and its spares.

The ability to identify the structure which fulfils the design objective is dependent on suitable selection criteria being evolved. The selection criteria must express the relative performance of each structure in terms of the degree of fulfilment of the design objective. Before the selection criteria can be specified, the parameter requiring maximisation, namely the airline profit, must be examined in detail.

## 2.2 The Cost Elements of the Airline Profit

An airline operating an aircraft of structural weight $W_s$ over a given service life receives a revenue R, from the passenger and freight fares, and has an expediture, due to the purchase cost and the operating costs of the aircraft, which can be defined as the life-cycle cost L.

The difference between the revenue and the expediture is the profit (or loss) P,

i.e. $P = R - L$ (2.1)

The main elements of the profit will now be examined.

### 2.2.1 The revenue

The revenue R obtained per aircraft from the passenger and freight charges, over its service life, is given by

$$R = L_F \cdot N \cdot S \cdot C_s \cdot T \qquad (2.2)$$

where R = revenue (£),

$L_F$ = average load factor over the aircraft's service life,

N = number of seats per aircraft,

S = block speed (m.p.h.),

$C_s$ = seat mile charge (£/seat mile),

T = service life (hrs.)

The average payload weight $W_{py}$ per aircraft is

$$W_{py} = L_F \cdot N \cdot W_p \qquad (2.3)$$

where $W_p$ = the design weight of a passenger plus baggage (lb.)

### 2.2.2 The life-cycle cost

The total cost to the airline of purchasing and operating the aircraft over its service life is defined as the life-cycle cost L. Fig. 2.1 gives an indication of the magnitude of the life-cycle cost for a long haul civil aircraft.

The life-cycle cost L may be sub-divided into direct and indirect operating costs, giving

$$L = D.O.C. + I.O.C. \qquad (2.4)$$

where D.O.C. = the direct cost of operating the aircraft over its service life, including the amortisation of the first cost (£),

I.O.C. = the proportion of the airline's indirect operating cost allocated to the aircraft over its service life (£).

(a) <u>the direct operating cost</u>

The main cost elements of which the direct operating cost, D.O.C., is composed, are

$$D.O.C. = C_B + C_C + C_F + C_M \qquad (2.5)$$

where $C_B$ = insurance, interest and depreciation costs (£),

$C_C$ = crew costs (£),

$C_F$ = fuel and oil costs (£),

$C_M$ = engine, airframe and equipment maintenance costs (£).

Fig. 2.2 gives an indication of the relative proportion of the direct operating cost that each cost element occupies, for a typical civil subsonic aircraft.(9)

The combined insurance, interest and depreciation cost $C_B$ can be expressed as

$$C_B = K_2 \cdot C_A \qquad (2.6)$$

where $K_2$ = a constant dependent on the aircraft type,

$C_A$ = aircraft first cost (£)

Crew cost $C_C$ are directly proportional to the number of crew per aircraft, which is dependent on aircraft size. However, the crew size is not a linear function of aircraft size, but increases in a number of discrete steps.

(b) <u>the indirect operating cost</u>

The main cost elements of which the indirect operating cost, I.O.C., is composed, are

$$I.O.C. = C_H + C_{SP} + C_G + C_P \qquad (2.7)$$

where $C_H$ = aircraft and traffic handling costs (£),

$C_{SP}$ = promotion and sales costs (£),

$C_G$ = administrative costs (£),

$C_P$ = passenger service costs (£).

Fig. 2.3 presents the breakdown of the indirect operating cost elements for T.W.A. in the financial year 1967/8.[24]

Typically the indirect operating costs are of the order of 70 to 130 per cent of the direct operating cost, depending on an airline's size, efficiency and the type of operation it undertakes. As an example, the indirect operating costs of B.O.A.C. were 94 per cent of the direct operating costs in the financial year 1968/9.[10] Ref. 10 states that the aircraft designer is probably responsible for at least 60 per cent of the direct operating cost and can influence 30 to 40 per cent of the indirect operating cost.

## 2.3 The Derivation of the Break-Even Exchange Rate Value

Equation (2.1) defines the profit $P$ for an aircraft of structural weight $W_s$ as

$$P = R - L$$

It is the influence of the structural weight on the profit that is being investigated. If an incremental decrease $\delta W_s$ is made in the structural weight of the aircraft due to a design improvement, then, using the calculus of variations, the resulting change in profit $\delta P$ is given by

$$\delta P = \frac{\partial P}{\partial R} \cdot \frac{\partial R}{\partial W_s} \cdot \delta W_s + \frac{\partial P}{\partial L} \cdot \frac{\partial L}{\partial W_s} \cdot \delta W_s \qquad (2.8)$$

Since the total revenue cannot increase even if the number or size of aircraft is increased, and the life-cycle cost is incurred whether passengers are carried or not, if one omits the small change in fuel costs with different payload weights, to the first order of approximation the revenue may be assumed to be independent of the life-cycle cost, hence $\frac{\partial P}{\partial R} = 1$ and $\frac{\partial P}{\partial L} = -1$, so that equation (2.8) reduces to

$$\delta P = \left( \frac{\partial R}{\partial W_s} - \frac{\partial L}{\partial W_s} \right) \cdot \delta W_s \qquad (2.9)$$

In the preliminary design stage, when the basic aircraft and its powerplant have been specified, savings in structural weight can be used either:

i) to increase the revenue- earning weight by replacing structural weight with payload, this being termed the upper bound case, since it attaches the maximum cost value to the weight saving, or

ii) to reduce the fuel cost element of the direct operating cost, due to the lower fuel requirements of the lighter aircraft, this being termed the lower bound case, since it attaches the minimum cost value to the weight saving.

These cost benefits from the saving of weight are obtained at the expense of an increased first cost, since it usually costs more to produce a lighter structure than a heavier, less complex structure, as is shown diagrammatically in fig. 2.4 for the case of a compression panel.

A parameter, known as the break-even exchange rate, is introduced which forms the basis of the selection criteria used in the optimisation process. The break-even exchange rate value $V_B$ is defined as the cost incurred in saving unit structural weight, for which there is no overall change in the profit P,

$$\text{i.e.} \quad V_B = \left( \frac{\partial C_A}{\partial W_s} \right)_{\delta P = 0} \tag{2.10}$$

In the mathematical derivation of the break-even exchange rate value the following assumptions are made:

i) the airframe maintenance cost $C_M$ is based on the A.T.A. maintenance cost equations presented in ref. 25, with

$$C_M = K_3 \cdot C_A + K_4 \cdot W_s \tag{2.11}$$

where $K_3$ = first cost constant

and $K_4$ = structural weight constant (£/lb.),

which are dependent on the aircraft type,

ii) the indirect operating cost I.O.C. and the crew cost $C_C$ are assumed unaffected by the incremental change

$\delta W_s$ in structural weight, so that

$$\frac{\partial \text{I.O.C.}}{\partial W_s} = \frac{\partial C_C}{\partial W_s} = 0 \qquad (2.12)$$

The break-even exchange rate values are evaluated using upper and lower bound considerations, an operative value being suggested.

### 2.3.1 The upper bound case

In the upper bound case the saving in structural weight is used to generate extra revenue by increasing the aircraft's payload. For the upper bound case to be applicable, the following conditions must all apply:

i) the aircraft must be weight limited, as is often the case when flying from hot and high airfields,

ii) sufficient volume must exist to accommodate the extra payload,

iii) the flight must be overbooked in order that the additional payload can exist,

iv) the structural weight saved must be equal to, or greater than, the weight of the extra payload, which in the case of an extra passenger is 200 lb.

For the upper bound case, the zero fuel weight of the aircraft is unchanged, since the structural weight saved is replaced by payload, so that the aircraft's fuel consumption, and hence its fuel cost, remain the same,

$$\text{i.e.} \quad \frac{\partial C_F}{\partial W_s} = 0 \qquad (2.13)$$

Applying the conditions specified by equations (2.5), (2.6), (2.11) and (2.12) in equation (2.9),

$$\text{i.e.} \quad \delta P = \left( \frac{\partial R}{\partial W_s} - \frac{\partial C_B}{\partial W_s} - \frac{\partial C_M}{\partial W_s} \right) \cdot \delta W_s$$

$$\delta P = \left( \frac{\partial R}{\partial W_s} - (K_2 + K_3) \cdot \frac{\partial C_A}{\partial W_s} - K_4 \right) \cdot \delta W_s \qquad (2.14)$$

The break-even exchange rate value $V_B$ is based on the condition that there is no change in profit, i.e. $\delta P = 0$.

$\therefore$ The upper bound value $V_{B_u}$ of the break-even exchange rate is obtained by re-arranging equation (2.14),

$$\text{i.e. } V_{B_u} = \left( \frac{\partial C_A}{\partial W_s} \right)_{\delta P = 0} = \frac{1}{(K_2 + K_3)} \cdot \left( \frac{\partial R}{\partial W_s} - K_4 \right) \qquad (2.15)$$

From equations (2.2) and (2.3), the extra revenue $\delta R$ generated by the increase $\delta W_{py}$ in payload, which is equal to the decrease $\delta W_s$ in structural weight, is

$$\frac{\partial R}{\partial W_s} = \frac{C_s \cdot S \cdot T}{W_p} \qquad (2.16)$$

Substituting in equation (2.15) from (2.16) gives the upper bound value $V_{B_u}$ of the break-even exchange rate as

$$V_{B_u} = \frac{1}{(K_2 + K_3)} \cdot \left( \frac{C_s \cdot S \cdot T}{W_p} - K_4 \right) \qquad (2.17)$$

### 2.3.2 The lower bound case

In the lower bound case the structural weight saved is used to reduce the fuel cost, because the

lighter aircraft has a lower fuel consumption.

There is no change in revenue,

$$\text{i.e.} \quad \frac{\partial R}{\partial W_s} = 0 \tag{2.18}$$

Applying the conditions specified by equations (2.5), (2.6), (2.11), (2.12) and (2.18) in equation (2.9),

$$\text{i.e.} \quad \delta P = - \left( \frac{\partial C_B}{\partial W_s} + \frac{\partial C_M}{\partial W_s} + \frac{\partial C_F}{\partial W_s} \right) \cdot \delta W_s$$

$$\delta P = - \left( (K_2 + K_3) \cdot \frac{\partial C_A}{\partial W_s} + K_4 + \frac{\partial C_F}{\partial W_s} \right) \cdot \delta W_s \tag{2.19}$$

The break-even exchange rate value $V_B$ is based on the condition that there is no change in profit,

i.e. $\delta P = 0$.

∴ The lower bound value $V_{B_L}$ of the break-even rate is obtained by re-arranging equation (2.19),

$$\text{i.e.} \quad V_{B_L} = \left( \frac{\partial C_A}{\partial W_s} \right)_{\delta P = 0} = - \frac{1}{(K_2 + K_3)} \cdot \left( \frac{\partial C_F}{\partial W_s} + K_4 \right) \tag{2.20}$$

According to Gerard[8], the reduction $\delta C_F$ in fuel cost over the aircraft's life $T$ (hr.), due to the reduction $\delta W_s$ in structural weight, is

$$\frac{\partial C_F}{\partial W_s} = - \frac{F \cdot T \cdot S \cdot (G - 2)}{R_A} \tag{2.21}$$

where $F$ = fuel cost per unit weight (£/lb.),

$G$ = gross weight - structural weight growth factor,

$R_A$ = aircraft range (miles).

Substituting in equation (2.20) from (2.21) gives the lower bound value $V_{B_L}$ of the break-even exchange rate as

$$V_{B_L} = \frac{1}{(K_2 + K_3)} \cdot \left( \frac{F \cdot T \cdot S \cdot (G - 2)}{R_A} - K_4 \right) \quad (2.22)$$

### 2.3.3 The operative value of the break-even exchange rate

The conditions, specified in section 2.3.1, which must be fulfilled for the upper bound case to apply exist for only a small fraction $x$ of the total service life, whilst the lower bound case applies for the remainder of the time.

Hence the operative value $V_{B_o}$ of the break-even exchange rate is given by

$$V_{B_o} = x \cdot V_{B_u} + (1 - x) \cdot V_{B_L} \quad (2.23)$$

Substituting from equations (2.17) and (2.20) into (2.23), gives the operative value as

$$V_{B_o} = \frac{S.T. \left( x.C_s.R_A + (1-x) \cdot (G-2).F.W_p \right) - K_4.R_A.W_p}{R_A \cdot W_p \cdot (K_2 + K_3)} \quad (2.24)$$

The variation of the operative value of the break-even exchange rate with aircraft speed is presented in fig. 2.5, for the conditions listed in Table 2.1.

## 2.4 The Definition of the Global Exchange Rate

In practice, the operating airline would not merely want to break even on any structural alterations incorporated in

the aircraft, but would require a definite increase in the profit, in which case an exchange rate, which is less than the break-even value, must be used.

The exchange rate adopted by the airline or the aircraft manufacturer, as a means of improving the profitability of an aircraft by reducing its structural weight, will be defined as the global exchange rate, which has a value $V_G$ given by

$$V_G = V_{B_o} - \frac{\delta P}{\delta W_s} \tag{2.25}$$

Ideally, the airline would like to apply a global exchange rate having zero value, in order to obtain the saving in weight for no increase in cost. In this case the increase in profit due to the saving in weight, $\frac{\delta P}{\delta W_s}$, is obtained from equation (2.25) as

$$\frac{\delta P}{\delta W_s} = V_{B_o}$$

It is not generally the case that the required saving in weight can be acquired at zero cost. Fig. 2.6 illustrates the variation of the magnitude of the increase in profit for different values of the global exchange rate.

Many factors influence the global value adopted for a given aircraft project, including the limits introduced by ref. 10, as follows:

i) the limitation on the amount the airline will pay, applied by market cost considerations,

ii) the limitation on the amount of capital investment which can be undertaken to enable new structural types to be introduced.

The exchange rate value, derived above, was based on a

consideration of civil aircraft costs, because of the straightforward manner in which a monetary value could be attached to the reduction in weight.

The exchange rate concept may also be applied to the design of military aircraft, but the monetary value of saving weight is not readily obvious. For military aircraft it is the gain in mission capability, in terms of an increased weapons load or an improved radius of action, for example, which must determine the monetary value of saving weight.

Quoted values of the global exchange rate range from £10/lb.,[11] for a simple turboprop airliner, up to £2000 + /lb.,[12] for orbital payloads. A spectrum of global exchange rate values is presented in fig. 2.7.

## 2.5 The Definition of the Detail Exchange Rate

A further exchange rate must be introduced to enable the structure with the optimal characteristics, as specified by the design objective, to be identified. This will be defined as the detail exchange rate, the value for which will be derived from a consideration of the following example:

Let two structural designs fulfil the same requirements. The datum design has a production cost per unit weight $S_1$ and a structural weight $W_1$, giving a production cost $C_1 = S_1 \cdot W_1$. The alternative design has a higher production cost per unit weight $S_2$, but a structural weight $W_2$ which is a fraction y of the weight of the datum design, that is $W_2 = y \cdot W_1$. The production cost $C_2$ of the alternative design is $C_2 = y \cdot W_1 \cdot S_2$.

If the second design is used rather than the first, the extra cost needed for the reduction in weight, which defines the value $V_D$ of the detail exchange rate, is given by

$$V_D = \frac{C_2 - C_1}{W_1 - W_2} = \frac{y \cdot S_2 - S_1}{1 - y} \qquad (2.26)$$

Hence if the global exchange rate value $V_G$ is greater than the detail exchange rate value $V_D$, it is worth incorporating the lighter, more expensive structure in the aircraft in order to increase the airline's profit.

The cost and weight values used in the detail exchange rate equation must be carefully specified, since the incorporation of a component into a structure can influence the cost and weight variation of the structure as a whole, as is demonstrated in Chapter 10.

The component cost used in the detail exchange rate equation must include:

i) the raw material cost of the component,

ii) the production cost of the component,

iii) the variable cost of the complete structure due to the inclusion of the component.

The component weight used in the detail exchange rate equation must include:

i) the component weight,

ii) the variable weight of the complete structure due to the inclusion of the component.

## 2.6 The Definition of the Merit Function

The merit function parameter, which was evolved by Alvey

Emero,[2] allows the relative performance of different systems, in terms of the degree of fulfilment of the design objective, to be compared. The merit function value M (lb.) of the structure, having a weight W and a cost C, is defined as

$$M = W + \frac{C}{V_G} \qquad (2.27)$$

where W = component weight (lb.), as defined in section 2.5,

C = component cost (£), as defined in section 2.5.

By definition, the minimum value of the merit function identifies the optimal structure.

The application of the merit function parameter in the design process will be demonstrated for the following example: Suppose a component in aluminium alloy weighs 200 lb., with a cost per unit weight of £15/lb., giving a component cost of £3000. The same component fabricated in titanium alloy weighs 150 lb., has a cost per unit weight of £40/lb., giving a component cost of £6000.

The value $V_D$ of the detail exchange rate between the structures is given by equation (2.26),

$$\text{i.e.} \quad V_D = \frac{C_2 - C_1}{W_1 - W_2} = \frac{6000 - 3000}{200 - 150} = £60/\text{lb.}$$

The merit function value $M_A$ for the aluminium alloy structure is

$$M_A = 200 + \frac{3000}{V_G} \qquad \text{(lb.)}$$

The merit function value $M_T$ for the titanium alloy structure is

$$M_T = 150 + \frac{6000}{V_G} \qquad \text{(lb.)}$$

At a global exchange rate value of £60/lb.,

$$M_A = M_T = 250 \quad \text{(lb.)}.$$

Thus the merit function analysis indicates structures having equal merit in terms of the degree of fulfilment of the design objective. At a higher value of the global exchange rate, the merit function analysis predicts that the lighter, more expensive structure will give the optimal solution, since $M_A$ is greater than $M_T$ when $V_G$ is greater than $V_D$.

TABLE 2.1 The specimen values used in the break-even exchange rate example presented in fig. 2.5.

| | | |
|---|---|---|
| Seat mile charge | $C_s$ | = £0.055/mile |
| Fuel cost per unit weight | F | = £0.011/lb. |
| Growth factor | G | = 4 |
| Combined constants | $(K_2 + K_3)$ | = 1.7 |
| Structural weight constant | $K_4$ | = £12/lb. |
| Aircraft range | $R_A$ | = 3000 mile |
| Service life | T | = 30,000 hr. |
| Time factor | x | = 0.01 |
| Passenger weight | $W_p$ | = 200 lb. |

FIG. 2.1 THE MAGNITUDE OF AN AIRCRAFT'S LIFE-CYCLE COST

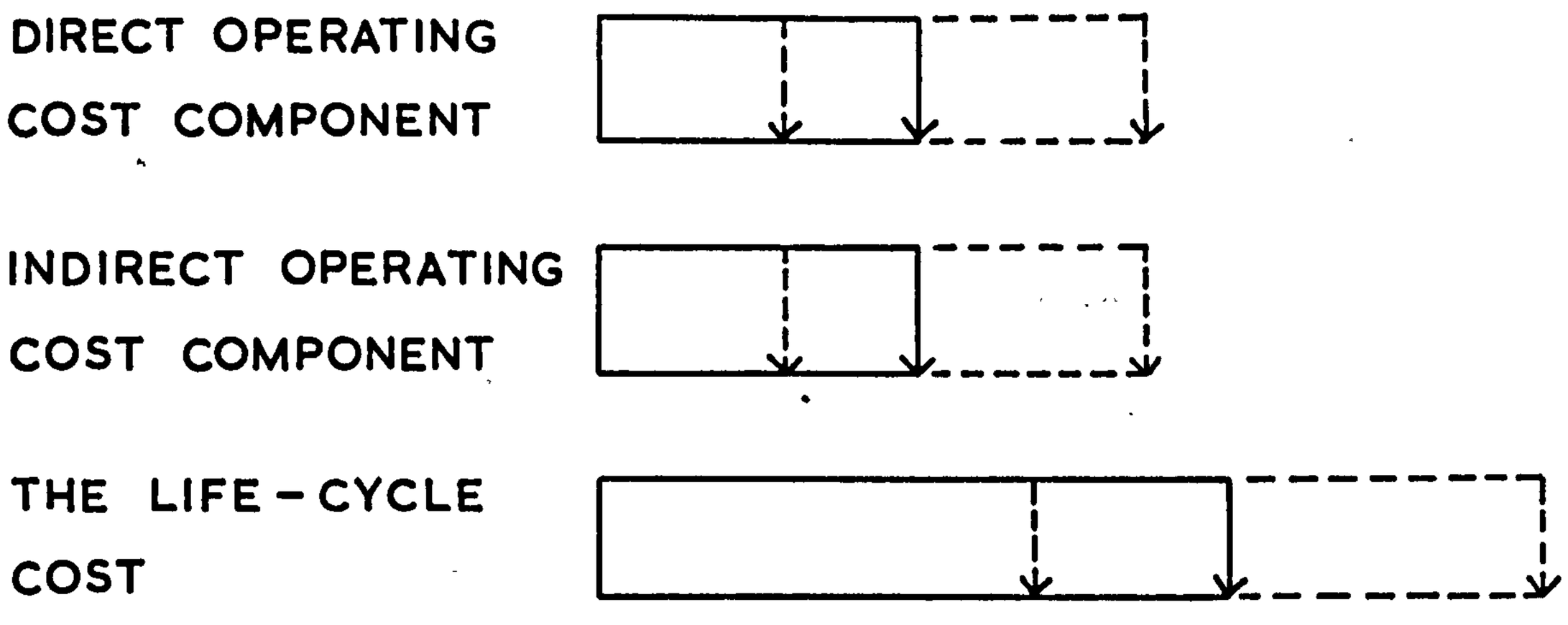


BASED ON DATA PUBLISHED IN REF. 24

FIG. 2.2 A DIRECT OPERATING COST BREAKDOWN

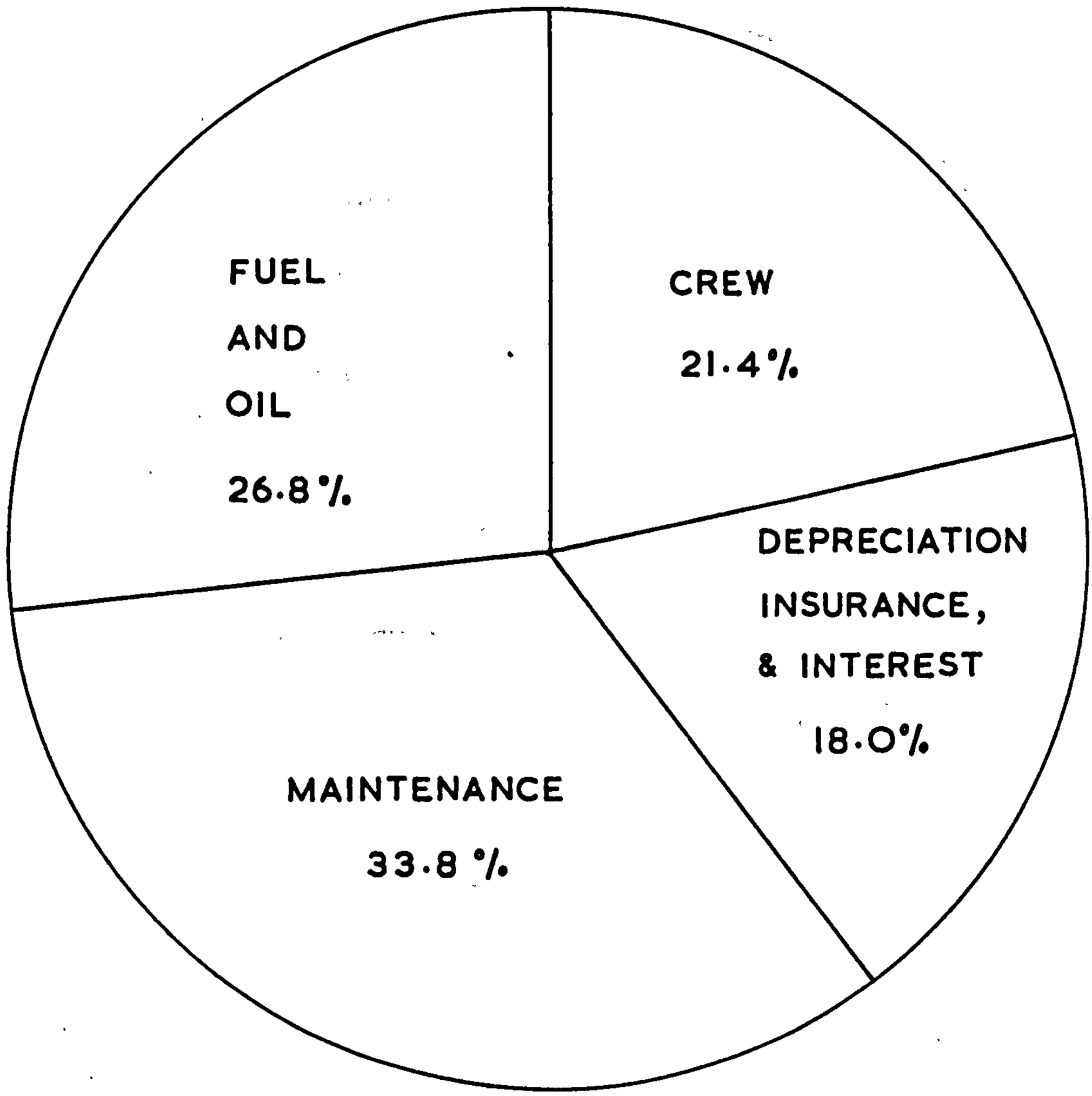


AIRCRAFT TYPE : BOEING 707

BASED ON DATA PUBLISHED IN REF. 9

FIG. 2.3 AN INDIRECT OPERATING COST BREAKDOWN

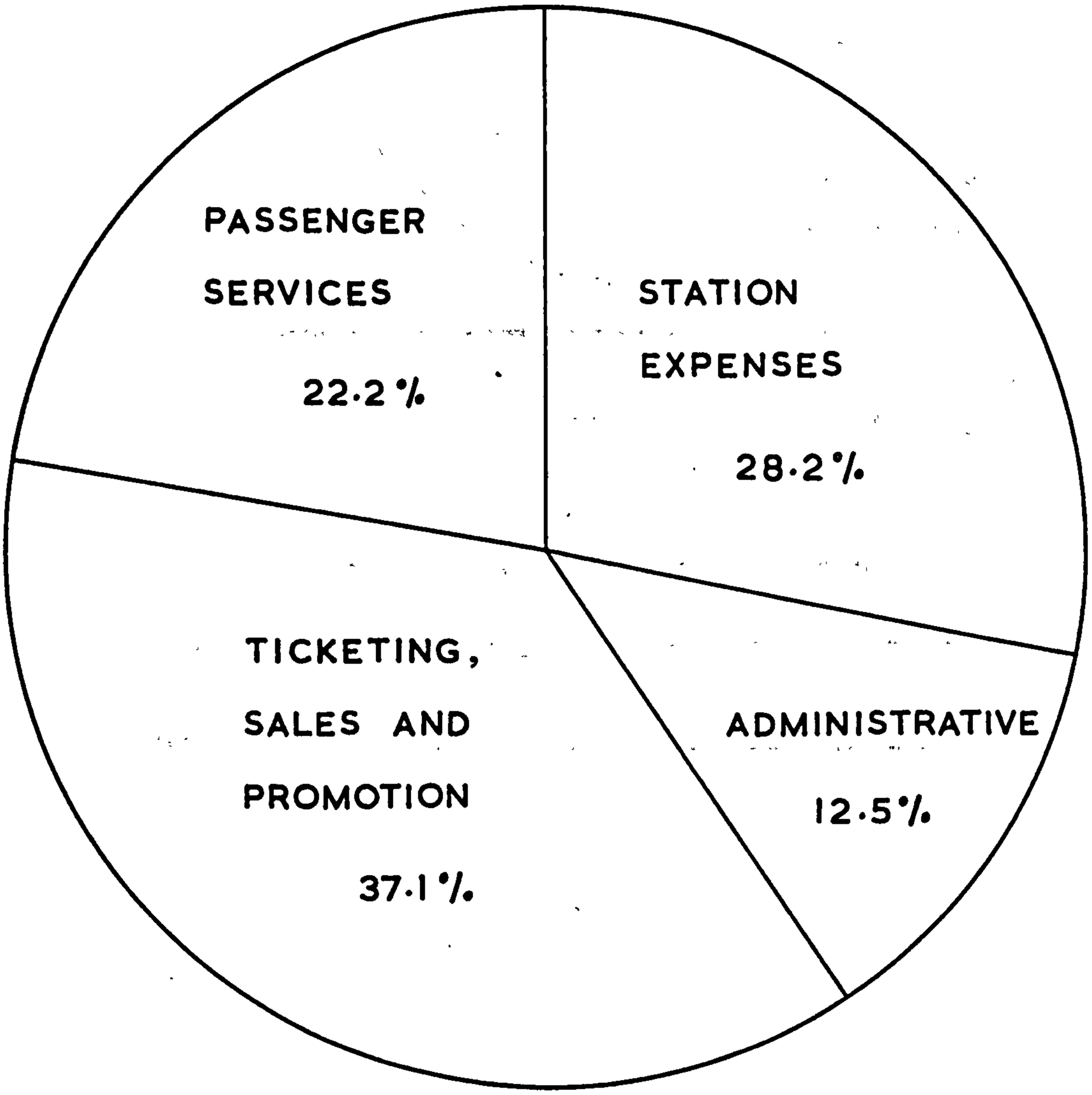


DATA FOR TRANS WORLD AIRLINES

SOURCE : REFERENCE 24

FIG. 2.4 THE VARIATION OF THE WEIGHT AND COST OF A TYPICAL AIRFRAME COMPONENT WITH STRUCTURAL EFFICIENCY

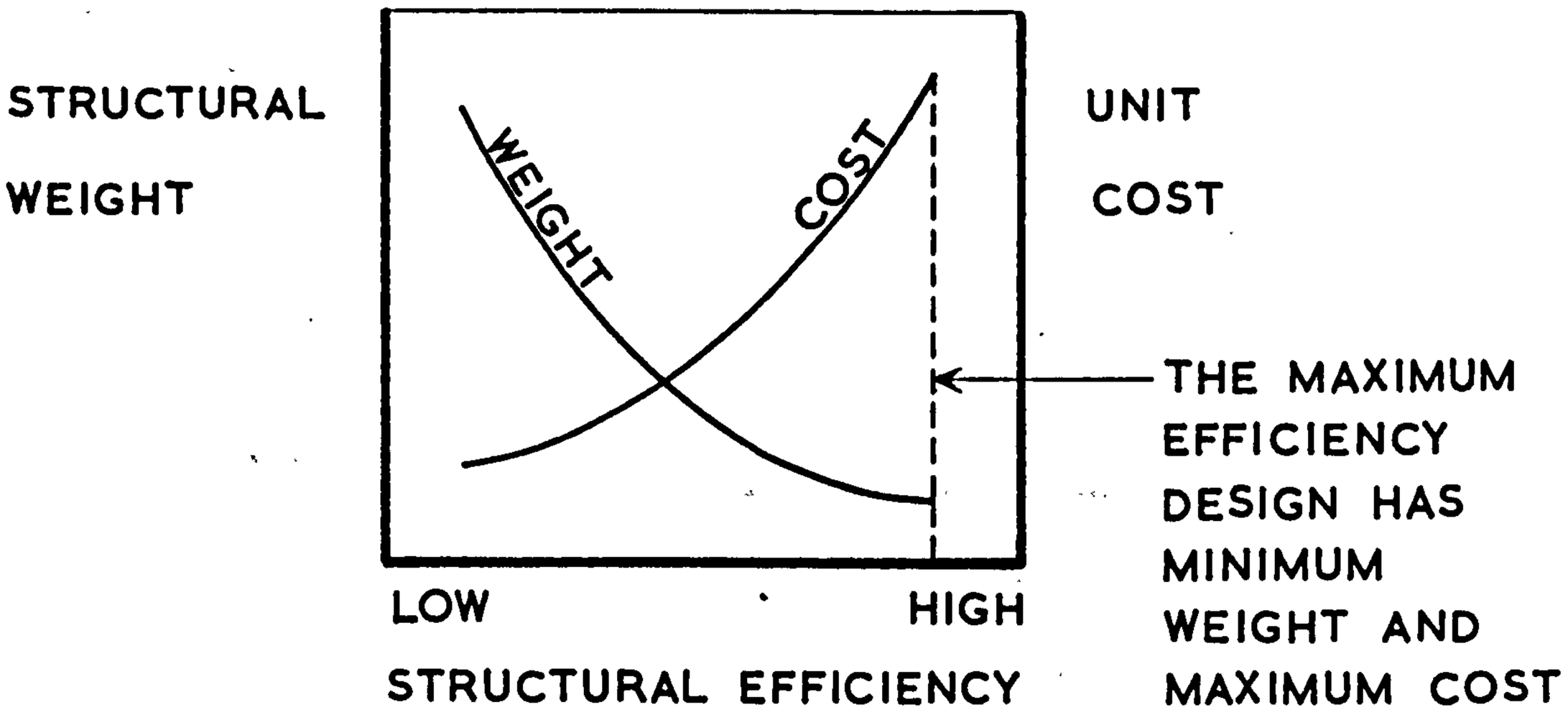


FIG. 2.5 THE VARIATION OF THE BREAK-EVEN EXCHANGE RATE WITH CRUISE SPEED

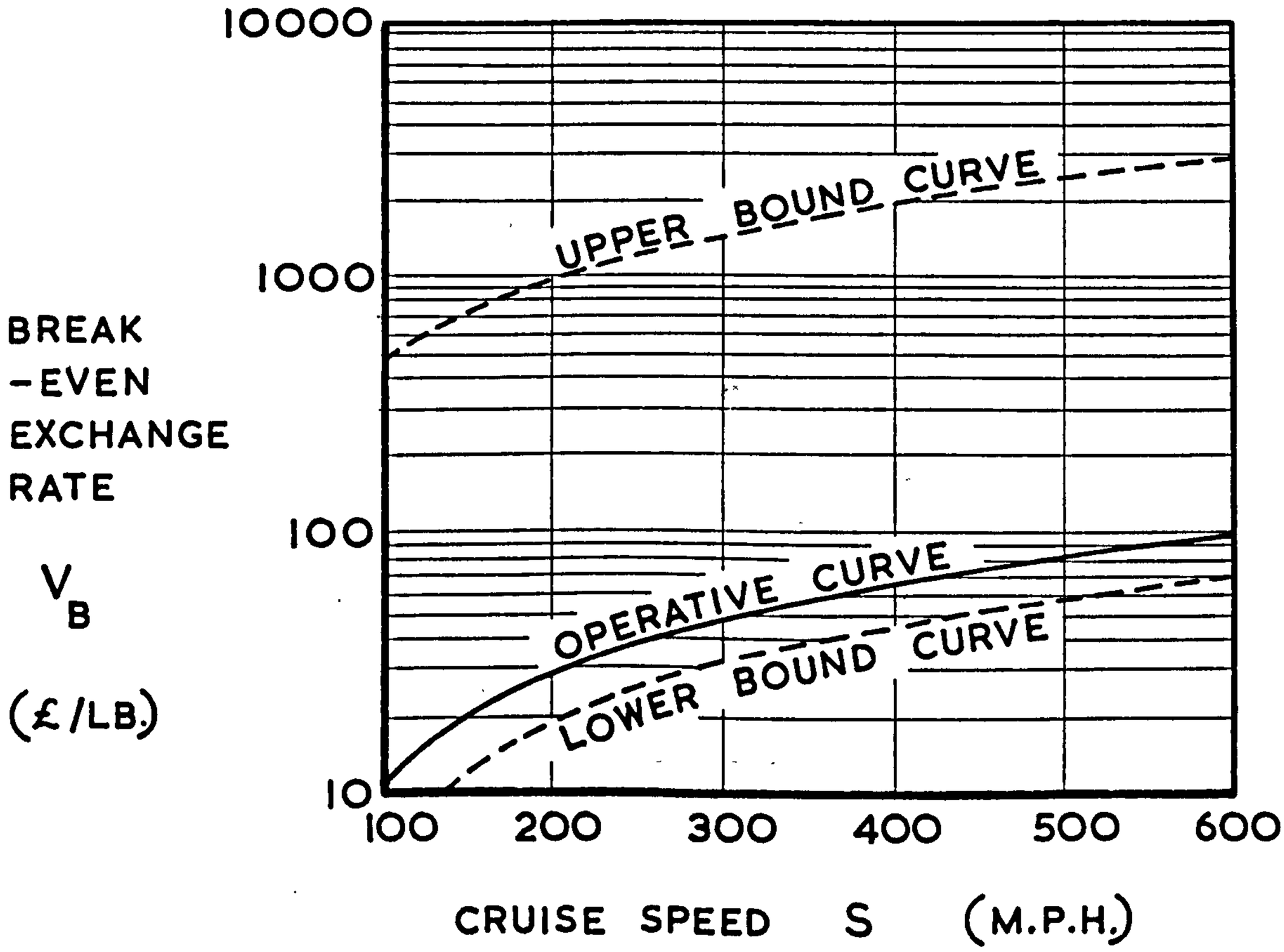

FIG. 2.6 A CHART FOR THE SELECTION OF THE GLOBAL EXCHANGE RATE VALUE

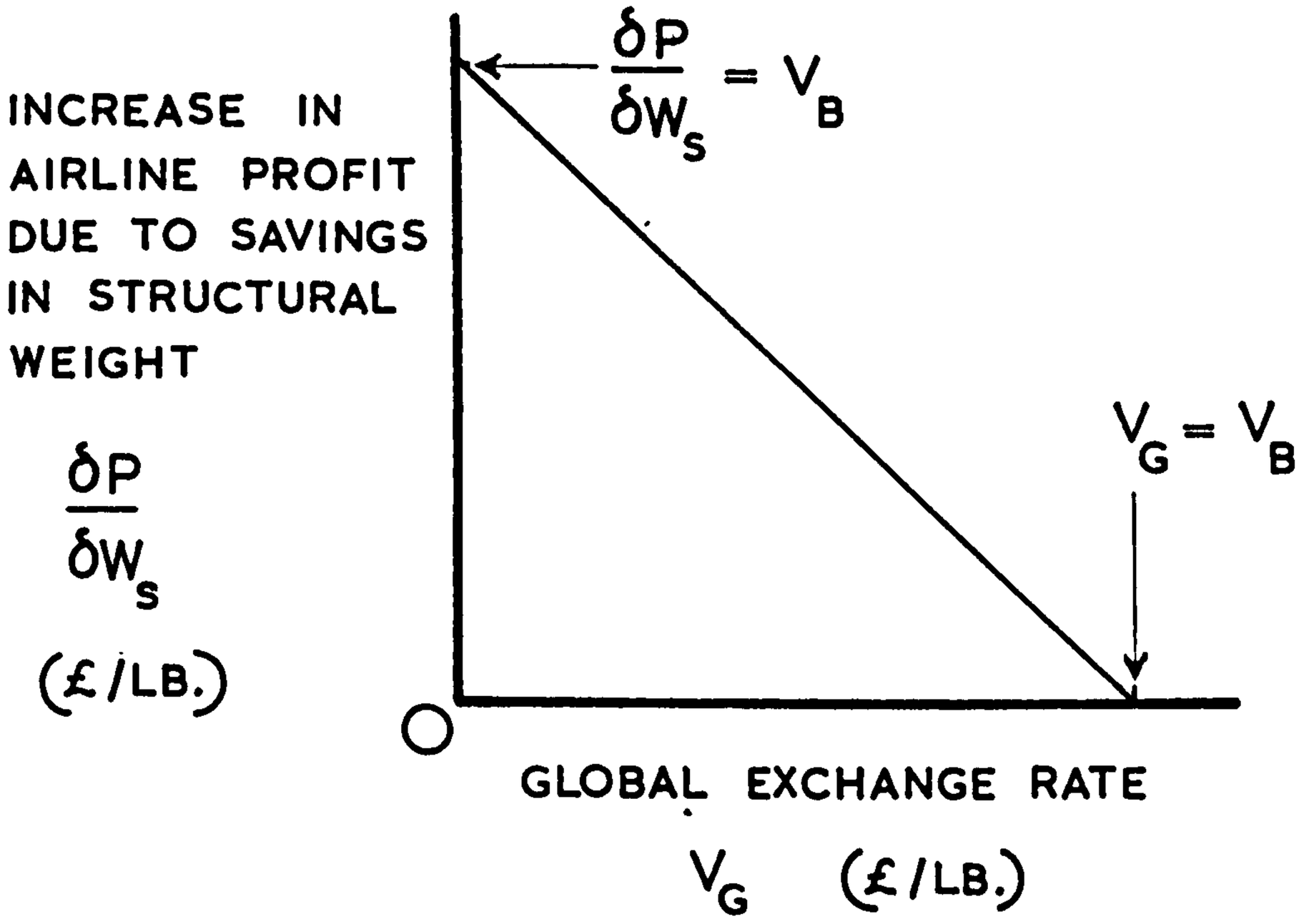


FIG. 2.7 A GLOBAL EXCHANGE RATE SPECTRUM

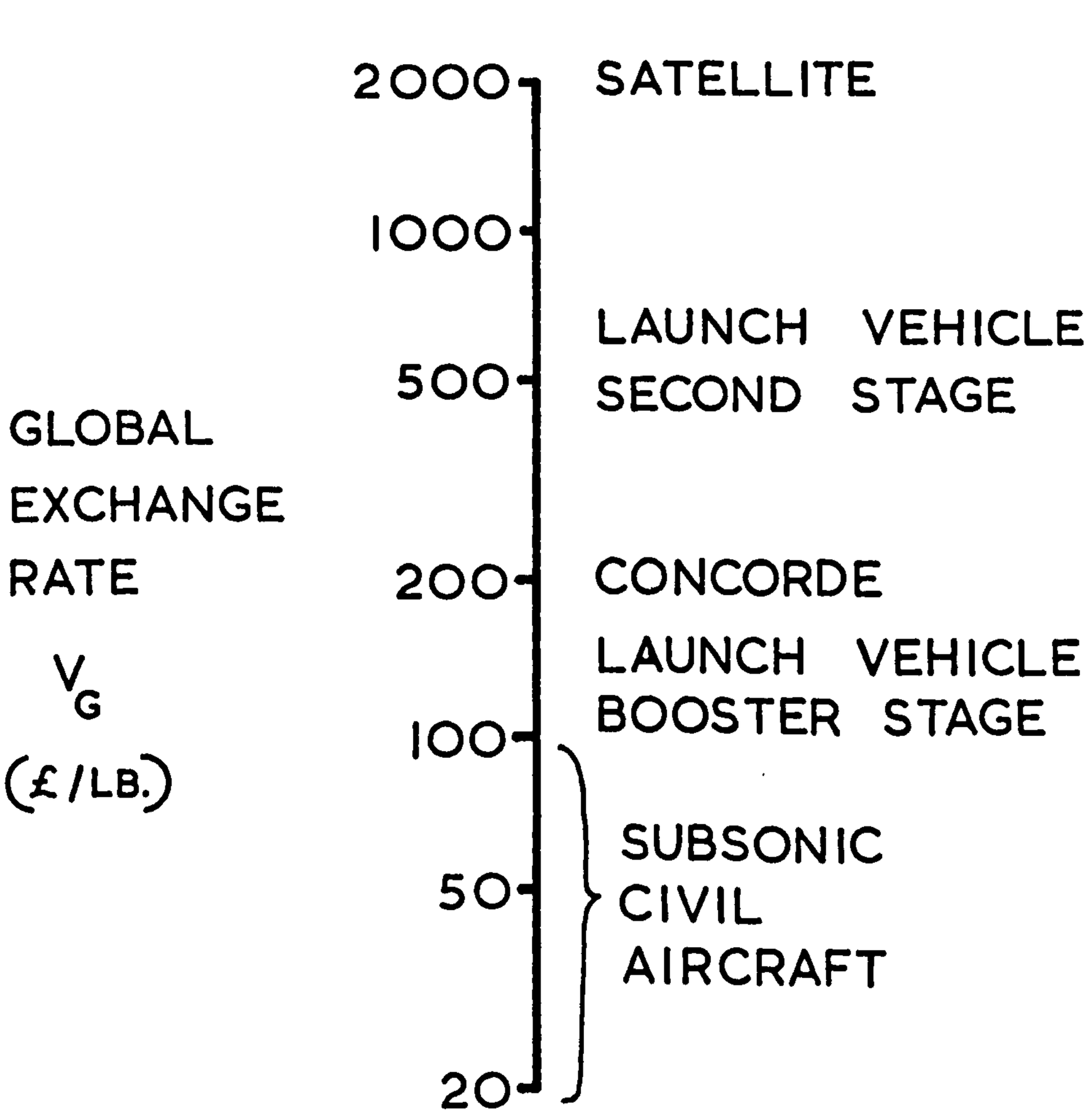

# P A R T  2 :

# THE OPTIMAL ANALYSIS OF A SPECIMEN STRUCTURE

# INTRODUCTION

The analysis of the specimen structure was undertaken with two main objectives, as follows:

i) to provide results of practical value,

ii) to demonstrate the modus operandi of the design process presented in Part 1.

The specimen structure was an essentially practical structure in concept, although several simplifications were introduced into the design model to ease the task of analysis.

As described in section 1.3, the design model prescribes the manner in which the system values are evaluated in order to allow the equitable comparison of different structural systems. The design model for the specimen structure was sub-divided into two section, as follows:

i) the structural model, presented in Chapter 3, which specifies the geometric constraints to be applied to each structural system,

ii) the cost model, presented in Chapter 4, which specifies the method of allocation of the cost elements to each structural system.

# C H A P T E R  3

# THE DEFINITION OF THE STRUCTURAL MODEL

## 3.1 Introduction

As defined in section 1.3, the structural model delimits the extent of the structural item under analysis and sets a series of geometric requirements to be satisfied by each structural system.

The specimen structure chosen for optimisation was a cantilever box beam, which can be considered as an idealised aircraft wing.

The loading system applied to the specimen structure consisted of compressive and tensile end loads, of magnitude $N_x$, applied to the upper and lower covers, respectively, by the maximum positive bending case. A negative bending case of half the positive case was considered. A shear load, of magnitude $V_s$, was applied to each spar. It was assumed that zero torque load was applied to the box beam section.

Each structural system examined consisted of the following structural items:

i) upper cover,

ii) lower cover,

iii) front spar,

iv) rear spar,

v) transverse ribs.

The dominant loadings in the upper and lower covers were the compressive and tensile end loads, respectively, due to the maximum positive bending case. Henceforth, the upper

cover will be termed the compression cover and the lower cover will be termed the tension cover.

Each structural system had to satisfy certain geometric constraints prescribed by the structural model. The geometric constraints imposed were of three types, as follows:

i) geometric constraints imposed on the external dimensions of the box beam,

ii) geometric constraints imposed on the internal dimensions by the structural design equations,

iii) geometric constraints imposed on the internal dimensions by producibility requirements.

Each case will be examined in turn.

## 3.2 The Specification of the External Dimensions

In the interest of clarity, it was decided to maintain the same external dimensions of the box beam throughout the analysis. The external dimensions of the box beam were held constant at a span of 100 in., a chord of 50 in., and a depth of 15 in. The planform dimensions were chosen since they approximate to a standard sheet size used in industry.

The dimensions represent a cantilever box planform aspect ratio of 2 and a box thickness/chord ratio of 0.3. In general, the torsion box of a wing occupies approximately half of the wing chord. Hence the box beam was commensurate with a wing having a thickness/chord ratio of approximately 15 per cent. Subsonic civil aircraft have wing thickness/chord ratios in the range of 10 to 18 per cent, generally.

## 3.3 The Structural Design Equations

The following structural design equations imposed a set of geometric constraints on each structural system, which ensured that a system capable of carrying the design loading without failure was obtained.

The structural design equations make use of the efficiency factor form of structural analysis due to Farrar.[13] The equations are applicable to any type of wide column structure for which the requisite efficiency factor design charts are available. The design charts, which specify the dimensions of Z stringer-stiffened covers[13] and L stringer-stiffened covers,[14] are presented in figs. 3.1 and 3.2, respectively.

The following assumptions are made in the analysis:

i) the compression cover is considered as a wide column simply supported by the transverse ribs, hence wide column theory may be used to determine the cover thickness,

ii) buckling of the cover is coincident with cover failure,

iii) the ribs, which are of stiffened web construction, satisfy wide column theory, in order that stability failure of the ribs, when subjected to the Brazier loads introduced by bending of the wing, may be examined,

iv) the spars carry the total shear load and provide negligible edge restraint to the cover.

The structural design equations governing the main structural components are now presented.

### 3.3.1 Compression cover and ribs

The compression cover is designed to an applied compressive loading per unit width, $N_x$, which corresponds to the maximum positive bending case.

The ribs are designed to an applied compressive loading per unit width, $N_R$, due to the bending of the wing under the applied moment $M = N_x \cdot d$.

From fig. 3.3

$$N_R = 2 \cdot N_x \sin(\theta/2)$$

i.e. $$N_R = N_x \cdot \frac{a}{R}$$

$$M = N_x \cdot d$$

$$I = t_c \cdot d^2/2$$

From bending theory, $\frac{M}{I} = \frac{E}{R}$

Thus $$R = \frac{E \cdot t_c \cdot d}{2 \cdot N_x}$$

$\therefore$ $$N_R = \frac{2 \cdot a \cdot N_x^2}{E \cdot t_c \cdot d} \qquad (3.1)$$

The following design cases are applicable to the compression cover and the ribs. In each case the relevant quantities are presented in non-dimensional form.

#### 3.3.1.1 Minimum gauge cover

This condition applies in the outboard wing section. The rib spacing a is arranged to cause failure by panel buckling and is obtained from the thickness equation derived by Farrar[13]:

$$t_c = \frac{1}{F}\sqrt{\frac{a \cdot N_x}{E}} \qquad (3.2)$$

since $t_c = t_{c\ min}$,

$$\frac{a}{t_{c\ min}} = t_{c\ min} \cdot F^2 \cdot \frac{E}{N_x} \qquad (3.3)$$

The weight per unit planform area $W$ of the compression cover and ribs is

$$W = p \cdot (t_c + \frac{d}{a} \cdot t_R) \qquad (3.4)$$

a. Minimum gauge ribs

With $t_R = t_{R\ min}$, and substituting for $a$ from (3.3) the weight/unit planform area is

$$\frac{W}{p \cdot t_{c\ min}} = 1 + \frac{d \cdot N_x \cdot t_{R\ min}}{t_{c\ min}^3 \cdot F^2 \cdot E} \qquad (3.5)$$

Rib thickness $t_R = t_{R\ min}$

$$\therefore \quad \frac{t_R}{t_{R\ min}} = 1 \qquad (3.6)$$

b. Stability failure of ribs

If the ribs are considered as a stiffened web of efficiency $F_R$ the rib thickness $t_R$ obtained by applying equation (3.2) is

$$t_R = \frac{1}{F_R}\sqrt{\frac{d \cdot N_R}{E}}$$

from equation (3.1),

$$t_R = \frac{N_x}{F_R \cdot E} \sqrt{\frac{2\,a}{t_c}} \qquad (3.7)$$

Since $t_c = t_{c\ min}$,

$$\frac{t_R}{t_{R\ min}} = \frac{F}{F_R \cdot t_{R\ min}} \left( \frac{2 \cdot t_{c\ min} \cdot N_x}{E} \right)^{\frac{1}{2}} \qquad (3.8)$$

Weight per unit area $W = p \cdot (t_c + \frac{d}{a} \cdot t_R)$

$$\therefore \frac{W}{p \cdot t_{c\ min}} = 1 + \frac{2^{\frac{1}{2}} \cdot d \cdot N_x^{3/2}}{F \cdot F_R \cdot E^{3/2} \cdot t_{c\ min}^{5/2}} \qquad (3.9)$$

c. <u>Strength failure of ribs</u>

If designed to the yield stress, the rib thickness $t_R$ is

$$t_R = \frac{N_R}{\sigma_c}$$

substituting for $N_R$ from (3.3) gives

$$t_R = \frac{2 \cdot a \cdot N_x^{\ 2}}{E \cdot t_c \cdot d \cdot \sigma_c} \qquad (3.10)$$

Since $t_c = t_{c\ min}$, substituting for $a$ from (3.3) gives

$$\frac{t_R}{t_{R\ min}} = \frac{2 \cdot N_x \cdot t_{c\ min} \cdot F^2}{d \cdot \sigma_c \cdot t_{R\ min}} \qquad (3.11)$$

Since weight per unit area $W = p \cdot (t_c + \frac{d}{a} \cdot t_R)$

applying equations (3.3) and (3.11) gives

$$\therefore \frac{W}{p \cdot t_{c\ min}} = 1 + \frac{2 \cdot N_x^{\ 2}}{E \cdot \sigma_c \cdot t_{c\ min}^{\ 2}} \qquad (3.12)$$

The maximum loading for the minimum gauge cover cases occurs when the cover yield stress is reached,

$$\text{i.e.} \quad \sigma_c = \frac{N_x}{t_{c\ min}}$$

Hence these cases are only applicable for values of the loading coefficient

$$\frac{N_x}{\sigma_c \cdot t_{c\ min}} \leq 1 \qquad (3.13)$$

3.3.1.2 <u>Cover thickness fixed by stability require-</u>

<u>ments</u>

In this case the cover thickness is varied to satisfy equation (3.2),

$$\text{i.e.} \quad t_c = \frac{1}{F}\sqrt{\frac{a \cdot N_x}{E}}$$

a. <u>Minimum gauge ribs</u>

Rib thickness $t_R = t_{R\ min}$,

$$\text{i.e.} \quad \frac{t_R}{t_{R\ min}} = 1 \qquad (3.14)$$

Weight per unit area W is

$$W = p \cdot \left(\frac{1}{F}\sqrt{\frac{a \cdot N_x}{E}} + \frac{d}{a} \cdot t_{R\ min}\right)$$

The optimum rib spacing is found by differentiating with respect to a to obtain the minimum weight, giving

$$\frac{a_o}{t_{c\ min}} = \left( \frac{4 \cdot F^2 \cdot d^2 \cdot t_{R\ min}^2 \cdot E}{N_x \cdot t_{c\ min}^3} \right)^{\frac{1}{3}} \qquad (3.15)$$

To obtain the minimum weight $W_o$, substitute $a = a_o$,

$$\text{i.e. } \frac{W_o}{p \cdot t_{c\ min}} = 1.5 \left( \frac{2 \cdot N_x \cdot d \cdot t_{R\ min}}{E \cdot F^2 \cdot t_{c\ min}^3} \right)^{\frac{1}{3}} \qquad (3.16)$$

b. <u>Stability failure of ribs</u>

Rib thickness $t_R$ is given by equation (3.7),

$$\text{i.e. } t_R = \frac{N_x}{F_R \cdot E} \sqrt{\frac{2 \cdot a}{t_c}}$$

Weight per unit area $W$ is

$$W = p \cdot \left( \frac{1}{F} \sqrt{\frac{a \cdot N_x}{E}} + \frac{d}{a} \cdot t_R \right) \qquad (3.17)$$

The optimum rib spacing $a_o$ is found by differentiating with respect to $a$ to obtain the minimum weight, giving

$$\frac{a_o}{t_{c\ min}} = \left( \frac{9 \cdot d^2 \cdot F^3 \cdot N_x^{\frac{1}{2}}}{2 \cdot F_R^2 \cdot E^{\frac{1}{2}} \cdot t_{c\ min}^{5/2}} \right)^{2/5} \qquad (3.18)$$

To obtain the minimum weight $W_o$, substitute $a = a_o$.

$$\text{i.e. } \frac{W_o}{p \cdot t_{c\ min}} = \left( \frac{9 \cdot d^2 \cdot N_x^3}{2 \cdot F_R^2 \cdot E^3 \cdot F^2 \cdot t_{c\ min}^5} \right)^{1/5} \cdot \left(1 + \tfrac{2}{3}\right) \qquad (3.19)$$

From (3.2), (3.7) and (3.18) rib thickness for minimum weight is:

$$\frac{t_R}{t_{R\,min}} = \left( \frac{12 \cdot N_x^4 \cdot F^4 \cdot d}{E^4 \cdot F_R^6 \cdot t_{R\,min}^5} \right)^{1/5} \qquad (3.20)$$

c. Strength failure of ribs

Rib thickness $t_R$ is given by equation (3.10),

$$\text{i.e.} \quad t_R = \frac{2 \cdot a \cdot N_x^2}{E \cdot t_c \cdot d \cdot \sigma_c}$$

The optimum rib spacing is found by differentiating (3.17) with respect to $a$ to obtain the minimum weight, giving

$$\frac{a_o}{t_{c\,min}} = \frac{2 \cdot N_x \cdot F^2}{\sigma_c \cdot t_{c\,min}} \qquad (3.21)$$

To obtain the minimum weight $W_o$, substitute

$a = a_o$

$$\text{i.e.} \quad \frac{W_o}{p \cdot t_{c\,min}} = \frac{2^{3/2} \cdot N_x}{E^{\frac{1}{2}} \cdot \sigma_c^{\frac{1}{2}} \cdot t_{c\,min}} \qquad (3.22)$$

Rib thickness for minimum weight is

$$\frac{t_R}{t_{R\,min}} = \frac{2^{3/2} \cdot N_x^2 \cdot F^2}{E^{\frac{1}{2}} \cdot d \cdot \sigma_c^{3/2} \cdot t_{R\,min}} \qquad (3.23)$$

The cases where the cover thickness is fixed by stability requirements are only applicable for values of the weight coefficient

$$\frac{W_o}{p \cdot t_{c\,min}} \geq 1 \qquad (3.24)$$

3.3.1.3 Cover thickness fixed by strength requirements

At high values of the applied loading the cover yield stress may be reached. If designed to the yield stress, the cover thickness is given by

$$t_c = \frac{N_x}{\sigma_c} \qquad (3.25)$$

To determine the rib spacing a, equate equation (3.25) to equation (3.2),

$$\text{i.e.} \quad \frac{a}{t_{c\,min}} = \frac{N_x \cdot E \cdot F^2}{\sigma_c^2 \cdot t_{c\,min}} \qquad (3.26)$$

a. Minimum gauge ribs

Rib thickness $t_R = t_{R\,min}$

$$\text{i.e.} \quad \frac{t_R}{t_{R\,min}} = 1 \qquad (3.27)$$

Weight per unit area W is given by

$$\frac{W}{p \cdot t_{c\,min}} = \frac{N_x}{\sigma_c \cdot t_{c\,min}} + \frac{d \cdot \sigma_c^2 \cdot t_{R\,min}}{N_x \cdot E \cdot F^2 \cdot t_{c\,min}} \qquad (3.28)$$

b. Stability failure of ribs

Rib thickness $t_R$ is found by substituting for a and $t_c$ in equation (3.7),

$$\text{i.e.} \quad \frac{t_R}{t_{R\,min}} = \frac{2^{\frac{1}{2}} \cdot N_x \cdot F}{F_R \cdot E^{\frac{1}{2}} \cdot \sigma_c^{\frac{1}{2}} \cdot t_{R\,min}} \qquad (3.29)$$

Weight per unit area $W$ is given by

$$\frac{W}{p \cdot t_{c\,min}} = \frac{N_x}{\sigma_c \cdot t_{c\,min}} + \frac{d}{F \cdot F_R \cdot t_{c\,min}} \cdot \left(\frac{2 \cdot \sigma_c^3}{E^3}\right)^{\frac{1}{2}} \qquad (3.30)$$

c. <u>Strength failure of ribs</u>

Rib thickness $t_R$ is found by substituting for $a$ and $t_c$ in equation (3.10),

$$\text{i.e.} \quad \frac{t_R}{t_{R\,min}} = \frac{2 \cdot N_x^2 \cdot F^2}{d \cdot \sigma_c^2 \cdot t_{R\,min}} \qquad (3.31)$$

Weight per unit area $W$ is given by

$$\frac{W}{p \cdot t_{c\,min}} = \frac{N_x}{t_{c\,min}} \cdot \left(\frac{1}{\sigma_c} + \frac{2}{E}\right) \qquad (3.32)$$

The cases where the cover thickness is fixed by strength requirements are only applicable for values of the weight coefficient

$$\frac{W_o}{p \cdot t_{c\,min}} \geq 1 \qquad (3.33)$$

3.3.2 <u>Tension cover</u>

The tension cover is designed to three loading cases:

a. Maximum tensile loading $N_x$ for the positive bending case.

b. Fatigue failure due to the oscillatory loading experienced in practice. To cater for this case

the cover is designed to a reduced stress level $\sigma_f$.

c. Negative bending case causing the lower cover to experience a compressive loading. A negative loading of half the positive loading is assumed, i.e. $N_x/_2$.

A minimum gauge constraint is applied to the tension cover. The following equations define the tension cover weight:

3.3.2.1 Minimum gauge case

The tension cover weight/unit area $W_T$ is

$$W_T = p \cdot t_{c\ min}$$

$$\text{i.e.} \quad \frac{W_T}{p \cdot t_{c\ min}} = 1 \qquad (3.34)$$

A loading coefficient based on $\sigma_c$ will be adopted, hence replacing $\sigma_t$ with $\sigma_c$, where $\sigma_{t/\sigma_c} = K_1$.

This case is only applicable for values of the loading coefficient

$$\frac{N_x}{\sigma_t \cdot t_{c\ min}} \leq 1, \text{ i.e. } \frac{N_x}{\sigma_c \cdot t_{c\ min}} \leq K_1 \qquad (3.35)$$

3.3.2.2 Maximum tensile stress case

The tension cover weight/unit area $W_T$ is

$$W_T = \frac{p \cdot K_2 \cdot N_x}{\sigma_t}$$

where $K_2$ = weight penalty factor due to rivet holes in the cover.

$$\text{i.e.} \quad \frac{W_T}{p \cdot t_{c\,min}} = \frac{K_2 \cdot N_x}{\sigma_t \cdot t_{c\,min}} \qquad (3.36)$$

This case is only applicable for values of the loading coefficient

$$\frac{N_x}{\sigma_t \cdot t_{c\,min}} \geq 1$$

$$\text{i.e.} \quad \frac{N_x}{\sigma_c \cdot t_{c\,min}} \geq K_1 \qquad (3.37)$$

3.3.2.3 Fatigue case

For the fatigue case the tension cover is designed to a reduced stress level $\sigma_f$, where $\sigma_f/\sigma_c = K_3$.

The weight/unit area $W_T$ of the tension cover is

$$\frac{W_T}{p \cdot t_{c\,min}} = \frac{K_2 \cdot N_x}{\sigma_f \cdot t_{c\,min}} \qquad (3.38)$$

This case is only applicable for values of the loading coefficient

$$\frac{N_x}{\sigma_f \cdot t_{c\,min}} \geq 1$$

$$\text{i.e.} \quad \frac{N_x}{\sigma_c \cdot t_{c\,min}} \geq K_3 \qquad (3.39)$$

$\sigma_f$ if a function of the number of cycles applied by particular types of loading. It is assumed that there is one critical type of loading which produces the majority of the fatigue damage.

$\sigma_f^1$ is the allowable stress level to prevent fatigue failure from this source, and is much lower than the ultimate tensile strength of the material.

For this case, $N_x$ is the end loading in the wing covers corresponding to this critical fatigue loading case (instead of the maximum positive or negative bending loading cases used previously).

As the equations use $N_x$ based on the maximum positive bending case then $\sigma_f$ must be factored by the ratio

$$\frac{N_x \text{ (max. positive bending case)}}{N_x \text{ (fatigue loading case)}} = K_5$$

$$\text{where } \sigma_f = K_5 \cdot \sigma_f^1$$

3.3.2.4 Negative bending case

In the negative bending case there are two considerations depending on whether the cover thickness is fixed by stability or strength requirements.

a. Cover thickness fixed by stability requirements

The thickness of the cover is given by equation (3.2) with $N_x$ replaced by $N_{x/2}$

$$\text{i.e. } t_c = \frac{1}{F}\sqrt{\frac{a_o \cdot N_x}{2 \cdot E}}$$

where $a_o$ is the rib spacing which gives the

minimum compression cover and rib weight compatible with the design requirements.

∴ The tension cover weight/unit area $W_T$ is

$$\frac{W_T}{p \cdot t_{c\ min}} = \frac{1}{F \cdot t_{c\ min}} \cdot \sqrt{\frac{a_o \cdot N_x}{2 \cdot E}} \qquad (3.40)$$

This case is only applicable for values of the weight coefficient

$$\frac{W_T}{p \cdot t_{c\ min}} \geq 1 \qquad (3.41)$$

It is assumed that the tension and compression covers are designed to the same value of efficiency factor. However, if the operative design case for the lover cover is not the negative bending case, the lowest value of the tension cover efficiency factor $F_T$, which still satisfies the negative bending case 3.3.2.4 (a) is

$$F_T = \frac{1}{t_{c_T}} \sqrt{\frac{a_o \cdot N_x}{2 \cdot E}} \qquad (3.42)$$

where $t_{c_T}$ = tension cover thickness given by the operative design case.

b. <u>Cover thickness fixed by compressive strength requirements</u>

The cover thickness $t_c = \frac{N_x}{2 \cdot \sigma_c}$

∴ The weight/unit area $W_T$ of the tension cover is

$$\frac{W_T}{p \cdot t_{c\ min}} = \frac{N_x}{2 \cdot \sigma_c \cdot t_{c\ min}} \qquad (3.43)$$

This case is only applicable for values of the loading coefficient

$$\frac{N_x}{\sigma_c \cdot t_{c\ min}} \geq 1 \qquad (3.44)$$

In general b is covered by the maximum tensile stress case 3322, since the negative bending case has a loading of half the tensile loading, whereas normally $\sigma_c/\sigma_t > \frac{1}{2}$.

### 3.3.3 Spars

The total shear force applied to the idealised wing is carried by two spars. The influence of any torque applied to the wing would be to increase the load in one spar and to reduce the load in the other. In the box beam analysis an equal shear load $V_s$ in each spar was assumed.

Each spar consisted of top and bottom spar booms and a spar web stiffened by vertical stiffeners. The operative rib pitch, specified by the structural design equations of section 3.3.1, imposed a constraint on the pitch of the spar web stiffeners, since the rib pitch was arranged as an integer multiple of the stiffener pitch. An existing computer program[15], based on the method of diagonal tension analysis presented in ref. 16, was utilised to expedite the evaluation of the spar weights.

Further details of the computer program are presented in section A1.2 of appendix 1.

### 3.3.4 The interpretation of the structural design equations

The operative criteria specifying the internal dimensions of the box beam were determined in the following manner:

i) the rib thickness $t_R$, for a given loading, had to be equal to the greatest thickness required for any individual case 3.3.1.1 to 3.3.1.3,

ii) the normalised rib pitch $\frac{a}{t_{c\ min}}$ had to be greater than 1 for theoretical considerations and greater than 300 for production considerations, the latter value being dependent on the value of $t_{c\ min}$,

iii) the compression cover thickness $tc_c$ had to be equal to the greatest thickness required for any individual case 3.3.1.1 to 3.3.1.3,

iv) the tension cover thickness $tc_T$ had to be equal to the greatest thickness required for any individual case 3.3.2.1 to 3.3.2.4.

The manner in which the operative design cases, governing the rib thickness, the rib pitch, the compression cover thickness and the tension cover thickness, vary with loading coefficient are illustrated in figs. 3.4 to 3.7, respectively, for the aluminimum alloy

material values used in the analysis of the specimen structure.

A comparison of the internal dimensions required by the aluminium alloy and titanium alloy box beams to satisfy the structural design equations are presented in figs. 3.8 to 3.11. The values used in the structural design equations, for the aluminium alloy and titanium alloy materials, are presented in Table 3.1.

### 3.3.5 The determination of the cover geometry

The structural design equations only indicate the generalised cover thickness necessary for structural integrity. In the formulation of practical designs, the internal arrangement of the cover geometry, in terms of the dimensions of the skin and stringers, had to be known.

The internal geometry was designed to satisfy two conditions, as follows:

i) the skin and stringer dimensions were varied to satisfy the equation

$$tc = t + \frac{A_{ST}}{b} \qquad (3.45)$$

where tc = the cover thickness indicated by the operative design case,

t = skin thickness,

$A_{ST}$ = stringer area,

b = stringer pitch,

ii) the combination of stringer to skin thickness

ratio $\frac{ts}{t}$ and the stringer to skin area ratio $\frac{A_{ST}}{b.t}$ had to specify a design of the correct efficiency factor value. A suitable arrangement of the cover geometry was obtained using the appropriate design chart for the cover configuration, chosen from the design charts presented in figs. 3.1 and 3.2.

## 3.4 The Geometric Constraints Imposed by Producibility Requirements

Producibility considerations imposed certain constraints on the internal geometry of the structural configurations.

For example, it was a basic requirement that each structural system should include upper and lower covers having a flush finish to improve the aerodynamic performance of the idealised wing. If a cut-countersink riveted structure was envisaged, there was a minimum skin gauge in which a cut-countersink could be made, the value of which depended on the rivet diameter and the rivet head angle. Hence the production method imposed a minimum gauge constraint on the skins of the upper and lower covers.

Damage tolerance considerations when the aircraft is in service can also influence the minimum skin gauges used.

Other constraints imposed by producibility requirements included minimum stringer pitches and minimum rib pitches to allow the access of the operator and his equipment. Further details of the producibility constraints imposed on the internal geometry, for specific production methods, are given in Chapter 5.

TABLE 3.1 Specimen values used in the structural design equations.

| | Aluminium alloy structural systems | Titanium alloy structural systems |
|---|---|---|
| Modulus of elasticity E (lb/in$^2$) | 10 x 10$^6$ | 18 x 10$^6$ |
| 0.1% Proof stress $\sigma_c$ (lb/in$^2$) | 47,000 | 130,000 |
| Ultimate tensile stress $\sigma_t$ (lb/in$^2$) | 60,000 | 147,000 |
| Material density p (lb/in$^3$) | 0.098 | 0.158 |
| Cover efficiency factor F | 0.6 - 0.95 | 0.7 - 1.015 |
| Rib efficiency factor $F_R$ | 0.5 | 0.5 |
| Box beam depth d (in) | 15 | 15 |
| cover minimum gauge $t_{c\ min}$ (in) | 0.036 | 0.022 |
| Rib minimum gauge $t_{R\ min}$ (in) | 0.036 | 0.022 |
| Weight penalty factor $K_2$ | 1 | 1 |
| Fatigue stress factor $K_3$ | 1 | 1 |

# THE COVER DESIGN CHARTS

FIG. 3.1 THE Z-STRINGER STIFFENED COVER

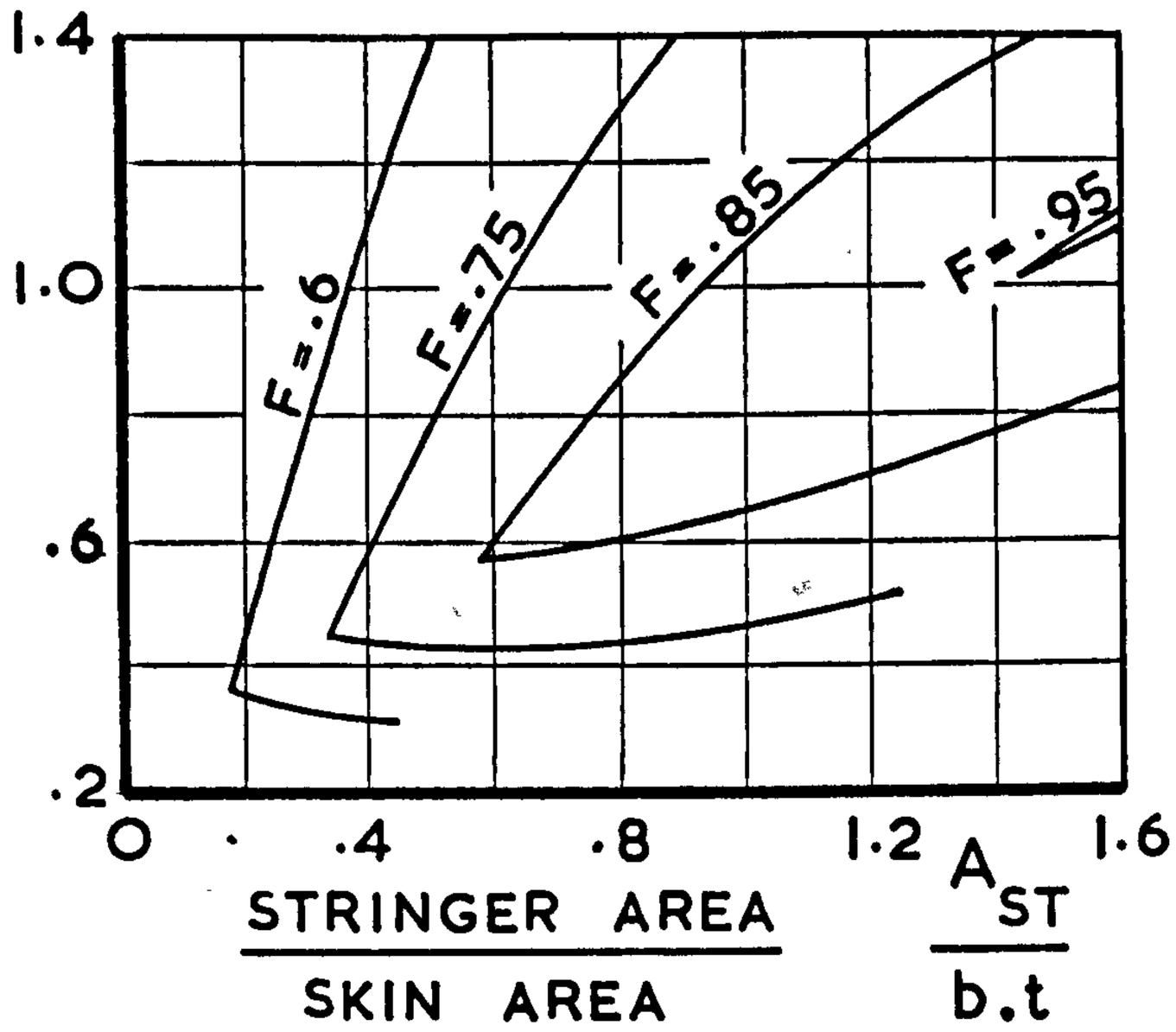


SOURCE : REF. 13

FIG. 3.2 THE L-STRINGER STIFFENED COVER

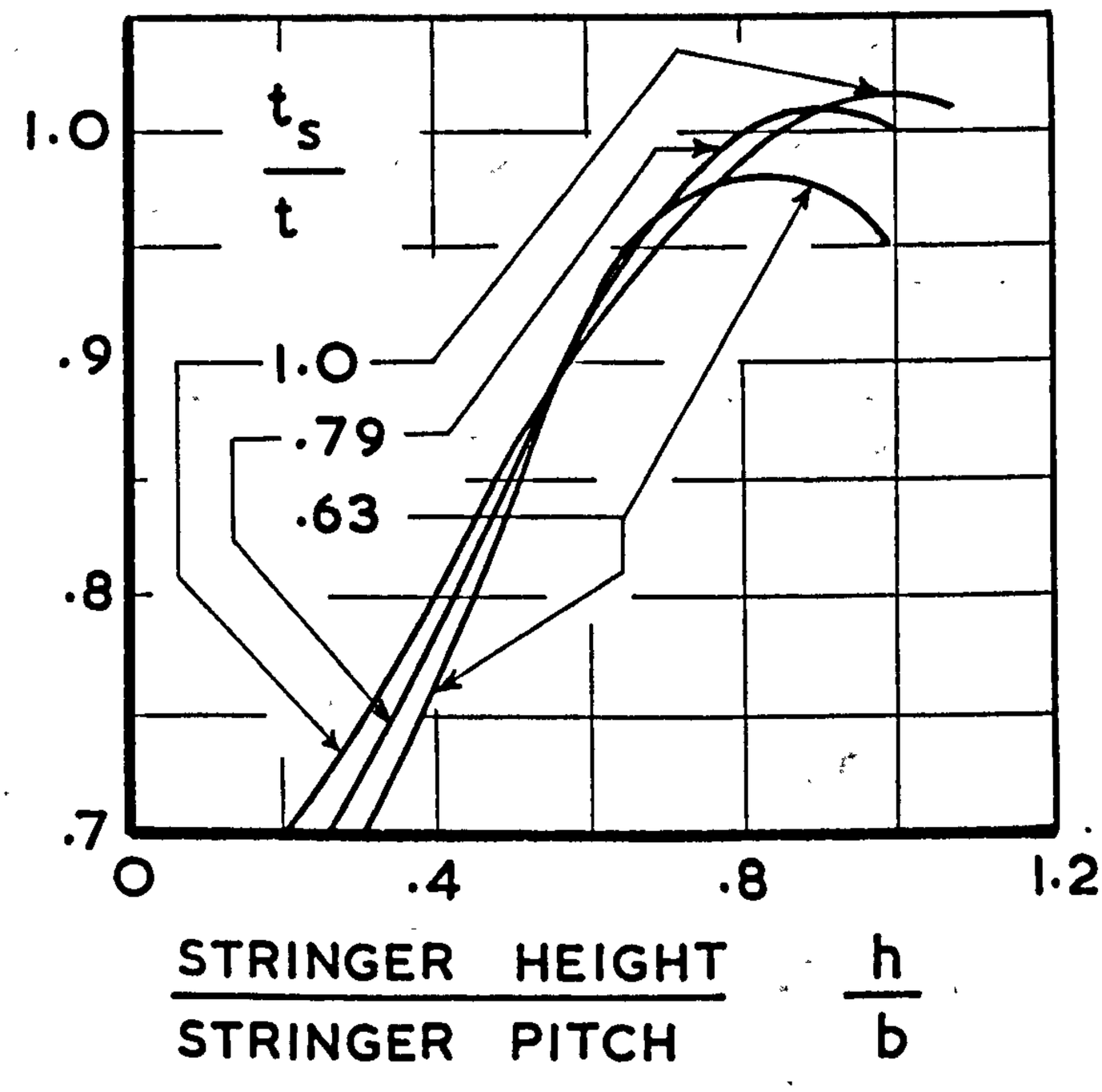


SOURCE : REF. 14

FIG. 3.3 THE BRAZIER LOADING APPLIED TO THE WING RIBS

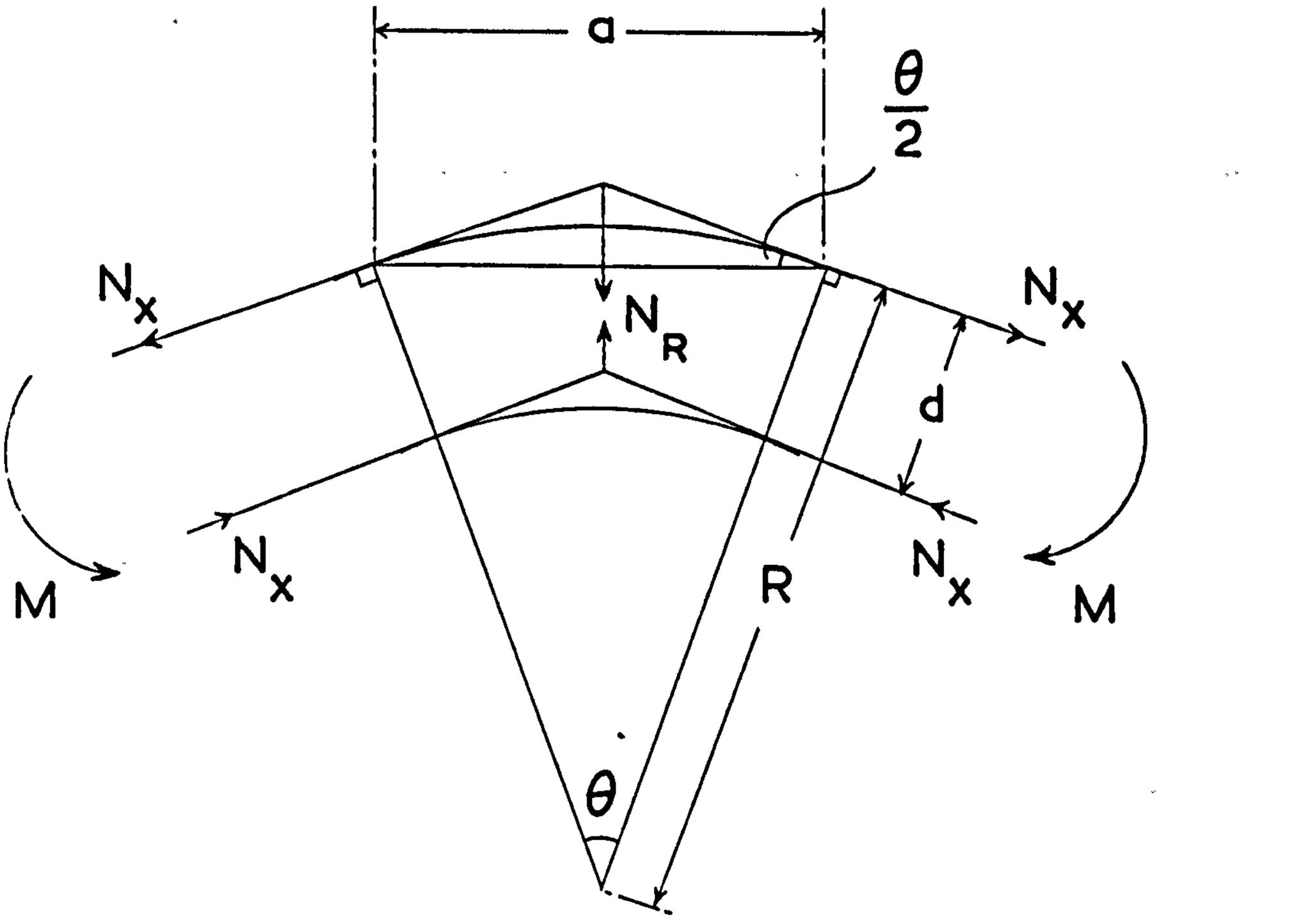


FIG. 3.4 THE RIB THICKNESS SPECIFIED BY THE STRUCTURAL DESIGN EQUATIONS

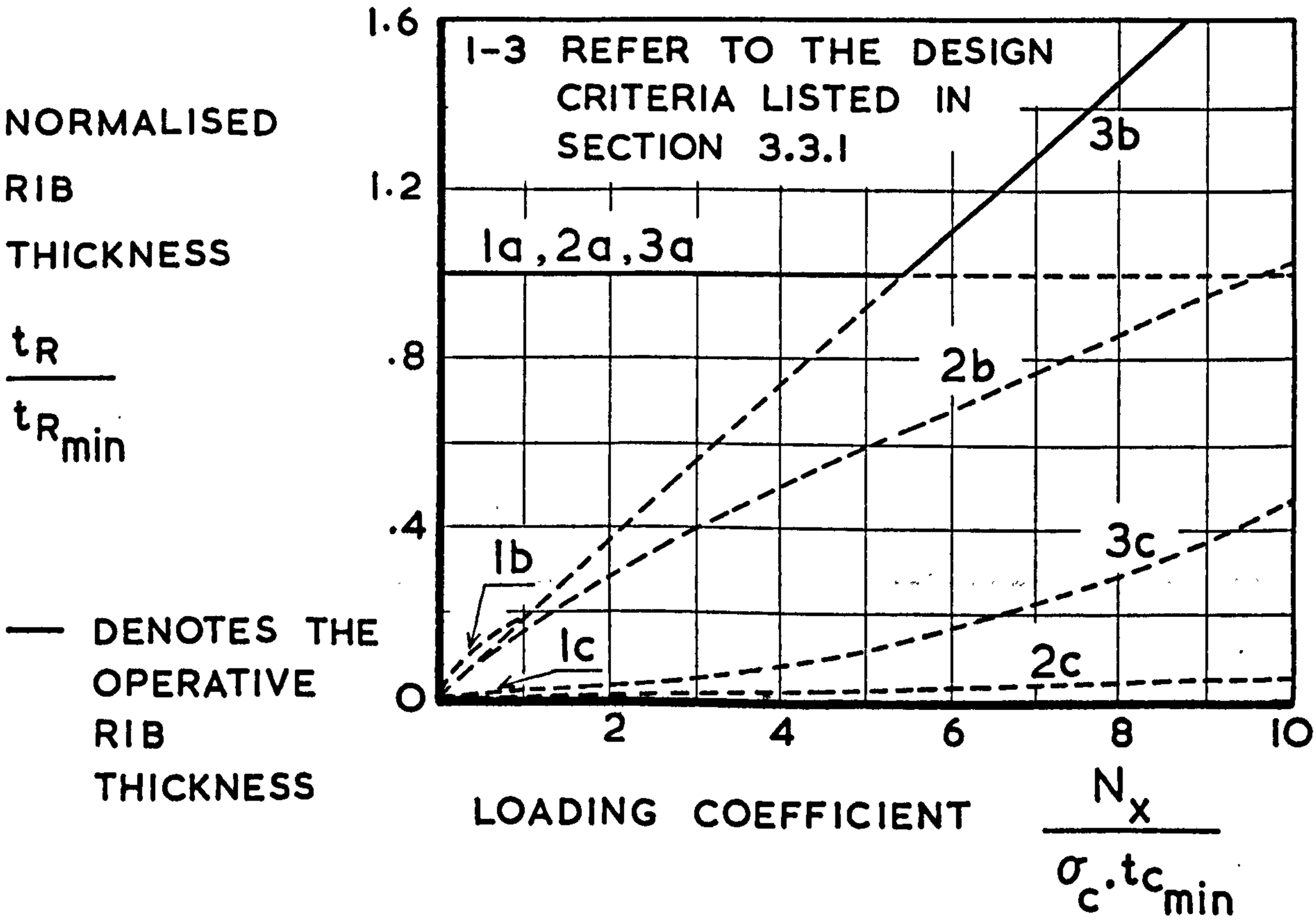

FIG. 3.5 THE RIB PITCH SPECIFIED BY THE STRUCTURAL DESIGN EQUATIONS

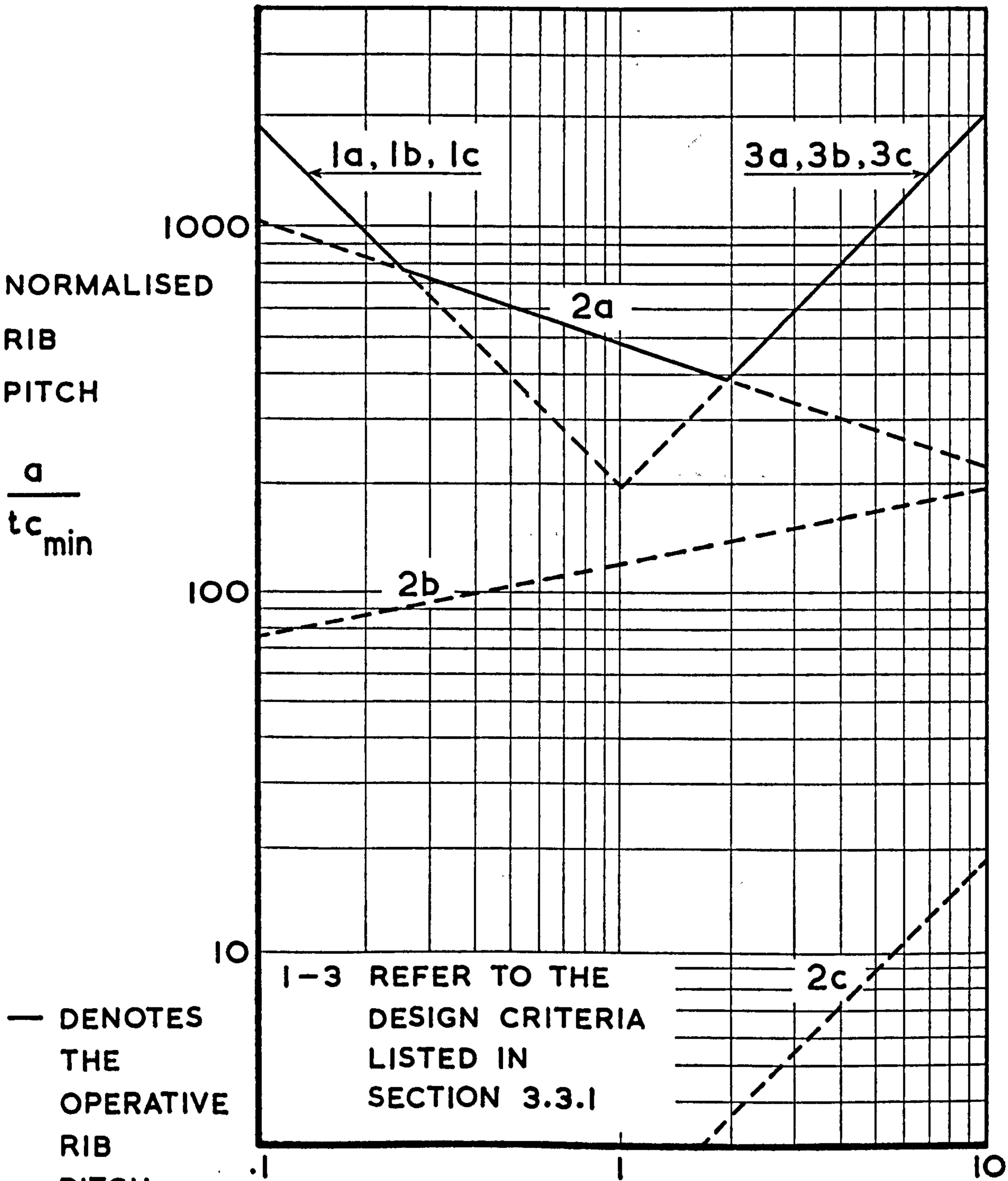

FIG. 3.6 THE COMPRESSION COVER THICKNESS SPECIFIED BY THE STRUCTURAL DESIGN EQUATIONS

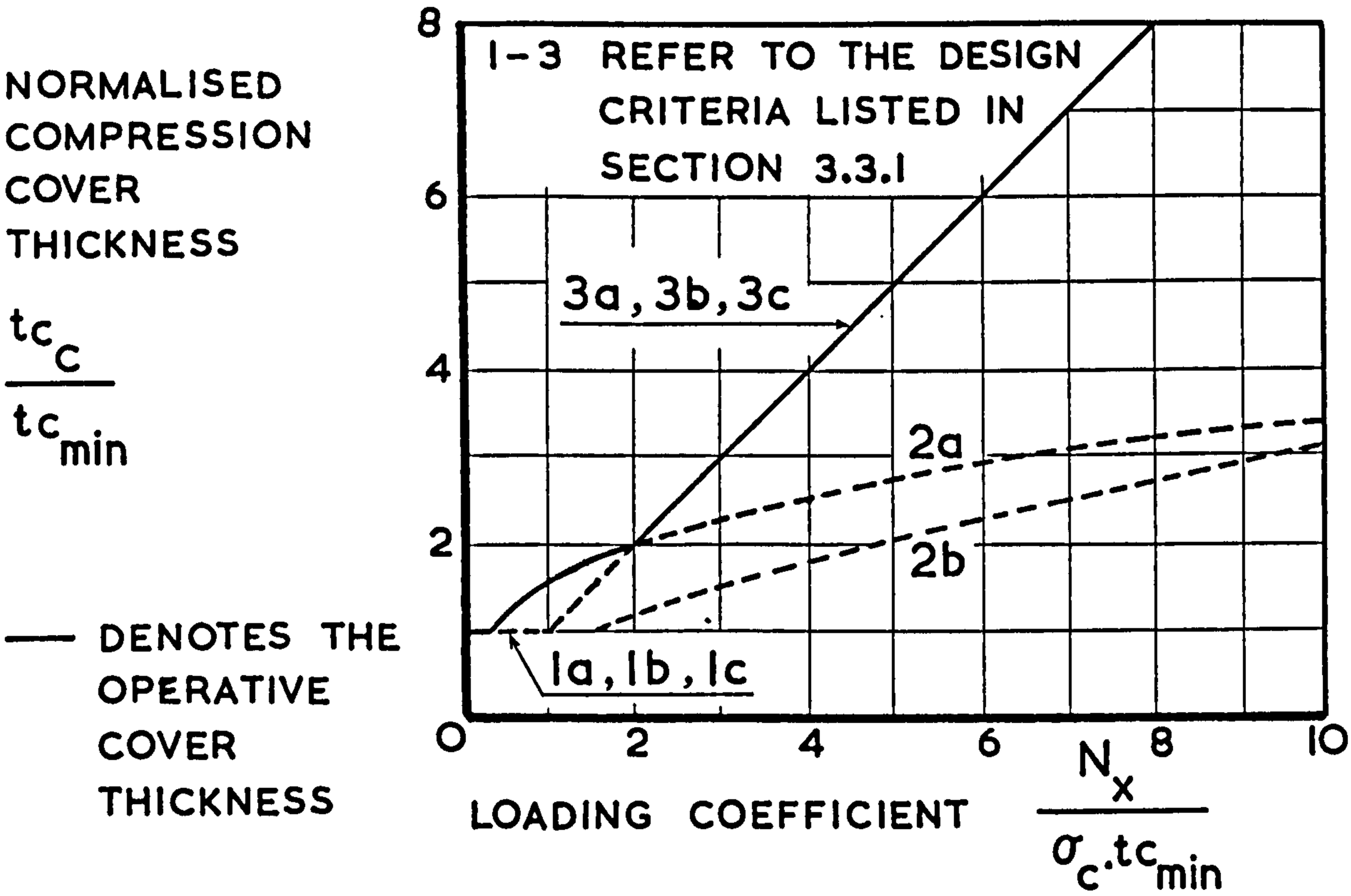


FIG. 3.7 THE TENSION COVER THICKNESS SPECIFIED BY THE STRUCTURAL DESIGN EQUATIONS

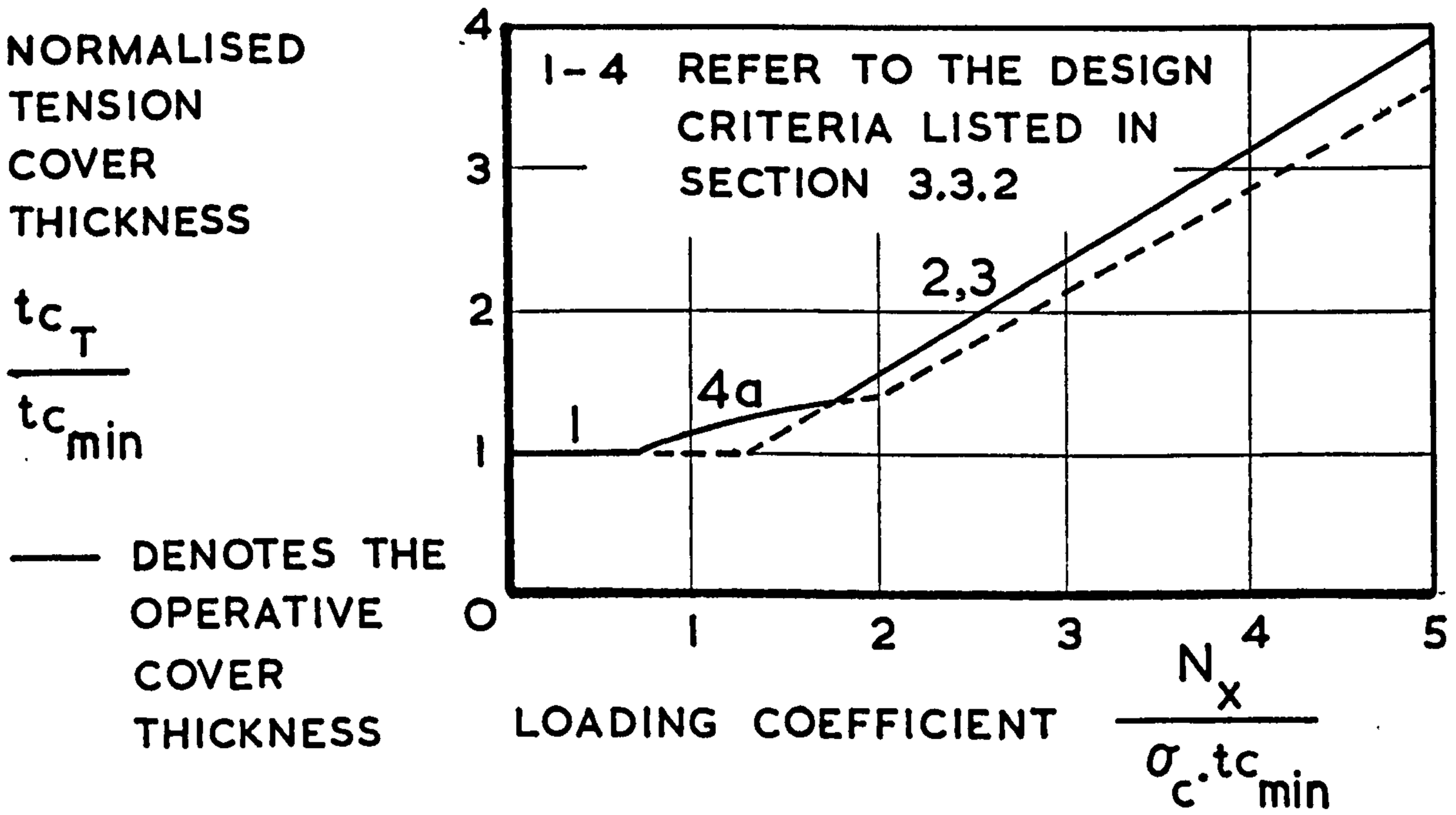

# A COMPARISON OF THE MAIN BOX DIMENSIONS FOR THE TWO STRUCTURAL MATERIALS

FIG. 3.8 THE RIB THICKNESS

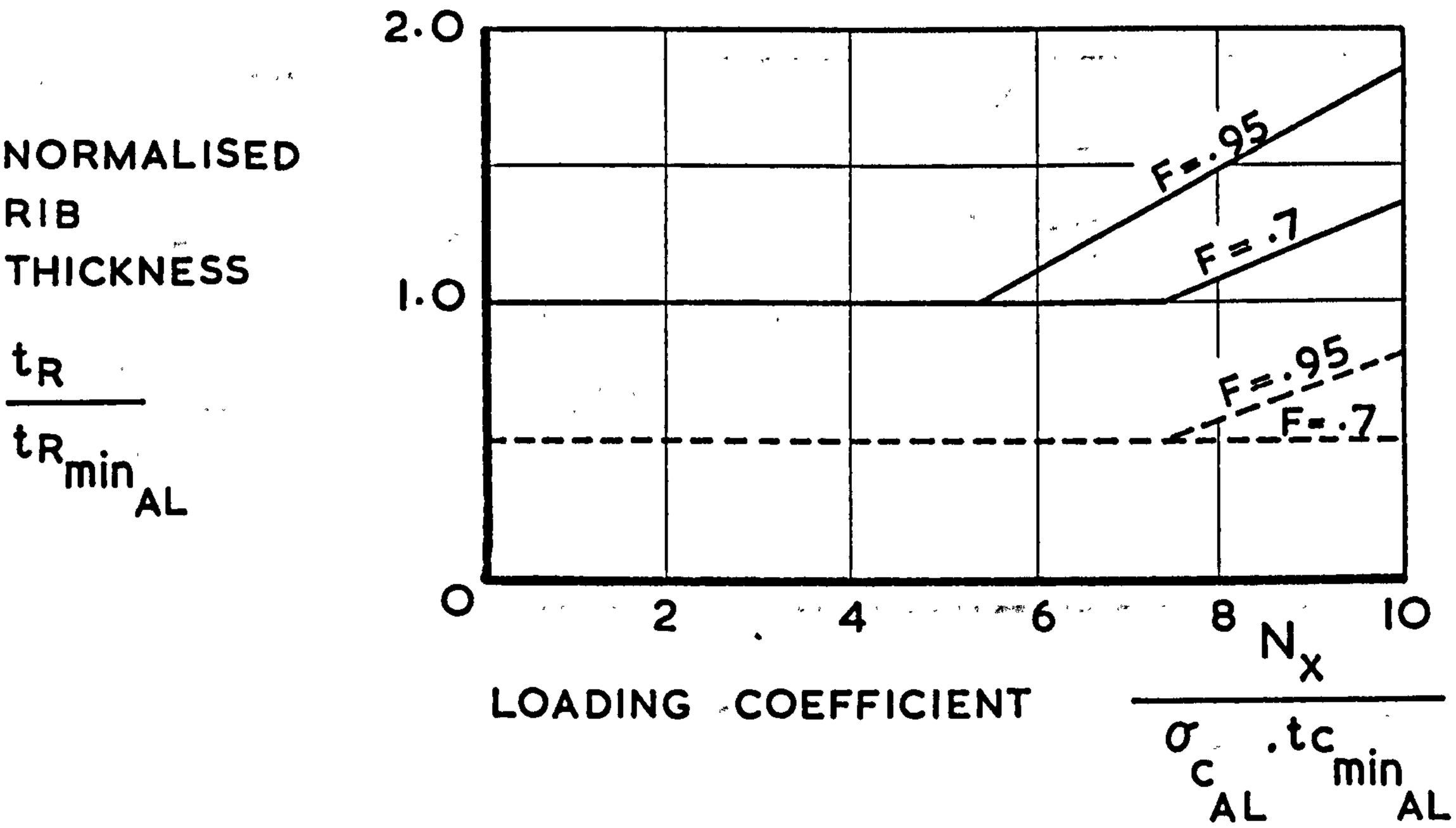


FIG. 3.9 THE RIB PITCH

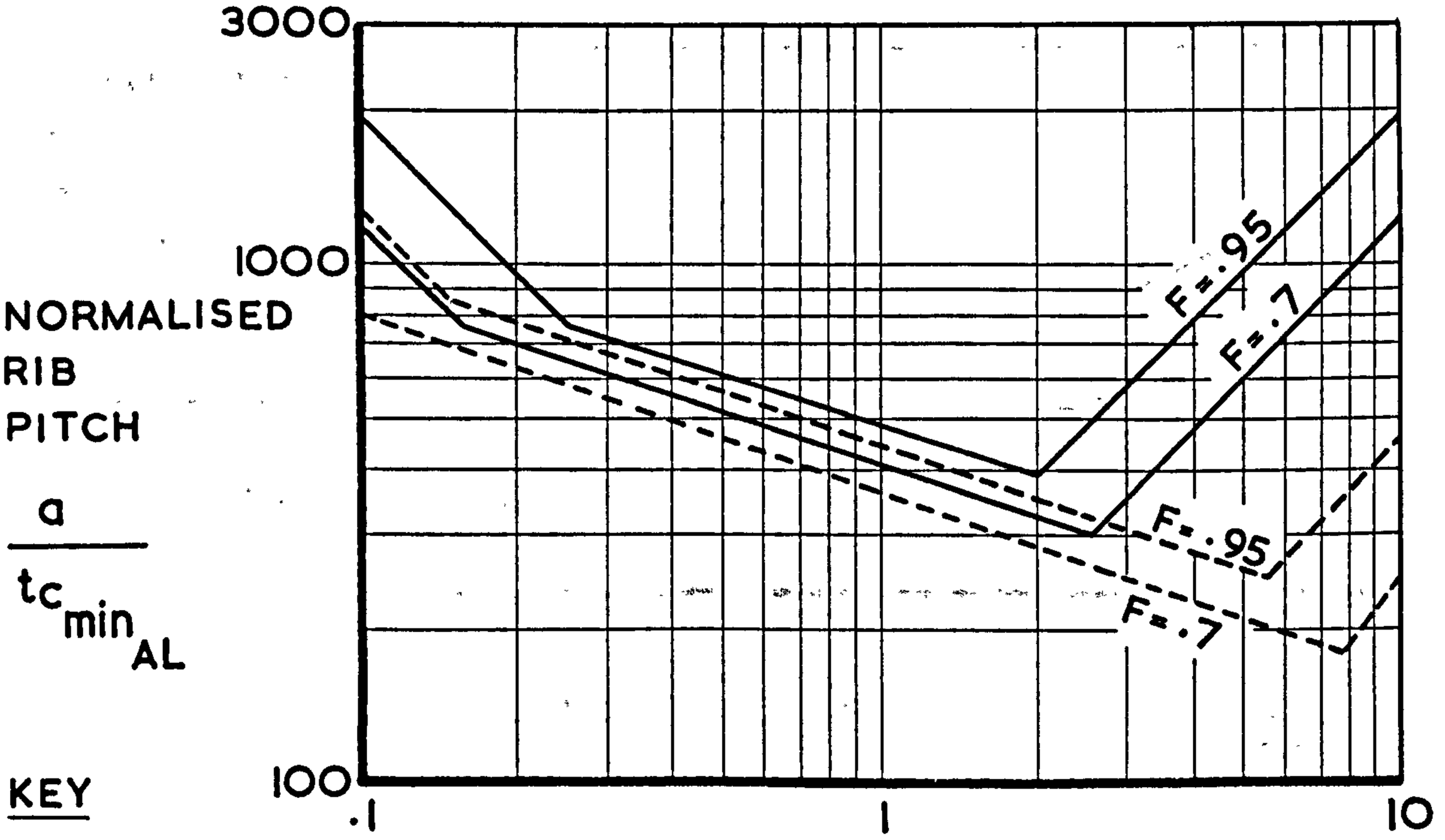

# A COMPARISON OF THE MAIN BOX DIMENSIONS FOR THE TWO STRUCTURAL MATERIALS

FIG. 3.10 THE COMPRESSION COVER THICKNESS

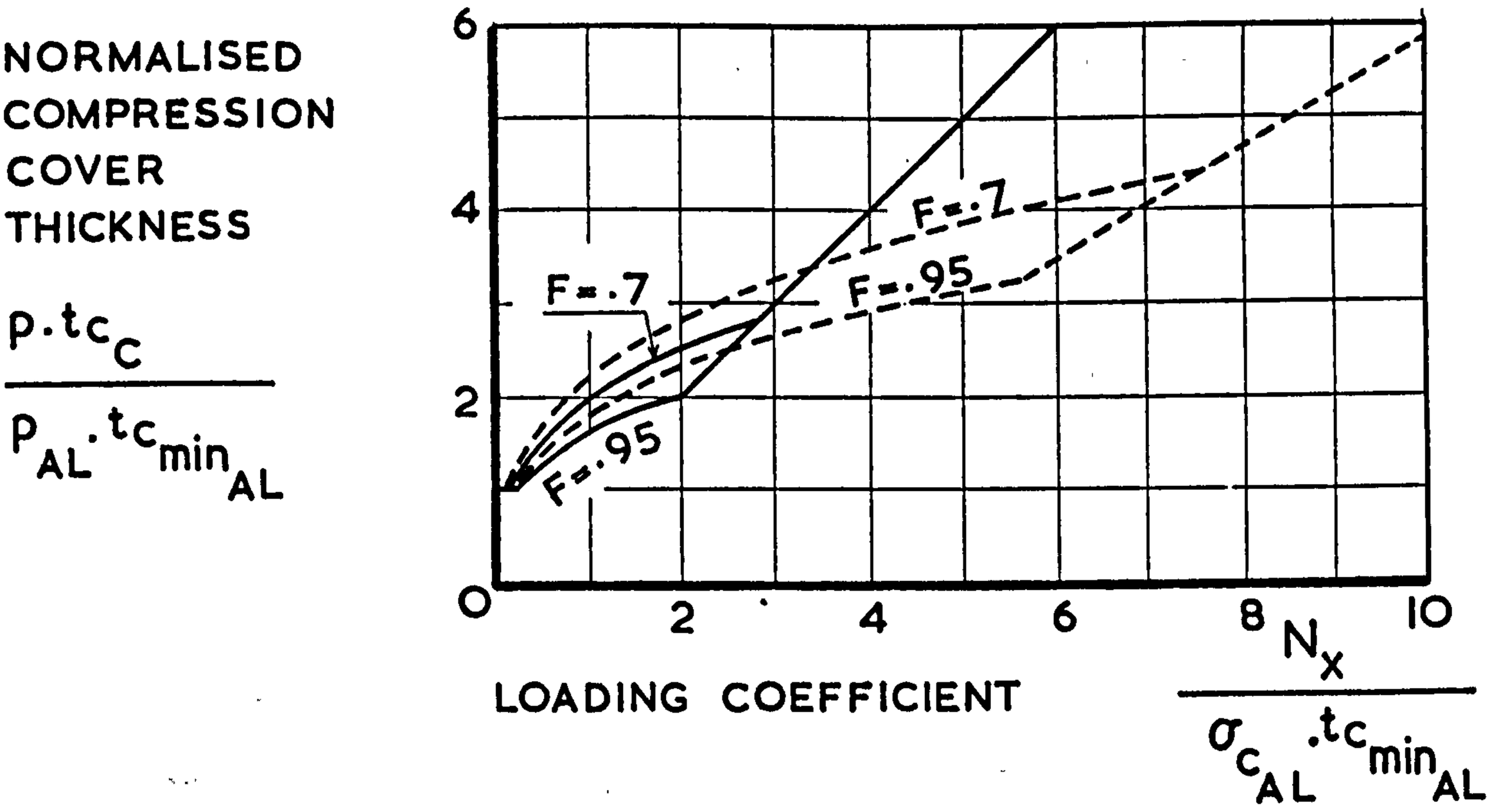


FIG. 3.11 THE TENSION COVER THICKNESS

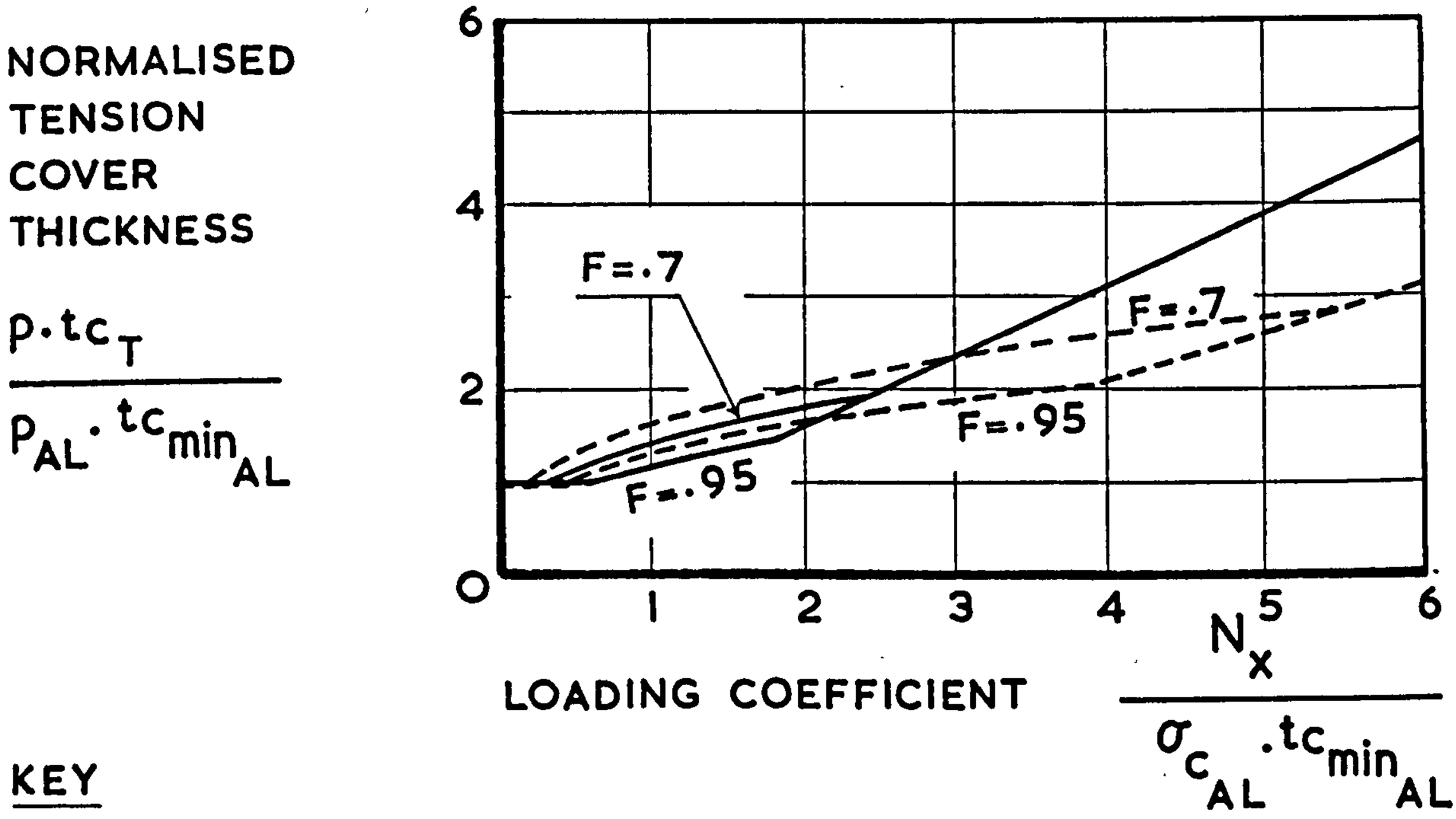


KEY

——— ALUMINIUM ALLOY

---- TITANIUM ALLOY

# C H A P T E R  4

# THE DEFINITION OF THE COST MODEL

## 4.1 Introduction

An essential feature of the design process was the definition of a standardised cost model governing the allocation of costs to each structural system. The cost model selected for the specimen structure allowed a realistic comparison of the costs of alternative structural systems to be made.

The cost $C$ of each system consisted of the following cost elements:

i) raw material cost $C_M$,

ii) production cost $C_p$, comprising the direct labour cost plus the overhead allowance for the $200^{th}$ production item,

iii) production learning cost $C_L$, to allow for the initial components which were more costly to produce,

iv) tooling cost $C_T$.

Henceforth the term "unit cost" will represent the summation of these cost elements, where the unit cost $C$ is

$$C = C_M + C_p + C_L + C_T \qquad (4.1)$$

## 4.2 The Composition of the First Cost of an Aircraft

The price at which an airline purchases an aircraft from the manufacturer may be defined as the first cost of the

aircraft. Neglecting any profit, or loss, involved in the transaction, the first cost of an aircraft may be separated into the following cost categories incurred by the aircraft manufacturer:

i) Variable costs:

direct labour cost,

raw material cost,

bought out item cost,

variable production overhead.

ii) Fixed costs:

fixed production overhead,

company overhead.

iii) Launching costs:

research and development cost,

design cost,

tooling cost,

sales cost,

production learning cost.

Fig. 4.1 presents a first cost breakdown for a typical civil subsonic aircraft, obtained from ref. 17, to illustrate the relationship between the cost elements. Since the total launching costs for a given aircraft project can, to a first approximation, be considered independent of the production quantity, the launching cost segment of the aircraft first cost is highly dependent on the proposed production quantity.

A comparison of the cost elements of the unit cost with the aircraft first cost categories indicates several omissions and the re-grouping of certain cost elements, the reasons for which will now be detailed:

i) Bought out item cost

Items not produced by the aircraft manufacturer, but purchased from outside suppliers, form a substantial proportion of the first cost. Typical bought out items include electrical, hydraulic and pneumatic systems, engines and furnishings. Since the analysis was confined to a structural optimisation, the cost of brought out items was omitted from the unit cost specified by the cost model.

ii) The allocation of overheads

Overheads can be considered in three categories, as follows:

a) variable production overheads

Variable production overheads comprise those costs which can be charged against specific processes, including the power consumption and depreciation costs of machines.

b) fixed production overheads

The fixed production overheads comprise those indirect costs, involved in production, which are difficult to allocate to specific processes. The dominant cost items forming the fixed production overheads include heating and lighting costs, the factory rent, the cost of production control departments and the cost of the indirect materials involved in production, especially paperwork costs.

c) Company overheads

Company overheads include the cost of rents, rates and insurance of general offices, the salaries of office workers, advertising and legal costs, and bank charges.

A widely used method of fixed overhead allocation involves the application of a fixed overhead rate to the direct labour time expended on each production process, this being termed the direct labour hour rate method(18).

In general, it is preferable to allocate the variable production overheads to the specific processes involved. However, it is common practice in industry to cover the variable production overheads by increasing the direct labour hour rates and treating the variable overheads as part of the fixed overheads, because of the difficulty of determining appropriate variable rates.

The above method of overhead allocation was used in the cost model because of the lack of information on variable rates. A total overhead rate of 350 per cent was applied to the direct labour time of each process, giving an absolute cost of £3 per direct labour hour, at 1970 cost values. The overhead rate of 350 per cent emphasises the great influence overheads have on determining the magnitude of production costs, the above

values being typical for the aircraft industry at the present time.

iii) Launching costs

With the exception of production learning costs and tooling costs, which will be dealt with separately, it was assumed that each design concept had received the requisite amount of launching cost funding to bring them to the stage of being producible using the production schemes detailed in Chapter 5, prior to the commencement of the cost analysis. This approach was adopted because of the difficulty of determining variable launching costs applicable to the different design concepts.

In general launching costs are a function of aircraft size, technological innovation and complexity.

## 4.3 The Composition of the Unit Cost

As defined by equation (4.1), the unit cost $C$ of each system is

$$C = C_M + C_p + C_L + C_T \qquad (4.1)$$

Each element of the unit cost will now be discussed.

### 4.3.1 The specification of the material cost

The material cost $C_{M_c}$ of each structural component included in a system is

$$C_{M_c} = \frac{C_s \cdot W_c}{U_F} \qquad (4.2)$$

where $C_{M_c}$ = component material cost (£),

$U_F$ = material utilisation factor,

$C_s$ = raw material cost per unit weight (£/lb),

$W_c$ = component weight (lb.).

The total material cost $C_M$ for the system is given by the summation of the component material costs $C_{M_c}$.

The material utilisation factor, which is an important factor in equation (4.2), expresses the percentage of the basic raw material remaining in the finished structural item. The efficiency of utilisation of the material is highly dependent on the production method employed. For example, an integrally stiffened skin, machined from a billet, may have a material utilisation factor of 10 per cent, or less. A utilisation factor of only 7 per cent was achieved for the example of the skin plank quoted in ref. 19. Typical values of the material utilisation factor for aluminium alloy built up structures range from 20 to 50 per cent.

In this study a utilisation factor of 50 per cent was applied to both aluminium alloy and titanium alloy structural systems. This figure is representative of present day structures subjected to careful production design.

The raw material cost per unit weight values used in the analysis were based on quotations issued by the leading suppliers of raw materials to the aircraft

industry. Care was taken to reflect the variations of material cost per unit weight with changes in material gauge.

The cost of titanium alloy material has been reduced considerably over the last decade and will probably be subjected to further cost reductions in the near future, with the advent of new material production techniques to meet an increasing demand. Hence it is very difficult to determine titanium alloy material costs which are applicable over any period of time.

The aluminium alloy and titanium alloy material cost per unit weight values used in the analysis are presented on Table 4.1.

### 4.3.2 The specification of the production cost

The production cost of each structural system was composed of the direct labour cost plus a proportion of the total overheads.

A series of production cost equations were evolved to facilitate the evaluation of the direct labour time required to produce each structural system. As described in section 4.2, a cost of £3 per direct labour hour was applied to the direct labour time to give the production cost.

The production cost equations were based on the dominant operations of the relevant production method described in Chapter 5, with appropriate scale factors being applied to give realistic costs. The process of

solving the production cost equations was expedited by the development of computer programs to undertake the task. The production cost equations, together with the appropriate computer program listings and the values of the parameters used in the equations, are presented in Appendix 2.

The values of the production process rates were based on the values experienced in industry. The production rates were quoted for the $200^{th}$ production item, when the learning curve had flattened out. The method of allocating the learning costs incurred by items up to the $200^{th}$ will be defined in the next section.

### 4.3.3 The specification of the production learning cost

It is an accepted principle in the aircraft industry that the time taken to produce structural items decreases with increasing production quantity. This phenomenon is known as the learning effect and its influence on aircraft production costs was first studied by T. P. Wright.[20]

Important factors which give rise to the reduction in production cost with increasing production quantity include:

i) job familiarisation of the operatives due to the repetition of operations,

ii) improvement in production methods, program planning and production management,

iii) an improved parts supply system,

iv) development of more efficient tooling.

The cost $C_n$ of producing the $n^{th}$ item is defined by the unit learning curve equation[21] as

$$C_n = C_1 \cdot r^{\frac{\log_e n}{\log_e 2}} \qquad (4.3)$$

where $C_1$ = the production cost of the first item (£),

$r$ = learning factor.

In this study a learning factor $r$ having a value of 0.8 was assumed. The variation of cost with production quantity for the above learning factor value is presented in fig. 4.2.

As mentioned in section 4.3.2, the production rates used in this investigation were based on the $200^{th}$ production item. The shaded area of fig. 4.2 represents the learning costs incurred by items up to the $200^{th}$. This additional cost due to learning was treated as a launching cost and was apportioned equally between the 200 items, in the following manner:

The total additional cost $C_A$ due to learning is

$$C_A = \int_1^{n_1} C_1 \cdot r^{\frac{\log_e n}{\log_e 2}} \cdot dn - n_1 \cdot C_1 \cdot r^{\frac{\log_e n_1}{\log_e 2}} \qquad (4.3)$$

The solution of the integral of equation (4.3), presented in appendix 4, gives the total additional cost due to learning as

$$C_A = \left[ \frac{C_1 \cdot n \cdot r^{\frac{\log_e n}{\log_e 2}}}{\frac{\log_e r}{\log_e 2} + 1} \right]_1^{50} - n_1 \cdot C_1 \cdot r^{\frac{\log_e n_1}{\log_e 2}} \qquad (4.4)$$

The learning cost $C_L$ per item is

$$C_L = \frac{C_A}{n_1} = \frac{1}{n_1} \cdot \left[ \frac{C_1 \cdot n \cdot r^{\frac{\log_e n}{\log_e 2}}}{\frac{\log_e r}{\log_e 2} + 1} \right]_1^{n_1} - C_1 \cdot r^{\frac{\log_e n_1}{\log_e 2}} \qquad (4.5)$$

For a learning factor $r$ of 0.8 and an $n_1$ value of 200 items, the learning cost $C_L$ per item given by equation (4.5) is

$$C_L = 0.0795 \cdot C_1 \qquad (4.6)$$

The learning cost $C_L$ per item, expressed in terms of the production cost $C_{200}$ of the $200^{th}$ item, is given by substituting equation (4.3) in (4.6), where

$$C_L = 0.44 \cdot C_{200} \qquad (4.7)$$

Using the result given in equation (4.7), the production cost element of the unit cost for each design was increased by 44 per cent to allow for production learning costs.

### 4.3.4 The specification of the tooling cost

The costs of the jigs and tools required to produce an airframe are influenced by many factors. The planned aircraft production quantity determines the level of

sophistication of the tooling to be adopted. Tooling of great sophistication may help to reduce the production time a component spends in a jig, at the expense of an increased tooling cost.

The time a component spends in a jig imposes a constraint on the production rate which the jig is capable of sustaining. If a jig cannot achieve the planned rate of production, duplication of jigs may have to be undertaken, with the resulting tooling cost increases, to avoid delays in the airframe production program. Thus the rate of production, as well as the total number planned, affects the tooling costs.

Tooling costs were amortised over the planned production quantity of 200 items specified in the cost model. It was assumed that all jigs and tools were capable of sustaining a rate of production of 2 items per month.

The estimates of the jig and tool costs for the aluminium alloy structures, were developed with the assistance of the Tooling Cost Estimating Department of Hawker Siddeley Aviation Ltd. The estimates covered the cost of tooling for detail manufacture, including drill bars and rubber press tools, sub assembly tooling, including tack riveting fixtures, and the final assembly tooling, comprising the fixture in which the box beams were completed.

The exact tooling requirements of the titanium alloy systems were difficult to ascertain. For this reason, the tooling cost estimates for the titanium

alloy systems were developed by applying a relative cost factor to the estimates for the aluminium alloy systems. A relative cost factor having a value of 3, as recommended in ref. 11, was used.

TABLE 4.1 Raw material cost per unit weight values

| Material gauge (s.w.g.) | 12 | 14 | 16 | 18 | 20 | 22 | 24 | 26 | 28 |
|---|---|---|---|---|---|---|---|---|---|
| Cost per unit weight of aluminium alloy material (£/lb.) | 0.27 | 0.28 | 0.29 | 0.30 | 0.33 | 0.37 | 0.40 | 0.45 | 0.48 |
| Cost per unit weight of titanium alloy material (£/lb.) | 6.07 | 6.35 | 6.70 | 7.00 | 7.50 | 8.10 | 8.76 | 9.90 | 10.71 |

FIG. 4.1 A BREAKDOWN OF THE FIRST COST OF A TYPICAL SUBSONIC CIVIL AIRCRAFT

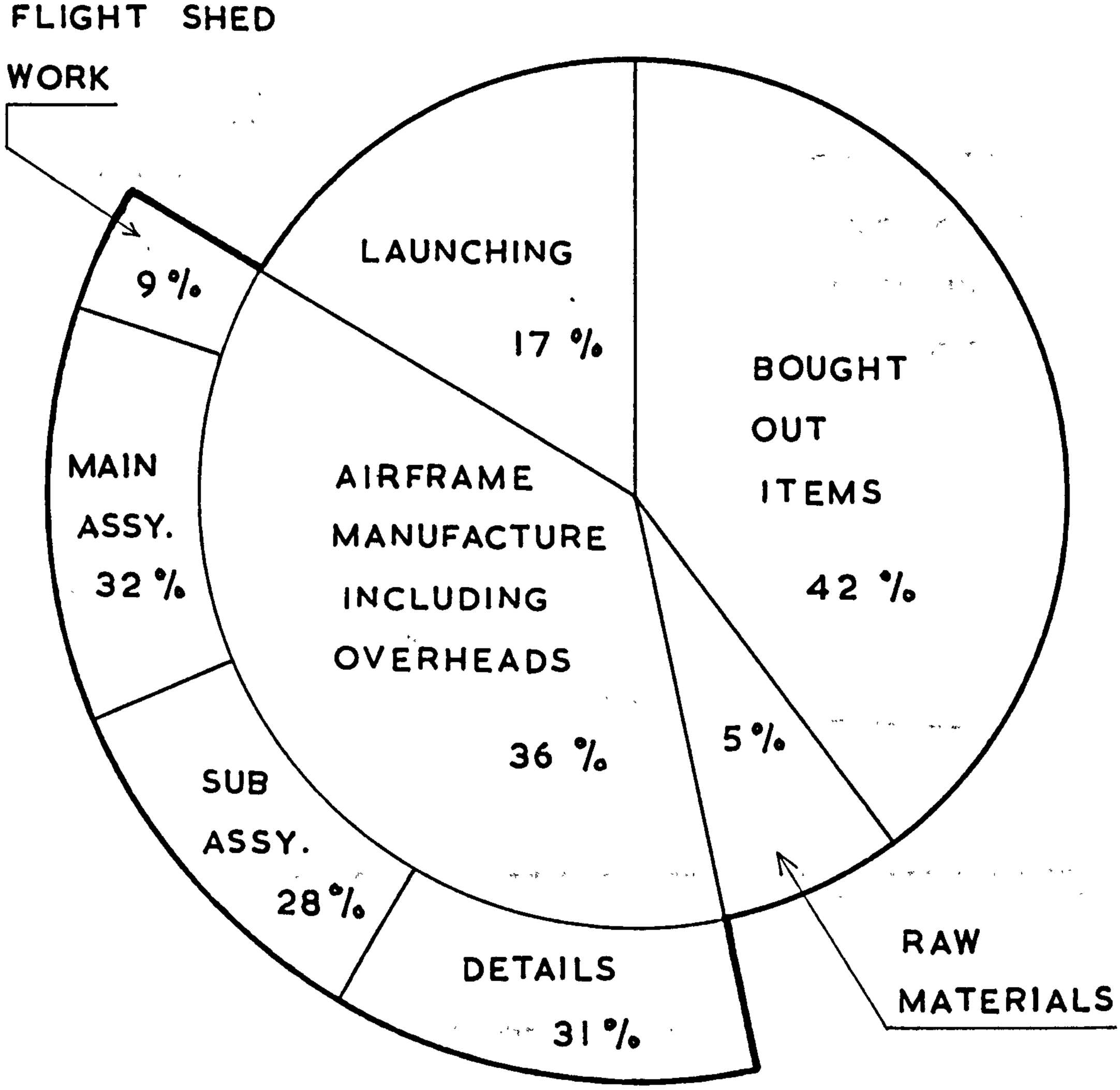


BASED ON THE COST BREAKDOWN PRESENTED IN REF. 17

FIG. 4.2 THE LEARNING CURVE FOR A LEARNING FACTOR r = 0·8

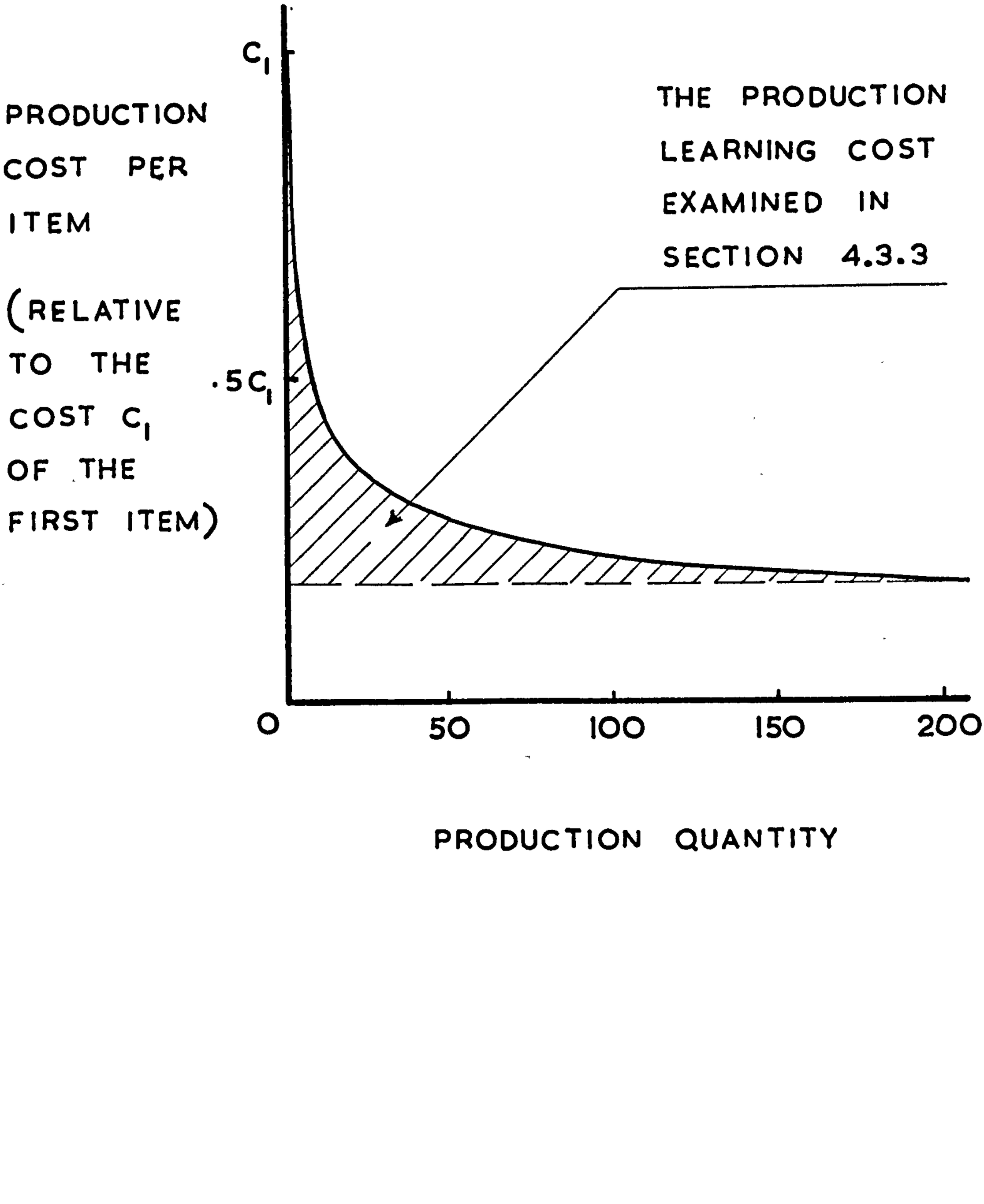

# C H A P T E R  5

# A DESCRIPTION OF THE ALTERNATIVE STRUCTURAL SYSTEMS

## 5.1 Introduction

The design process was used to compare alternative structural systems made from two structural materials and employing various production methods.

As an example of existing airframe construction techniques, structural systems of riveted construction and employing aluminium alloy material, were examined.

A titanium alloy structural system of welded construction was analysed to determine if any economic benefits were to be gained by resorting to new materials and new production methods for airframe applications. The term "new" is used relative to the accepted practices of the present time, where aluminium alloy is the dominant structural material and mechanical fastening is the usual method of attachment for most aircraft structures.

A description of the producibility constraints imposed, the production method employed, and the physical characteristics of each structural system, is now given. The nomenclature used in the production method descriptions for the component parts of the specimen structure is defined in fig. 5.1.

## 5.2 The Aluminium Alloy Structural Systems

The properties of the aluminium alloy material used in the weight analysis are given in Table 3.1.

The aluminium alloy structural systems investigated were of all-riveted construction and consisted of the following component parts:

i) upper and lower covers having skins stabilised by Z section stringers,

ii) front and rear spars having angle section booms and webs stiffened by angle section stiffeners,

iii) transverse ribs having flat webs stiffened by Z section stiffeners.

### 5.2.1. The producibility requirements

The stringers were attached to the skins of the upper and lower covers using countersink head rivets to satisfy the design requirement, introduced in section 3.4, demanding a flush finish.

A minimum gauge of 18 s.w.g. is required for the use of cut-countersinking of skins to accommodate $\frac{1}{8}$" diameter rivets. At low values of the applied end loading the structural design equations of section 3.3 may indicate a skin thickness less than this minimum value. For example, in the case of an aluminium alloy cover having the maximum efficiency factor value of 0.95 attainable from the Z stringer configuration, the critical loading value is 5640 lb/in for the design values presented in Table 3.1.

Producible cover designs may be achieved at load levels below the critical loading level by:

i) Chemically etching an 18 s.w.g. skin to the required thickness and leaving lands for the

attachment of the stringers using cut-countersink techniques. The introduction of lands leads to a weight penalty compared to the ideal structure.

ii) Employing spin dimpling to achieve a flush finish without the weight penalty of the stringer land

The following producibility requirements were applied to all designs:

i) the ribs were attached to the skins if the distance $x$ between stringers, illustrated in fig. 5.2, was greater than 1.5 in.,

ii) for riveted attachment to the skin, a minimum value of 0.5 in. for the lower flange width of a $Z$ stringer was assumed,

iii) minimum and maximum values of 0.5 in. and 1.5 in., respectively, were assumed for the rivet spacing, with the spacing being determined by inter-rivet buckling considerations and by the applied load per inch,

iv) the number of ribs $n$ per box beam was given by

$$n = 1 + \frac{l}{a} \tag{5.1}$$

where $l$ = box beam length (in.),

and $a$ = optimal rib pitch given by the structural design equations of section 3.3 (in.).

An integer number of ribs was not fixed since this would unfairly bias certain cases, being solely dependent on the box length assumed in the analysis.

Aluminium alloy structural systems of four design types were examined, as follows:

i) the basic design, which employed automatic riveting of the covers, was operative above the critical loading value,

ii) the chemically etched design, which utilised the same production method as the basic design, was operative below the critical loading value,

iii) the spin dimpled design was operative below the critical loading value,

iv) the component part, consisting of the compression cover and rib elements of the complete structure, which was examined in the sensitivity analysis detailed in Chapter 10.

The production method employed for each type of aluminium alloy structural system is now described.

### 5.2.2 The production method for the basic design of aluminium alloy structural system

The production cost element of the unit cost was based on a manufacturing method which employed the following stages:

i) the detail manufacture stage

The skins of the panels and the ribs, the stringers of panels 1 and 2, the spar boom angles, the spar web stiffeners and the rib stiffeners were cut to size. The stringers and stiffeners, which were to be automatically

riveted in the sub assembly stage, had one tenth of the rivet positions pre-drilled in readiness for the tack riveting operation.
The items, which were to be manually riveted in the sub assembly stage, had all rivet positions pre-drilled.
Stringer cut-outs were routed in the rib blanks and the rib webs were pressed on a rubber press.
Usually, the structural design equations indicated panel 1 and 2 skin thickness of non standard gauges for those structural systems having covers with the maximum efficiency configurations. The chemical etching of standard sheets was undertaken to achieve the requisite skin thickness for maximum structural efficiency. This case differed from the design type described in section 5.2.3, since no weight penalty was involved.

ii) <u>the sub-assembly stage</u>

The stiffeners for the skins of panels 1, 2, 3 and for the rib webs were attached using a Drivmatic automatic riveting machine. These items were manually tack riveted in a sub assembly fixture before transfer to the Drivmatic machine for the automatic riveting process. In the tack riveting process the items were positioned, drilled off and pegged

up progressively. The pegs were then removed, the items deburred and countersunk, if applicable, and protective treatment was applied.

The items were re-positioned, pegged up and manually riveted, the pegs being removed progressively as the riveting proceeded.

The tack riveted assemblies were automatically riveted using the Drivmatic machine, which automatically drills and countersinks the hole, inserts and forms the rivet at a rate which is dependent on stock thickness, material type and rivet diameter.

iii) <u>the final assembly stage</u>

Panels 1, 2, 3 and the ribs were positioned in the final assembly fixture. The rib flange holes, spar boom holes, stringer cleat holes and spar web stiffener holes were drilled off. The items were removed, deburred, and countersunk, if applicable, then cleaned, treated, re-positioned and riveted up complete. Two coats of protective treatment were applied to the assembly and the joints were fillet sealed to give a fuel-tight final assembly.

Panel 4 was positioned to the riveted assembly, and the spar boom holes and web stiffener holes were drilled off. The panel was removed, deburred, cleaned, treated, re-positioned and riveted up using blind rivets. Fillet sealing was carried out in the panel 4 area when the

assembly had been removed from the fixture.

5.2.3 The production method for the chemically etched design

Although chemical etching of the covers was employed in certain instances for the designs described in sections 5.1.2 and 5.1.4, the structural systems of the chemically etched design type differed from systems of other design types in that a weight penalty existed relative to the ideal structure, due to the lands left for the attachment of stringers and ribs. The resulting form of the stringer lands is illustrated on fig. 5.3. Depending on the skin thickness indicated by the structural design equations, chemical etching of the skins of one or both covers had to be undertaken.

The production method employed for the chemically etched design was the same as for the basic design described in section 5.2.2, with the inclusion of the chemical etch operation in the detail manufacture stage.

5.2.4 The production method for the spin dimpled design

Structural systems of the spin dimpled type employed spin dimpling as the countersinking method to achieve the requisite flush finish. The production costs were based on a manufacturing method employing the following stages:

i) the detail manufacture stage

The detail stage was basically the same as in the production method description given in section 5.2.2. However, the use of manual riveting, rather than automatic riveting, for the attachment of stringers to panels 1 and 2 required more pre-drilling and deburring of stringers.

Generally the structural design equations dictated panel 1 and 2 skin thicknesses of non standard gauge for the maximum efficiency configurations. The requisite thicknesses were achieved by chemically etching standard gauge sheets. However, the spin dimpled designs did not suffer from a weight penalty.

ii) the sub-assembly stage

The stiffeners for the skin of panel 3 and for the rib webs were attached using the automatic riveting process described in section 5.2.2. The holes in the stringers and skins of panels 1 and 2 and in the rib flanges were drilled off in a sub-assembly fixture.

The skin, stringer and rib flanges were spin dimpled and the stringers were attached to the skins using countersink rivets to form complete panel assemblies.

iii) the final assembly stage

Panels 1, 2, 3 and the ribs were positioned in the final assembly fixture. The spar boom holes, spar web stiffener holes and the stringer cleat

holes were drilled off. The items were removed, deburred, cleaned, treated, re-positioned and riveted up complete. The rib flanges were countersink riveted to the skins of panels 1 and 2. The attachment of panel 4 to the assembly and the application of sealing compound followed the procedure described in section 5.2.2.

5.2.5 The production method for a component part of the specimen structure

An important aspect of the research program was the examination of the sensitivity of the selection process to the degree of structural completeness. The analysis of a structural component of the specimen structure, namely the compression cover and rib elements, formed a major part of this investigation.

The production cost of the structural component was based on a manufacturing method which employed the following stages:

i) the detail manufacture stage

Items of the structural component common to the complete structure underwent the operations of detail manufacture described in section 5.2.2.

At load levels below the critical loading value, the required skin thickness of the cover was obtained by chemically etching a standard gauge skin and leaving lands for stringer and rib attachment, as described in section 5.2.3.

ii) the sub-assembly stage

The stiffeners for the skin of the cover and for the rib webs were attached using a Drivmatic automatic riveting machine. These items had one tenth of the holes manually tack riveted in a sub-assembly fixture, before being transferred to the Drivmatic machine for the insertion of the remaining 90 per cent of the total rivets by the automatic process described in section 5.2.2.

iii) the final assembly stage

The ribs were attached to the compression cover by riveting through the rib flange and the compression cover skin and through the rib cleats and the webs of the compression cover stringers.

The final assembly stage was performed in the sub-assembly fixture to which rib boards were attached for the location of the ribs. This removed the need for a separate final assembly fixture and so reduced the tooling cost of the structural component relative to the tooling cost of the specimen structure.

## 5.3 The Titanium Alloy Structural Systems

Recently titanium alloys have found increasing applications in aircraft structures. Two factors have given rise to this enthusiasm for titanium alloy as a structural material:

i) The kinetic heating effects, experienced by aircraft having cruising speeds greater than a Mach number of 2.5,

exclude the use of aluminium alloy for airframes due to the degradation of material properties. Titanium alloy, however, retains its properties over a greater temperature range than aluminium alloy, as is illustrated in fig. 5.4 for the variation of ultimate tensile stress with temperature.(22)

The Anglo-French Concorde supersonic transport relies on aluminium alloy as the structural material, since it has a cruise Mach number of 2.01, whereas the now defunct American supersonic transport study, the Boeing 2707, had a design Mach number of 2.7 and was designed mainly in titanium alloy material.

ii) Titanium alloy can provide substantial savings in structural weight at high values of the load level relative to aluminium alloy, as is illustrated in fig. 3.10 for the variation of compression cover weight. This is an important consideration in a weight conscious application, providing the cost penalty incurred is not too severe.

It was with its increasing popularity in mind that titanium alloy was chosen as the structural material to be compared with the dominant structural material in use today, aluminium alloy. The comparison was restricted to the material properties experienced in room temperature conditions, as presented in Table 3.1.

Structural systems of welded construction were investigated, since titanium alloys are readily weldable and yield good quality welds. The advantages of using a welded titanium alloy structure are as follows:

i) welded structures are lighter than mechanically fastened structures, due to the reduction or elimination of joint weights,

ii) welded structures are structurally more sound than structures employing mechanical fasteners, due to the absence of stress raising holes,

iii) it is possible to obtain leak proof structures by seam welding at the fuel tank boundaries.

The titanium alloy structural systems consisted of the following component parts:

i) upper and lower covers having skins stabilised by L section stringers, in the manner illustrated in fig. 5.5,

ii) front and rear spars having angle section booms and webs stiffened by angle section stiffeners,

iii) transverse ribs having flat webs stiffened by L section stiffeners.

### 5.3.1 The production method for the titanium alloy structural systems

A method of producing the titanium alloy structures was devised in the light of existing knowledge. However, the lack of precise information on the production of full size structures in titanium alloy made the production cost, which was based on this production method, susceptible to considerable variations. The proposed production method employed the following stages:

i) the detail manufacture stage

The skins of the panels and the ribs, the stringers

of panels 1 and 2, the spar boom angles, the spar stiffeners and the rib stiffeners were cut to size.

The stiffeners and spar booms of panel 4 were pre-drilled and deburred to cater for the riveted attachment of panel 4 to the assembly, which gave a semi-accessible design compared with a totally welded structure.

Stringer cut outs were routed in the rib blanks and the rib webs were formed in a press having heated dies.

The chemical etching of standard sheets was undertaken to achieve the requisite skin thickness for panels 1 and 2 of these structural systems having covers with the maximum efficiency configurations. The cost of the chemical etch operation for the titanium alloy structures was determined by applying a relative cost factor having a value of 3, as recommended in ref. 11, to the estimates for the aluminium alloy systems.

ii) <u>the sub-assembly stage</u>

The stiffeners for the skins of panels 1, 2, 3 and for the rib webs were attached using the draw welding technique. The stringers and skin of each panel were rigidly clamped in a fixture to which tension was applied. The welding operation was performed by plasma arc welding equipment using either fillet or burn-through welding, depending on the material gauge being welded. The distorsion

of the panels caused by heating was minimised using this procedure.

Prior to welding, the relevant areas were cleaned and had scale removed by means of a suitable treatment process. After welding, the panels were trued up in a combined hot sizing and stress relieving operation.

The rear spar booms were attached to panel 4 and to the front spar booms, and the rib flange angles were attached to panels 1 and 2, using tungsten inert gas (T.I.G.) welding equipment.

iii) <u>the final assembly stage</u>

Panels 1, 2 and the ribs were clamped in the final assembly fixture and the rib webs were T.I.G. welded to the rib flange angles. The panel 4 stiffeners were clamped to the rib webs and to the upper and lower spar booms and were then T.I.G. welded in situ. The skin of panel 4 was clamped to the main assembly and was back drilled through the pre-drilled holes of the stiffeners and the spar booms, access being gained through the open panel 3 area. The clamping pegs were removed and the items were deburred.

The next step in the final assembly sequence involved the attachment of panel 3 to the main assembly. When panel 3 had been suitably clamped in position, it was T.I.G. welded to panels 1 and 2 and to the ribs, access being gained through the open panel 4 area.

The remaining operation was the attachment of panel 4 to the assembly to complete the box structure. Sealant was applied in the relevant areas to give a leak proof structure. The skin of panel 4 was pegged in position and was attached using blind rivets, the pegs being removed progressively.

In the production method given above it was assumed that welding apparatus, capable of performing the tasks outlined, existed. In all welding operations it was assumed that prior to the commencement of welding the relevant areas underwent suitable cleaning and treatment processes, and after welding operations suitable inspection of the weld quality was undertaken.

FIG. 5.1 THE TERMINOLOGY APPLIED TO THE BOX BEAM COMPONENT PARTS

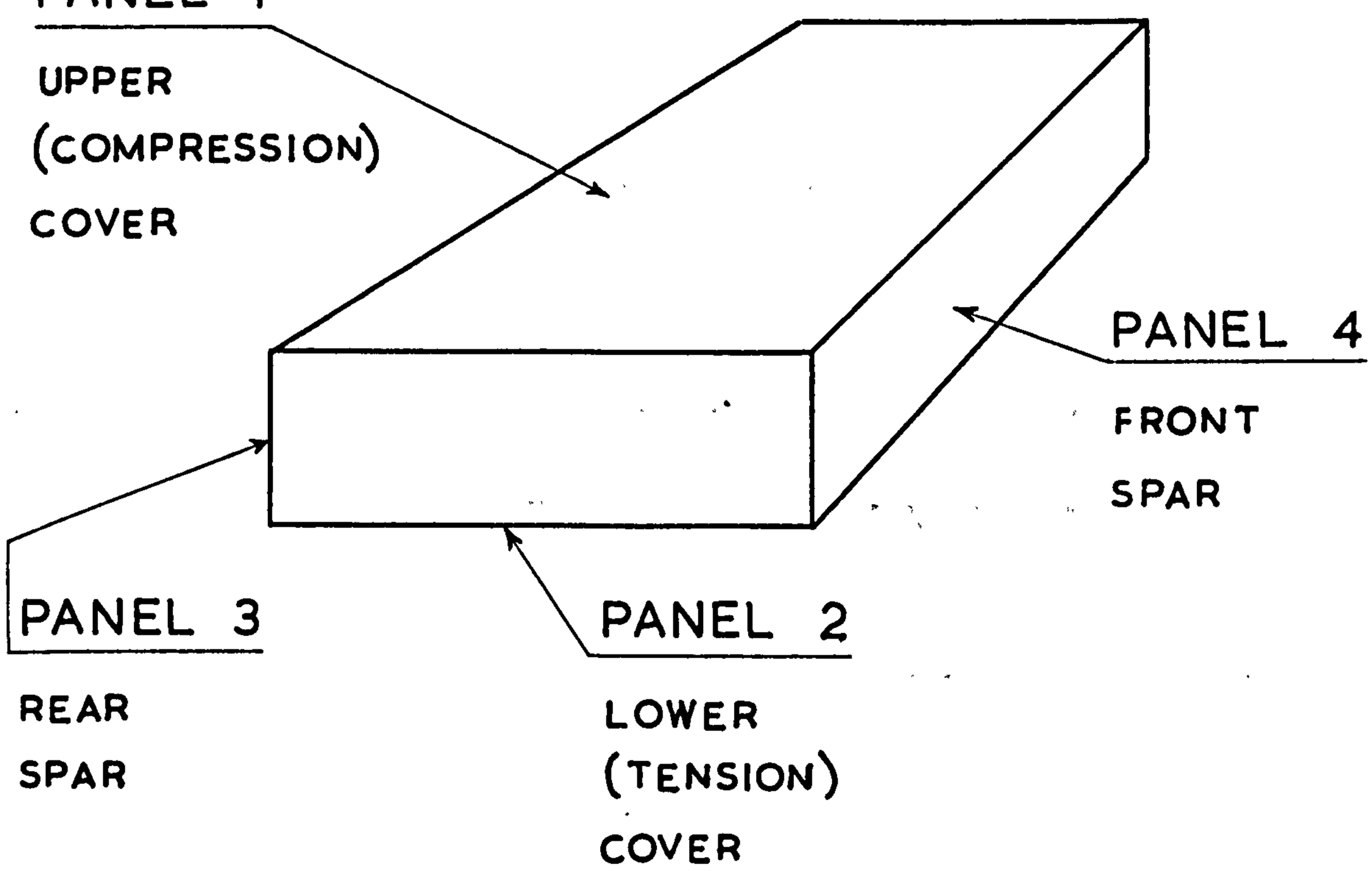


FIG. 5.2 ARRANGEMENT OF THE Z - STRINGER STIFFENED COVER

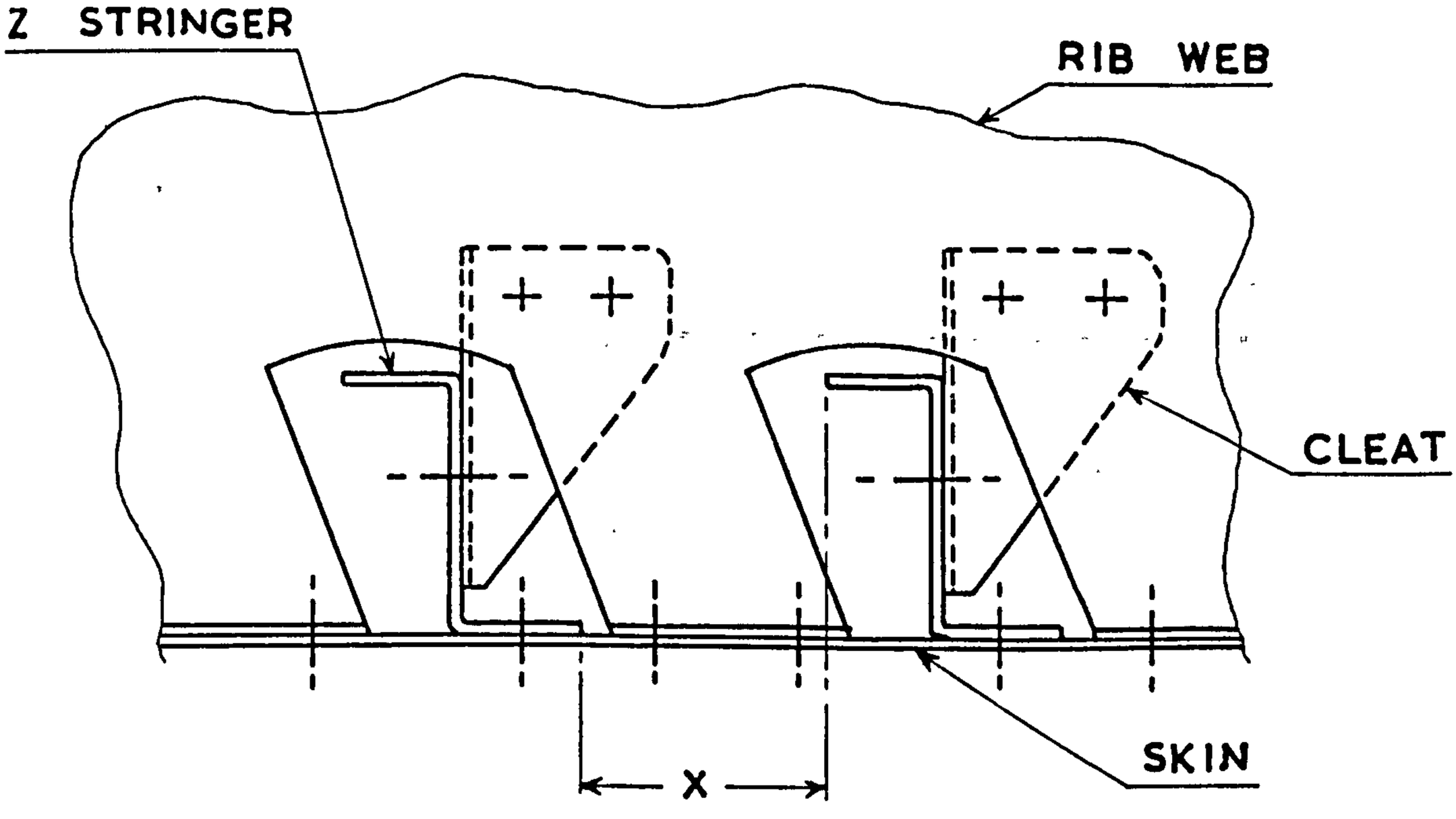

FIG. 5.3 STRINGER LANDS OBTAINED BY CHEMICALLY ETCHING THE SKINS

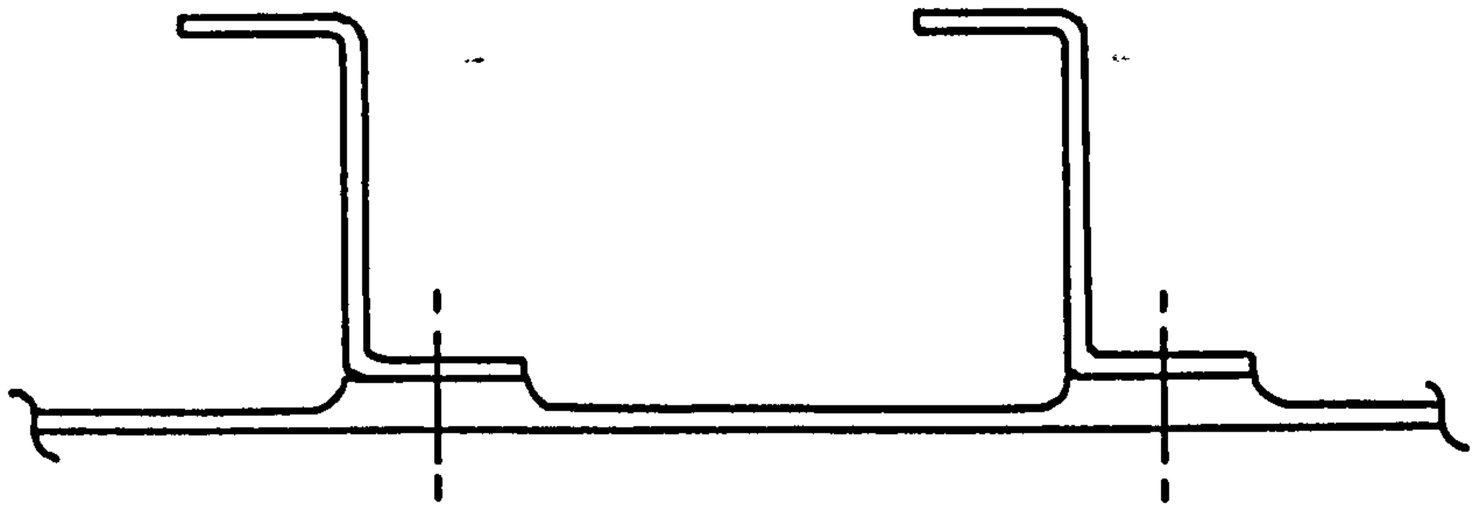

FIG. 5.4 THE VARIATION OF MATERIAL STRENGTH WITH TEMPERATURE

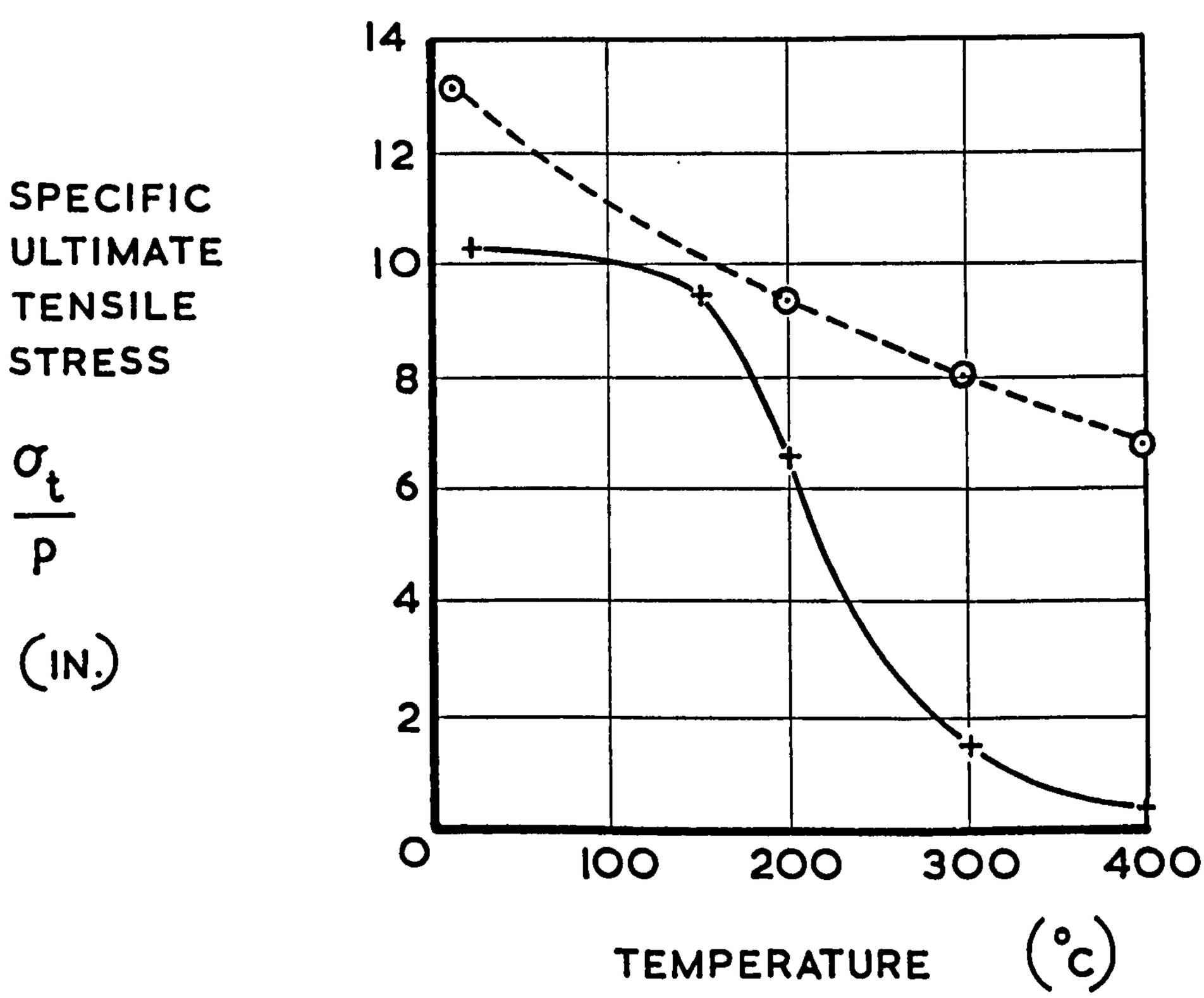

FIG. 5.5 THE ARRANGEMENT OF THE L - STRINGER STIFFENED COVER

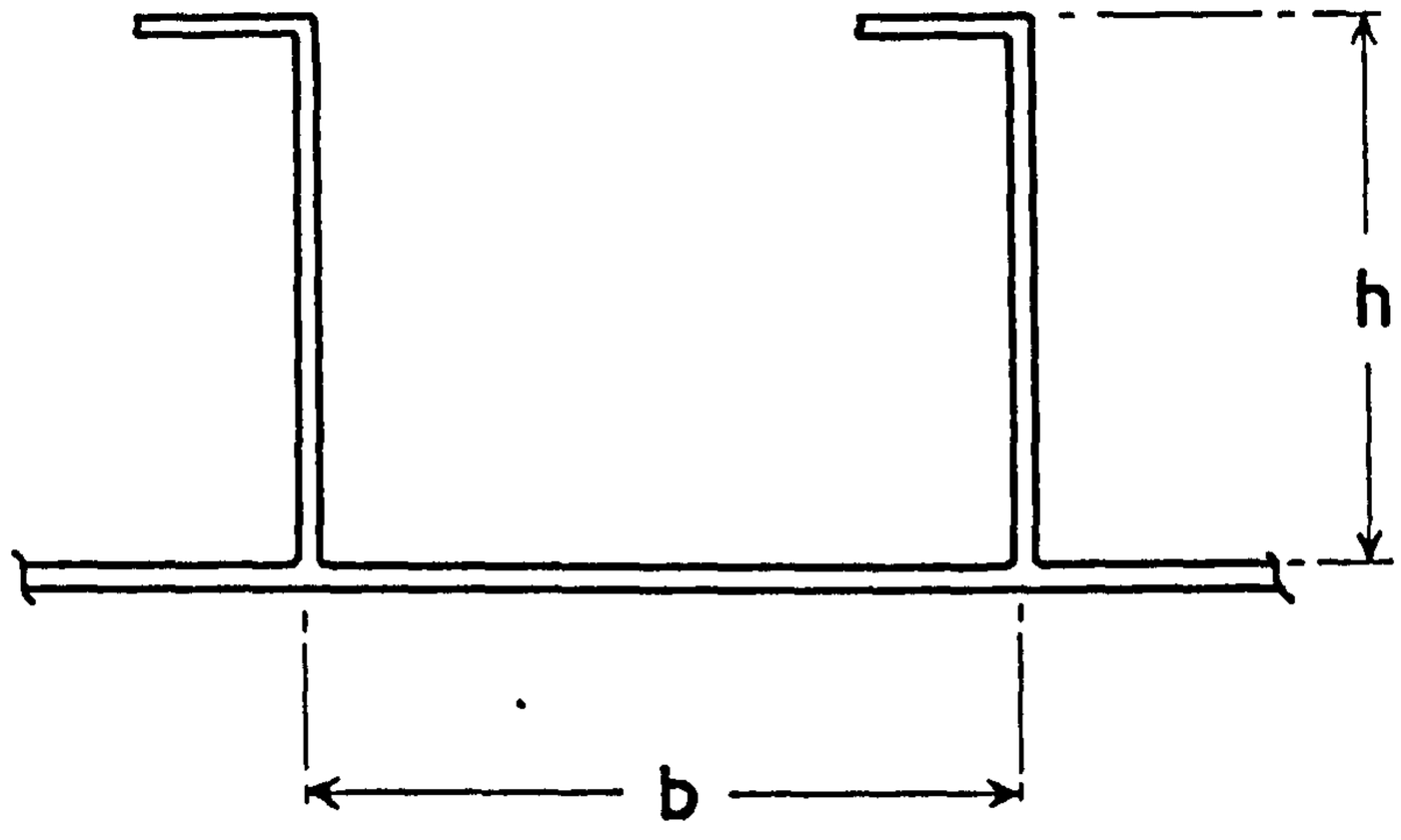

# C H A P T E R  6

# THE PRESENTATION OF THE SYSTEM VALUES

## 6.1 Introduction

The comparison of the alternative structural systems was undertaken using the merit function parameter introduced in section 2.6. The system values, which define the merit function value of a particular system, comprise the structural weight and the unit cost. The structural weight value and the unit cost value of each system were derived in the manner specified by the design model..

The optimisation procedure was carried out at a series of values of the cover end loading which encompass the loading spectrum likely to be encountered in a traverse along a typical aircraft wing, the values being 1,000 lb/in, 2,500 lb/in, 5,000 lb./in. and 10,000 lb./in.

At each value of the cover end loading the structural weight and the unit cost values of each system were evaluated for configurations of the system having varying values of structural efficiency. This procedure enabled the variation of the optimal configuration for a given structural system with global exchange rate to be examined. Structural weight and unit cost values were evaluated for configurations having compression cover efficiency factor values of 0.6, 0.7, 0.8 and 0.95 for the aluminium alloy systems, and 0.7, 0.8, 0.9 and 1.015 for the titanium alloy systems. In each case the upper limit of efficiency factor represents the maximum value attainable from the cover configuration in use,

whereas the lower limit represents the minimum efficiency factor value designated on the appropriate design chart.

## 6.2 The Definition of the Internal Dimensions

The definition of the internal dimensions of each structural system represents the first step in the process of evaluating the structural weight and the unit cost values. The structural design equations specified the internal dimensions of each structural system.

The cover dimensions required for the structural integrity of the aluminium alloy systems and the titanium alloy systems are presented in Tables 6.1 and 6.2, respectively. The arrangement of the skin and stringers to give a cover configuration, having the required value of efficiency factor, was determined using the technique described in section 3.3.5.

The relevant dimensions, specifying the internal geometry of the aluminium alloy and the titanium alloy structural systems, are presented in Tables 6.3 and 6.4, respectively.

## 6.3 The Structural Weight Values of Each System

The structural weight values were derived directly from the structural dimensions given in the previous section. Breakdowns of the structural weight values, for the various designs of aluminium alloy system described in sections 5.2.2, 5.2.3, 5.2.4 and 5.2.5, and for the titanium alloy systems described in section 5.3, are presented in Tables 6.5 and 6.6, respectively.

## 6.4 The Unit Cost Values of Each System

The unit cost of each structural system was derived in the manner specified by the cost model presented in Chapter 4. Breakdowns of the unit cost values, for the aluminium alloy and titanium alloy systems, are presented in Tables 6.7 and 6.8, respectively.

## 6.5 The Cost Per Unit Weight Values of Each System

Straight forward manipulation of the unit cost and the structural weight values enabled the cost per unit weight values of each system to be determined. The cost per unit weight values for the aluminium alloy and the titanium alloy systems are presented in Tables 6.9 and 6.10, respectively. The cost per unit weight variation for each system, presented in fig. 6.1, illustrates two effects, found in practice, which are not widely appreciated, as follows:

i) at each value of the applied end loading, the cost per unit weight value of a system increases as the efficiency of the structural configuration, expressed in terms of an efficiency factor value, increases, since it is generally more expensive to produce a structure having high efficiency and a low weight than a heavier, less efficient structure,

ii) the cost per unit weight value of each system increases with decreasing end loading at a particular value of efficiency factor, since a reduction in end loading implies the use of thinner materials, with the associated production difficulties and higher material costs.

## 6.6 The Normalisation of the Results

With the alternative structural systems having structural weight and unit cost values of varying magnitudes, the form of the results, as evaluated, tended to be misleading. It was decided to normalise the results by dividing throughout by appropriate standard weight and standard cost values to improve the presentation and to aid interpretation.

A different normalisation technique was specified for the comparative analysis of the aluminium alloy and titanium alloy systems compared to the normalisation technique specified for the examination of the sensitivity of the selection process to structural completeness.

The requirements of each case were as follows:

i) the relative magnitudes of the structural weight and unit cost values of each system were of prime importance in the comparative analysis of the aluminium alloy and titanium alloy systems. The normalisation technique was designed to emphasise the comparative nature of the analysis.

The structural weight and the unit cost values for the configuration of the aluminium alloy system having the maximum efficiency factor value were designated as the standard weight value $W_{ST}$ end the standard cost value $C_{ST}$, for each value of cover end loading. As discussed in section 5.2, two design types of aluminium alloy system exist below the critical value of the end loading, namely the spin dimpled design and the chemically etched design. The system values for the

maximum efficiency configuration of the chemically etched design were arbitrarily chosen as the standards to be adopted. The standard weight and standard cost values, used in the comparative analysis, are presented in Table 6.11.

The normalisation of the results for the aluminium alloy and titanium alloy systems were accomplished by dividing the structural weight values, W, and the unit cost values, C, by the appropriate standard values to give normalised weight values, $W_N$, and normalised cost values, $C_N$, where

$$W_N = \frac{W}{W_{ST}} \qquad (6.1)$$

and

$$C_N = \frac{C}{C_{ST}} \qquad (6.2)$$

The normalised weight and cost values for the aluminium alloy systems and the titanium alloy systems are presented in Tables 6.12 and 6.13, respectively.

ii) In the sensitivity analysis the structural weight and the unit cost values for the complete structure were normalised using the standard values quoted above. However, since the scale of the structural component and the complete structure differed markedly, a different set of standard values had to be adopted for the normalisation of the system values of the structural component, in order to allow a direct comparison to be made of the weight and cost variations of both structual items. The configuration of the structural component having the maximum efficiency factor was used as the standard, for

each value of the cover end loading. The standard values for the structural component are presented in Table 6.14. The normalised weight and cost values for the component are presented in Table 6.15.

TABLE 6.1 The cover dimensions for the aluminium alloy systems.

| Applied end loading Nx (lb./in.) | 1000 | | | | 2500 | | | |
|---|---|---|---|---|---|---|---|---|
| Compression cover efficiency factor F | .6 | .7 | .8 | .95 | .6 | .7 | .8 | .95 |
| Compression cover equivalent thickness $t_{c_c}$ (in.) | .067 | .060 | .055 | .049 | .091 | .082 | .075 | .067 |
| Tension cover equivalent thickness $t_{c_T}$ (in.) | .047 | .043 | .039 | .035 | .064 | .058 | .053 | .047 |
| Operative tension cover efficiency factor $F_T$ | .6 | .7 | .8 | .95 | .6 | .7 | .8 | .95 |

TABLE 6.1 CONTINUED

| Applied end loading Nx (lb./in.) | 5000 | | | | 10000 | | | |
|---|---|---|---|---|---|---|---|---|
| Compression cover efficiency factor F | .6 | .7 | .8 | .95 | .6 | .7 | .8 | .95 |
| Compression cover equivalent thickness $t_{c_c}$ (in.) | .115 | .106 | .106 | .106 | .213 | .213 | .213 | .213 |
| Tension cover equivalent thickness $t_{c_T}$ (in.) | .083 | .083 | .083 | .083 | .167 | .167 | .167 | .167 |
| Operative tension cover efficiency factor $F_T$ | .58 | .63 | .72 | .86 | .54 | .63 | .72 | .86 |

TABLE 6.2 The cover dimensions for the titanium alloy systems

| Applied end loading Nx (lb./in.) | 1000 | | | | 2500 | | | |
|---|---|---|---|---|---|---|---|---|
| Compression cover efficiency factor F | .7 | .8 | .9 | 1.015 | .7 | .8 | .9 | 1.015 |
| Compression cover equivalent thickness $t_{c_c}$ (in.) | .042 | .039 | .036 | .033 | .057 | .052 | .048 | .045 |
| Tension cover equivalent thickness $t_{c_T}$ (in.) | .030 | .027 | .025 | .023 | .040 | .037 | .034 | .032 |
| Operative tension cover efficiency factor $F_T$ | .7 | .8 | .9 | 1.015 | .7 | .8 | .9 | 1.015 |

TABLE 6.2 CONTINUED

| Applied end loading Nx (lb./in.) | 5000 | | | | 10000 | | | |
|---|---|---|---|---|---|---|---|---|
| Compression cover efficiency factor F | .7 | .8 | .9 | 1.015 | .7 | .8 | .9 | 1.015 |
| Compression cover equivalent thickness $t_{c_c}$ (in.) | .072 | .066 | .061 | .056 | .091 | .083 | .077 | .077 |
| Tension cover equivalent thickness $t_{c_T}$ (in.) | .051 | .047 | .043 | .040 | .068 | .068 | .068 | .068 |
| Operative tension cover efficiency factor $F_T$ | .7 | .8 | .9 | 1.015 | .66 | .69 | .72 | .81 |

TABLE 6.3 The definition of the internal geometry for the aluminium alloy designs.

| End loading Nx (lb./in.) | | 1000 | | | | 2500 | | | |
|---|---|---|---|---|---|---|---|---|---|
| Compression cover efficiency factor F | | 0.6 | 0.7 | 0.8 | 0.95 | 0.6 | 0.7 | 0.8 | 0.95 |
| Compression Cover Data | Skin thickness t (in.) | .048 | .040 | .032 | .020 | .072 | .064 | .048 | .027 |
| | Stringer thickness $t_s$ (in.) | .048 | .040 | .032 | .021 | .048 | .032 | .036 | .028 |
| | Stringer pitch b (in.) | 6.1 | 4.7 | 3.2 | 1.68 | 6.1 | 4.3 | 3.2 | 1.68 |
| | No. of stringers per panel | 8 | 10 | 15 | 29 | 8 | 11 | 15 | 29 |
| Tension Cover Data | Skin thickness t (in.) | .036 | .028 | .022 | .014 | .048 | .040 | .036 | .019 |
| | Stringer thickness $t_s$ (in.) | .036 | .028 | .022 | .015 | .040 | .036 | .032 | .020 |
| | Stringer pitch b (in.) | 7.2 | 4.5 | 3.1 | 1.68 | 6.2 | 4.8 | 3.1 | 1.68 |
| | No. of stringers per panel | 6 | 11 | 16 | 29 | 8 | 10 | 16 | 29 |
| Rib Data | Rib thickness $t_R$ (in.) | .036 | .036 | .036 | .036 | .036 | .036 | .036 | .036 |
| | Rib pitch a (in.) | 16.1 | 17.9 | 19.5 | 21.9 | 11.9 | 13.2 | 14.4 | 16.2 |
| | No. of ribs per box | 7.2 | 6.6 | 6.1 | 5.6 | 9.4 | 8.6 | 7.9 | 7.2 |
| Spar Data | Spar web thickness (in.) | .024 | .024 | .024 | .024 | .028 | .028 | .028 | .028 |
| | Stiffener area ($in.^2$) | .032 | .032 | .032 | .032 | .055 | .055 | .055 | .055 |
| | Stiffener pitch (in.) | 8.1 | 8.9 | 9.8 | 10.9 | 11.9 | 13.2 | 7.2 | 8.1 |
| | No. of stiffeners per box | 13 | 12 | 11 | 10 | 9 | 8 | 14 | 13 |
| | Boom area per spar ($in.^2$) | .376 | .376 | .376 | .376 | .606 | .606 | .606 | .606 |

TABLE 6.3 CONTINUED

| End loading Nx (lb./in.) | | 5000 | | | | 10000 | | | |
|---|---|---|---|---|---|---|---|---|---|
| Compression cover efficiency Factor F | | 0.6 | 0.7 | 0.8 | 0.95 | 0.6 | 0.7 | 0.8 | 0.95 |
| Compression Cover Data | Skin thickness t (in.) | .092 | .080 | .072 | .043 | .176 | .160 | .144 | .085 |
| | Stringer thickness $t_s$ (in.) | .056 | .048 | .048 | .045 | .104 | .092 | .092 | .089 |
| | Stringer pitch b (in.) | 5.9 | 4.4 | 3.2 | 1.68 | 5.9 | 4.4 | 3.1 | 1.68 |
| | No of stringer per panel | 8 | 11 | 15 | 29 | 8 | 11 | 15 | 29 |
| Tension Cover Data | Skin thickness t (in.) | .064 | .064 | .056 | .048 | .128 | .128 | .116 | .104 |
| | Stringer thickness $t_s$ (in.) | .056 | .048 | .048 | .040 | .128 | .092 | .092 | .064 |
| | Stringer pitch b (in.) | 7.1 | 6.1 | 4.3 | 2.6 | 7.9 | 5.9 | 4.3 | 2.4 |
| | No of stringer per panel | 7 | 8 | 11 | 19 | 6 | 8 | 11 | 20 |
| Rib Data | Rib thickness $t_R$ (in.) | .036 | .036 | .036 | .036 | .036 | .036 | .036 | .039 |
| | Rib pitch a (in.) | 9.4 | 11.1 | 14.5 | 20.4 | 16.3 | 22.2 | 29.0 | 40.9 |
| | No of ribs per box | 11.6 | 10.0 | 7.9 | 5.9 | 7.1 | 5.5 | 4.5 | 3.4 |
| Spar Data | Spar web thickness (in.) | .036 | .036 | .036 | .036 | .036 | .036 | .036 | .036 |
| | Stiffener area ($in.^2$) | .065 | .065 | .065 | .065 | .087 | .087 | .087 | .087 |
| | Stiffener pitch (in.) | 9.4 | 11.1 | 7.3 | 10.2 | 8.2 | 7.4 | 9.7 | 8.1 |
| | No of stiffeners per box | 11 | 10 | 14 | 10 | 13 | 14 | 11 | 13 |
| | Boom area per spar ($in.^2$) | .748 | .748 | .748 | .748 | 1.09 | 1.09 | 1.09 | 1.09 |

TABLE 6.4 The definition of the internal geometry for the titanium alloy designs.

| End loading Nx (lb./in.) | | 1000 | | | | 2500 | | | |
|---|---|---|---|---|---|---|---|---|---|
| Compression cover efficiency factor F | | 0.7 | 0.8 | 0.9 | 1.015 | 0.7 | 0.8 | 0.9 | 1.015 |
| Compression Cover Data | Skin thickness t (in.) | .033 | .026 | .021 | .014 | .045 | .034 | .028 | .020 |
| | Stringer thickness $t_s$ (in.) | .033 | .026 | .021 | .014 | .045 | .034 | .028 | .020 |
| | Stringer pitch b (in.) | 7.5 | 3.8 | 2.6 | 1.5 | 7.5 | 3.8 | 2.6 | 1.5 |
| | No. of stringers per panel | 6 | 13 | 19 | 33 | 6 | 13 | 19 | 33 |
| Tension Cover Data | Skin thickness t (in.) | .024 | .018 | .014 | .014 | .032 | .024 | .020 | .014 |
| | Stringer thickness $t_s$ (in.) | .024 | .018 | .014 | .014 | .032 | .024 | .020 | .014 |
| | Stringer pitch b (in.) | 7.5 | 3.8 | 2.6 | 2.6 | 7.5 | 3.8 | 2.6 | 1.5 |
| | No. of stringers per panel | 6 | 13 | 19 | 19 | 6 | 13 | 19 | 33 |
| Rib Data | Rib thickness $t_R$ (in.) | .022 | .022 | .022 | .022 | .022 | .022 | .022 | .022 |
| | Rib pitch a (in.) | 15.7 | 17.1 | 18.5 | 20.1 | 11.5 | 12.6 | 13.6 | 14.8 |
| | No. of ribs per box | 7.4 | 6.9 | 6.4 | 6.0 | 9.7 | 9.0 | 8.4 | 7.8 |
| Spar Data | Spar web thickness (in.) | .014 | .014 | .014 | .014 | .014 | .014 | .014 | .014 |
| | Stiffener area ($in.^2$) | .021 | .021 | .021 | .021 | .032 | .032 | .032 | .032 |
| | Stiffener pitch (in.) | 7.9 | 8.6 | 9.3 | 10.0 | 11.5 | 12.6 | 13.6 | 14.8 |
| | No. of stiffeners per box | 13 | 12 | 11 | 11 | 9 | 8 | 8 | 7 |
| | Boom area per spar ($in.^2$) | .238 | .238 | .238 | .238 | .34 | .34 | .34 | .34 |

TABLE 6.4 CONTINUED

| End loading Nx (lb./in.) | | 5000 | | | | 10000 | | | |
|---|---|---|---|---|---|---|---|---|---|
| Compression cover efficiency factor F | | 0.7 | 0.8 | 0.9 | 1.015 | 0.7 | 0.8 | 0.9 | 1.015 |
| Compression Cover Data | Skin thickness t (in.) | .057 | .044 | .035 | .024 | .072 | .055 | .044 | .034 |
| | Stringer thickness $t_s$ (in.) | .057 | .044 | .035 | .024 | .072 | .055 | .044 | .034 |
| | Stringer pitch b (in.) | 7.5 | 3.8 | 2.6 | 1.5 | 7.5 | 3.8 | 2.6 | 1.5 |
| | No. of stringers per panel | 6 | 13 | 19 | 33 | 6 | 13 | 19 | 33 |
| Tension Cover Data | Skin thickness t (in.) | .041 | .031 | .025 | .017 | .054 | .054 | .051 | .044 |
| | Stringer thickness $t_s$ (in.) | .041 | .031 | .025 | .017 | .054 | .054 | .051 | .044 |
| | Stringer pitch b (in.) | 7.5 | 3.8 | 2.6 | 1.5 | 7.5 | 7.5 | 5.8 | 3.5 |
| | No. of stringer per panel | 6 | 13 | 19 | 33 | 6 | 6 | 8 | 14 |
| Rib Data | Rib thickness $t_R$ (in.) | .022 | .022 | .022 | .022 | .022 | .022 | .022 | .022 |
| | Rib pitch a (in.) | 9.2 | 10.0 | 10.8 | 11.7 | 7.3 | 7.9 | 8.6 | 11.0 |
| | No. of ribs per box | 11.9 | 11.0 | 10.3 | 9.6 | 14.8 | 13.6 | 12.6 | 10.1 |
| Spar Data | Spar web thickness (in.) | .014 | .014 | .014 | .014 | .020 | .020 | .020 | .020 |
| | Stiffener area ($in.^2$) | .040 | .040 | .040 | .040 | .048 | .048 | .048 | .048 |
| | Stiffener pitch (in.) | 9.2 | 10.0 | 10.8 | 11.7 | 7.3 | 7.9 | 8.6 | 11.0 |
| | No. of stiffeners per box | 11 | 11 | 10 | 9 | 14 | 13 | 12 | 10 |
| | Boom area per spar ($in.^2$) | .494 | .494 | .494 | .494 | .62 | .62 | .62 | .62 |

TABLE 6.5 Structural weight breakdowns for the aluminium alloy designs.

| Applied end loading Nx (lb./in.) | | | 1000 | | | | 2500 | | | |
|---|---|---|---|---|---|---|---|---|---|---|
| Compression cover efficiency factor | | | 0.6 | 0.7 | 0.8 | 0.95 | 0.6 | 0.7 | 0.8 | 0.95 |
| Basic Design (see section 5.2.2) | Compression cover weight | (lb.) | - | - | - | - | 47.3 | - | - | - |
| | Tension cover weight | (lb.) | - | - | - | - | 33.3 | - | - | - |
| | Rib weight | (lb.) | - | - | - | - | 26.7 | - | - | - |
| | Spar weight | (lb.) | - | - | - | - | 22.9 | - | - | - |
| | Total weight | (lb.) | - | - | - | - | 130.2 | - | - | - |
| Chemically Etched Design (see section 5.2.3) | Compression cover weight | (lb.) | 34.9 | 31.7 | 30.1 | 29.6 | - | 42.6 | 39.0 | 38.3 |
| | Tension cover weight | (lb.) | 25.0 | 23.9 | 22.9 | 23.6 | - | 30.6 | 28.6 | 29.3 |
| | Rib weight | (lb.) | 20.8 | 18.4 | 16.5 | 13.6 | - | 24.1 | 21.4 | 17.6 |
| | Spar weight | (lb.) | 16.3 | 16.1 | 17.5 | 17.5 | - | 22.6 | 23.2 | 23.1 |
| | Total weight | (lb.) | 97.0 | 90.1 | 87.0 | 84.3 | - | 119.9 | 112.4 | 108.3 |
| Spin Dimpled Design (see section 5.2.4) | Compression cover weight | (lb.) | 34.9 | 31.2 | 28.6 | 25.5 | - | 42.6 | 39.0 | 34.9 |
| | Tension cover weight | (lb.) | 24.4 | 22.4 | 20.3 | 18.2 | - | 30.2 | 27.6 | 24.5 |
| | Rib weight | (lb.) | 20.8 | 18.4 | 16.5 | 13.6 | - | 24.1 | 21.4 | 17.6 |
| | Spar weight | (lb.) | 16.3 | 16.1 | 17.5 | 17.5 | - | 22.6 | 23.2 | 23.1 |
| | Total weight | (lb.) | 96.4 | 88.1 | 82.9 | 74.8 | - | 119.5 | 111.4 | 100.1 |
| Component Design (see section 5.2.5) | Compression cover weight | (lb.) | 34.9 | 31.7 | 30.1 | 29.6 | 47.3 | 42.6 | 39.0 | 38.3 |
| | Rib weight | (lb.) | 20.8 | 18.4 | 16.5 | 13.6 | 26.7 | 24.1 | 21.4 | 17.6 |
| | Total weight | (lb.) | 55.7 | 50.1 | 46.6 | 43.2 | 74.0 | 66.7 | 60.4 | 55.9 |

TABLE 6.5 CONTINUED

| Applied end loading Nx (lb./in.) | | | 5000 | | | | 10000 | | | |
|---|---|---|---|---|---|---|---|---|---|---|
| Compression cover efficiency factor | | | 0.6 | 0.7 | 0.8 | 0.95 | 0.6 | 0.7 | 0.8 | 0.95 |
| Basic Design (see section 5.2.2) | Compression cover weight | (lb.) | 59.8 | 55.1 | 55.1 | 55.1 | 110.9 | 110.9 | 110.9 | 110.9 |
| | Tension cover weight | (lb.) | 43.2 | 43.2 | 43.2 | 43.2 | 86.8 | 86.8 | 86.8 | 86.8 |
| | Rib weight | (lb.) | 33.4 | 28.4 | 22.0 | 15.4 | 20.6 | 15.6 | 12.4 | 9.2 |
| | Spar weight | (lb.) | 28.4 | 28.2 | 28.9 | 28.4 | 37.0 | 37.0 | 36.4 | 37.0 |
| | Total weight | (lb.) | 164.8 | 154.9 | 149.2 | 142.1 | 255.3 | 250.3 | 246.5 | 243.9 |
| Chemically Etched Design (see section 5.2.3) | Compression cover weight | (lb.) | - | - | - | - | - | - | - | - |
| | Tension cover weight | (lb.) | - | - | - | - | - | - | - | - |
| | Rib weight | (lb.) | - | - | - | - | - | - | - | - |
| | Spar weight | (lb.) | - | - | - | - | - | - | - | - |
| | Total weight | (lb.) | - | - | - | - | - | - | - | - |
| Spin Dimpled Design (see section 5.2.4) | Compression cover weight | (lb.) | - | - | - | - | - | - | - | - |
| | Tension cover weight | (lb.) | - | - | - | - | - | - | - | - |
| | Rib weight | (lb.) | - | - | - | - | - | - | - | - |
| | Spar weight | (lb.) | - | - | - | - | - | - | - | - |
| | Total weight | (lb.) | - | - | - | - | - | - | - | - |
| Component Design (see section 5.2.5) | Compression cover weight | (lb.) | 59.8 | 55.1 | 55.1 | 55.1 | 110.9 | 110.9 | 110.9 | 110.9 |
| | Rib weight | (lb.) | 33.4 | 28.4 | 22.0 | 15.4 | 20.6 | 15.6 | 12.4 | 9.2 |
| | Total weight | (lb.) | 93.2 | 83.5 | 77.1 | 70.5 | 131.5 | 126.5 | 123.3 | 120.1 |

TABLE 6.6 Structural weight breakdowns for the titanium designs.

| Applied end loading Nx (lb./in.) | | 1000 | | | | 2500 | | | |
|---|---|---|---|---|---|---|---|---|---|
| Compression cover efficiency factor F | | 0.7 | 0.8 | 0.9 | 1.015 | 0.7 | 0.8 | 0.9 | 1.015 |
| Compression cover weight | (lb.) | 33.2 | 30.8 | 28.5 | 26.1 | 45.1 | 41.1 | 37.9 | 35.6 |
| Tension cover weight | (lb.) | 23.7 | 21.4 | 19.8 | 18.2 | 31.6 | 29.2 | 26.9 | 25.3 |
| Rib weight | (lb.) | 20.0 | 18.1 | 16.4 | 14.5 | 26.3 | 23.6 | 21.5 | 17.6 |
| Spar weight | (lb.) | 15.6 | 15.4 | 15.4 | 15.2 | 19.0 | 18.8 | 18.8 | 19.6 |
| Total weight | (lb.) | 92.5 | 85.7 | 80.1 | 74.0 | 122.0 | 112.7 | 105.1 | 98.1 |

TABLE 6.6 CONTINUED

| Applied end loading Nx (lb./in.) | | 5000 | | | | 10000 | | | |
|---|---|---|---|---|---|---|---|---|---|
| Compression cover efficiency factor F | | 0.7 | 0.8 | 0.9 | 1.015 | 0.7 | 0.8 | 0.9 | 1.015 |
| Compression cover weight | (lb.) | 56.9 | 52.1 | 48.2 | 44.3 | 71.9 | 65.6 | 60.9 | 60.9 |
| Tension cover weight | (lb.) | 40.3 | 37.2 | 34.0 | 31.6 | 53.7 | 53.7 | 53.7 | 53.7 |
| Rib weight | (lb.) | 32.3 | 29.1 | 26.4 | 21.6 | 40.2 | 36.4 | 33.1 | 24.7 |
| Spar weight | (lb.) | 24.2 | 24.2 | 24.2 | 24.0 | 33.0 | 32.6 | 32.4 | 31.8 |
| Total weight | (lb.) | 153.7 | 142.6 | 132.8 | 121.5 | 198.8 | 188.3 | 180.1 | 171.1 |

TABLE 6.7 Unit cost breakdowns for the aluminium alloy designs.

| Applied end loading Nx (lb./in.) | | | 1000 | | | | 2500 | | | |
|---|---|---|---|---|---|---|---|---|---|---|
| Compression cover efficiency factor F | | | 0.6 | 0.7 | 0.8 | 0.95 | 0.6 | 0.7 | 0.8 | 0.95 |
| Basic Design (see section 5.2.2) | Material cost | (£) | - | - | - | - | 108.4 | - | - | - |
| | Production cost* | (£) | - | - | - | - | 410.2 | - | - | - |
| | Tooling cost | (£) | - | - | - | - | 19.5 | - | - | - |
| | Unit cost | (£) | - | - | - | - | 538.1 | - | - | - |
| Chemically Etched Design (see section 5.2.3) | Material cost | (£) | 82.6 | 82.5 | 83.1 | 86.8 | - | 105.0 | 106.3 | 112.7 |
| | Production cost* | (£) | 488.1 | 631.8 | 757.1 | 881.0 | - | 585.1 | 704.3 | 1012.1 |
| | Tooling cost | (£) | 19.5 | 19.5 | 19.5 | 19.5 | - | 19.5 | 19.5 | 19.5 |
| | Unit cost | (£) | 590.2 | 733.8 | 859.7 | 987.3 | - | 709.6 | 830.1 | 1144.3 |
| Spin Dimpled Design (see section 5.2.4) | Material cost | (£) | 82.6 | 82.5 | 83.1 | 86.8 | - | 105.0 | 106.3 | 112.7 |
| | Production cost* | (£) | 586.1 | 705.0 | 923.2 | 1734.1 | - | 623.1 | 853.2 | 1630.1 |
| | Tooling cost | (£) | 19.5 | 19.5 | 19.5 | 19.5 | - | 19.5 | 19.5 | 19.5 |
| | Unit cost | (£) | 688.2 | 807.0 | 1025.8 | 1840.4 | - | 747.6 | 979.0 | 1762.3 |
| Component Design (see section 5.2.5) | Material cost | (£) | 43.1 | 40.8 | 40.5 | 40.9 | 56.9 | 54.3 | 57.7 | 60.4 |
| | Production cost* | (£) | 62.1 | 197.9 | 241.3 | 283.0 | 79.1 | 129.7 | 164.8 | 284.4 |
| | Tooling cost | (£) | 12.0 | 12.0 | 12.0 | 12.0 | 12.0 | 12.0 | 12.0 | 12.0 |
| | Unit cost | (£) | 117.2 | 250.7 | 293.8 | 335.9 | 148.0 | 196.0 | 234.5 | 356.8 |

*The production cost includes the direct labour cost, the overhead cost and the production learning cost.

TABLE 6.7 CONTINUED

| Applied end loading Nx (lb./in.) | | | 5000 | | | | 10000 | | | |
|---|---|---|---|---|---|---|---|---|---|---|
| Compression cover efficiency factor F | | | 0.6 | 0.7 | 0.8 | 0.95 | 0.6 | 0.7 | 0.8 | 0.95 |
| Basic Design (see section 5.2.2) | Material cost | (£) | 139.1 | 131.7 | 136.6 | 150.9 | 198.8 | 193.6 | 199.6 | 146.2 |
| | Production cost* | (£) | 452.5 | 465.3 | 494.0 | 697.2 | 412.2 | 398.5 | 420.1 | 691.4 |
| | Tooling cost | (£) | 19.5 | 19.5 | 19.5 | 19.5 | 19.5 | 19.5 | 19.5 | 19.5 |
| | Unit cost | (£) | 611.1 | 616.5 | 650.1 | 867.6 | 630.5 | 611.6 | 639.2 | 957.1 |
| Chemically Etched Design (see section 5.2.3) | Material cost | (£) | - | - | - | - | - | - | - | - |
| | Production cost* | (£) | - | - | - | - | - | - | - | - |
| | Tooling cost | (£) | - | - | - | - | - | - | - | - |
| | Unit cost | (£) | - | - | - | - | - | - | - | - |
| Spin Dimpled Design (see section 5.2.4) | Material cost | (£) | - | - | - | - | - | - | - | - |
| | Production cost* | (£) | - | - | - | - | - | - | - | - |
| | Tooling cost | (£) | - | - | - | - | - | - | - | - |
| | Unit cost | (£) | - | - | - | - | - | - | - | - |
| Component Design (see section 5.2.5) | Material cost | (£) | 71.1 | 69.4 | 69.3 | 70.9 | 94.2 | 92.4 | 106.4 | 124.5 |
| | Production cost* | (£) | 100.5 | 119.9 | 134.3 | 288.6 | 70.1 | 80.0 | 92.5 | 284.0 |
| | Tooling cost | (£) | 12.0 | 12.0 | 12.0 | 12.0 | 12.0 | 12.0 | 12.0 | 12.0 |
| | Unit cost | (£) | 183.6 | 201.3 | 215.6 | 371.5 | 176.3 | 184.4 | 210.9 | 420.5 |

*The production cost includes the direct labour cost, the overhead cost and the production learning cost.

TABLE 6.8 Unit cost breakdowns for the titanium alloy designs.

| Applied end loading Nx (lb./in.) | 1000 | | | | 2500 | | | |
|---|---|---|---|---|---|---|---|---|
| Compression cover efficiency factor F | 0.7 | 0.8 | 0.9 | 1.015 | 0.7 | 0.8 | 0.9 | 1.015 |
| Material cost (£) | 1561.2 | 1531.8 | 1481.0 | 1483.2 | 1929.8 | 1872.8 | 1896.8 | 1936.2 |
| Production cost* (£) | 1237.5 | 1600.1 | 1910.2 | 3058.0 | 1291.1 | 1647.6 | 1989.6 | 3578.8 |
| Tooling cost (£) | 60.0 | 60.0 | 60.0 | 60.0 | 60.0 | 60.0 | 60.0 | 60.0 |
| Unit cost (£) | 2858.7 | 3191.9 | 3451.2 | 4601.2 | 3280.9 | 3580.4 | 3946.4 | 5575.0 |

*The production cost includes the direct labour cost, the overhead cost and the production learning cost.

TABLE 6.8 CONTINUED

| Applied end loading Nx (lb./in.) | 5000 | | | | 10000 | | | |
|---|---|---|---|---|---|---|---|---|
| Compression cover efficiency factor F | 0.7 | 0.8 | 0.9 | 1.015 | 0.7 | 0.8 | 0.9 | 1.015 |
| Material cost (£) | 2331.8 | 2286.6 | 2183.2 | 2144.2 | 2873.0 | 2778.8 | 2716.4 | 2648.8 |
| Production cost* (£) | 1398.0 | 1759.9 | 2072.2 | 3601.5 | 1561.1 | 1700.5 | 1879.5 | 3084.3 |
| Tooling cost (£) | 60.0 | 60.0 | 60.0 | 60.0 | 60.0 | 60.0 | 60.0 | 60.0 |
| Unit cost (£) | 3789.8 | 4106.5 | 4315.4 | 5805.7 | 4494.1 | 4539.3 | 4655.9 | 5793.1 |

*The production cost includes the direct labour cost, the overhead cost and the production learning cost.

TABLE 6.9 The cost per unit weight values (in £/lb.) for the aluminium alloy structures.

| | | | Efficiency factor F | | | |
|---|---|---|---|---|---|---|
| | | | 0.6 | 0.7 | 0.8 | 0.95 |
| Applied end loading Nx (lb./in.) | 1000 | chemically etched | 6.1 | 8.1 | 9.9 | 11.7 |
| | | spin dimpled | 7.1 | 9.2 | 12.4 | 24.6 |
| | 2500 | basic design | 4.1 | - | - | - |
| | | chemically etched | - | 5.9 | 7.4 | 10.6 |
| | | spin dimpled | - | 6.3 | 8.8 | 17.6 |
| | 5000 | | 3.7 | 4.0 | 4.4 | 6.1 |
| | 10000 | | 2.5 | 2.5 | 2.6 | 3.9 |

TABLE 6.10 The cost per unit weight values (in £/lb.) for the titanium alloy structures.

| | | Efficiency factor F | | | |
|---|---|---|---|---|---|
| | | 0.7 | 0.8 | 0.9 | 1.015 |
| Applied end loading Nx (lb./in.) | 1000 | 30.9 | 37.2 | 43.1 | 62.2 |
| | 2500 | 26.9 | 31.8 | 37.6 | 56.9 |
| | 5000 | 24.7 | 28.8 | 32.5 | 47.8 |
| | 10000 | 22.6 | 24.1 | 25.8 | 33.8 |

TABLE 6.11 The standard values for the comparative analysis.

| | Applied end loading Nx (lb./in.) | | | |
|---|---|---|---|---|
| | 1000 | 2500 | 5000 | 10000 |
| Standard cost $C_{ST}$ (£) | 987.3 | 1144.3 | 867.6 | 957.1 |
| Standard weight $W_{ST}$ (lb.) | 84.3 | 108.3 | 142.1 | 243.9 |

The standards are based on the maximum efficiency of the chemically etched design for sub-critical loads and on the maximum efficiency of the basic aluminium alloy design for super-critical loads.

TABLE 6.12 The normalised cost and weight values for the aluminium alloy structures.

(a) Normalised Cost ($C/C_{ST}$)

| | | | Efficiency factor F | | | |
|---|---|---|---|---|---|---|
| | | | 0.6 | 0.7 | 0.8 | 0.95 |
| Applied end loading Nx (lb./in.) | 1000 | spin dimpled | 0.697 | 0.817 | 1.039 | 1.864 |
| | | chemically etched | 0.598 | 0.743 | 0.871 | 1.0 |
| | 2500 | spin dimpled | - | 0.653 | 0.856 | 1.540 |
| | | chemically etched | - | 0.620 | 0.725 | 1.0 |
| | 5000 | | 0.704 | 0.711 | 0.749 | 1.0 |
| | 10000 | | 0.659 | 0.639 | 0.668 | 1.0 |

(b) Normalised Weight ($W/W_{ST}$)

| | | | Efficiency factor F | | | |
|---|---|---|---|---|---|---|
| | | | 0.6 | 0.7 | 0.8 | 0.95 |
| Applied end loading Nx (lb./in.) | 1000 | spin dimpled | 1.144 | 1.045 | 0.983 | 0.887 |
| | | chemically etched | 1.151 | 1.069 | 1.032 | 1.0 |
| | 2500 | spin dimpled | - | 1.103 | 1.027 | 0.924 |
| | | chemically etched | - | 1.107 | 1.038 | 1.0 |
| | 5000 | | 1.160 | 1.090 | 1.050 | 1.0 |
| | 10000 | | 1.047 | 1.026 | 1.011 | 1.0 |

TABLE 6.13 The normalised cost and weight values for the titanium alloy structures.

(a) Normalised Cost $(C/C_{ST})$

| | | Efficiency factor F | | | |
|---|---|---|---|---|---|
| | | 0.7 | 0.8 | 0.9 | 1.015 |
| Applied end loading Nx (lb./in.) | 1000 | 2.896 | 3.233 | 3.496 | 4.660 |
| | 2500 | 2.867 | 3.129 | 3.449 | 4.872 |
| | 5000 | 4.368 | 4.733 | 4.974 | 6.692 |
| | 10000 | 4.696 | 4.743 | 4.865 | 6.053 |

(b) Normalised Weight $(W/W_{ST})$

| | | Efficiency factor F | | | |
|---|---|---|---|---|---|
| | | 0.7 | 0.8 | 0.9 | 1.015 |
| Applied end loading Nx (lb./in.) | 1000 | 1.097 | 1.017 | 0.950 | 0.878 |
| | 2500 | 1.127 | 1.041 | 0.970 | 0.905 |
| | 5000 | 1.082 | 1.004 | 0.935 | 0.855 |
| | 10000 | 0.815 | 0.772 | 0.738 | 0.702 |

TABLE 6.14 The standard values for the component structure.

| | Applied end loading Nx (lb./in.) | | | |
|---|---|---|---|---|
| | 1000 | 2500 | 5000 | 10000 |
| Standard cost $C_{ST}$ (£) | 335.9 | 356.8 | 371.5 | 420.5 |
| Standard weight $W_{ST}$ (lb.) | 43.2 | 55.9 | 70.5 | 120.1 |

The standards are based on the maximum efficiency configuration of the component.

TABLE 6.15 The normalised cost and weight values for the component structure.

(a) Normalised Cost $(C/C_{ST})$

| | | Efficiency factor F | | | |
|---|---|---|---|---|---|
| | | 0.6 | 0.7 | 0.8 | 0.95 |
| Applied end loading Nx (lb./in.) | 1000 | 0.349 | 0.746 | 0.875 | 1.0 |
| | 2500 | 0.415 | 0.549 | 0.657 | 1.0 |
| | 5000 | 0.494 | 0.542 | 0.580 | 1.0 |
| | 10000 | 0.419 | 0.439 | 0.502 | 1.0 |

(b) Normalised Weight $(W/W_{ST})$

| | | Efficiency factor F | | | |
|---|---|---|---|---|---|
| | | 0.6 | 0.7 | 0.8 | 0.95 |
| Applied end loading Nx (lb./in.) | 1000 | 1.289 | 1.160 | 1.079 | 1.0 |
| | 2500 | 1.324 | 1.193 | 1.081 | 1.0 |
| | 5000 | 1.322 | 1.184 | 1.094 | 1.0 |
| | 10000 | 1.095 | 1.053 | 1.027 | 1.0 |

FIG. 6.1 THE COST PER UNIT WEIGHT VALUES FOR THE SPECIMEN STRUCTURE

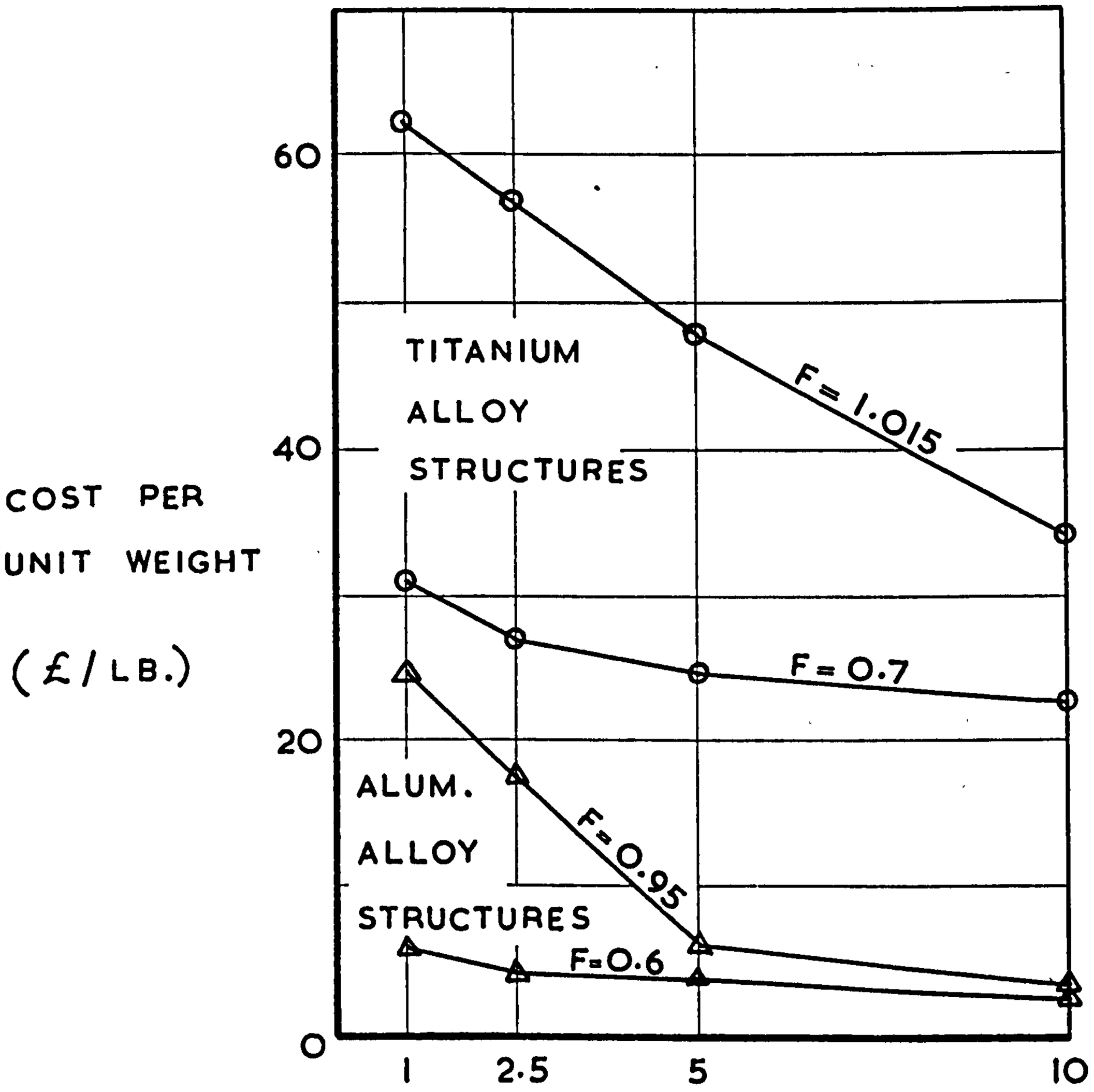

# C H A P T E R  7

# THE VARIATION OF THE OPTIMAL CONFIGURATION FOR EACH STRUCTURAL SYSTEM

## 7.1 Introduction

The configuration of a structural system is defined in terms of the arrangement of the main structural components, including the stringers and the ribs. When designed to a given global exchange rate value, there is a certain configuration which yields the optimal solution.

In the analysis of the specimen structure, the configuration of each structural system was defined in terms of an efficiency factor value. The examination of the variation of the optimal configuration with global exchange rate was an important aspect of the analysis.

## 7.2 Curve Fitting Using the Lagrange Interpolation Method

As mentioned in section 6.1, the structural weight and the unit cost values of each structural system had been evaluated for n different configurations, which may be defined in terms of cover efficiency factor values.

Let the n configurations, having efficiency factor values of $\{F_1 \ldots F_n\}$, possess structural weight and unit cost values of $\{W_1, C_1 \ldots W_n, C_n\}$. It was assumed that for each structural system the structural weight and the unit cost both varied with efficiency factor in a continuous manner within the data range considered.

The Lagrange interpolation method [23] allows a continuous curve equation $y(x)$ to be fitted between $n$ discrete points having values of $\{x_1, y_1 \ldots x_n, y_n\}$. The curve equation is given by the polynomial of the $(n-1)^{th}$ degree

$$y = \frac{(x - x_2) \cdot (x - x_3) \ldots (x - x_n)}{(x_1 - x_2) \cdot (x_1 - x_3) \ldots (x_1 - x_n)} \cdot y_1$$

$$+ \frac{(x - x_1) \cdot (x - x_3) \ldots (x - x_n)}{(x_2 - x_1) \cdot (x_2 - x_3) \ldots (x_2 - x_n)} \cdot y_2$$

$$+ \ldots + \frac{(x - x_1) \cdot (x - x_2) \ldots (x - x_{n-1})}{(x_n - x_1) \cdot (x_n - x_2) \ldots (x_n - x_{n-1})} \cdot y_n \qquad (7.1)$$

Incorporating the structural weight data $\{W_1 \ldots W_n\}$ in equation (7.1), the continuous curve equation giving the variation of structural weight $W$ with the structural configuration, expressed in terms of efficiency factor $F$, is

$$W = \frac{(F - F_2) \cdot (F - F_3) \ldots (F - F_n)}{(F_1 - F_2) \cdot (F_1 - F_3) \ldots (F_1 - F_n)} \cdot W_1$$

$$+ \frac{(F - F_1) \cdot (F - F_3) \ldots (F - F_n)}{(F_2 - F_1) \cdot (F_2 - F_3) \ldots (F_2 - F_n)} \cdot W_2$$

$$+ \ldots + \frac{(F - F_1) \cdot (F - F_2) \ldots (F - F_{n-1})}{(F_n - F_1) \cdot (F_n - F_2) \ldots (F_n - F_{n-1})} \cdot W_n \qquad (7.2)$$

Incorporating the unit cost data $\{C_1 \ldots C_n\}$ in equation (7.1), the continuous curve equation giving the variation of the unit cost $C$ with the structural configuration, expressed in terms of efficiency factor $F$, is

$$C = \frac{(F - F_2) \cdot (F - F_3) \cdot \ldots \cdot (F - F_n)}{(F_1 - F_2) \cdot (F_1 - F_3) \cdot \ldots \cdot (F_1 - F_n)} \cdot C_1$$

$$+ \frac{(F - F_1) \cdot (F - F_3) \cdot \ldots \cdot (F - F_n)}{(F_2 - F_1) \cdot (F_2 - F_3) \cdot \ldots \cdot (F_2 - F_n)} \cdot C_2$$

$$+ \ldots + \frac{(F - F_1) \cdot (F - F_2) \cdot \ldots \cdot (F - F_{n-1})}{(F_n - F_1) \cdot (F_n - F_2) \cdot \ldots \cdot (F_n - F_{n-1})} \cdot C_n \qquad (7.3)$$

The variations of the normalised weight and normalised cost with efficiency factor, given by equations (7.2) and (7.3), respectively, are presented in figs. 7.1 to 7.10 for each structural system.

## 7.3 The Location of the Optimal Configuration

The merit function value M, defined by equation (2.27) as

$$M = W + \frac{C}{V_G},$$

was used for the identification of the optimal configuration of a structural system.

It was decided to normalise the merit function values in order to facilitate interpretation of the results. Normalisation was accomplished by dividing by the appropriate standard weight value $W_{ST}$, introduced in section 6.6, since the merit function M has the dimensions of weight. Hence, the normalised merit function value $M_N$ is

$$M_N = \frac{M}{W_{ST}} = \frac{1}{W_{ST}} \cdot \left( W + \frac{C}{V_G} \right) \qquad (7.4)$$

The original intention had been to include the weight equation (7.2) and the cost equation (7.3) in the merit function equation (2.27), and then to differentiate with respect to efficiency factor F to determine the minimum value of merit function, which specifies the optimal configuration of the system. However, investigation revealed that unrealistic optimal efficiency values were given, due to the divergence of both curves when extrapolated beyond the data range.

To overcome this problem, the search for the optimal configuration was limited to interpolation within the data range examined. The computer program presented in Appendix 3 was written to carry out the complete optimisation analysis. Structural weight and unit cost values were evaluated at a series of efficiency factor values within the limits set. Since a computerised solution was adopted, the efficiency factor steps could be made as small as required. The merit function value was evaluated at each efficiency factor value and a step-wise comparative procedure was used to locate the minimum value of the merit function, which defines the optimal structural configuration.

As an illustration of the optimisation process, the optimal configuration for an aluminium alloy system was located graphically in fig. 7.11. The structural weight and unit cost values for the aluminium alloy system designed to an end load value of 5000 lb./in. were normalised and then incorporated in equations (7.2) and (7.3), respectively, to give the normalised weight and cost curves shown in fig. 7.11. At each value of efficiency factor the normalised merit

function value satisfying equation (7.4) was evaluated for a global exchange rate value $V_G$ of £20/lb. The minimum merit function value defines the optimal solution, hence the optimal configuration had an efficiency factor value of 0.825, where the normalised weight values was 1.042 and the normalised cost value was 0.771.

The variation of optimal configuration, expressed in terms of efficiency factor F, with global exchange rate $V_G$ is presented in figs. 7.12 to 7.21, for each structural system.

## 7.4 Discussion of the Results

Examination of figs. 7.1 to 7.10 reveals that the structural weight of each structural system decreases as efficiency factor increases, whereas the unit cost of each system increases with increasing efficiency factor. The configuration with the maximum structural efficiency attainable from the design type being considered gave the minimum structural weight and the maximum unit cost for each structural system.

For the weight and cost variations described above, the value of the efficiency factor defining the optimal configuration increases with increasing global exchange rate value. For each system, the maximum efficiency configuration gave the optimal solution above a certain global exchange rate value $V_{G_{MAX}}$, and these values are summarised in Table 7.1, for each load level examined. The constraint on the maximum value of structural efficiency factor was applied by the operative type of cover configuration, and could only be overcome by changing the design type.

Below a certain global exchange rate value $V_{G_{MIN}}$, the optimisation process sometimes gave the lower limit of the range of efficiency factor values examined, as the optimal configuration. As stated in section 6.1, the lower limit represents the minimum efficiency factor value designated on the appropriate design chart. The minimum efficiency factor case may not represent a true optimal solution, since configurations of lower efficiency having higher structural weight and lower unit cost can exist. For this reason, throughout this thesis, the curves defining the optimal configuration were discontinued below the exchange rate value $V_{G_{MIN}}$.

TABLE 7.1 The global exchange rate values (in £/lb.) above which the maximum efficiency configuration gives the optimal solution.

| Applied end loading Nx (lb./in.) | Aluminium alloy structures | | | Titanium alloy design |
|---|---|---|---|---|
| | Basic design | Chemically etched design | spin dimpled design | |
| 1000 | - | 50 | 120 | 320 |
| 2500 | - | 1560 | 98 | 420 |
| 5000 | 42 | - | - | 240 |
| 10000 | 1150 | - | - | 220 |

# COST AND WEIGHT CURVES AT THE LOAD LEVEL $N_x = 1000$ LB./IN.

FIG. 7.1 THE ALUMINIUM ALLOY CHEMICALLY ETCHED DESIGN

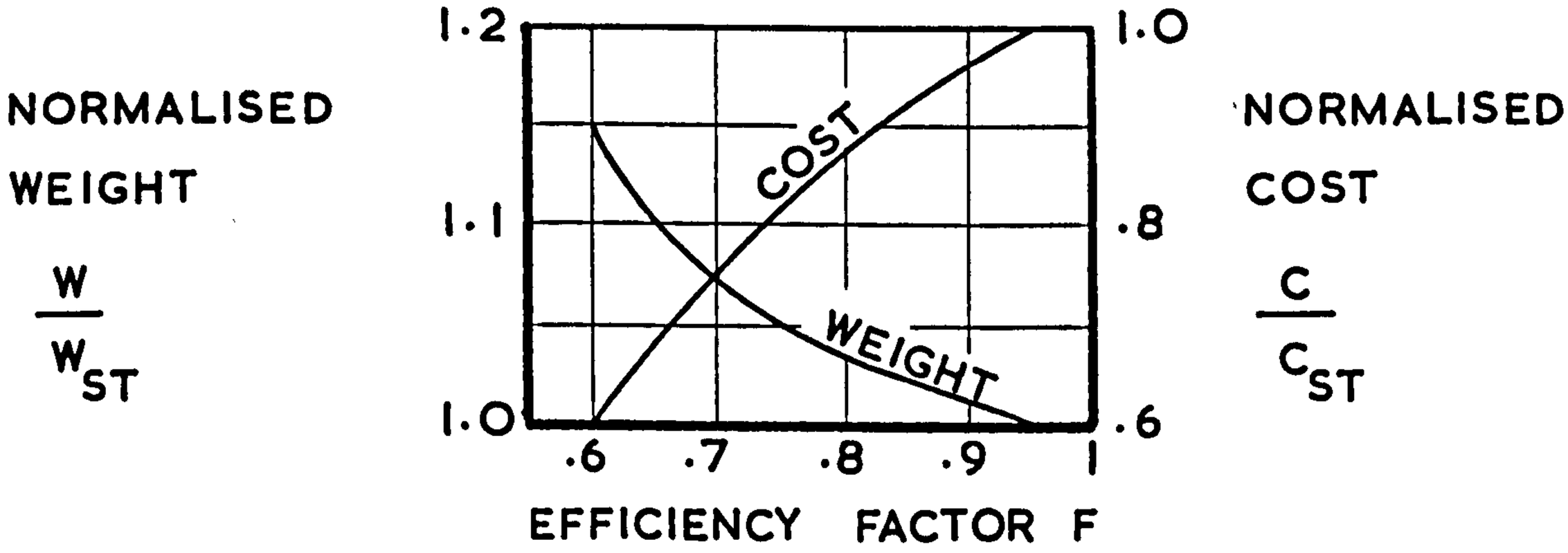


FIG. 7.2 THE ALUMINIUM ALLOY SPIN DIMPLED DESIGN

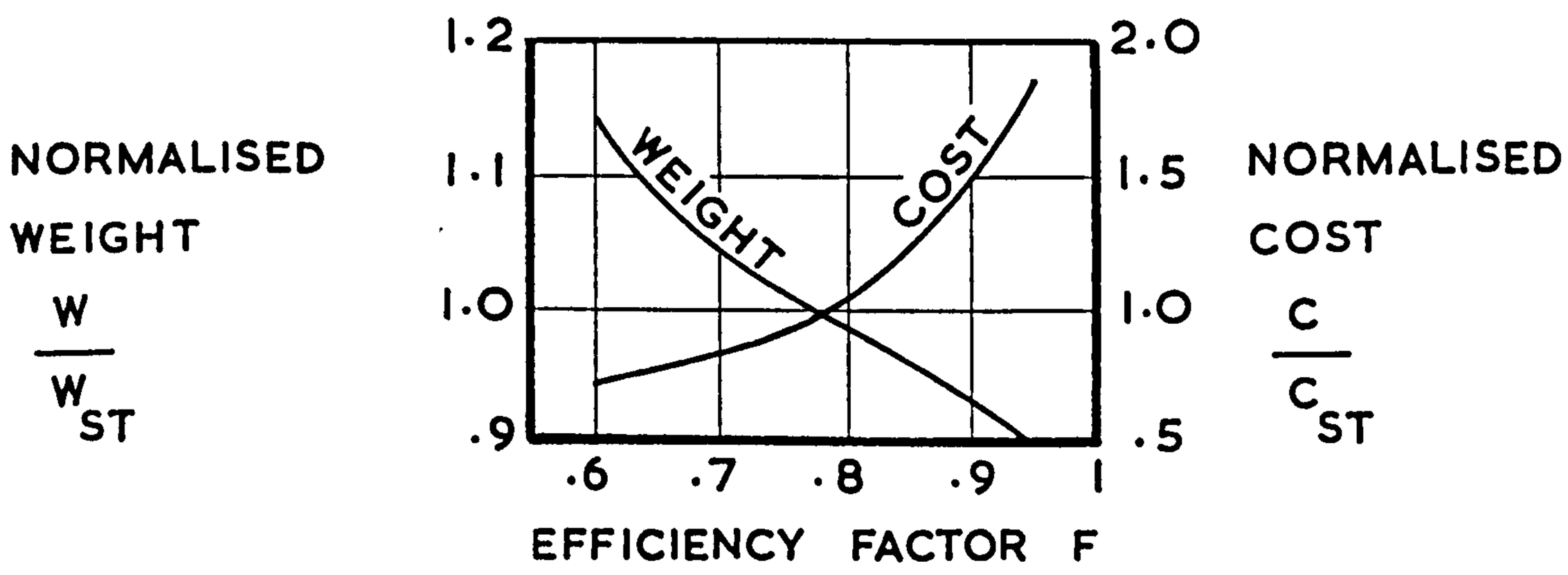


FIG. 7.3 THE TITANIUM ALLOY DESIGN

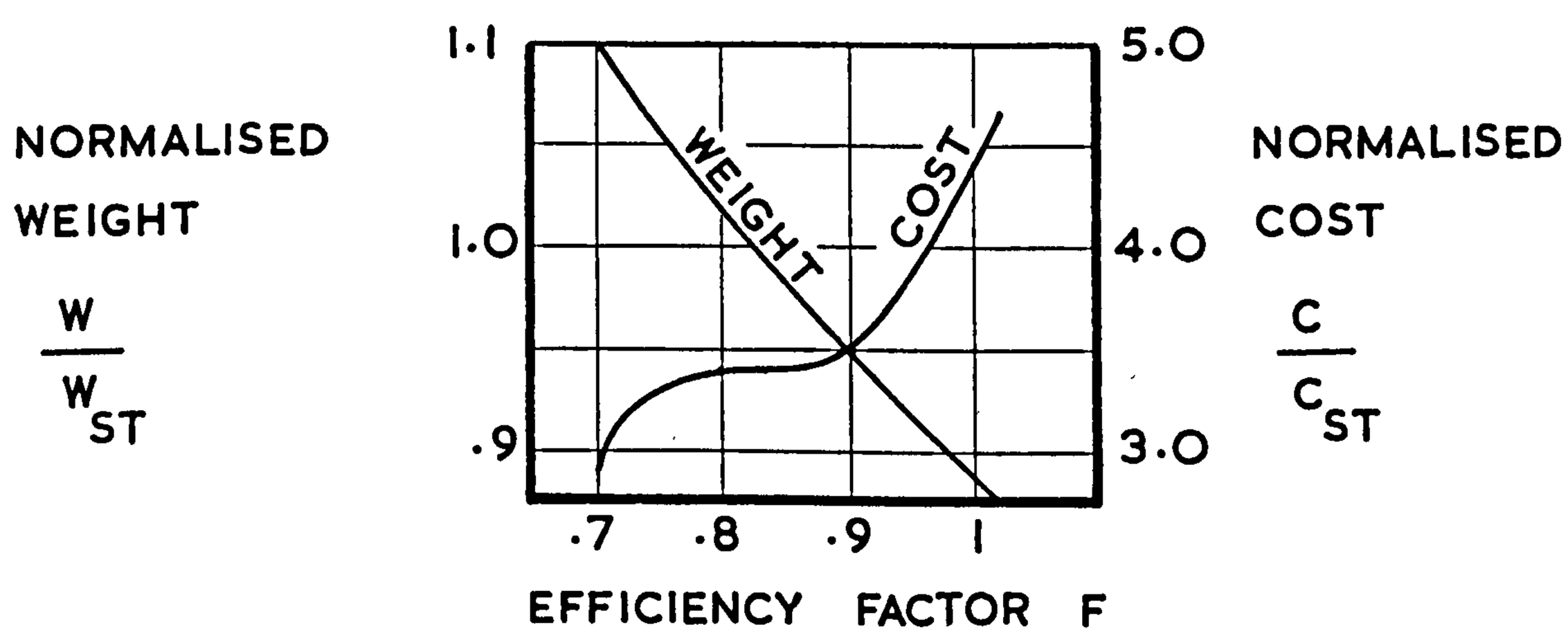

COST AND WEIGHT CURVES AT THE LOAD LEVEL $N_x$ = 2500 LB./IN.

FIG. 7.4 THE ALUMINIUM ALLOY CHEMICALLY ETCHED DESIGN

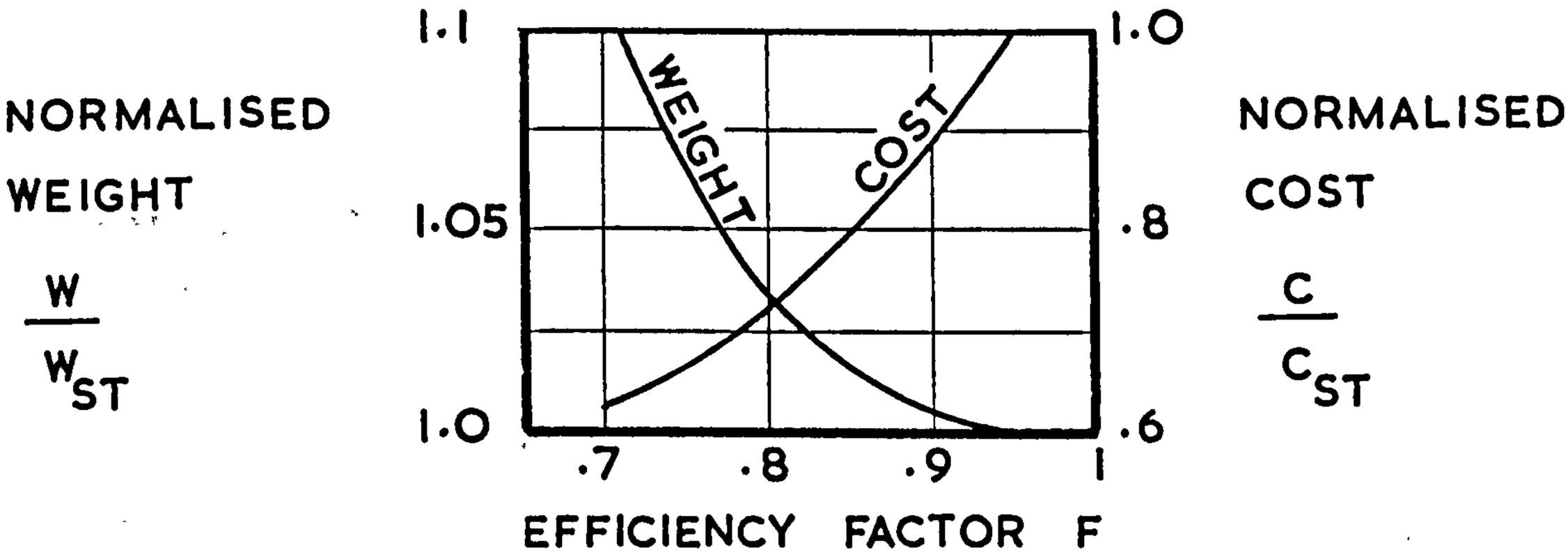


FIG. 7.5 THE ALUMINIUM ALLOY SPIN DIMPLED DESIGN

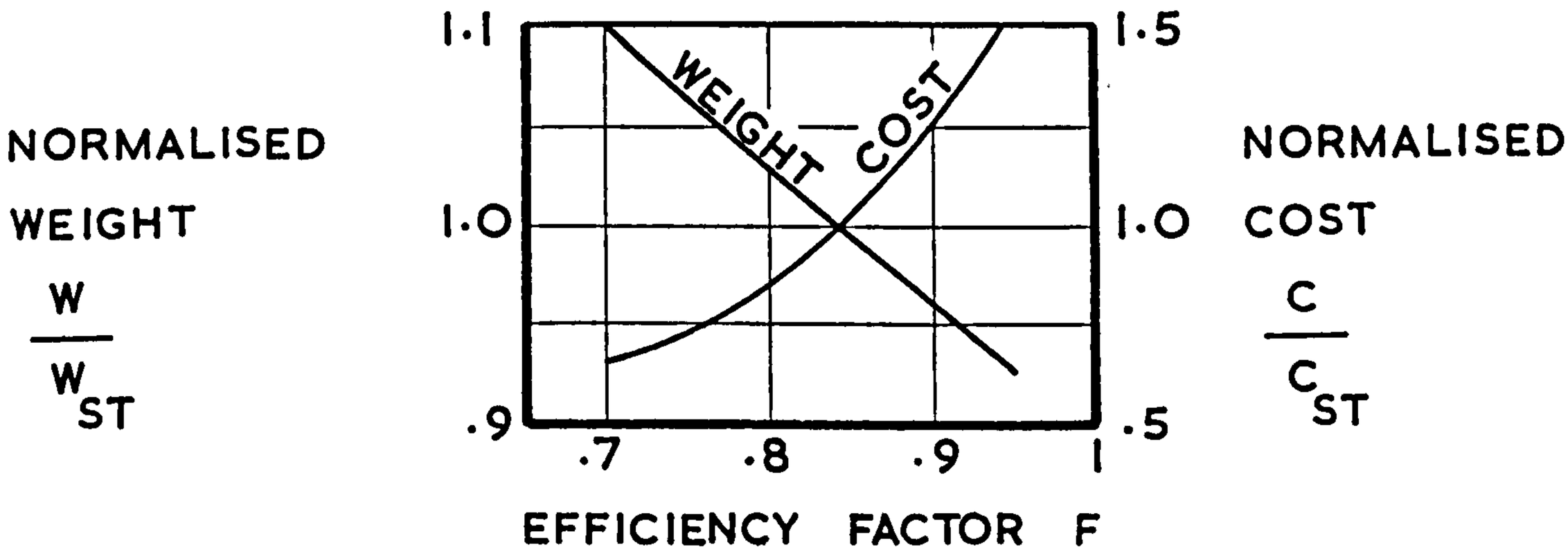


FIG. 7.6 THE TITANIUM ALLOY DESIGN

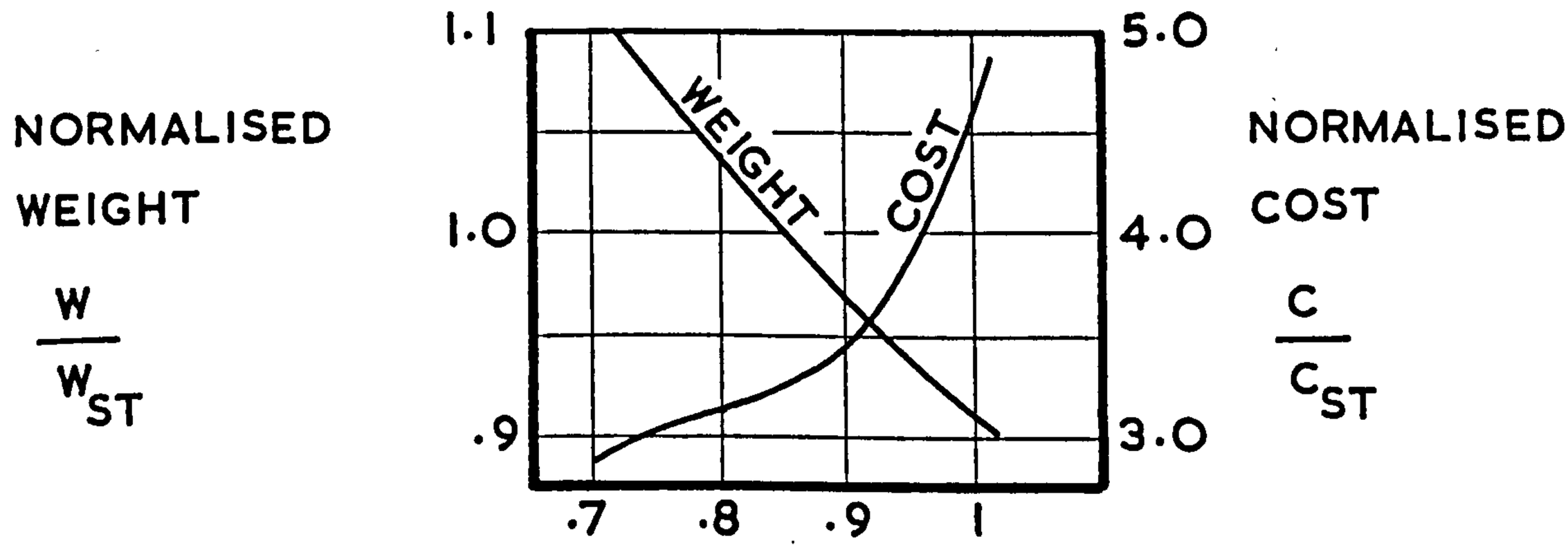

COST AND WEIGHT CURVES AT THE LOAD LEVEL $N_x = 5000$ LB./IN.

FIG. 7.7 THE BASIC ALUMINIUM ALLOY DESIGN

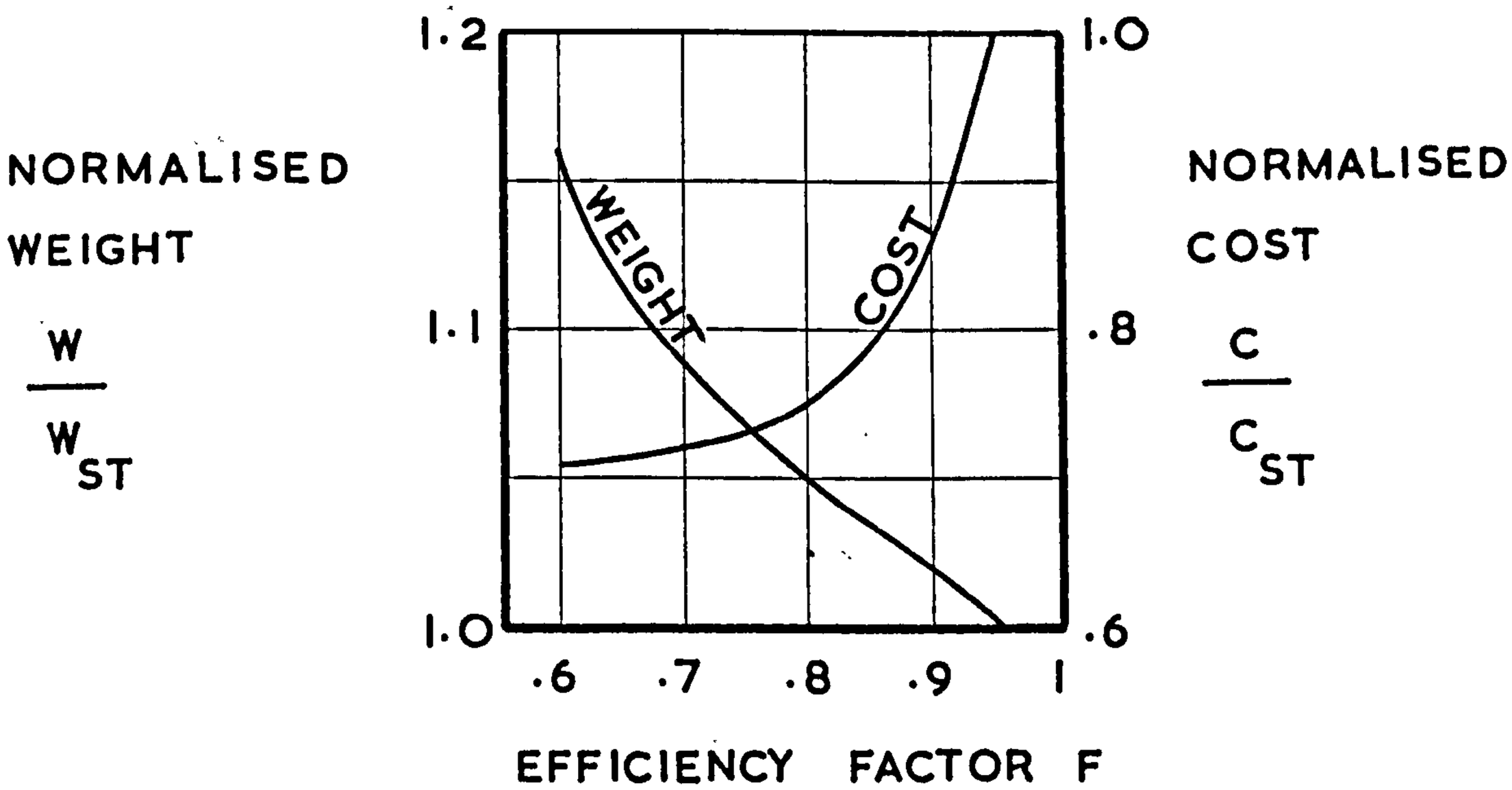


FIG. 7.8 THE TITANIUM ALLOY DESIGN

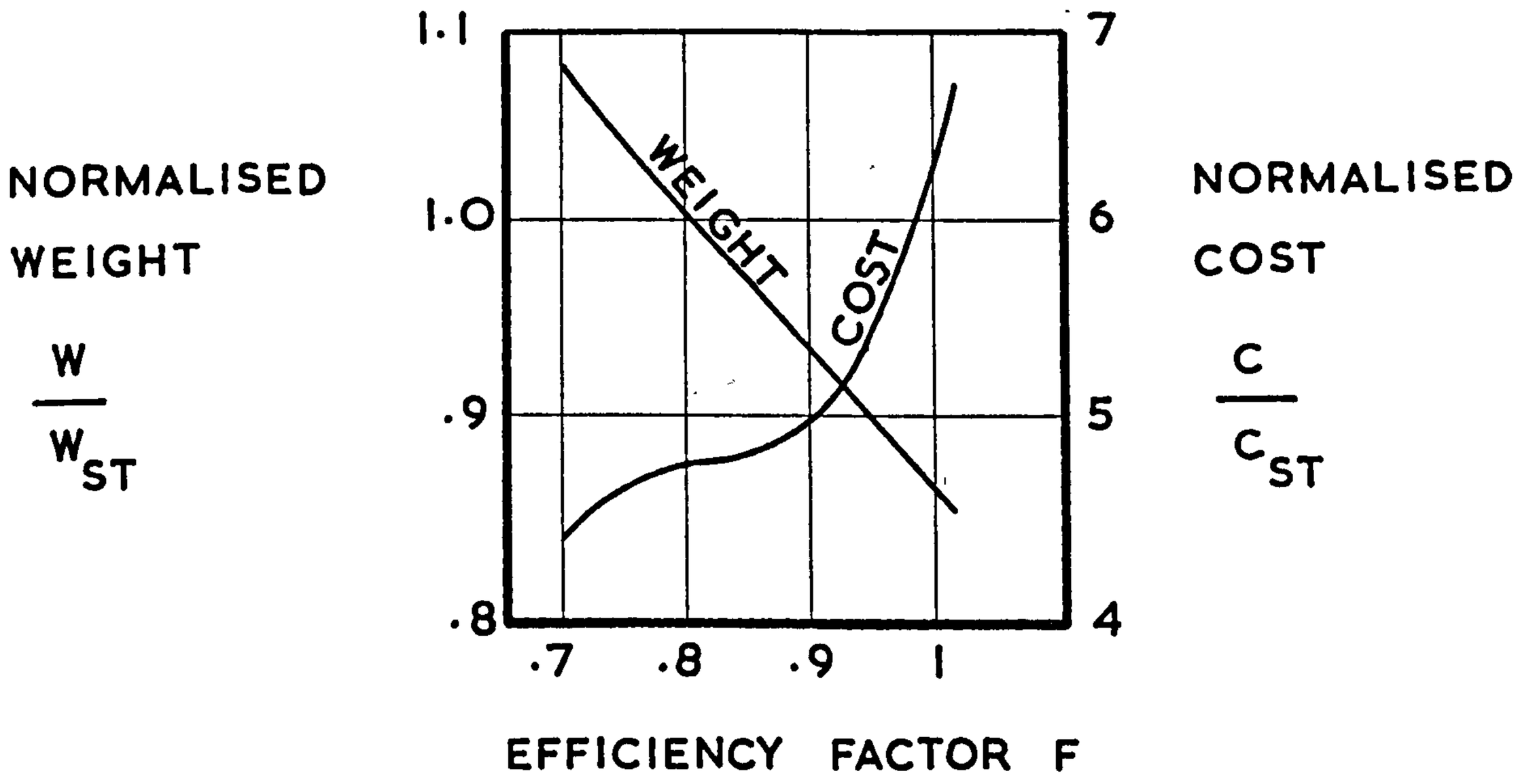

COST AND WEIGHT CURVES AT THE LOAD LEVEL $N_x = 10{,}000$ LB./IN.

FIG. 7.9 THE BASIC ALUMINIUM ALLOY DESIGN

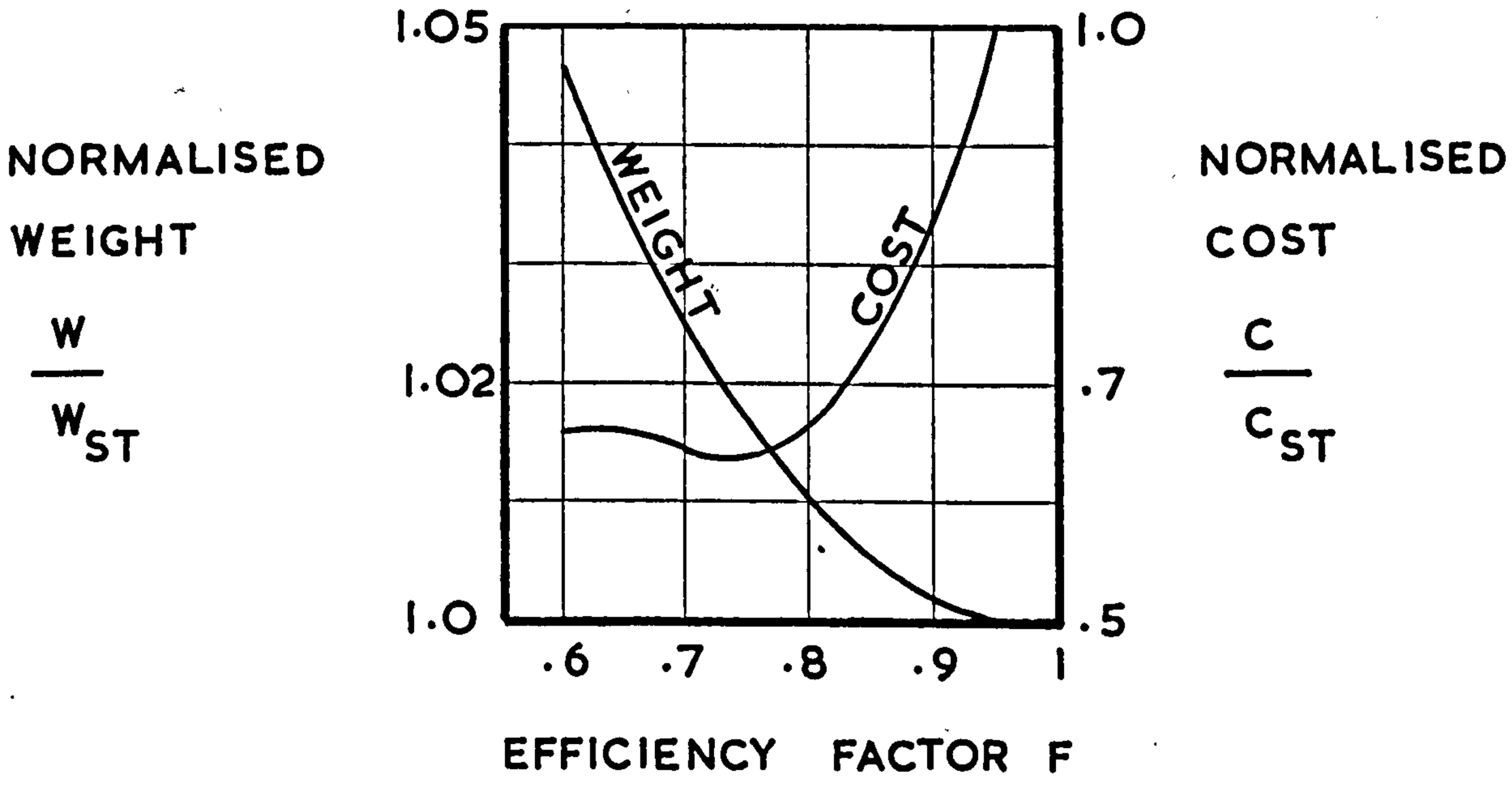


FIG. 7.10 THE TITANIUM ALLOY DESIGN

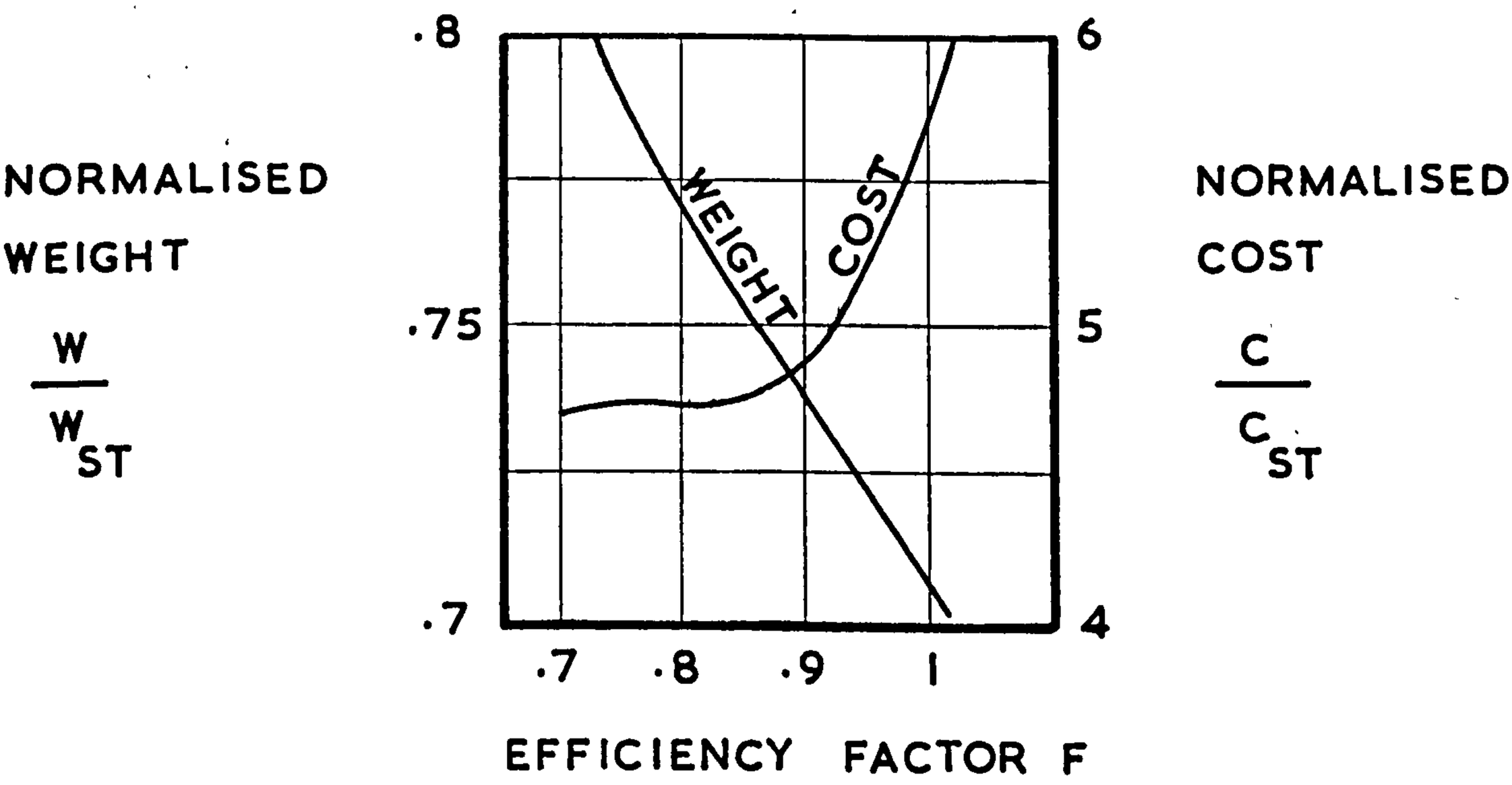

FIG. 7.11 THE USE OF THE MERIT FUNCTION PARAMETER FOR THE LOCATION OF THE OPTIMAL CONFIGURATION

(THE EXAMPLE USES THE BASIC ALUMINIUM ALLOY DESIGN AT A LOAD LEVEL $N_X$ OF 5000 LB./IN. FOR A GLOBAL EXCHANGE RATE VALUE $V_G$ OF £20/LB.)

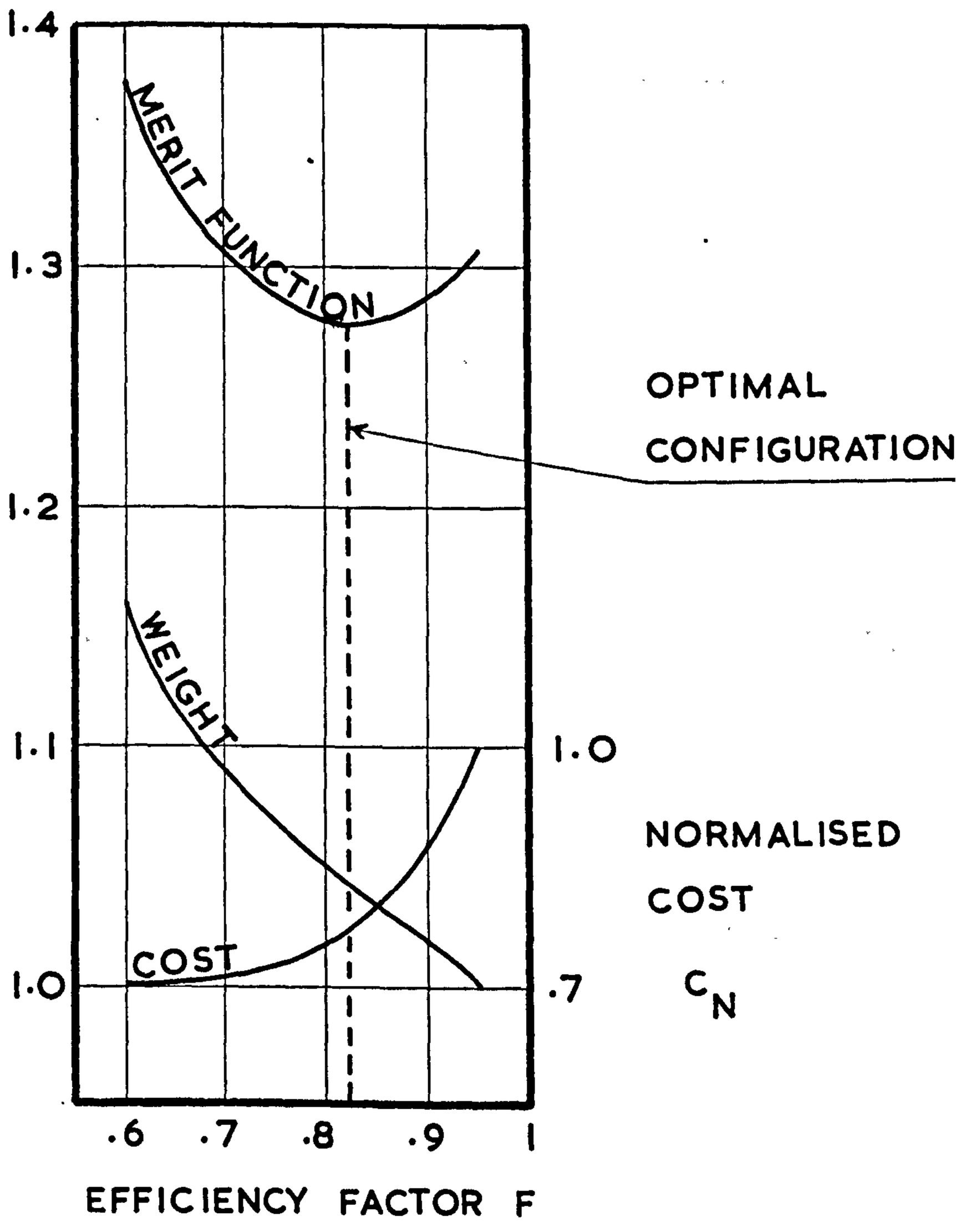

OPTIMAL EFFICIENCY FACTOR CURVES AT THE LOAD LEVEL $N_x$ =1000 LB./IN.

FIG. 7.12 THE ALUMINIUM ALLOY CHEMICALLY ETCHED DESIGN

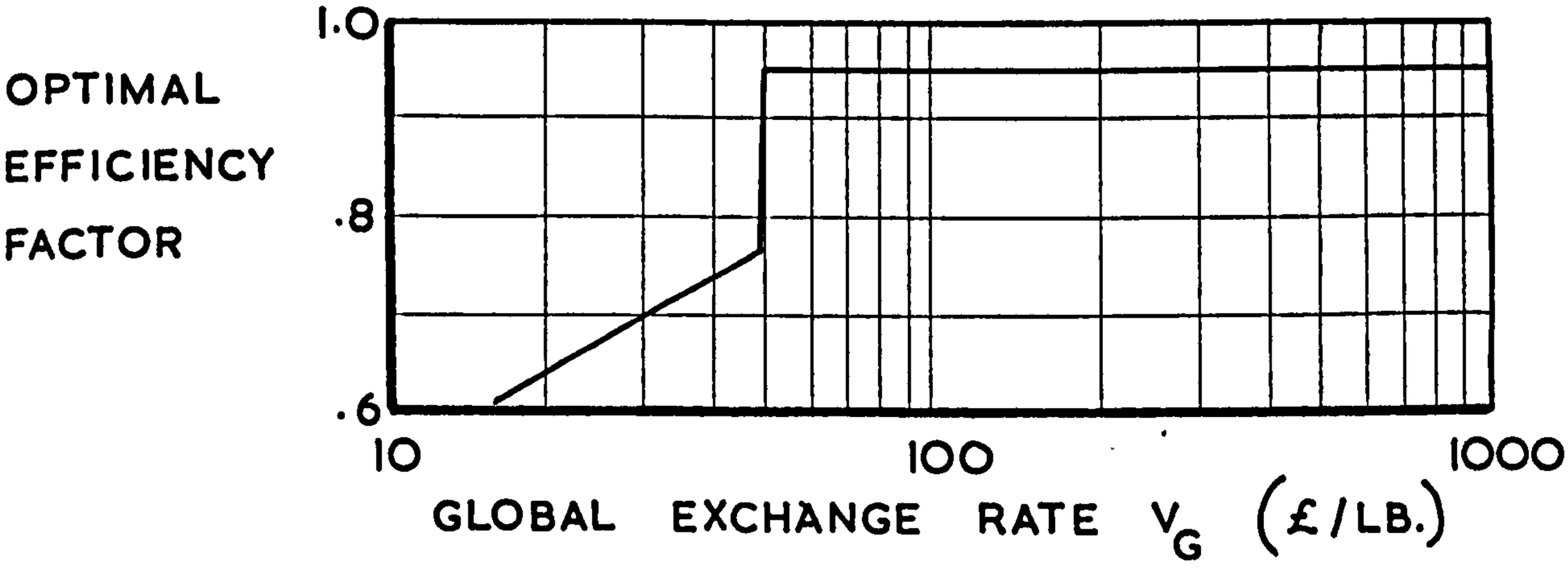


FIG. 7.13 THE ALUMINIUM ALLOY SPIN DIMPLED DESIGN

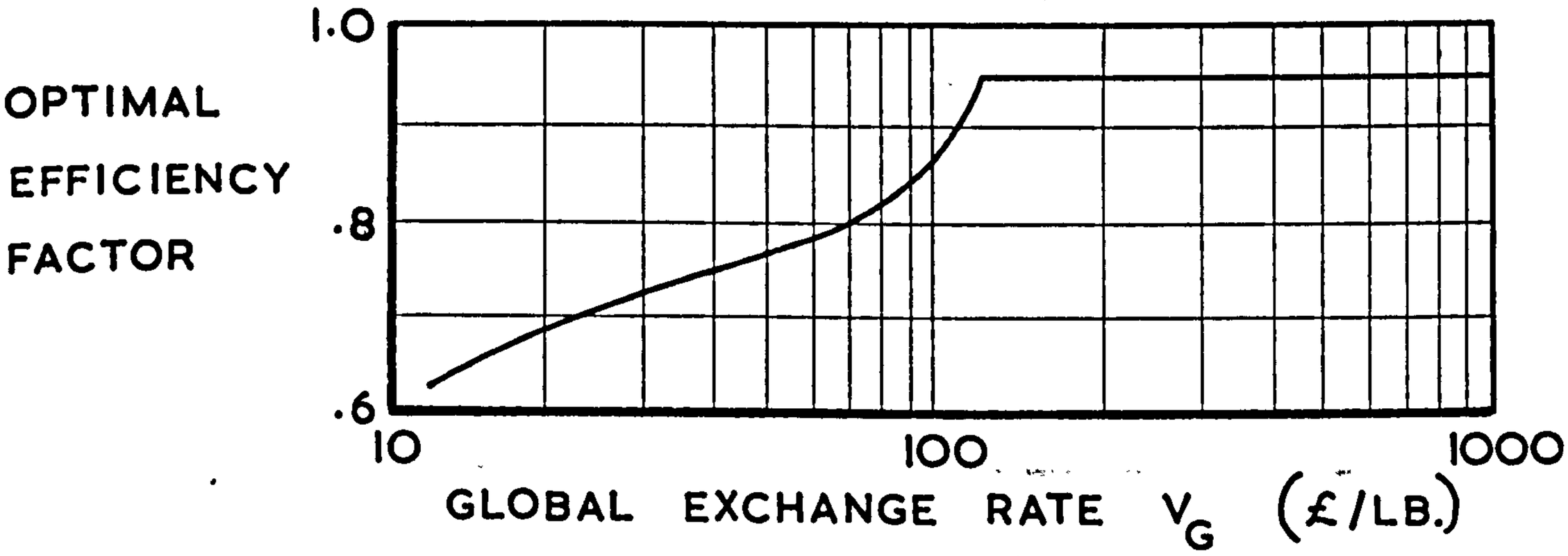


FIG. 7.14 THE TITANIUM ALLOY DESIGN

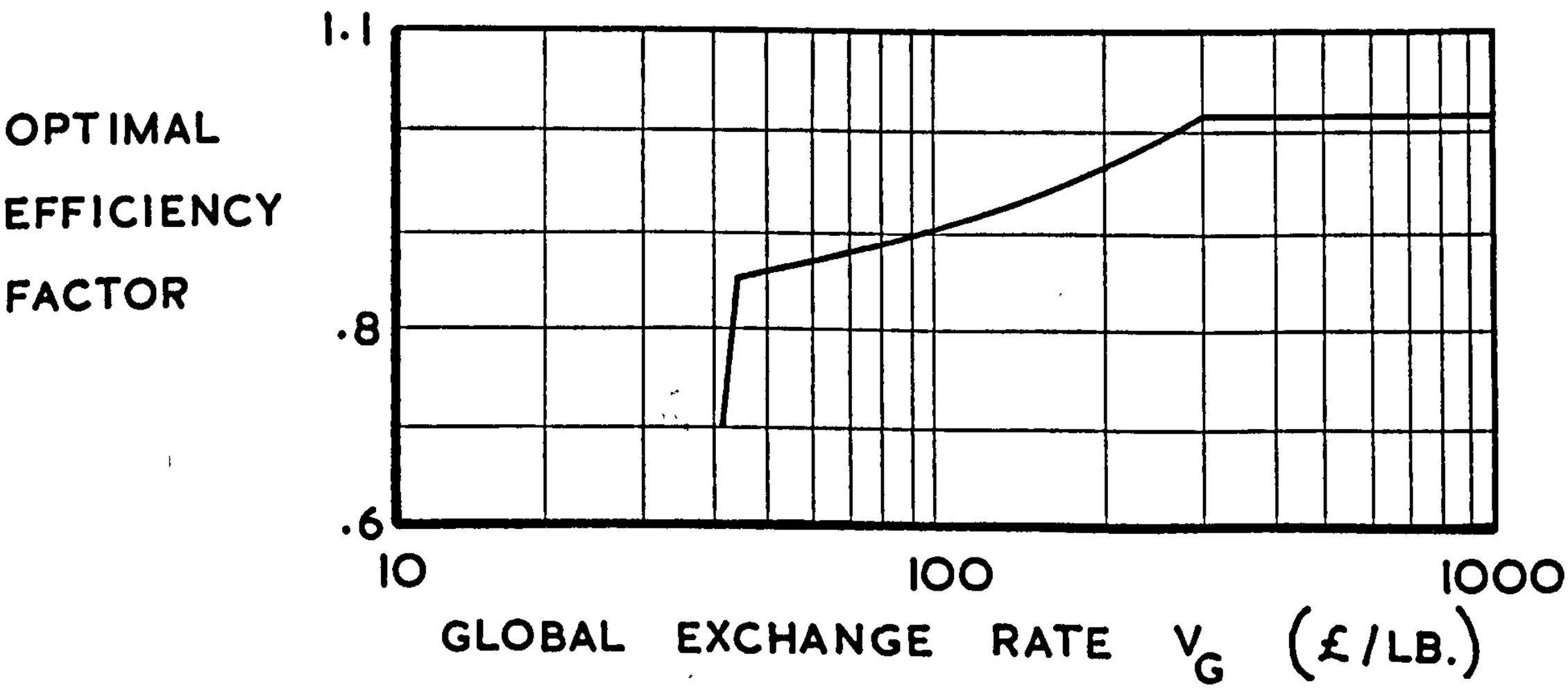

OPTIMAL EFFICIENCY FACTOR CURVES AT THE LOAD LEVEL $N_x = 2500$ LB./IN.

FIG. 7.15 THE ALUMINIUM ALLOY CHEMICALLY ETCHED DESIGN

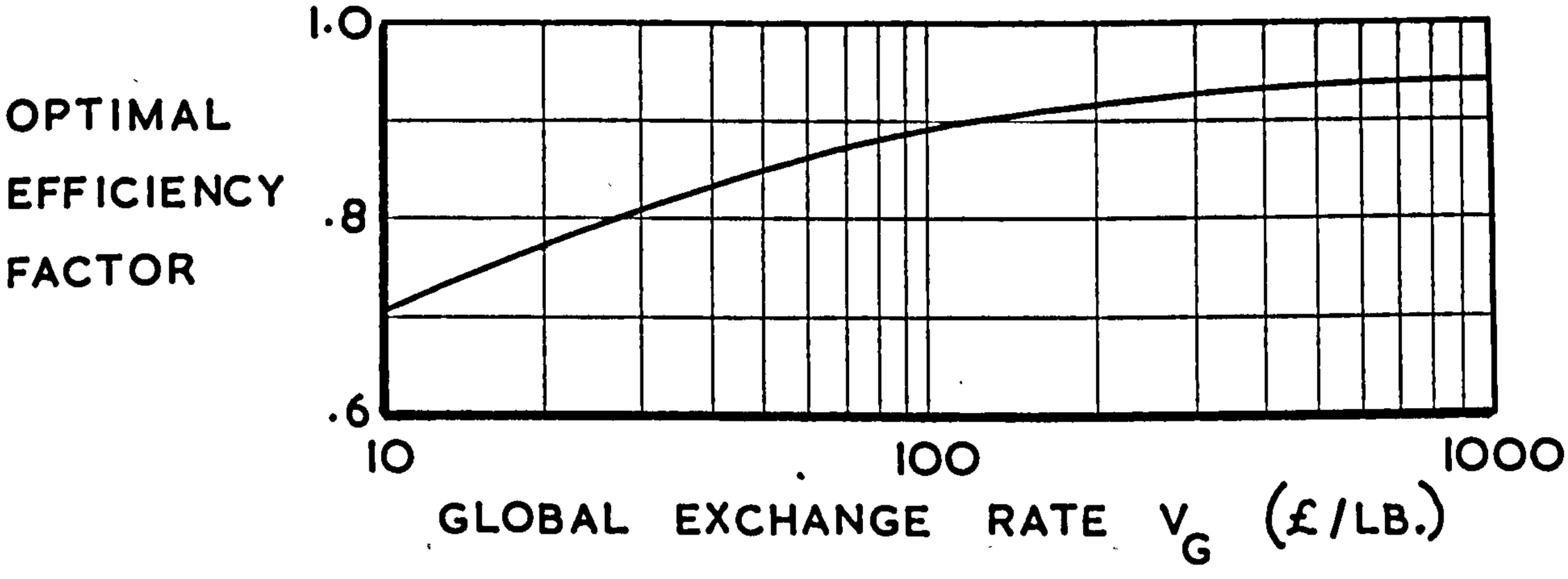


FIG. 7.16 THE ALUMINIUM ALLOY SPIN DIMPLED DESIGN

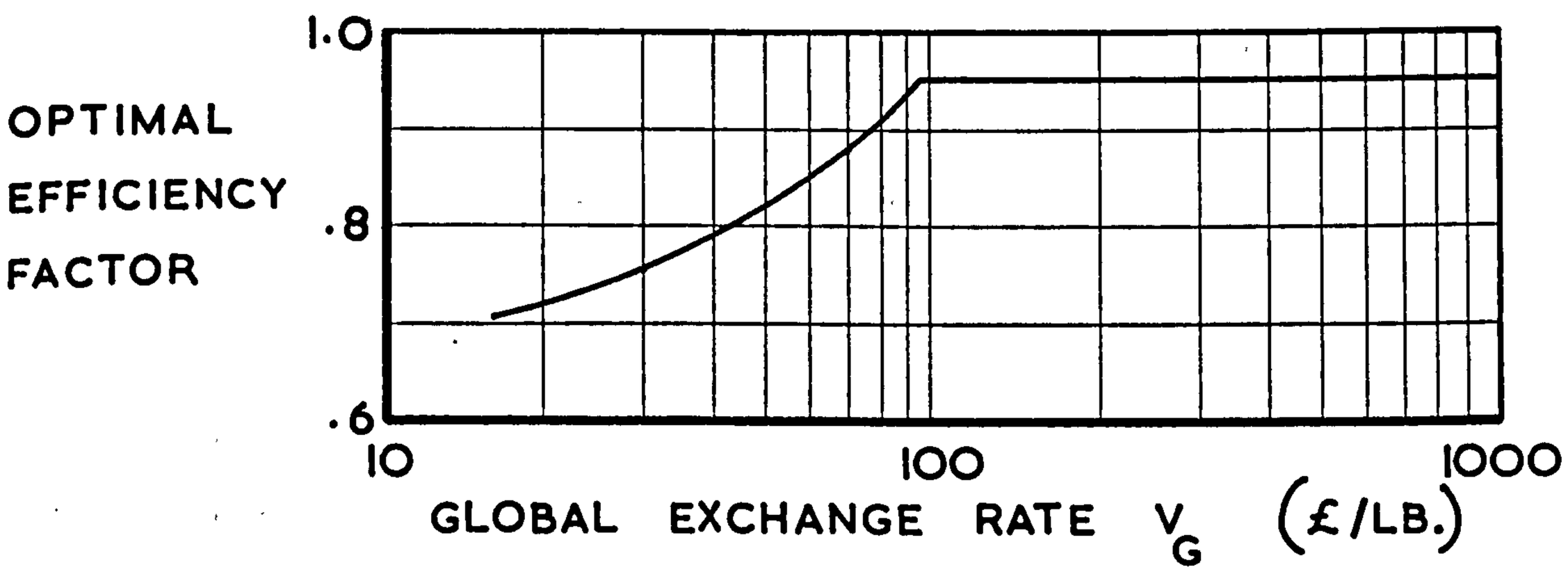


FIG. 7.17 THE TITANIUM ALLOY DESIGN

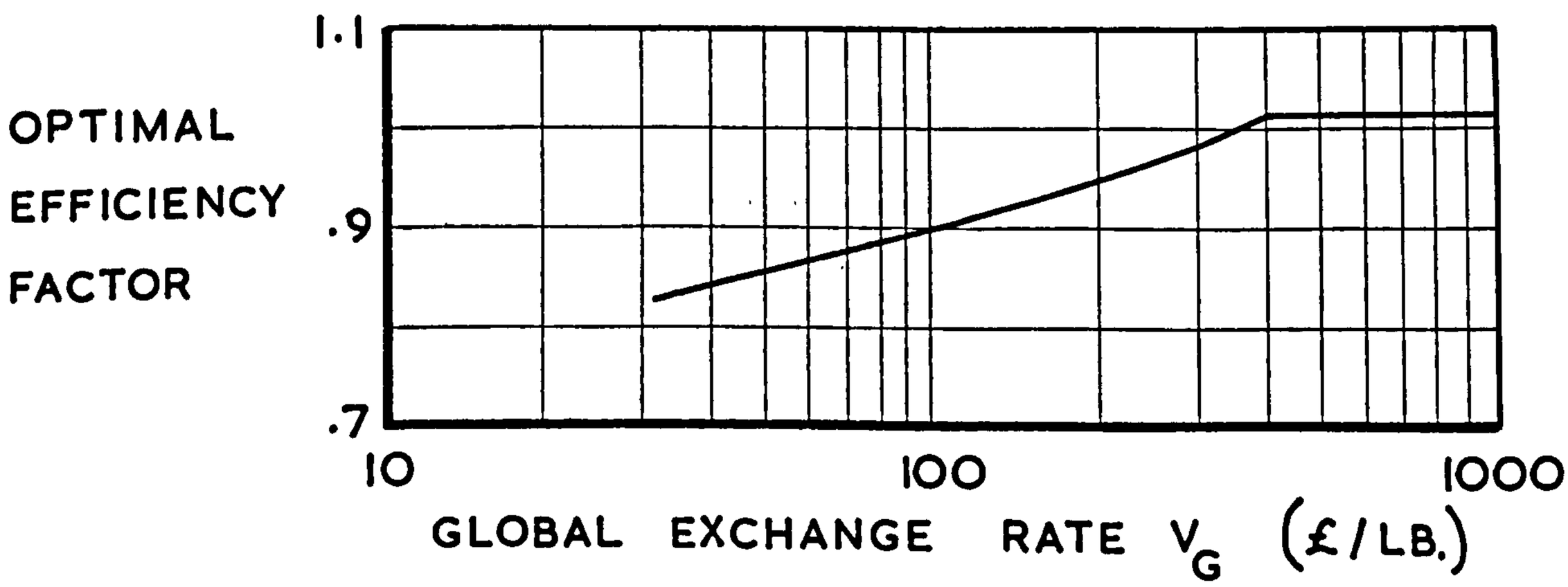

OPTIMAL EFFICIENCY FACTOR CURVES AT THE LOAD LEVEL $N_x = 5000$ LB./IN.

FIG. 7.18 THE BASIC ALUMINIUM ALLOY DESIGN

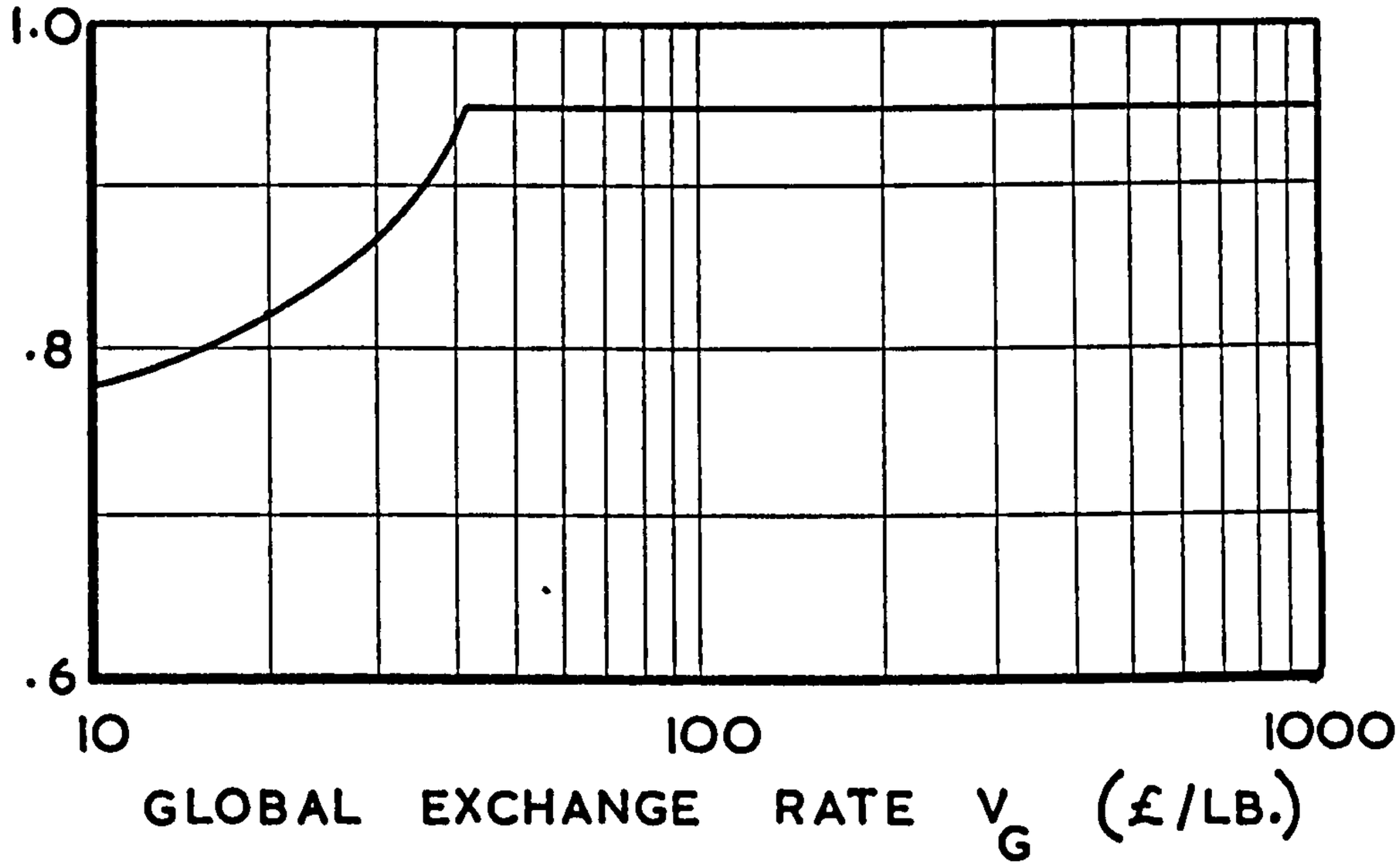


FIG. 7.19 THE TITANIUM ALLOY DESIGN

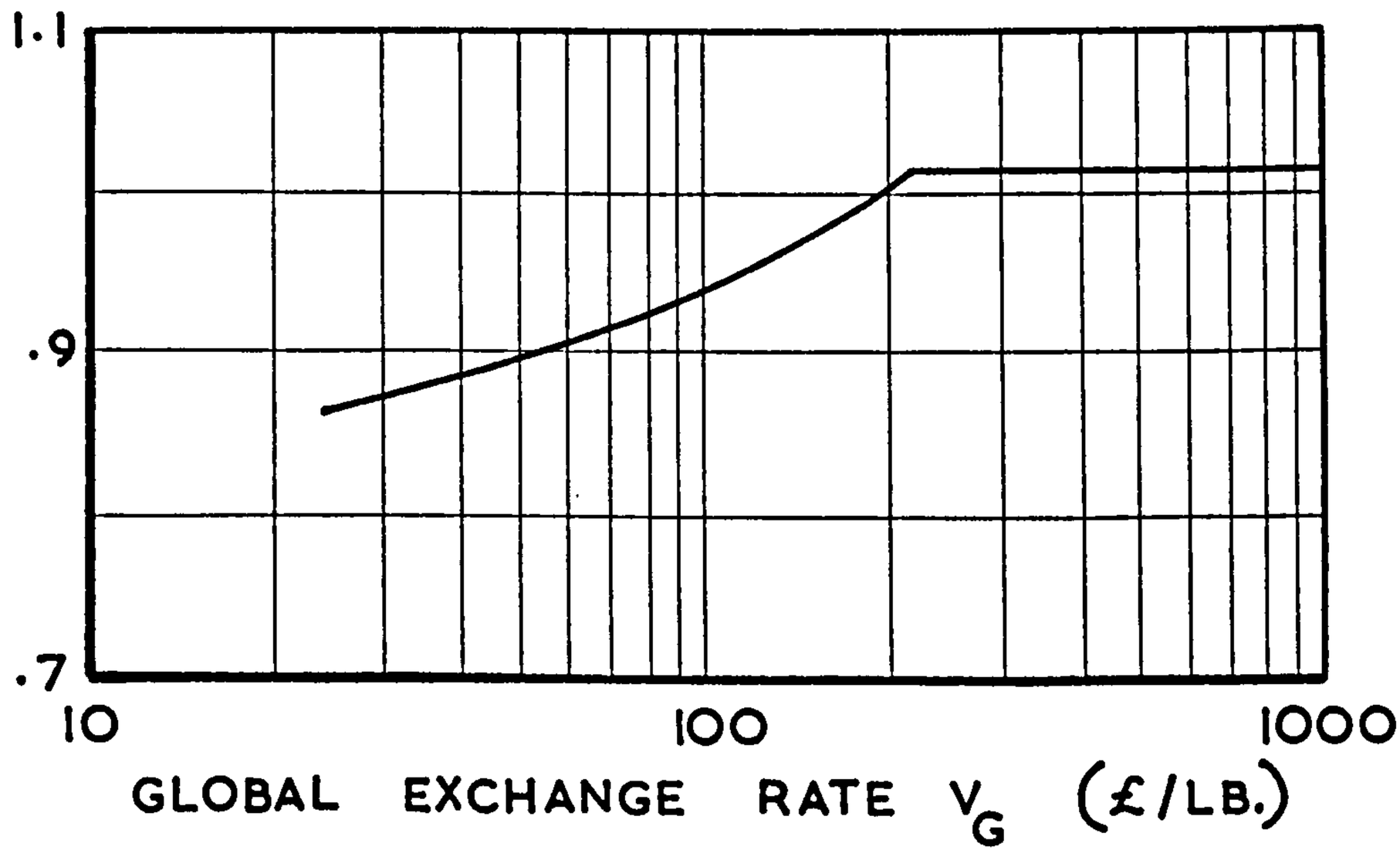

OPTIMAL EFFICIENCY FACTOR CURVES AT THE LOAD LEVEL $N_x$ = 10,000 LB./IN.

FIG. 7.20 THE BASIC ALUMINIUM ALLOY DESIGN

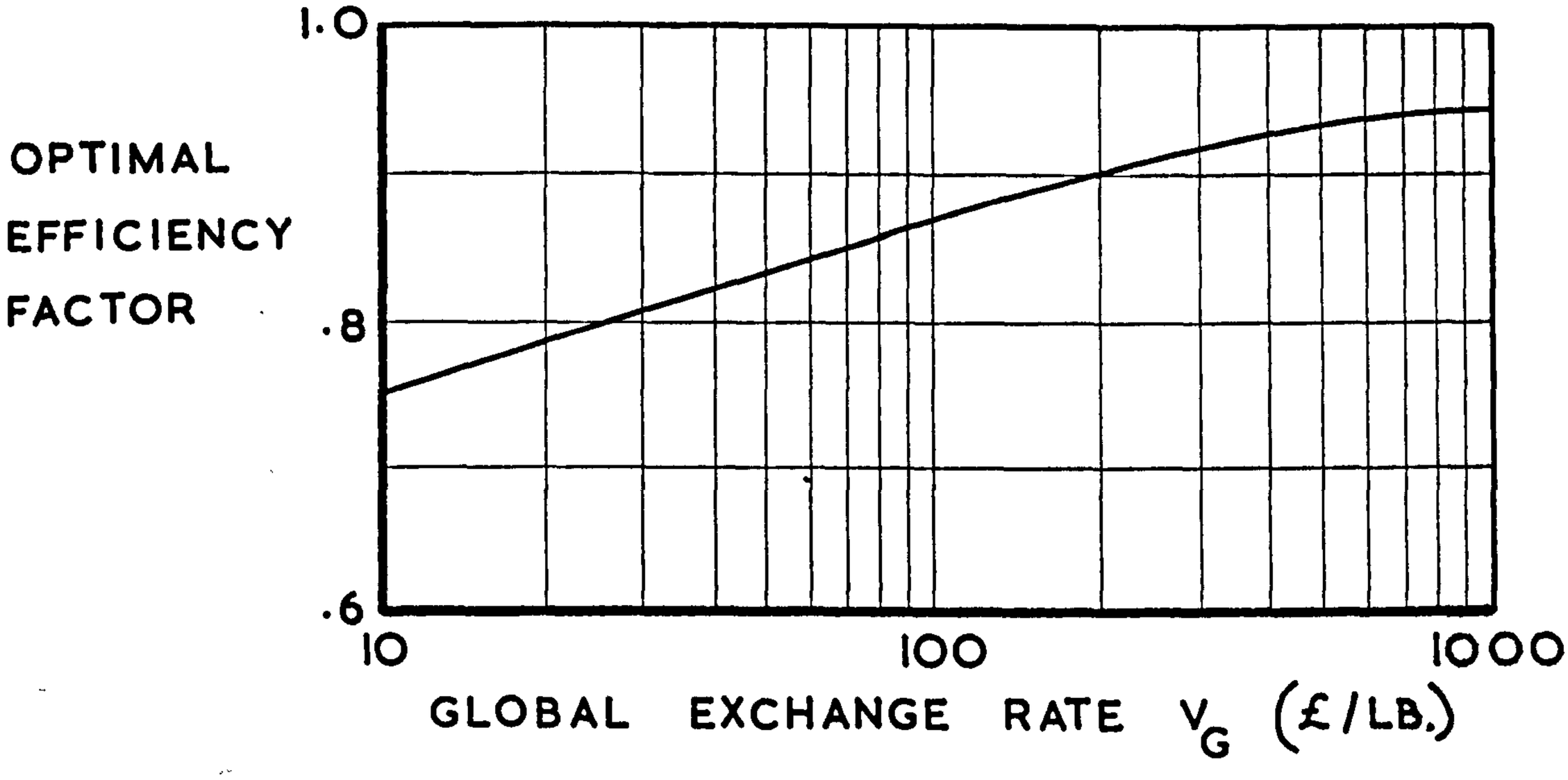


FIG. 7.21 THE TITANIUM ALLOY DESIGN

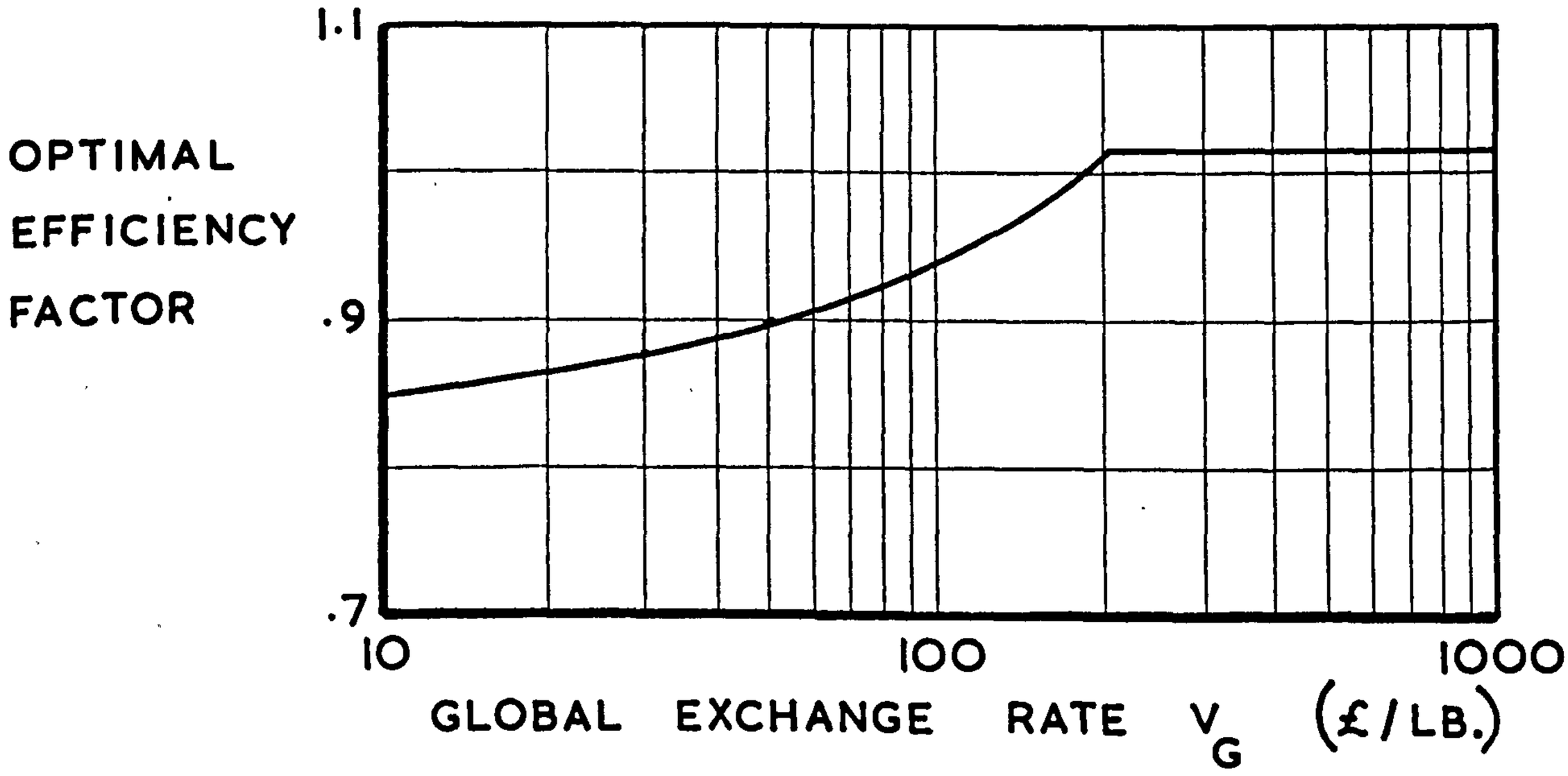

# C H A P T E R  8

# THE VARIATION OF THE OPTIMAL STRUCTURAL SYSTEM

## 8.1 Introduction

An important aspect of the research program was the examination of the manner in which the structural system giving the optimal solution varied as the operative design conditions, which specified the end loading and the global exchange rate values, were varied.

## 8.2 The Location of the Optimal System

At each value of the end loading, the merit function values of each system were generated by incorporating the structural weight equation (7.2) and the unit cost equation (7.3) in equation (2.27). The alternative configurations for each system, which were examined in Chapter 7, were retained in this analysis in order to compare the best configuration of each system. The procedure described in section 7.3 was used for the location of the system having the minimum value of the merit function, this being the optimal system.

The variations of the normalised merit function values, defining the variation of the optimal structural systems, with global exchange rate are presented in figs. 8.1 to 8.4 and the corresponding variations of the operative efficiency factor values of each optimal system are presented in figs. 8.5 to 8.9.

The global exchange rate values defining the change-over from one structural system to another, for the most efficient structure, are summarised in Table 8.1.

## 8.3 Discussion of the Results

As the global exchange rate values employed in existing aircraft projects may be assumed to lie within the £10/lb. to £300/lb. band, the results show that the titanium alloy systems only become viable propositions at load levels greater than 5,000 lb./in., when the weight saving potential of the titanium alloy material, relative to aluminium alloy, is exploited. In fact, the results of the analysis suggest that load levels in excess of 10,000 lb./in. are required for the most efficient incorporation of titanium alloy material in the airframes of subsonic civil aircraft, which are designed to global exchange rate values of the order of £50/lb.

At a load level of 1,000 lb./in. the titanium alloy system gave the optimal solution at a global exchange rate value of £3,451/lb., due to a small saving in weight compared to the aluminium alloy systems. The saving in weight only arose because the cover configuration of the titanium alloy system allowed a higher maximum efficiency factor to be attained, compared to the configuration of the aluminium alloy systems. The weight saving of the titanium alloy system would vanish if higher efficiency configurations were adopted for the aluminium alloy systems. Hence, the use of titanium alloy material in a low load level application would appear inefficient, unless dictated by other considerations such as the existence of a kinetic heating environment.

TABLE 8.1 The variation of the optimal structural type with global exchange rate.

| Applied end loading Nx (lb./in.) | Aluminium alloy structures | | | Titanium alloy design |
|---|---|---|---|---|
| | Basic design | Chemically etched design | Spin dimpled design | |
| 1000 | - | $V_G < 33$ | $33 < V_G < 3451$ | $V_G > 3451$ |
| 2500 | $V_G < 15$ | $15 < V_G < 85$ | $85 < V_G < 1906$ | $V_G > 1906$ |
| 5000 | $V_G < 240$ | - | - | $V_G > 240$ |
| 10000 | $V_G < 61$ | - | - | $V_G > 61$ |

Global exchange rate values in £/lb.

FIG. 8.1 THE OPTIMAL STRUCTURAL SYSTEMS AT THE LOAD LEVEL $N_x = 1000$ LB./IN.

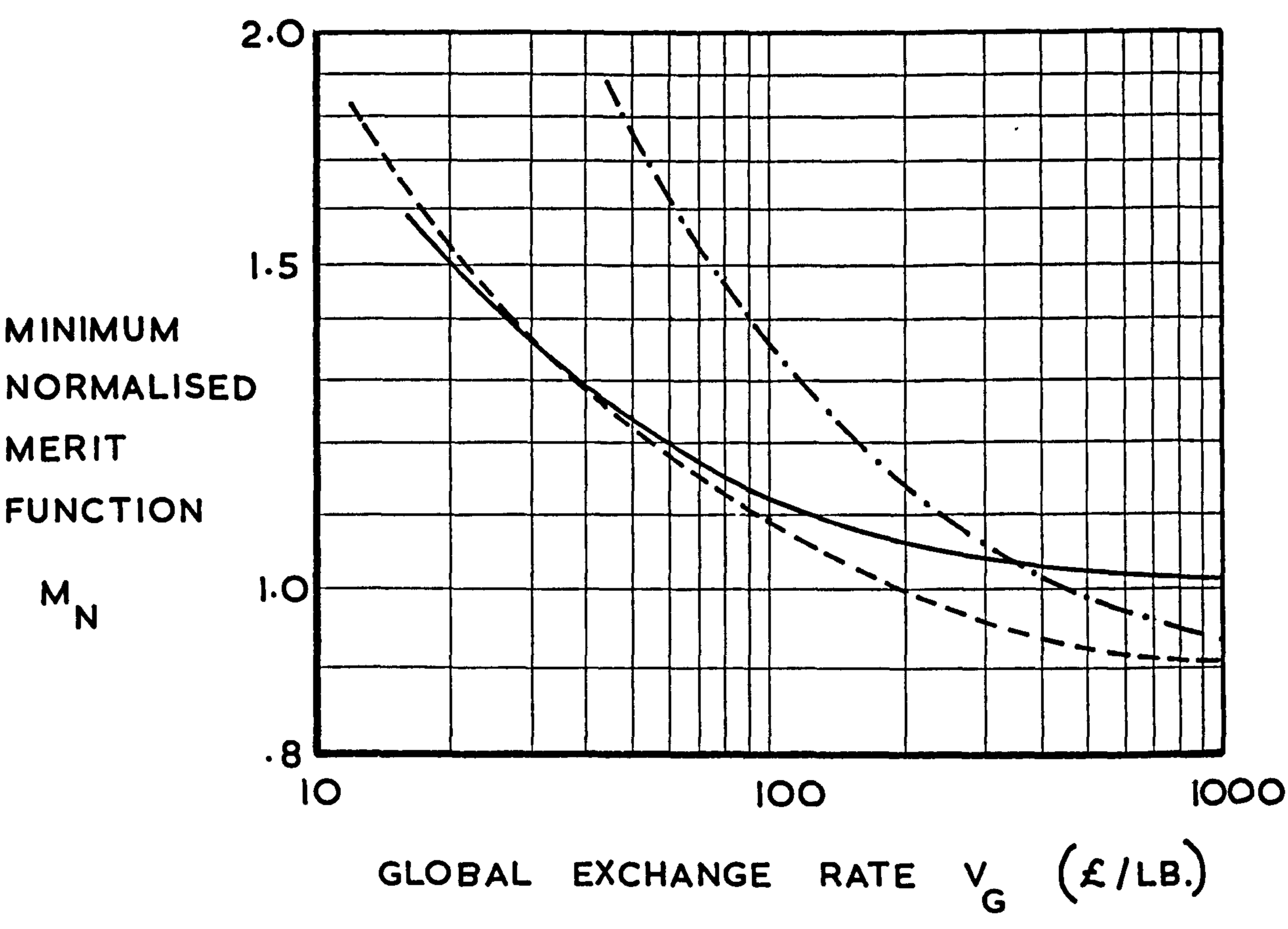


KEY

——— ALUMINIUM ALLOY CHEMICALLY ETCHED DESIGN

– – – ALUMINIUM ALLOY SPIN DIMPLED DESIGN

—·— TITANIUM ALLOY DESIGN

FIG. 8.2 THE OPTIMAL STRUCTURAL SYSTEMS AT THE LOAD LEVEL $N_x = 2500$ LB./IN.

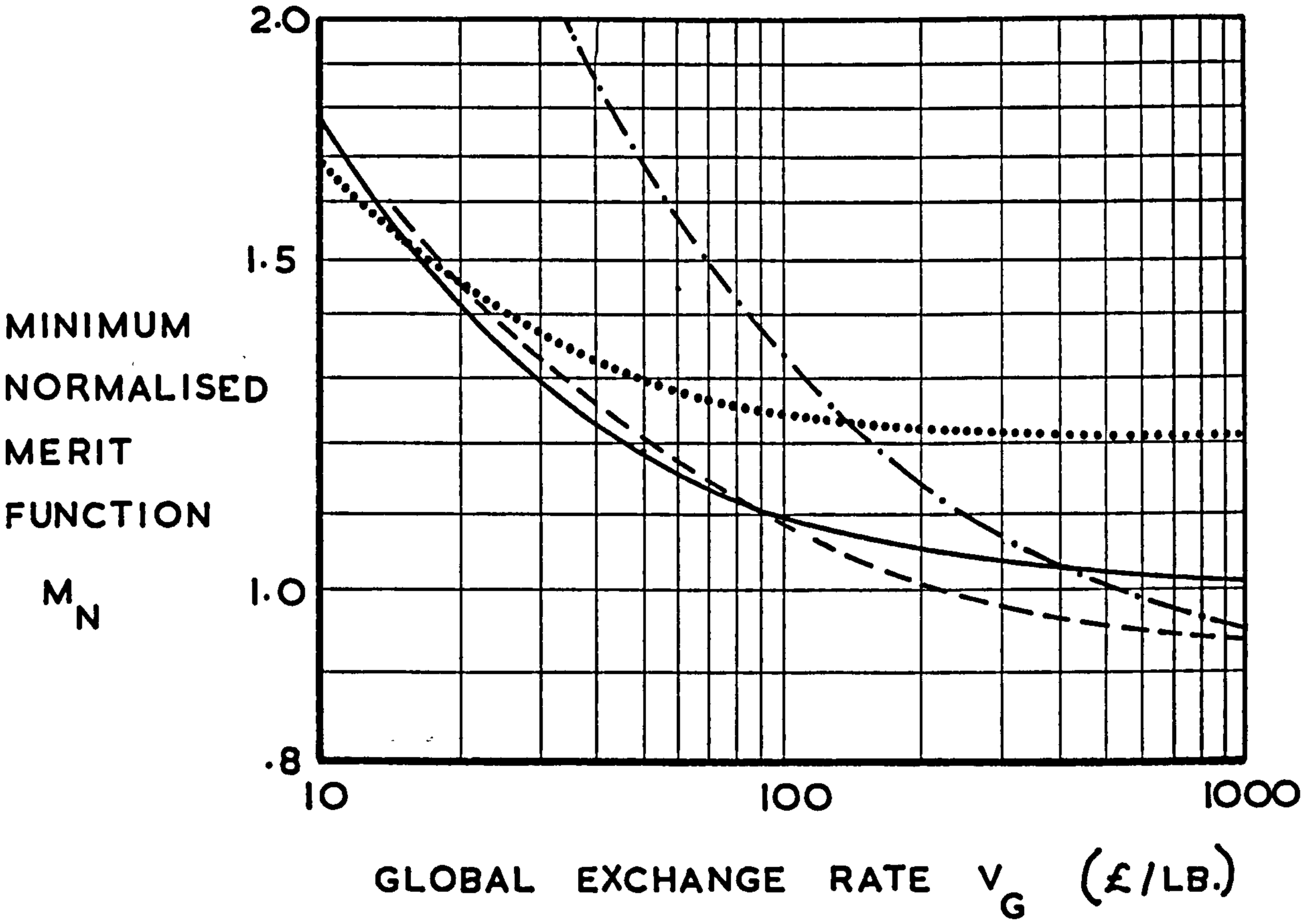


KEY

..... BASIC ALUMINIUM ALLOY DESIGN FOR AN EFFICIENCY FACTOR F = 0.6

——— ALUMINIUM ALLOY CHEMICALLY ETCHED DESIGN

– – – ALUMINIUM ALLOY SPIN DIMPLED DESIGN

—·— TITANIUM ALLOY DESIGN

FIG. 8.3 THE OPTIMAL STRUCTURAL SYSTEMS AT THE LOAD LEVEL $N_x = 5000$LB./IN.

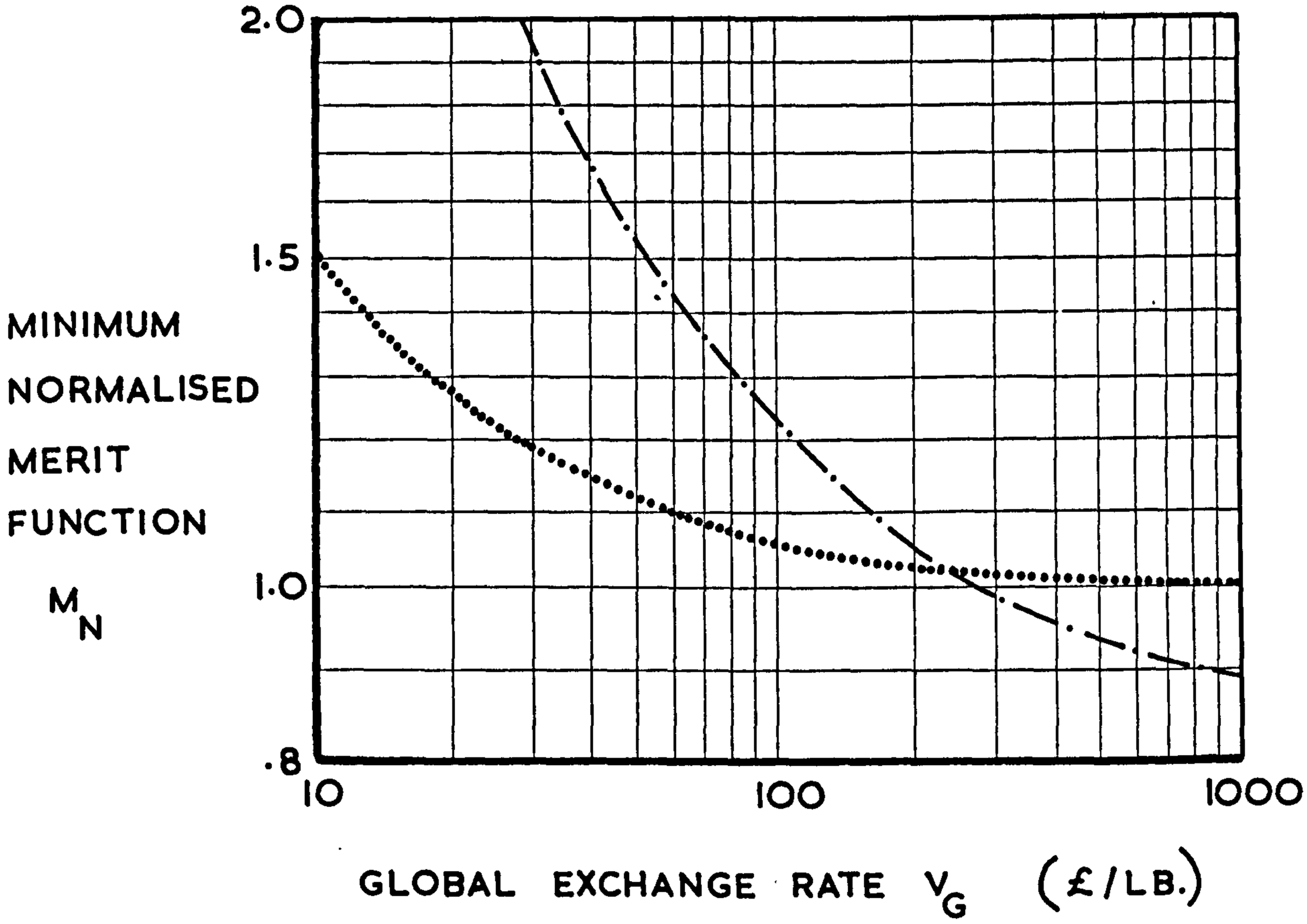


KEY

••••••••• BASIC ALUMINIUM ALLOY DESIGN

—·— TITANIUM ALLOY DESIGN

FIG. 8.4 THE OPTIMAL STRUCTURAL SYSTEMS AT THE LOAD LEVEL $N_x$ =10,000LB./IN.

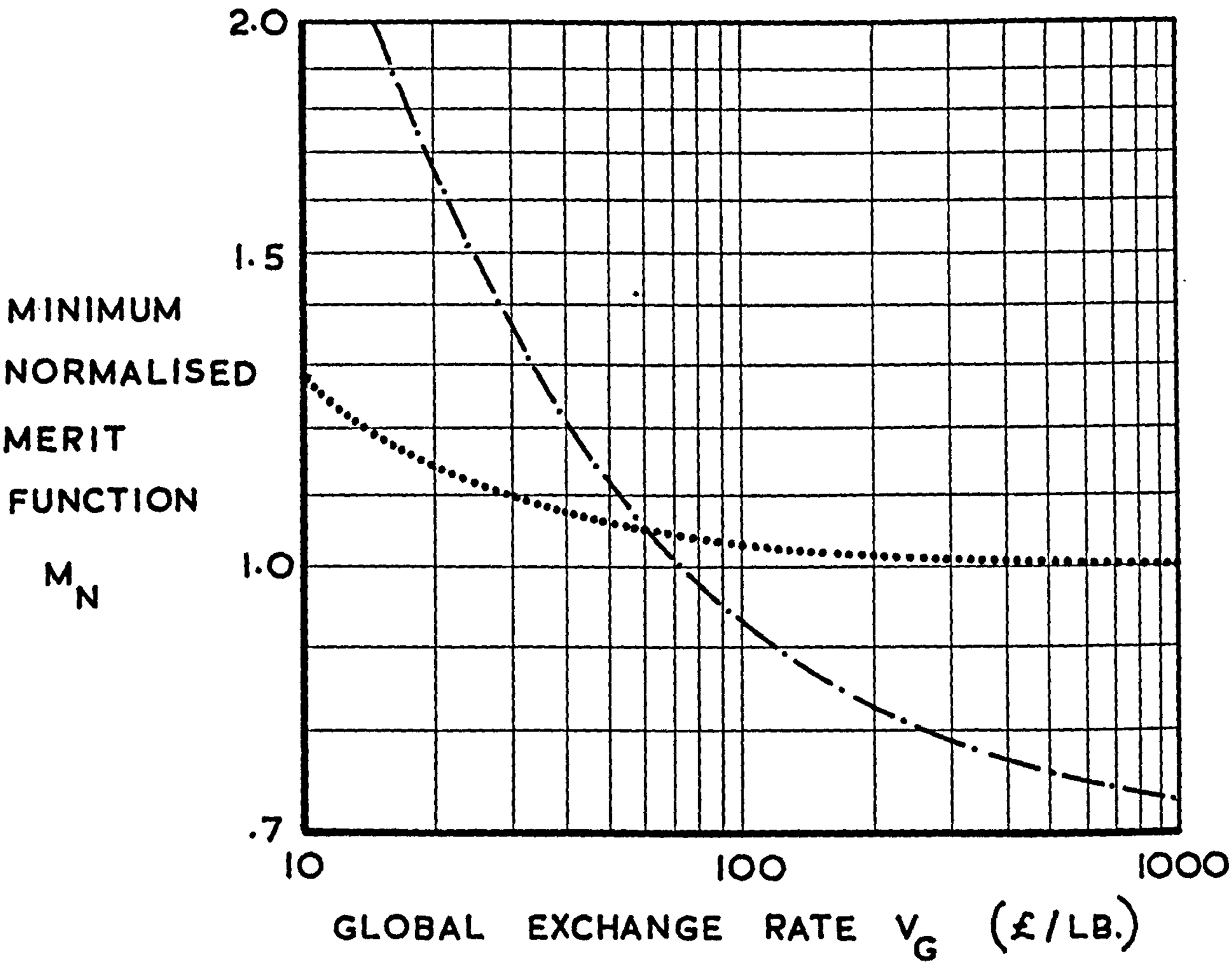


KEY

..... BASIC ALUMINIUM ALLOY DESIGN

—·— TITANIUM ALLOY DESIGN

FIG. 8.5 THE OPTIMAL STRUCTURAL CONFIGURATIONS AT THE LOAD LEVEL $N_x$ = 1000 LB./IN.

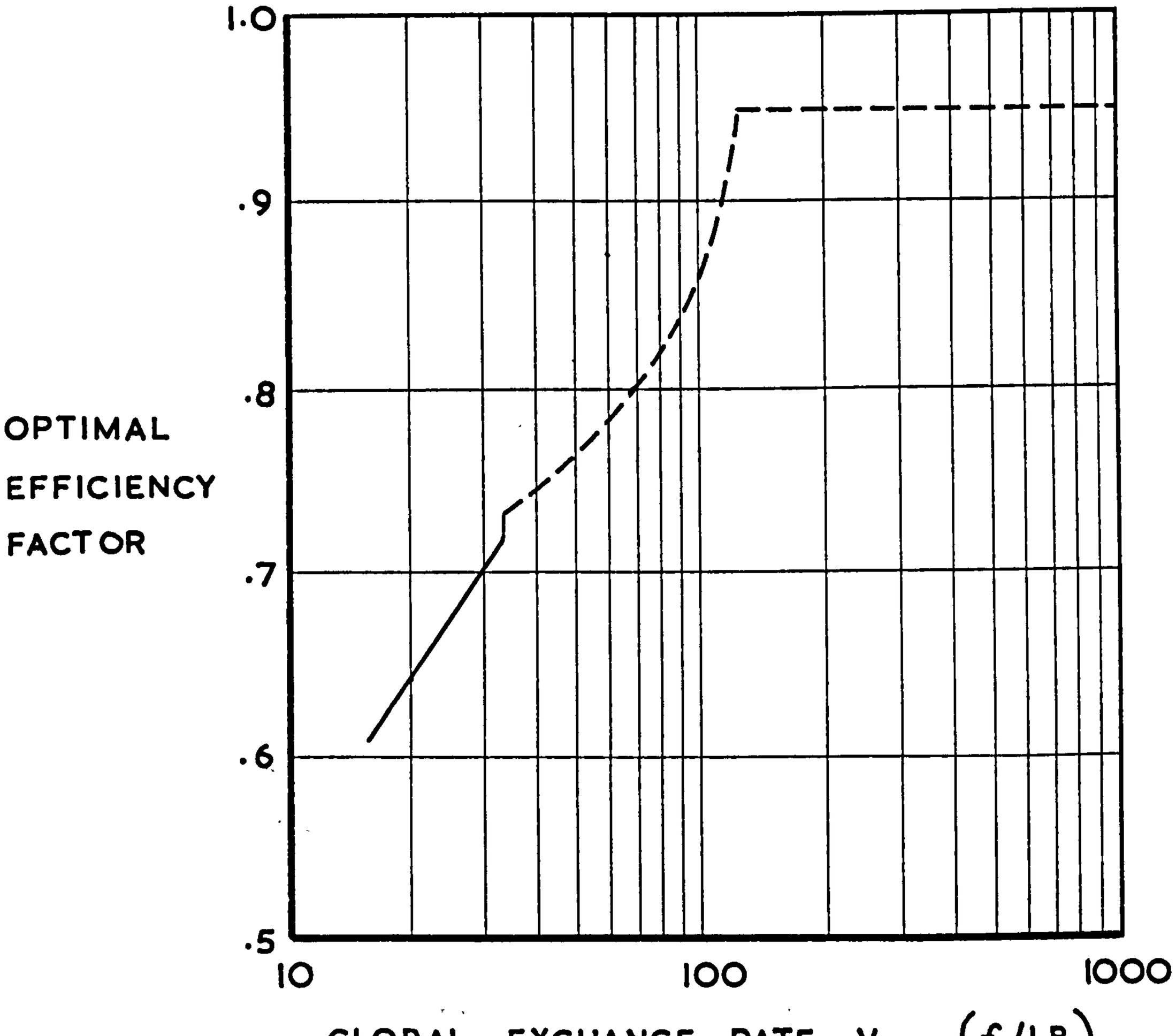


KEY

——— ALUMINIUM ALLOY CHEMICALLY ETCHED DESIGN

– – – ALUMINIUM ALLOY SPIN DIMPLED DESIGN

FIG. 8.6 THE OPTIMAL STRUCTURAL CONFIGURATIONS AT THE LOAD LEVEL $N_x = 2500$ LB./IN.

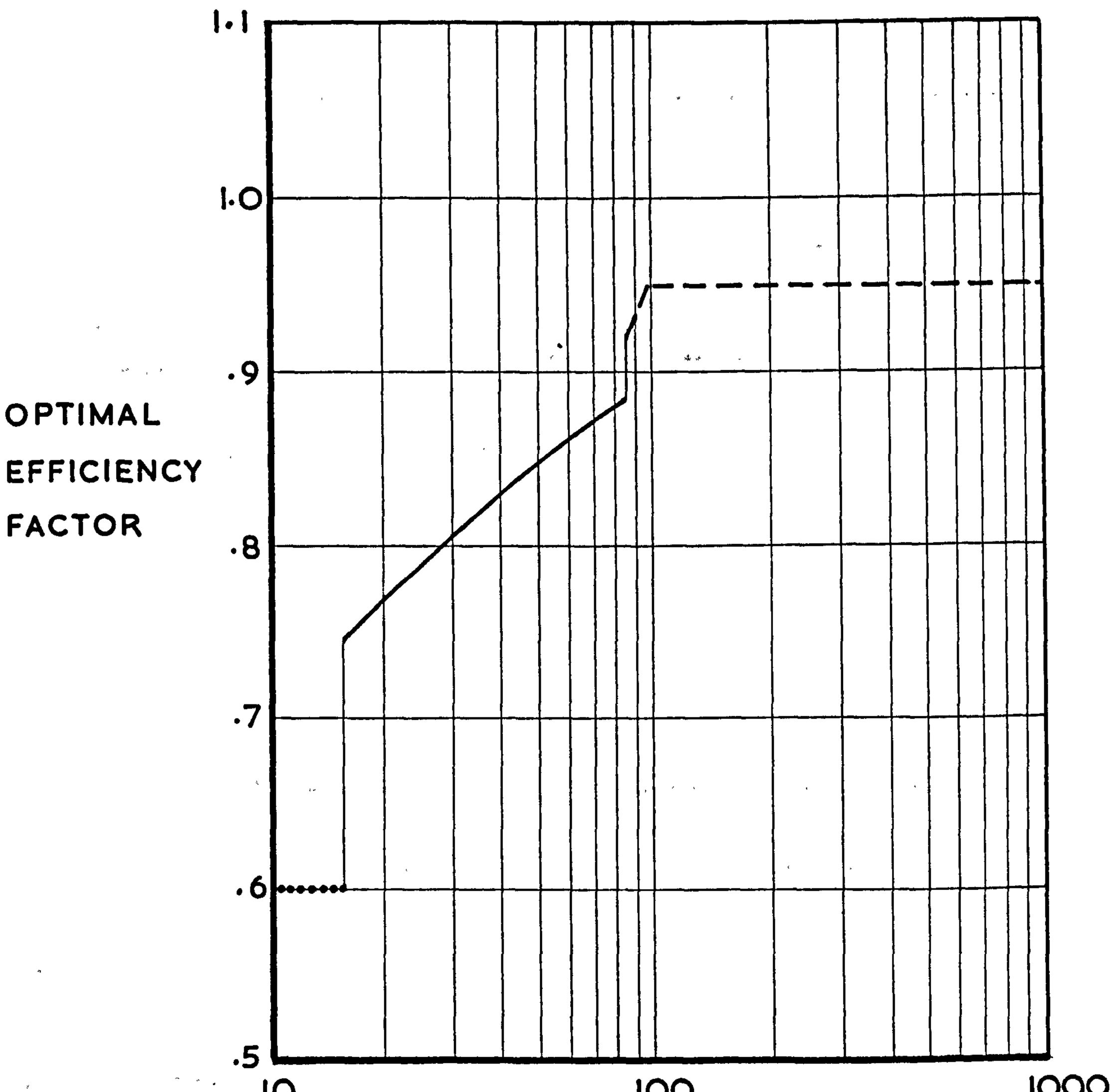

FIG. 8.7 THE OPTIMAL STRUCTURAL CONFIGURATIONS AT THE LOAD LEVEL $N_x = 5000$ LB./IN.

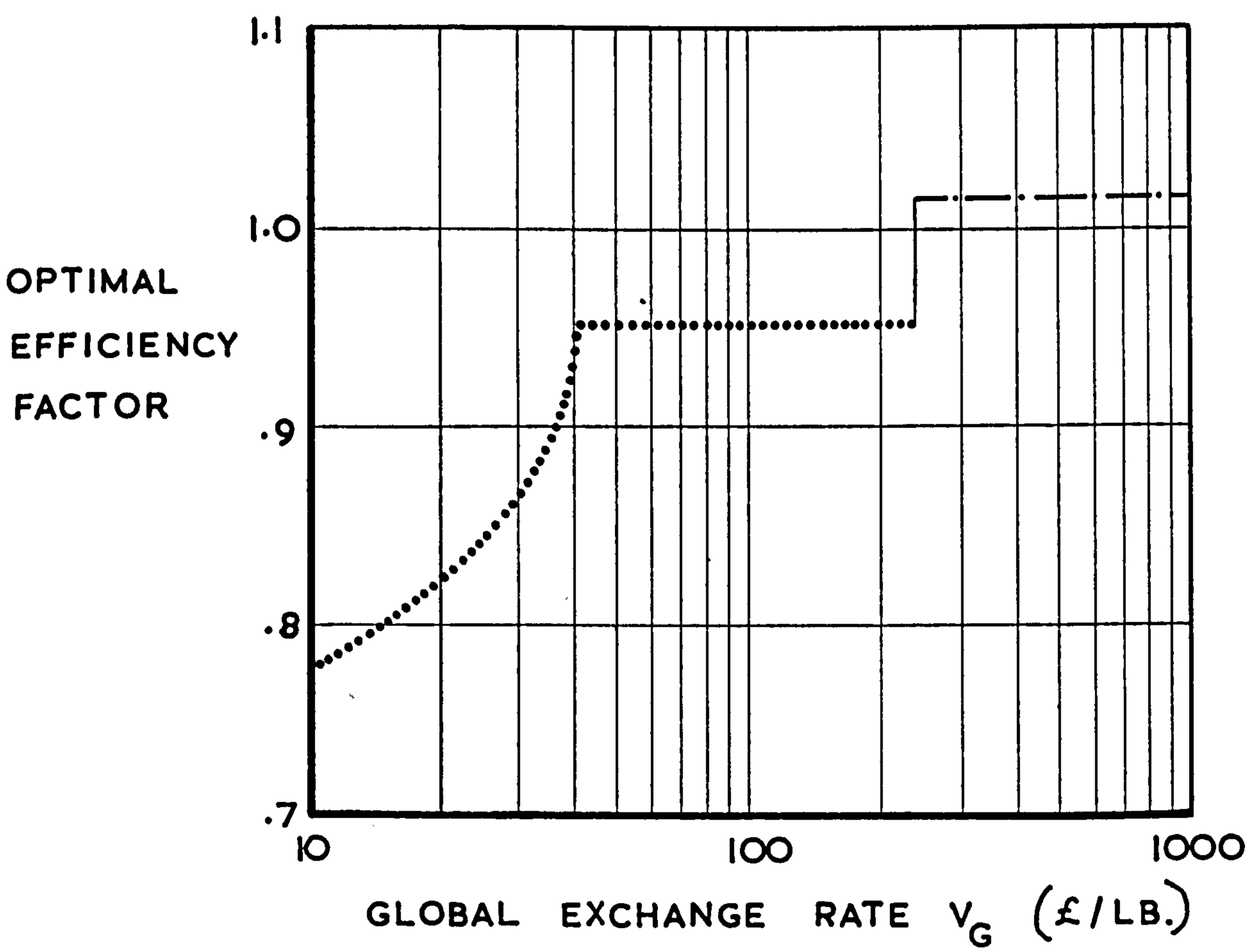


KEY

••••••••• BASIC ALUMINIUM ALLOY DESIGN

—·— TITANIUM ALLOY DESIGN

FIG. 8.8 THE OPTIMAL STRUCTURAL CONFIGURATIONS AT THE LOAD LEVEL $N_x = 10{,}000$ LB./IN.

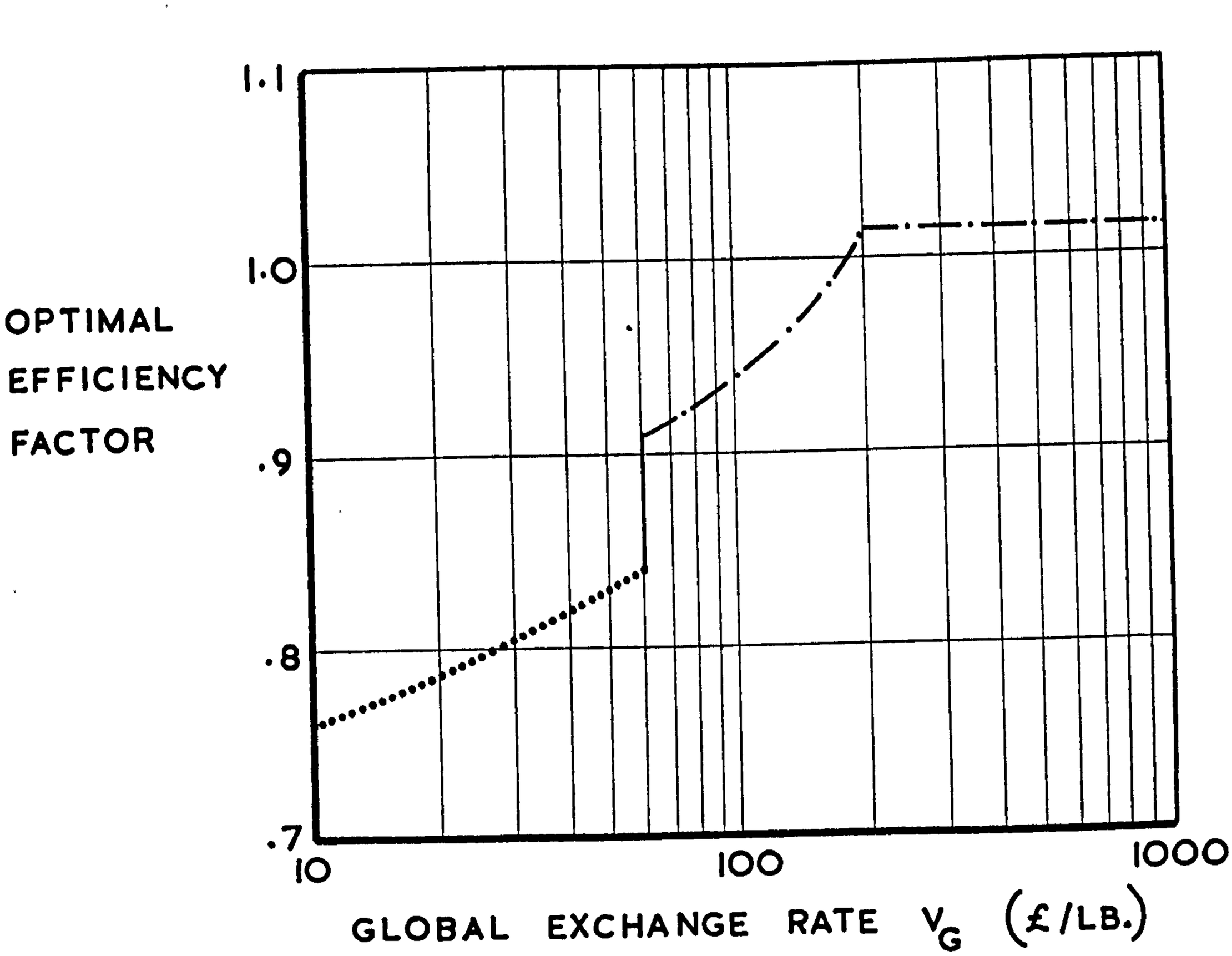


KEY

..... BASIC ALUMINIUM ALLOY DESIGN

—·— TITANIUM ALLOY DESIGN

# C H A P T E R  9

# THE SENSITIVITY OF THE SELECTION PROCESS TO ERRORS IN THE ESTIMATES FOR THE SYSTEM VALUES

## 9.1 Introduction

The results of the optimisation analyses, which are presented in Chapters 7 and 8, were derived subject to the qualifying assumption that the structural weight and the unit cost values used for each system were accurate.

In a practical situation, the estimates of the structural weight and the unit cost for alternative structures are liable to errors, the magnitudes of which are dependent on the methods of estimation employed.

The sensitivity of the selection process to these errors is of prime importance in determining the suitability of the method for the location of optimal solutions in a practical environment.

## 9.2 The Evaluation of Upper and Lower Bound Values for the Detail Exchange Rate

Assume that two structural systems, 1 and 2, have system values which are initially free from errors. Let the unit cost $C_2$ of system 2 and the structural weight $W_1$ of system 1 have the greatest magnitudes, giving

$$C_2 > C_1 \quad \text{and} \quad W_1 > W_2$$

Comparing systems 1 and 2, the change-over from one system to the other occurs at a specific value of the detail

exchange rate. This will be termed the median exchange rate value $V_{D_M}$, and is defined when the merit function values of the systems are equal,

$$\text{i.e.} \quad M_1 = M_2 = W_1 + \frac{C_1}{V_{D_M}} = W_2 + \frac{C_2}{V_{D_M}} ,$$

$$\text{giving} \quad V_{D_M} = \frac{C_2 - C_1}{W_1 - W_2} \tag{9.1}$$

In the presence of errors in the estimates for the system values, the change-over from one system to the other occurs somewhere within a band of detail exchange rate values, rather than at a specific value. The bandwidth determines the sensitivity of the analysis to errors in the estimating methods. The existence of a band of detail exchange rate values is shown diagrammatically in fig. 9.1, with the upper and lower bound values of the detail exchange rate indicated by $V_{D_u}$ and $V_{D_L}$, respectively.

Assume that the unit cost estimates of systems 1 and 2 are subjected to fractional errors of $\pm p_1$ and $\pm p_2$, respectively, and the structural weight estimates are subjected to fractional errors of $\pm r_1$ and $\pm r_2$, respectively.

The upper bound value $V_{D_u}$ of the detail exchange rate is defined by the intersection of the merit function equations, giving

$$(1 - r_1) \cdot W_1 + \frac{(1 - p_1) \cdot C_1}{V_{D_u}} = (1 + r_2) \cdot W_2 + \frac{(1 + p_2) \cdot C_2}{V_{D_u}}$$

$$\therefore V_{D_u} = \frac{(1 + p_2) \cdot C_2 - (1 - p_1) \cdot C_1}{(1 - r_1) \cdot W_1 - (1 + r_2) \cdot W_2} \tag{9.2}$$

The lower bound value $V_{D_L}$ of the detail exchange rate is defined by the equation

$$(1 + r_1) \cdot W_1 + \frac{(1 + P_1) \cdot C_1}{V_{D_L}} = (1 - r_2) \cdot W_2 + \frac{(1 - p_2) \cdot C_2}{V_{D_L}}$$

$$\therefore \quad V_{D_L} = \frac{(1 - p_2) \cdot C_2 - (1 + p_1) \cdot C_1}{(1 + r_1) \cdot W_1 - (1 - r_2) \cdot W_2} \tag{9.3}$$

The sensitivity equations, which express the fractional variation in detail exchange rate relative to the median value, are given by

$$\left( \frac{V_{D_U} - V_{D_M}}{V_{D_M}} \right)$$

$$= \frac{(W_1 - W_2) \cdot (p_1 \cdot C_1 + p_2 \cdot C_2) + (C_2 - C_1) \cdot (r_1 \cdot W_1 + r_2 \cdot W_2)}{(C_2 - C_1) \cdot [(1 - r_1) \cdot W_1 - (1 + r_2) \cdot W_2]} \tag{9.4}$$

and

$$- \left( \frac{V_{D_M} - V_{D_L}}{V_{D_M}} \right)$$

$$= \frac{-(W_1 - W_2) \cdot (p_1 \cdot C_1 + p_2 \cdot C_2) - (C_2 - C_1) \cdot (r_1 \cdot W_1 + r_2 \cdot W_2)}{(C_2 - C_1) \cdot [(1 + r_1) \cdot W_1 - (1 - r_2) \cdot W_2]} \tag{9.5}$$

The sensitivity equations are of great utility for practical investigations. The errors experienced with the estimating methods used in past aircraft programs may be evaluated statistically. If similar estimating techniques are to be employed for new projects, the sensitivity of the individual analyses may be examined by incorporating the appropriate error values in the sensitivity equations.

### 9.2.1 Errors in the cost estimates

If the cost estimates only are liable to errors, the equations governing the detail exchange rate band are obtained by substituting $r_1 = r_2 = 0$ in equations (9.2), (9.3), (9.4) and (9.5).

The upper bound value $V_{D_U}$ of the detail exchange rate reduces to

$$V_{D_U} = \frac{(1 + p_2) \cdot C_2 - (1 - p_1) \cdot C_1}{W_1 - W_2} \qquad (9.6)$$

The lower bound value $V_{D_L}$ of the detail exchange rate reduces to

$$V_{D_L} = \frac{(1 - p_2) \cdot C_2 - (1 + p_1) \cdot C_1}{W_1 - W_2} \qquad (9.7)$$

The sensitivity equations reduce to

$$\left(\frac{V_{D_U} - V_{D_M}}{V_{D_M}}\right) = \frac{p_1 \cdot C_1 + p_2 \cdot C_2}{C_2 - C_1} \qquad (9.8)$$

and

$$-\left(\frac{V_{D_M} - V_{D_L}}{V_{D_M}}\right) = -\left(\frac{p_1 \cdot C_1 + p_2 \cdot C_2}{C_2 - C_1}\right) \qquad (9.9)$$

### 9.2.2 Errors in the weight estimates

If the weight estimates only are liable to errors, the equations governing the detail exchange rate band are obtained by substituting $p_1 = p_2 = 0$ in equations (9.2), (9.3), (9.4) and (9.5)

The upper bound value $V_{D_U}$ of the detail exchange rate reduces to

$$V_{D_U} = \frac{C_2 - C_2}{(1 - r_1) \cdot W_1 - (1 + r_2) \cdot W_2} \qquad (9.10)$$

The lower bound value $V_{D_L}$ of the detail exchange rate reduces to

$$V_{D_L} = \frac{C_2 - C_1}{(1 + r_1) \cdot W_1 - (1 - r_2) \cdot W_2} \qquad (9.11)$$

The sensitivity equations reduce to

$$\left(\frac{V_{D_U} - V_{D_M}}{V_{D_M}}\right) = \frac{r_1 \cdot W_1 + r_2 \cdot W_2}{(1 - r_1) \cdot W_1 - (1 + r_2) \cdot W_2} \qquad (9.12)$$

and

$$-\left(\frac{V_{D_M} - V_{D_L}}{V_{D_M}}\right) = \frac{-r_1 \cdot W_1 - r_2 \cdot W_2}{(1 + r_1) \cdot W_1 - (1 - r_2) \cdot W_2} \qquad (9.13)$$

### 9.2.3 The sensitivity analysis of a practical example

The degradation of the ability to select a unique solution, in the presence of estimating errors, was investigated for a practial example. The maximum effic-iency configurations for the aluminium alloy and the titanium alloy systems, designed to a load level of 10,000 lb./in., were examined in the analysis.

Incorporation of the system values,whih are given in Tables 7.5 to 7.8, in equation (9.1) gave a median exchange rate value $V_{D_M}$ of £66/lb.

The influence of errors in the structural weight and the unit cost estimates separately, and together, were examined using the equations derived above. In each case fractional errors of $\pm$ 0.1 were assumed for each system. The results of each analysis are summarised in Table 9.1.

In this instance the errors in the weight estimates have a much greater effect on the detail exchange rate band width than the errors in the cost estimates, as is to be expected since W is a denominator term and C is a numerator term. This is confirmed by examination of the upper and lower bound values of the detail exchange rate associated with each type of error. The upper bound value of £154/lb. and the lower bound value of £42/lb. arising from the errors in the weight estimates make the task of locating a unique solution far more difficult than the corresponding values of £76/lb. and £57/lb. for the errors in the cost estimates.

It must be emphasised that the relative importance of the type of error varies with the application, and the influence of the errors should be analysed for individual cases.

## 9.3 The Introduction of Cost Estimating Errors into the Analysis of the Specimen Structure

The analysis of the specimen structure had been undertaken with ideal boundary conditions, that is the structural weight and unit cost values for each system were assumed accurate. However, in a practical environment errors would be encountered in all estimates, to a varying degree.

In order to assess the effect of errors in the cost estimates on the results, the analysis of the specimen structure was repeated with an error factor of $\pm$ 10 per cent applied to the cost estimates for each system. The structural weight

estimates were assumed to be made to a sufficiently high degree of accuracy as to be considered exact.

The analysis had been concerned with two aspects of optimisation, as follows:

i) the location of the optimal configuration for each structual system, the results being presented in Chapter 7,

ii) the selection of the optimal system from the alternative systems, the results being presented in Chapter 8.

The effects of the cost estimating errors on the results were assessed in the above areas.

### 9.3.1 The location of the optimal configuration

The ideal analysis had allowed a specific configuration, defined in terms of an efficiency factor value, to be isolated at each value of the global exchange rate, for each structural system. The resulting curves, which express the variation of the optimal efficiency factor with global exchange rate for each system, are presented in figs. 7.12 to 7.21.

With an error factor of $\pm$ 10 per cent applied to the unit cost values, a band of efficiency factor values exists at each value of the global exchange rate within which the optimal configuration is located, instead of a unique solution being defined.

The upper and lower bound curves expressing the variation of the optimal configuration with global

exchange rate for each system, when cost estimating errors exist, are presented in figs. 9.2 to 9.11.

The width of the efficiency factor band at each value of the global exchange rate, when used in conjunction with the associated curves of structural weight and unit cost variation, which are presented in figs. 7.1 to 7.10, determines the extent to which the errors in the cost estimates degrade the selection process.

### 9.3.2 The selection of the optimal structural system

As mentioned in section 9.2, upper and lower bound values may be applied to the detail exchange rate, which defines the change-over from one system to another, when errors occur in the methods of estimation. The equations developed in section 9.2 for the evaluation of the upper and lower bound values relate to the comparison of two systems having fixed structural configurations. In the comparison of the alternative systems the configuration of each system was varied systematically in order to allow the most efficient structural arrangement to be determined, hence the equations of section 9.2 were not applicable in this case.

The upper and lower bound values of the detail exchange rate were determined in the following manner:

The normalised merit function values, formed from cost values having 90 per cent and 110 per cent of the unit cost values presented in Chapter 6 to allow for the error factor of $\pm$ 10 per cent, were evaluated for each system. The variation of the minimum values

of the normalised merit function with global exchange rate exhibited a band of merit function values for each system, rather than the single curve of the ideal case. The extremes of the overlapping merit function bands of the alternative systems defined the upper and lower bound values. The greater the degree of overlap of the merit function bands of the alternative systems, the harder it is to define an optimal system at a given global exchange rate value.

The normalised merit function bands for the appropriate systems at the different load levels are presented on figs. 9.12 to 9.15. The upper and lower bound values of the detail exchange rate, within which the change-over from one structural system to another occurs, are summarised in Table 9.2.

## 9.4 Conclusions

In the presence of errors in the estimates for the system values, it is impossible to specify:

i) a unique value of the structural efficiency factor which defines the optimal configuration for a given structural system, or

ii) a unique value of the detail exchange rate which marks the change-over from one optimal system to another.

These effects were demonstrated in section 9.3 when the analysis of the specimen structure was repeated with errors in the cost estimates.

In those cases where a small percentage deviation in the costs produces a number of possible solutions, company policy could take one of the following decisions:

i) Choose the structural type of which there is the most knowledge.

ii) Choose the structure requiring the minimum modification to the existing manufacturing resources.

iii) Choose the structure giving the greatest utilisation of the manufacturing equipment.

iv) Choose the structure with the shortest timescale to completion of the batch.

TABLE 9.1 The detail exchange rate band values for the practical example presented in section 9.2.3.

| | Cost and weight estimation errors | Weight estimation errors only | Cost estimation errors only |
|---|---|---|---|
| $V_{D_U}$ (£/lb.) | 174.5 | 153.5 | 75.5 |
| $V_{D_L}$ (£/lb.) | 36.4 | 42.4 | 57.3 |
| $\left(\frac{V_{D_U} - V_{D_M}}{V_{D_M}}\right)$ | 1.63 | 1.31 | 0.14 |
| $-\left(\frac{V_{D_M} - V_{D_L}}{V_{D_M}}\right)$ | -0.45 | -0.36 | -0.14 |

TABLE 9.2 The detail exchange rate bounds for the comparison of two structural types with an error factor of ± 10 per cent applied to the cost estimates.

| | | Aluminium alloy structures | | | | | | | | |
|---|---|---|---|---|---|---|---|---|---|---|
| | | Basic design | | | Chemically etched design | | | Spin dimpled design | | |
| | End loading Nx (lb./in.) | $V_{D_L}$ | $V_{D_M}$ | $V_{D_U}$ | $V_{D_L}$ | $V_{D_M}$ | $V_{D_U}$ | $V_{D_L}$ | $V_{D_M}$ | $V_{D_U}$ |
| Titanium alloy design | 1000 | - | - | - | 296 | 351 | 405 | 2651 | 3451 | 4251 |
| | 2500 | 119 | 135 | 153 | 372 | 433 | 503 | 1373 | 1814 | 2255 |
| | 5000 | 207 | 240 | 272 | - | - | - | - | - | - |
| | 10000 | 53 | 61 | 69 | - | - | - | - | - | - |
| Aluminium alloy spin dimpled design | 1000 | - | - | - | <10 | 33 | 118 | | | |
| | 2500 | <10 | 19 | 29 | <10 | 85 | 119 | | | |
| | 5000 | - | - | - | - | - | - | | | |
| | 10000 | - | - | - | - | - | - | | | |
| Aluminium alloy chemically etched design | 1000 | - | - | - | | | | | | |
| | 2500 | <10 | 15 | 24 | | | | | | |
| | 5000 | - | - | - | | | | | | |
| | 10000 | - | - | - | | | | | | |

Exchange rate values in £/lb.

FIG. 9.1 A DIAGRAMMATIC REPRESENTATION OF THE DETAIL EXCHANGE RATE BANDS DUE TO ERRORS IN THE ESTIMATION METHODS

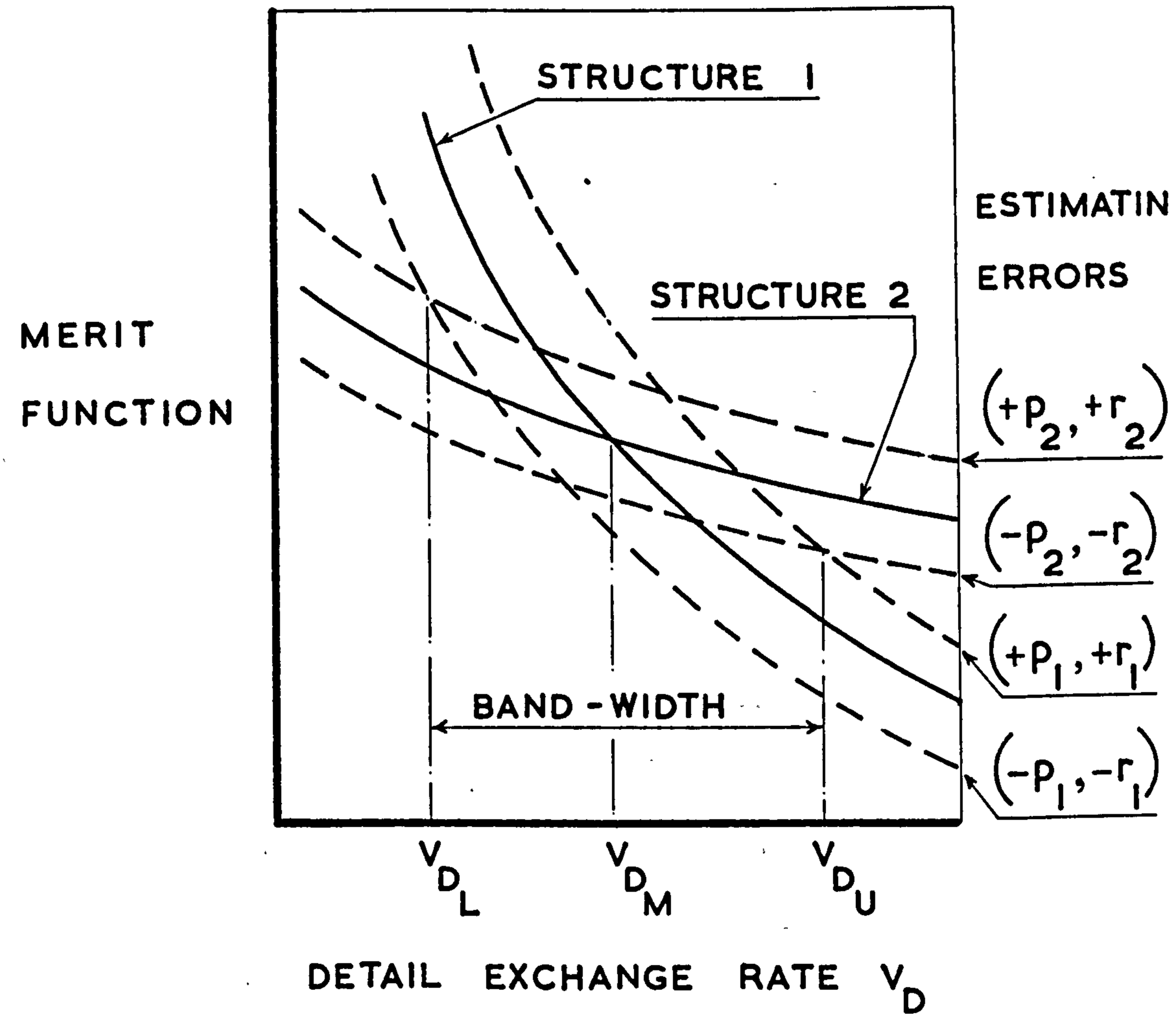

THE OPTIMAL EFFICIENCY FACTOR CURVES WITH ERRORS OF ± 10 % IN THE COST ESTIMATES AT THE LOAD LEVEL $N_x$ = 1000 LB./IN.

FIG. 9.2 THE ALUMINIUM ALLOY CHEMICALLY ETCHED DESIGN

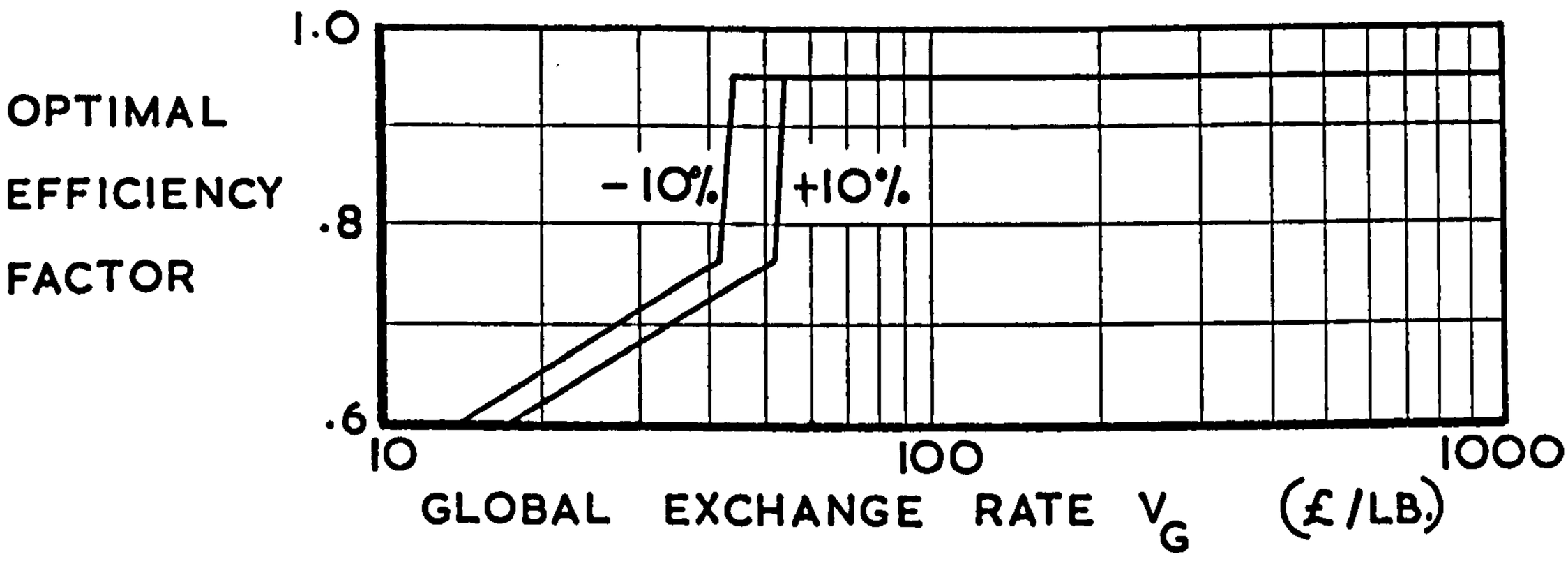


FIG. 9.3 THE ALUMINIUM ALLOY SPIN DIMPLED DESIGN

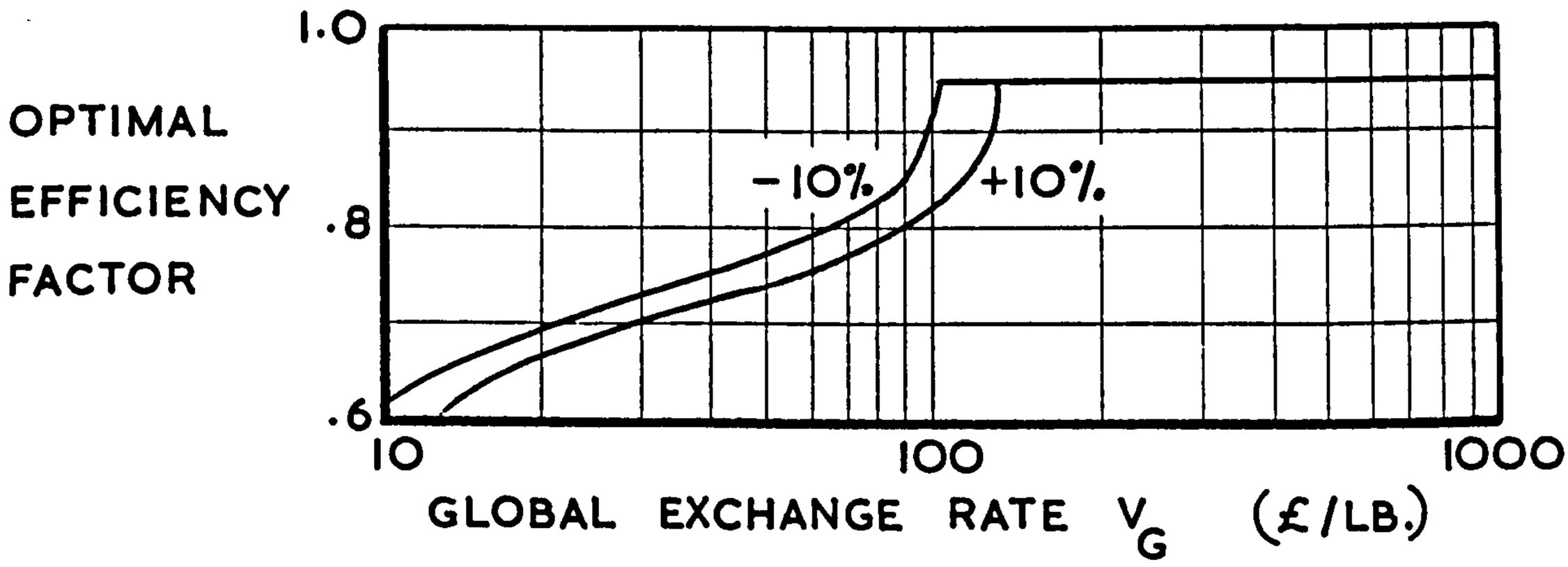


FIG. 9.4 THE TITANIUM ALLOY DESIGN

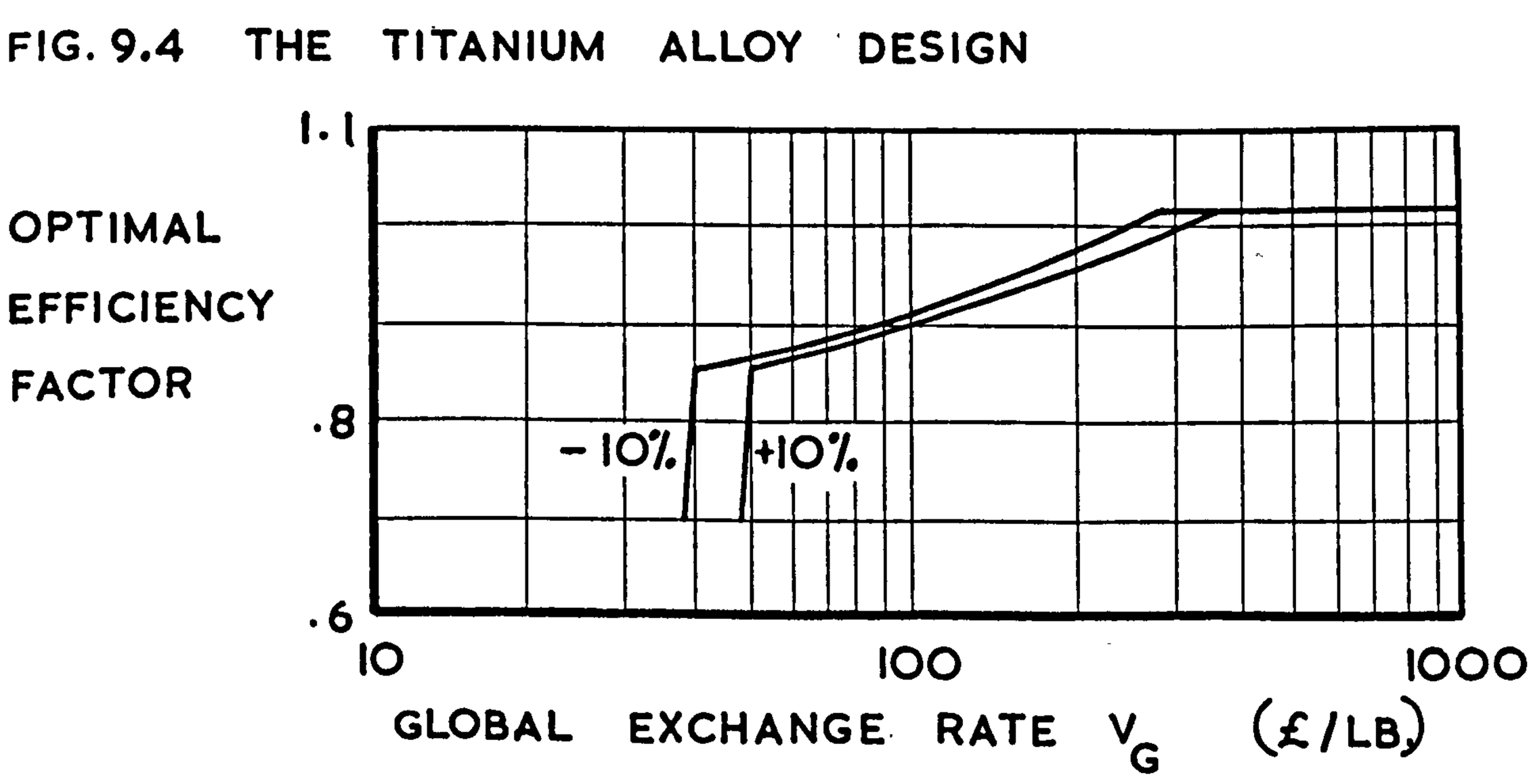

THE OPTIMAL EFFICIENCY FACTOR CURVES WITH ERRORS OF ±10% IN THE COST ESTIMATES AT THE LOAD LEVEL $N_x = 2500$ LB./IN.

FIG. 9.5 THE ALUMINIUM ALLOY CHEMICALLY ETCHED DESIGN

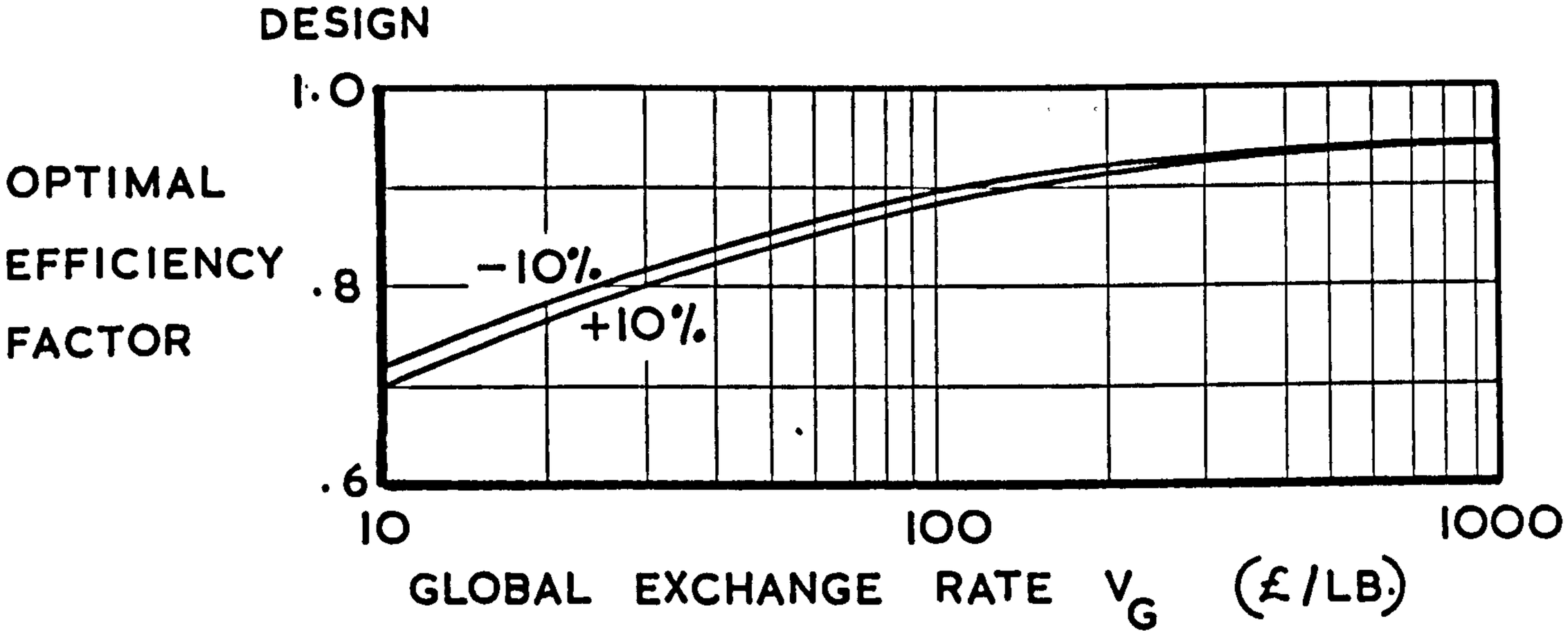


FIG. 9.6 THE ALUMINIUM ALLOY SPIN DIMPLED DESIGN

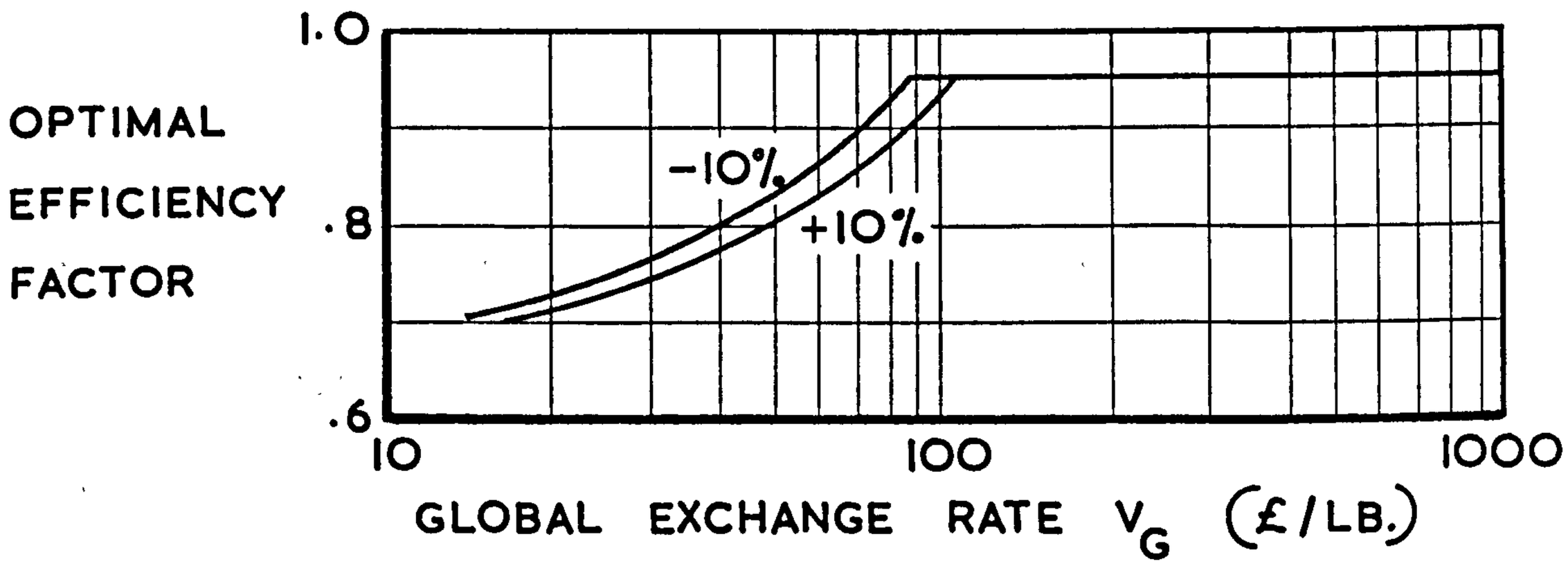


FIG. 9.7 THE TITANIUM ALLOY DESIGN

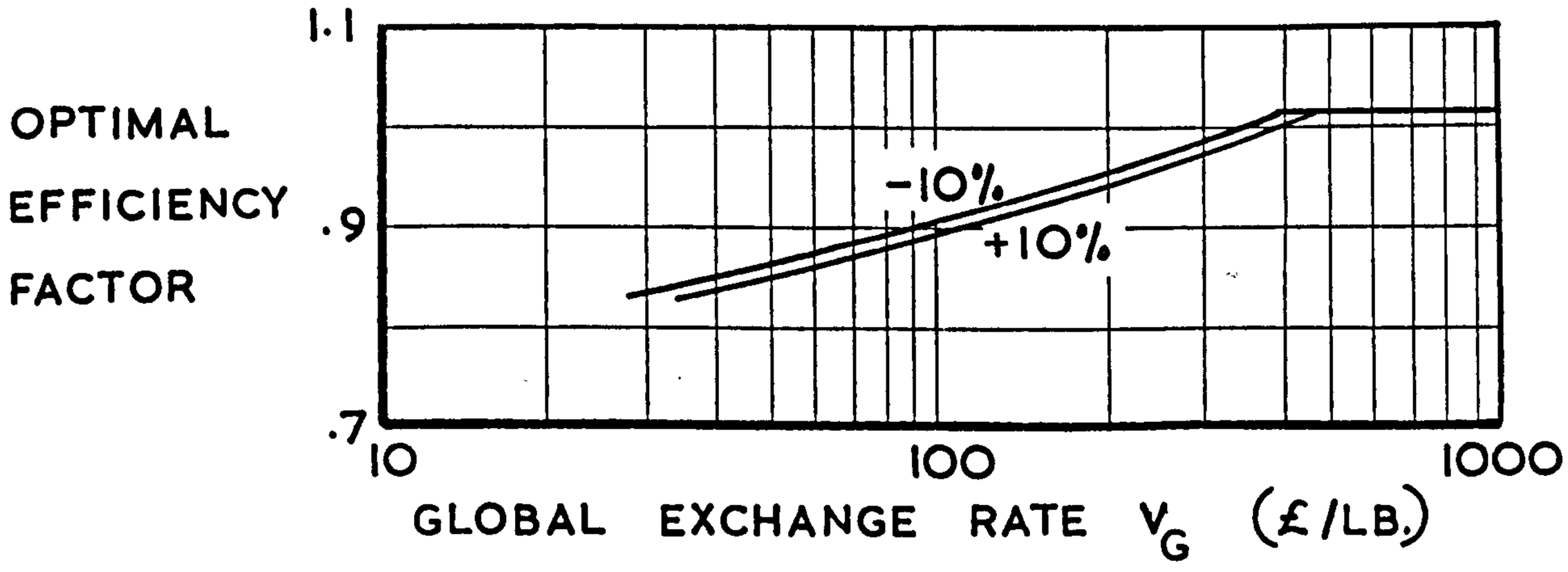

THE OPTIMAL EFFICIENCY FACTOR CURVES WITH ERRORS OF ±10% IN THE COST ESTIMATES AT THE LOAD LEVEL $N_x = 5000$ LB./IN.

FIG. 9.8 THE BASIC ALUMINIUM ALLOY DESIGN

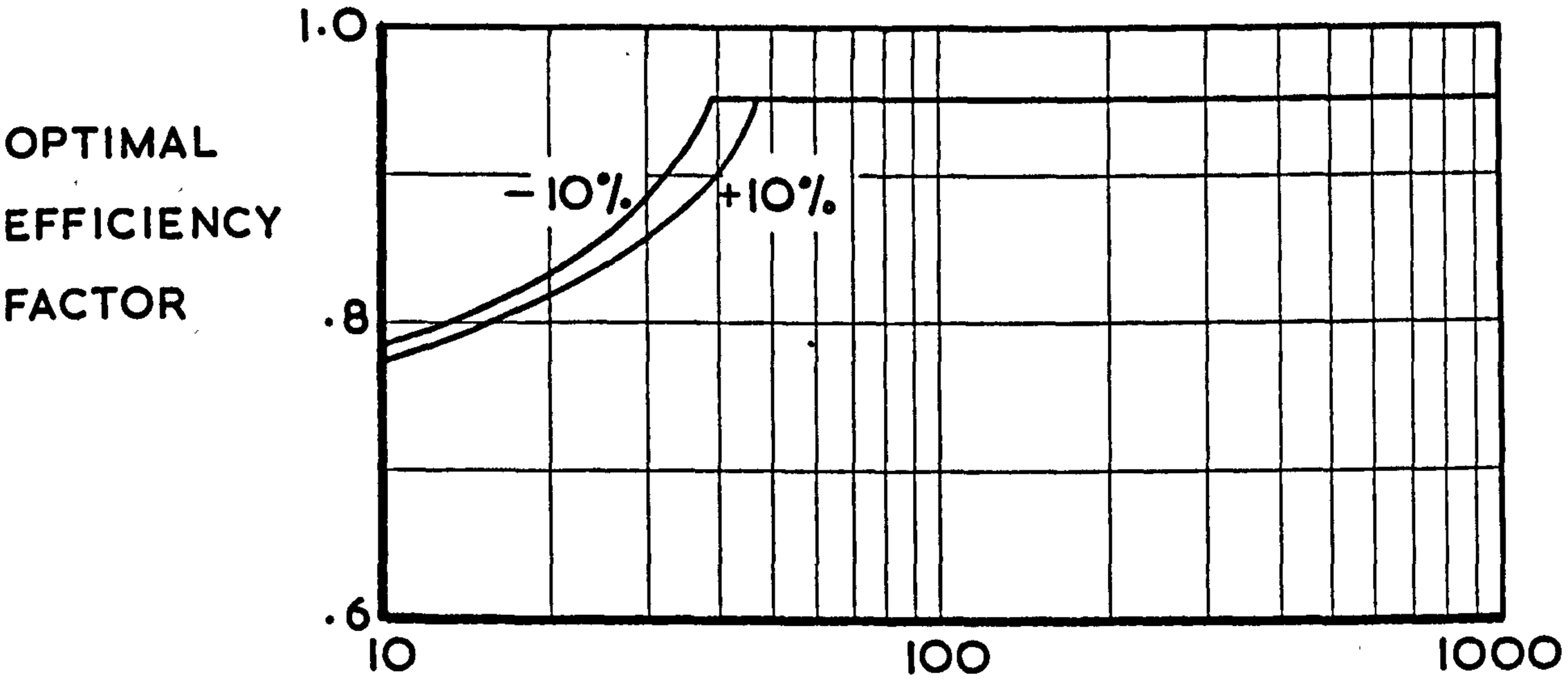


FIG. 9.9 THE TITANIUM ALLOY DESIGN

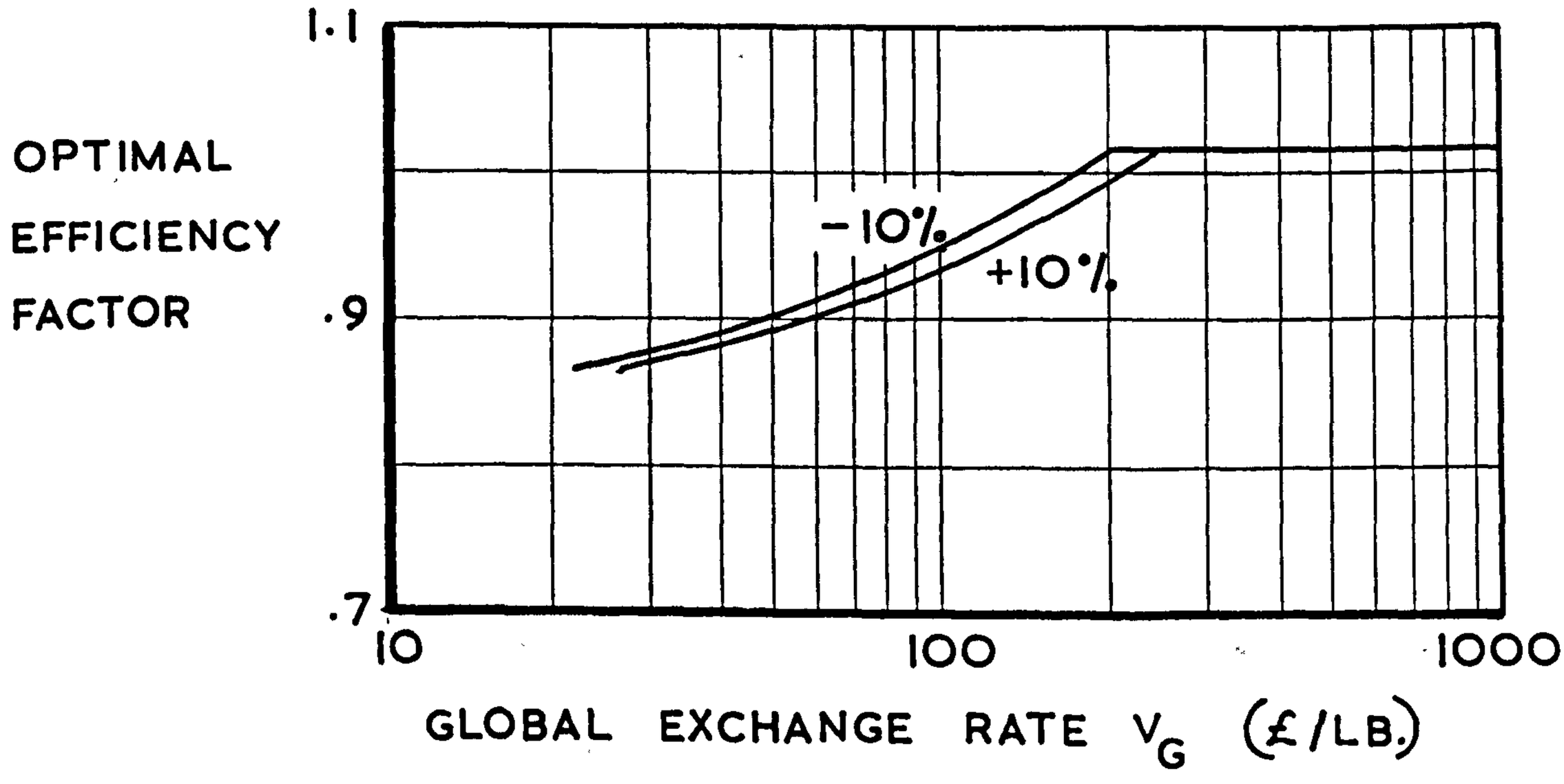

THE OPTIMAL EFFICIENCY FACTOR CURVES WITH ERRORS OF ±10% IN THE COST ESTIMATES AT THE LOAD LEVEL $N_x$ = 10,000 LB./IN.

FIG. 9.10 THE BASIC ALUMINIUM ALLOY DESIGN

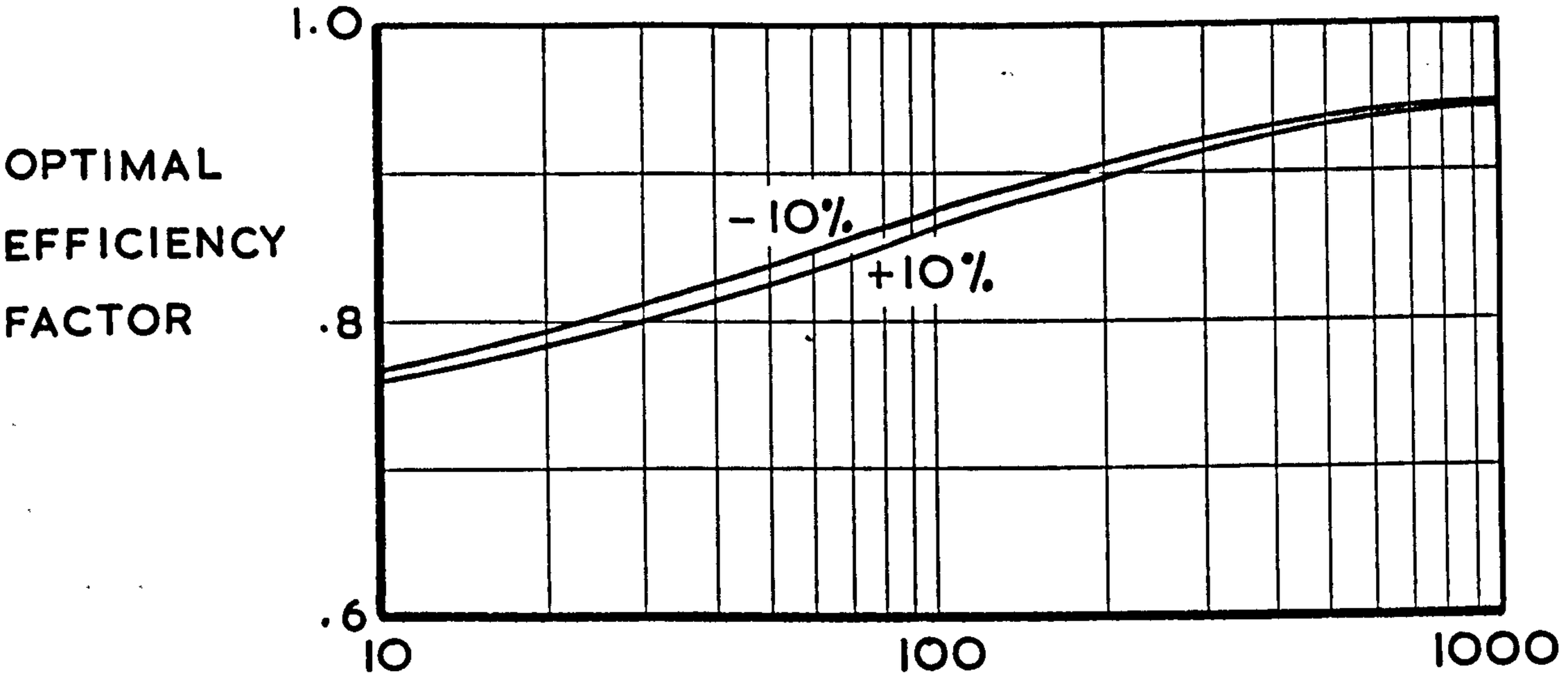


FIG. 9.11 THE TITANIUM ALLOY DESIGN

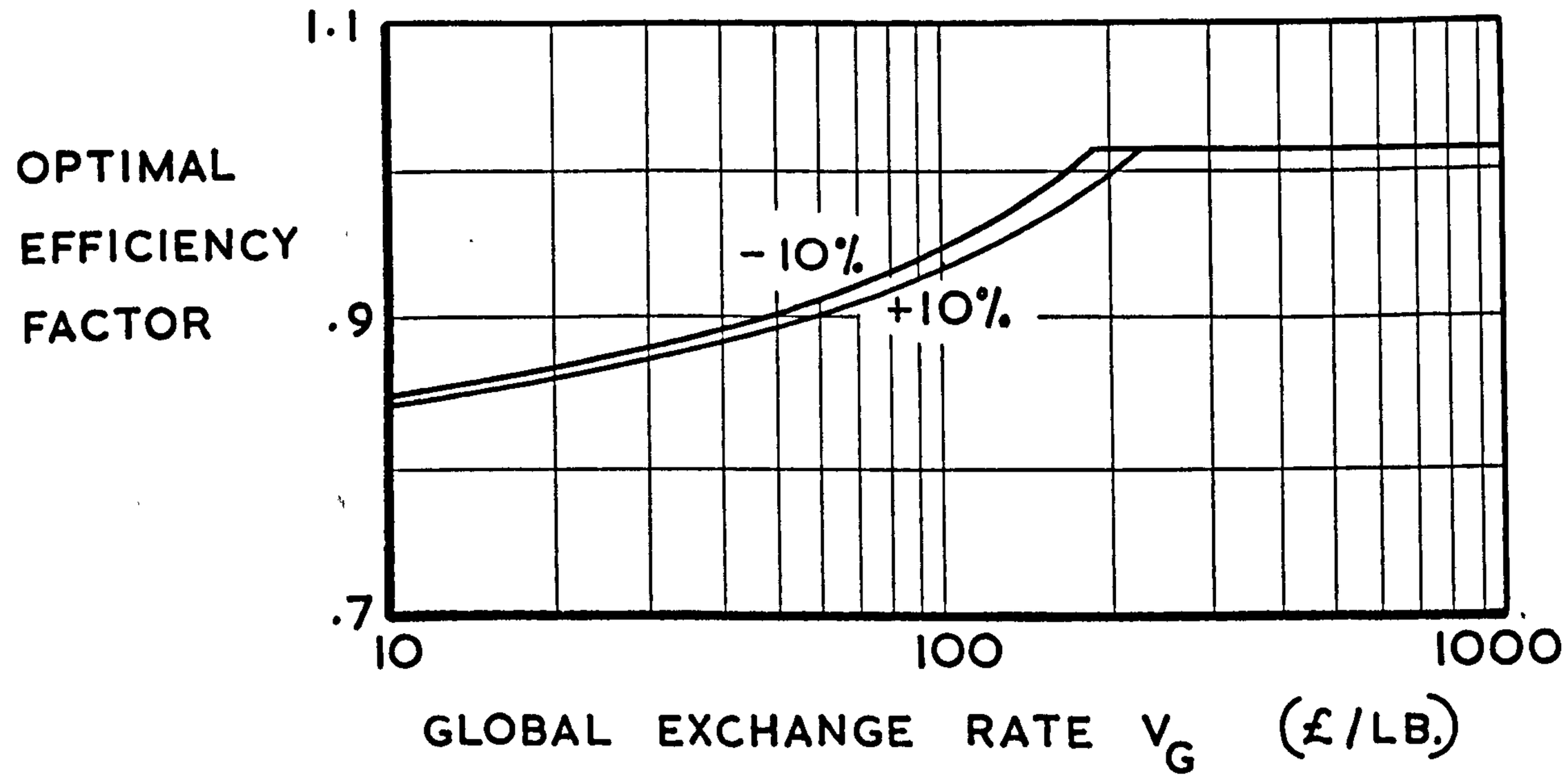

FIG. 9.12 THE OPTIMAL SYSTEM CURVES WITH ERRORS OF ±10% IN THE COST ESTIMATES AT THE LOAD LEVEL $N_x$ = 1000 LB./IN.

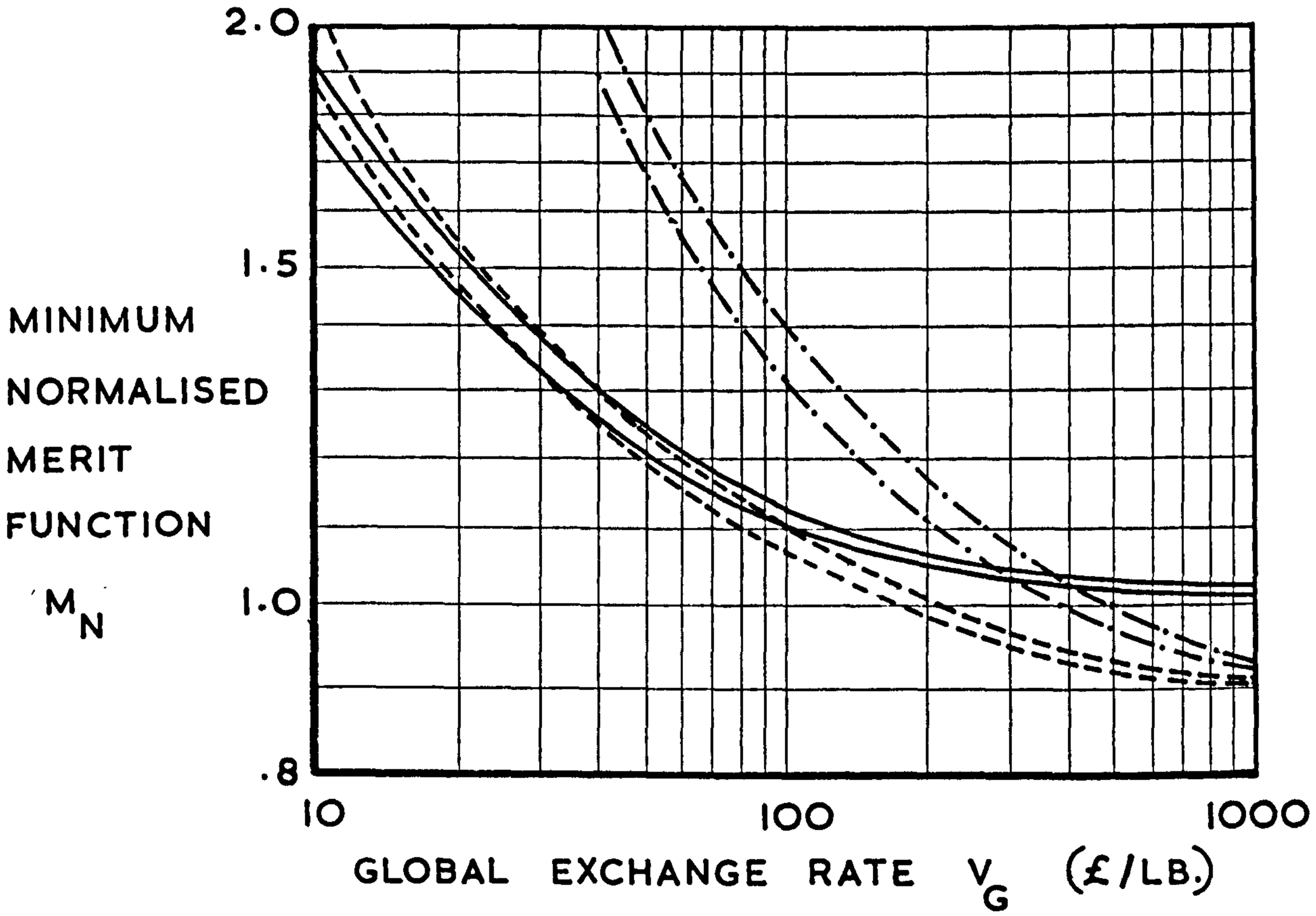


KEY

——— ALUMINIUM ALLOY CHEMICALLY ETCHED DESIGN

– – – ALUMINIUM ALLOY SPIN DIMPLED DESIGN

—·— TITANIUM ALLOY DESIGN

FIG. 9.13 THE OPTIMAL SYSTEM CURVES WITH ERRORS OF ±10% IN THE COST ESTIMATES AT THE LOAD LEVEL $N_x$ = 2500LB./IN.

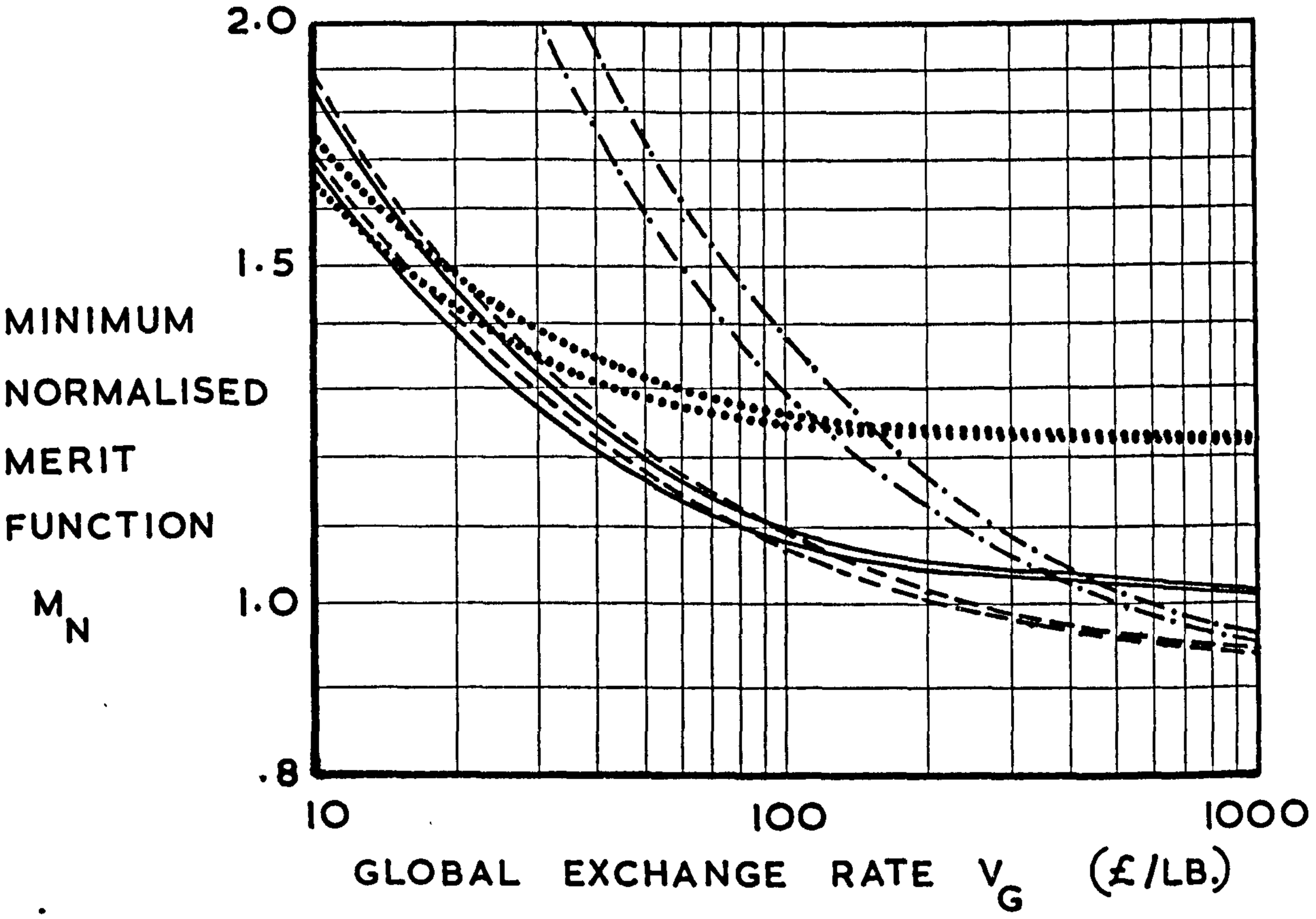


KEY

..... BASIC ALUMINIUM ALLOY DESIGN FOR AN EFFICIENCY FACTOR F 0.6

——— ALUMINIUM ALLOY CHEMICALLY ETCHED DESIGN

– – – ALUMINIUM ALLOY SPIN DIMPLED DESIGN

—·— TITANIUM ALLOY DESIGN

FIG. 9.14 THE OPTIMAL SYSTEM CURVES WITH ERRORS OF ±10% IN THE COST ESTIMATES AT THE LOAD LEVEL $N_x$ =5000LB./IN.

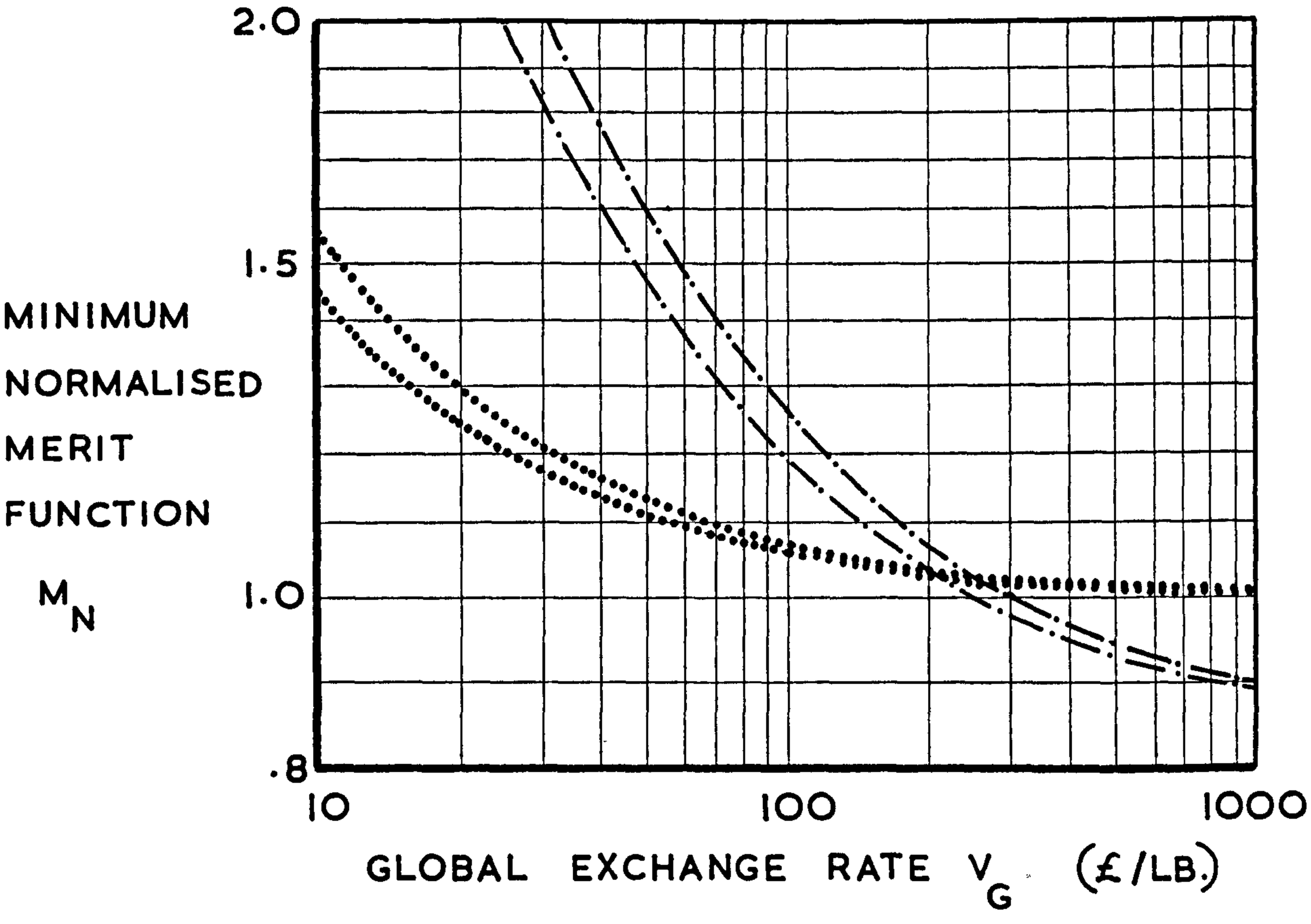


KEY

••••••••• BASIC ALUMINIUM ALLOY DESIGN

—·— TITANIUM ALLOY DESIGN

FIG. 9.15 THE OPTIMAL SYSTEM CURVES WITH ERRORS OF ±10% IN THE COST ESTIMATES AT THE LOAD LEVEL $N_x$ = 10,000 LB./IN.

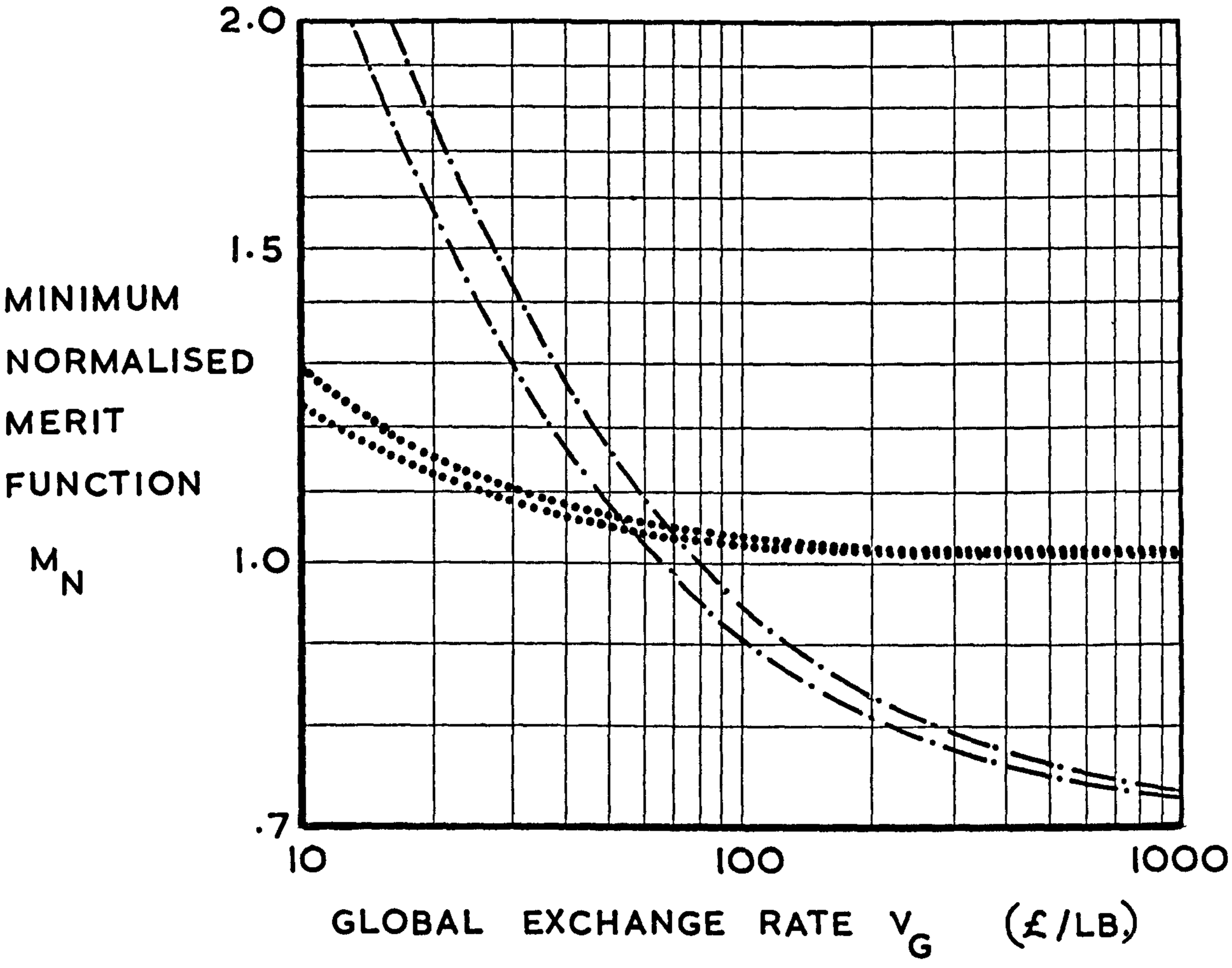


KEY

——— 

••••••••  BASIC ALUMINIUM ALLOY DESIGN

—·— TITANIUM ALLOY DESIGN

# C H A P T E R  1 0

# THE SENSITIVITY OF THE SELECTION PROCESS TO THE EFFECTS OF THE INTERACTION OF COMPONENTS

## 10.1 Introduction

If the effects of estimating errors are not too great, the selection process may be used for the definition of the optimal configuration of a structural component, inthe manner demonstrated in Chapter 7.

In the case of a complete structure made up of several component parts, each part may be analysed separately, giving a series of solutions which define the optimal configuration for each part. However, if the structure is analysed as a whole, the configuration defined as the optimum may differ radically from the configuration formed by an integration of the optimal solutions for the component parts.

The interactions of the component parts, when they are mated to form a complete structural assembly, give rise to joint weights and joint costs which vary in magnitude at different levels of structural efficiency. The separate optimisation of the components neglects the interaction effects, so that it is most important to specify a structural model which takes into account all relevant structural items.

## 10.2 The Examination of a Practical Example

Alvey and Emero[2] presented optimal design curves for various structural components, including tension covers and shear webs. However, the considerations discussed in section

10.1 suggest that such an approach to the optimal design of a complete structure might yield invalid results in practice.

In order to assess the influence of component interactions, it was decided to compare the configurations of a structure specified as the optimum in each case by the analyses of the structure as a whole and of its main component part.

The structure chosen for analysis was the aluminium alloybox beam of riveted construction. The component part consisted of the compression cover and rib elements of the box beam, since these items broadly define the layout of the other structural components.

Suppose the optimal configuration predicted by the analysis of the component occurs at an efficiency factor value Fc, for a specific value of the global exchange rate. Referring to the appropriate curves, giving the variations of the box beam weight and the box beam cost with efficiency factor, the component analysis predicts an optimal box weight W(Fc) and an optimal box cost C(Fc).

At the same global exchange rate value, let the true optimal configuration, as given by the analysis of the complete structure, occur at an efficiency factor value of $F_T$, giving a true optimal box weight $W(F_T)$ and a true optimal box cost $C(F_T)$.

The percentage difference in the box weight, $\Delta W$, between the optima given by the analyses of the complete structure and of the component are

$$\Delta W = \left( \frac{W(F_T) - W(F_c)}{W(F_T)} \right) \quad x\ 100 \qquad (10.1)$$

In a similar manner, the percentage difference in the box cost, $\Delta C$, between the optima given by analyses of the complete structure and of the component are

$$\Delta C = \left( \frac{C(F_c) - C(F_T)}{C(F_T)} \right) \quad x\ 100 \qquad (10.2)$$

### 10.2.1 The location of the optimal configuration

The optimal configurations for the box beam and for the component part were derived using the method described in Chapter 7, as follows:

The structural weight and the unit cost values of the box beam and the component part were determined at the series of efficiency factor values and for each value of the end loading examined in section 6.1.

The production cost element of the unit cost, for the box beam, was based on the production method descriptions given in sections 5.2.2 and 5.2.3, if the load level was above or below the critical loading value, respectively. The production cost element of the unit cost, for the component part, was based on the production method description given in section 5.2.5.

The structural weight and the unit cost values were normalised in the manner described in section 6.6, the normalised values being presented in Table 6.12 for the complete structure and in Table 6.15 for the component part.

Continuous curve equations, giving the variations of the normalised weight and the normalised cost with efficiency factor, were fitted to the discrete data using the Lagrange interpolation method described in section 7.2. The curves are presented in figs. 10.1 to 10.4.

Normalised merit function values were evaluated for the complete structure and for the component part in the manner described in section 7.3, enabling the optimal configuration, expressed in terms of an efficiency factor value, to be located for each case. The variation of the optimal configuration with global exchange rate is presented on figs 10.5 to 10.8, for each loading value. The efficiency factor values were used to determine the corresponding box weight and box cost values for inclusion in equations (10.1) and (10.2). Figs 10.9 to 10.12 give the variation of the percentage difference of the weight and the cost with global exchange rate.

### 10.2.2 Discussion of the results

Examination of the curves of structural weight variation with efficiency factor shows that the decrease in weight with increasing efficiency factor is less marked for the complete structure than for the component structure, for the following reasons:

When designated to satisfy stability requirements, the weight of the component is inversely proportional to efficiency factor to the index power $^{2}/_{3}$, as given

by equation (3.16). However, the inclusion of components, such as the tension cover and the spars, in the complete structure, which make up a large proportion of the structural weight but which exhibit little or no weight variation with efficiency factor, tends to reduce the overall weight variation of the complete structure with respect to efficiency factor, relative to the component part.

In a similar manner, the increase in cost with increasing efficiency factor is less marked for the complete structure than for the component part, for the following reasons:

The cost of fabricating a compression cover of high structural efficiency is markedly higher than the fabrication cost of a low efficiency cover. In general, a high efficiency factor implies a large number of stringers attached to a thin skin by many rivets in a mechanically fastened design, giving high fastening costs. The cost of the attachment of the ribs to the compression cover tends to reduce the cost variation of the component to some extent, since a high efficiency design has fewer ribs than a low efficiency design. However, the interaction of the other components of the box beam, in the final assembly stage, markedly reduces the cost variation of the box beam with efficiency factor, relative to the component part.

The optimal configuration curves presented in figs. 10.5 to 10.8 indicate that the configurations, defined by each analysis as the optimum, differ radically, until

a global exchange rate value is reached when both analyses specify the maximum efficiency configuration as the optimal solution. At this value the percentage difference in weight and the percentage difference in cost, given by equations (10.1) and (10.2), tend to zero. Below this value there are global exchange rate values at which a maximum percentage difference in weight and a maximum difference in cost, arising from the two analyses, occur; the global exchange rate values giving the maxima need not coincide, since the weight and cost curves are not identical. The relevant values are summarised in Table 10.1 for each load level examined.

## 10.3 Conclusions

The need to analyse all structural items having an influence on the optimal configuration of the structure as a whole is emphasised by the results of the analysis of the practical example, since the optimal configurations of the box beam, given by the analyses of the complete structure and of its main structural component, differ considerably.

Before a component part of a structure is optimised as a separate entity, it is essential to consider the interaction of the other component parts in terms of their influence on the structural weight and the unit cost of the structure as a whole. The results of the optimal analyses of component parts, such as those due to Alvey and Emero[2], should only be used with the utmost caution.

The results derived in section 10.2 had a major influence on the specimen structure chosen for analysis. Initially, it was intended to investigate a component composed of the compression cover and rib elements, since these items form the dominant component of the box beam structure and are amenable to analysis. However, in the light of the findings of the sensitivity analysis, it was decided to investigate a complete box beam, which, although being more difficult to analyse, is free from those interaction problems. It must be noted that the wing box has still to be mated to other wing boxes and to the fuselage, and these further interaction problems must be recognised when designing a complete aircraft.

TABLE 10.1 The maximum deviation of the box beam values.

| End loading Nx (lb./in.) | Global exchange rate value for maximum weight difference (£/lb.) | Maximum percentage weight difference % | Global exchange rate value for maximum cost difference (£/lb.) | Maximum percentage cost difference % |
|---|---|---|---|---|
| 1000 | 18 | 10.2 | 18 | 53.9 |
| 2500 | 16 | 15.5 | .16 | 67.4 |
| 5000 | 10 | 1.3 | 26 | 6.6 |
| 10000 | 110 | 0.3 | 130 | 26.8 |

# COST AND WEIGHT CURVES FOR THE COMPONENT STRUCTURE AND THE COMPLETE STRUCTURE

FIG. 10.1 THE LOAD LEVEL $N_X = 1000$ LB./IN.

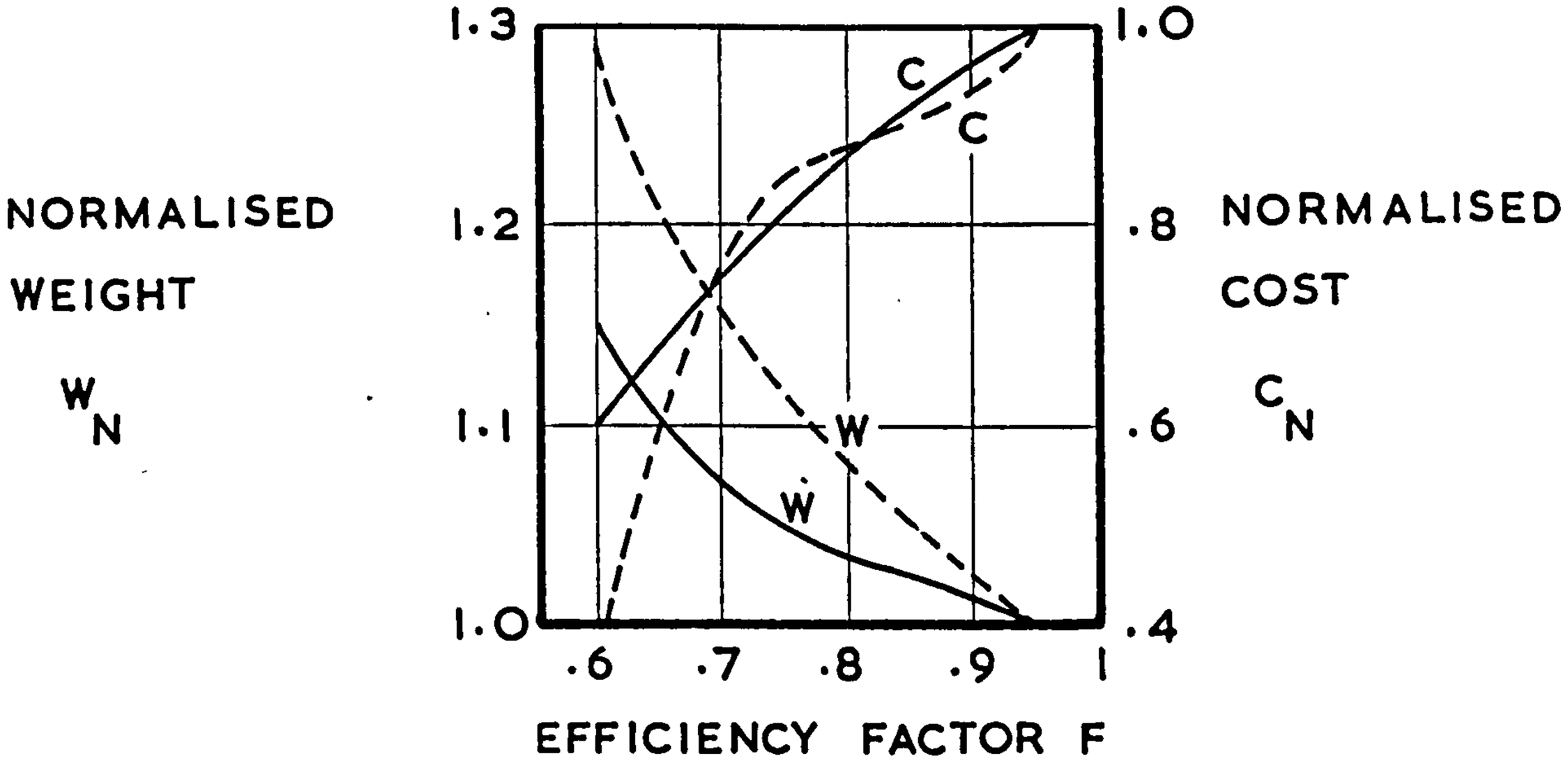


FIG. 10.2 THE LOAD LEVEL $N_X = 2500$ LB./IN.

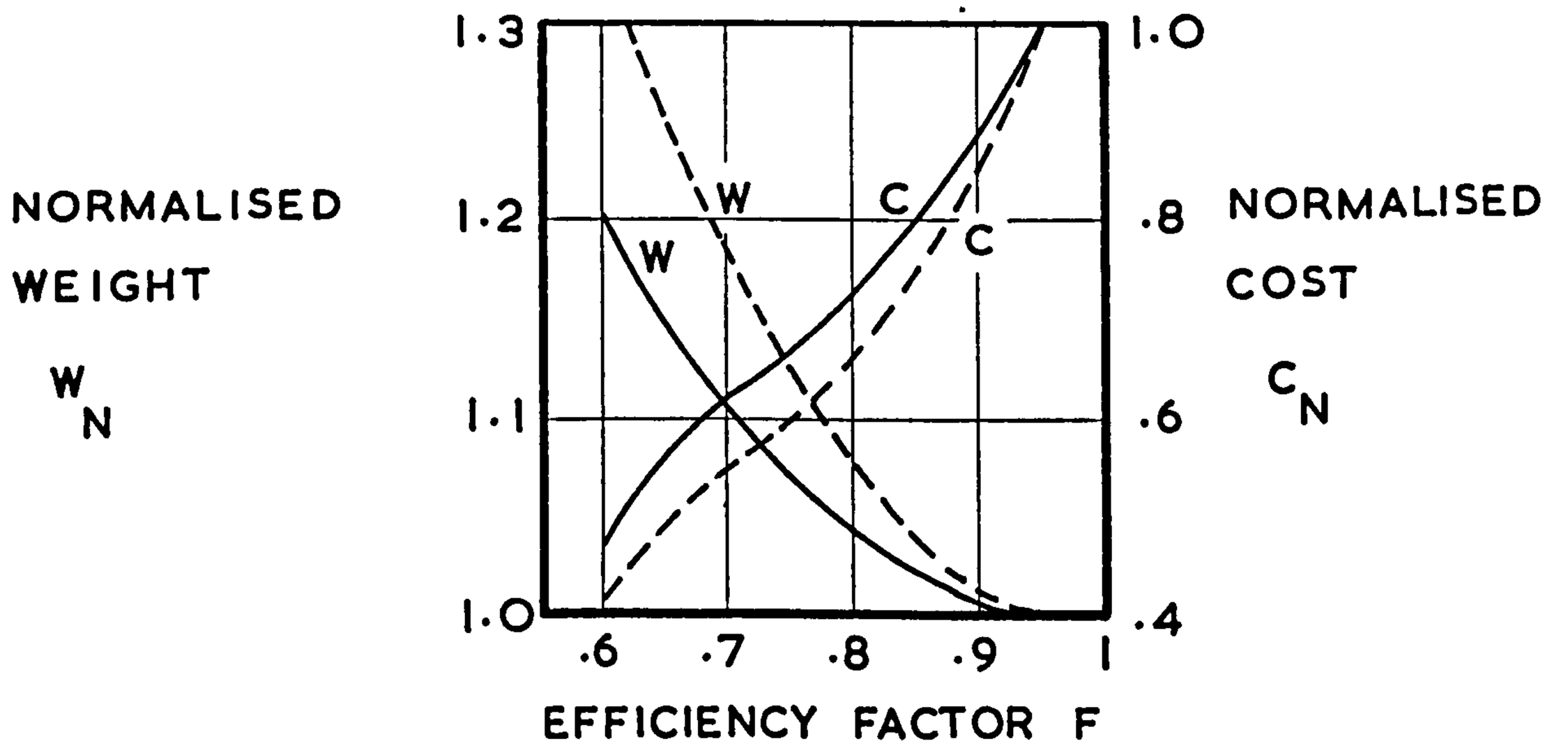


KEY

---- COMPONENT STRUCTURE

———— COMPLETE STRUCTURE

COST AND WEIGHT CURVES FOR THE COMPONENT STRUCTURE AND THE COMPLETE STRUCTURE

FIG. 10.3 THE LOAD LEVEL $N_X = 5000$ LB./IN.

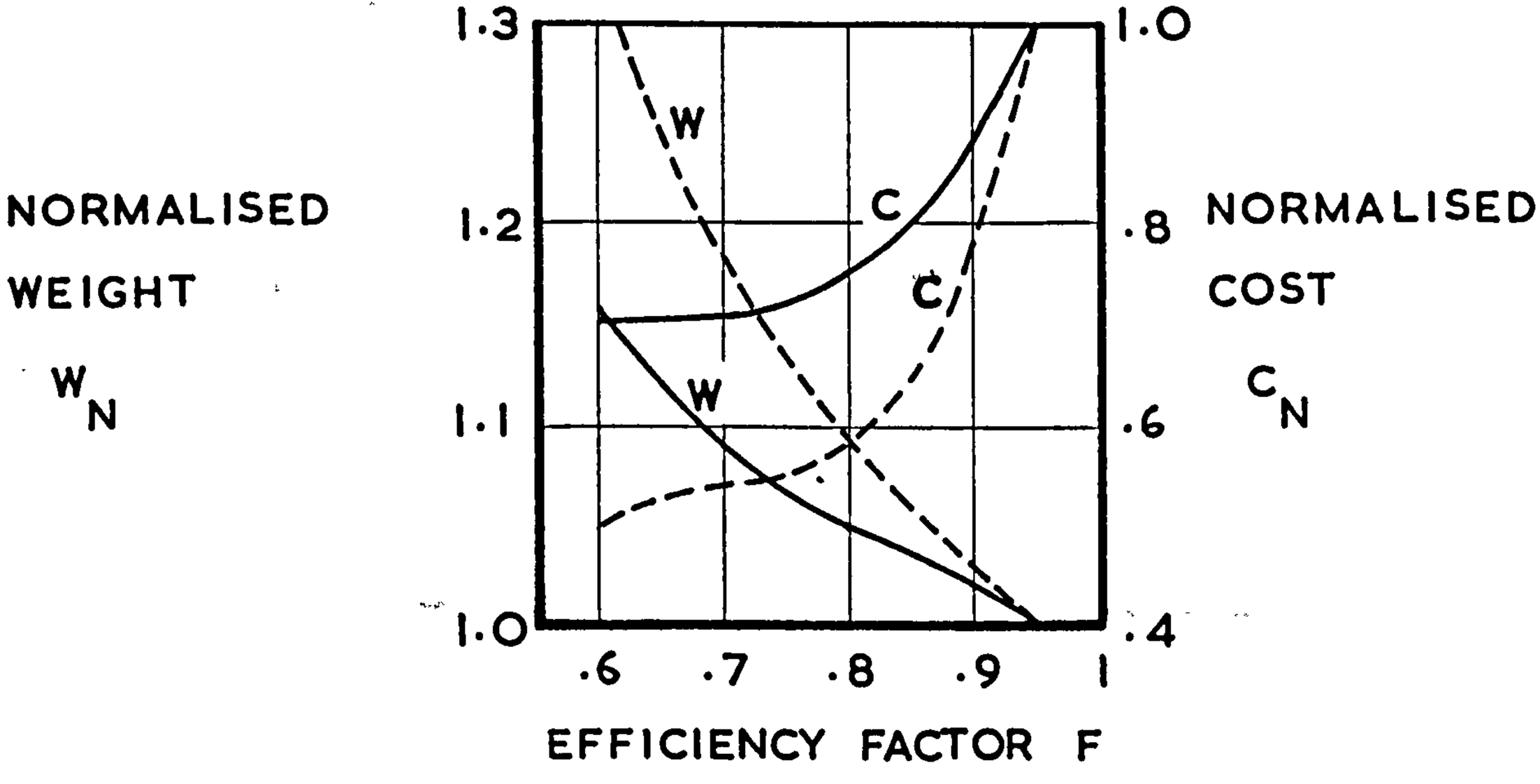


FIG. 10.4 THE LOAD LEVEL $N_X = 10{,}000$ LB./IN.

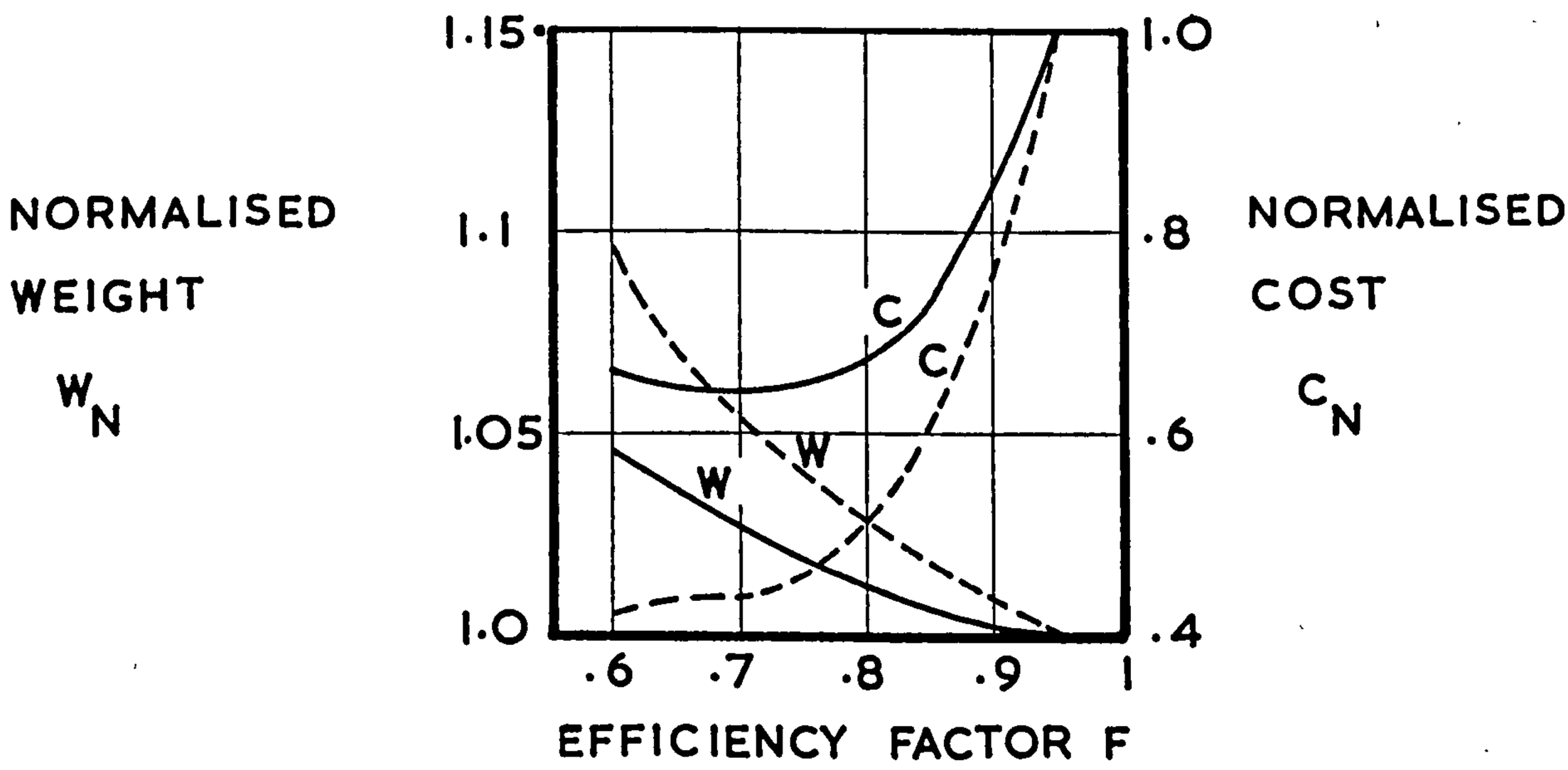


KEY

– – – – COMPONENT STRUCTURE

———— COMPLETE STRUCTURE

OPTIMAL EFFICIENCY FACTOR CURVES FOR THE COMPONENT STRUCTURE AND THE COMPLETE STRUCTURE

FIG. 10.5 THE LOAD LEVEL $N_X$ = 1000 LB./IN.

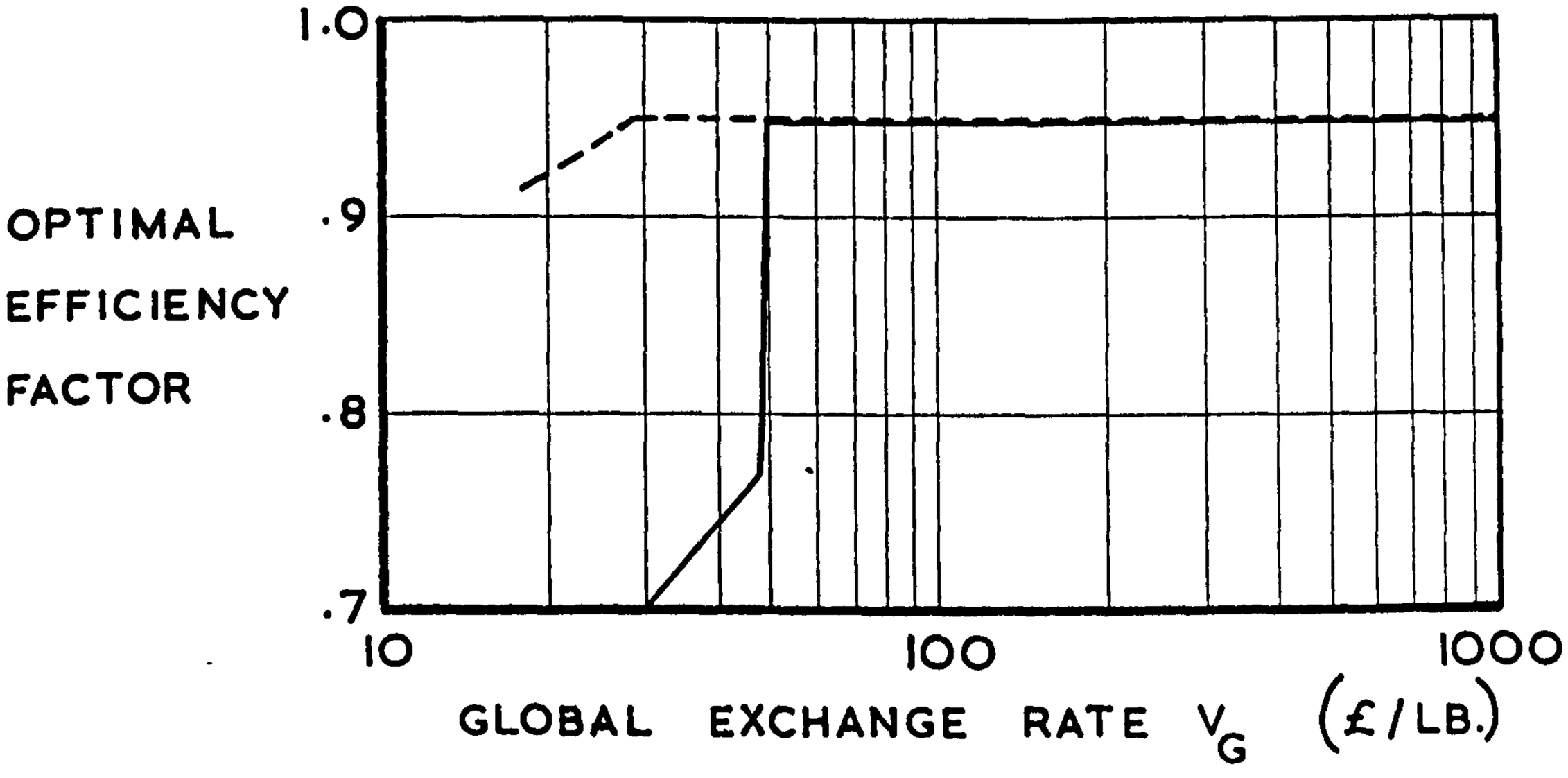


FIG. 10.6 THE LOAD LEVEL $N_X$ = 2500 LB./IN.

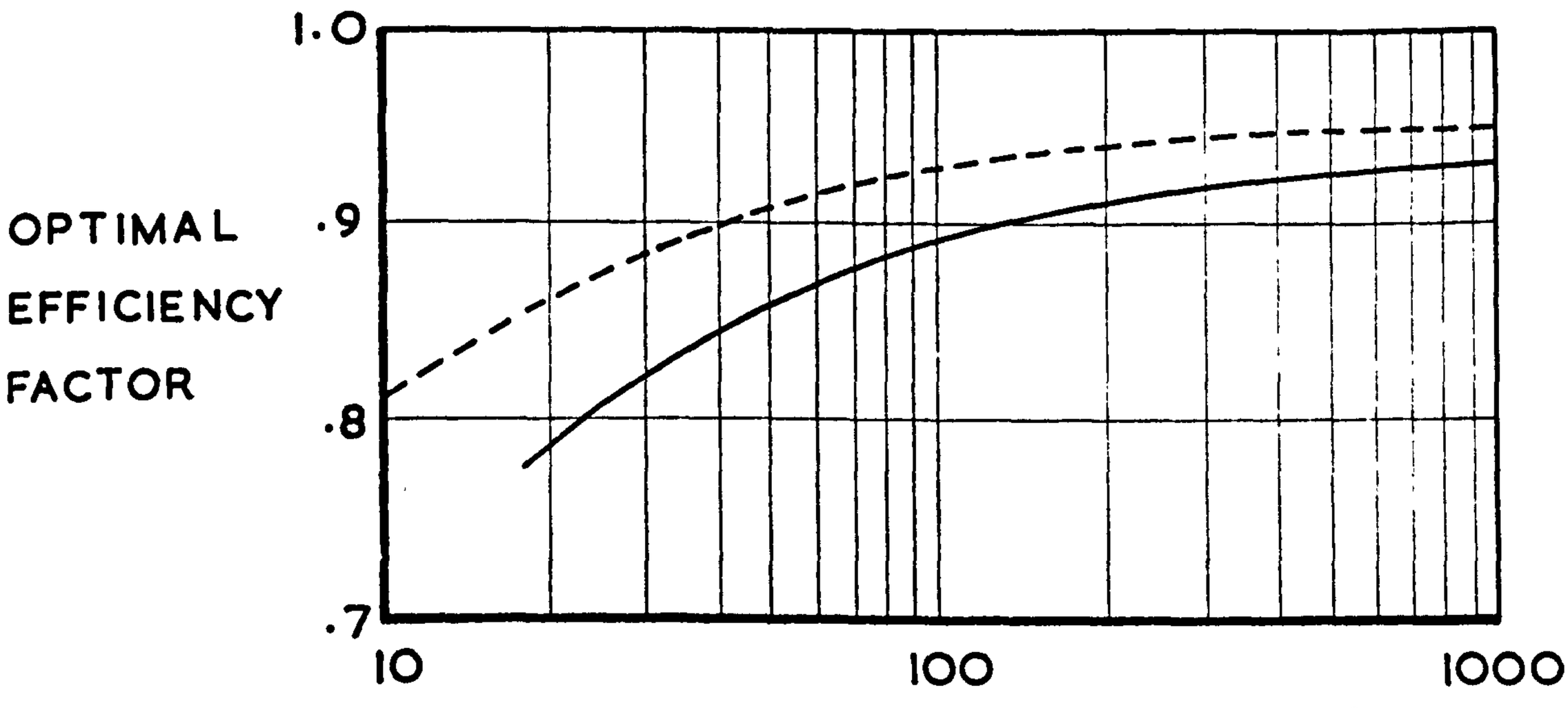


KEY

---- COMPONENT STRUCTURE

———— COMPLETE STRUCTURE

OPTIMAL EFFICIENCY FACTOR CURVES FOR THE COMPONENT STRUCTURE AND THE COMPLETE STRUCTURE

FIG. 10.7 THE LOAD LEVEL $N_X = 5000$ LB./IN.

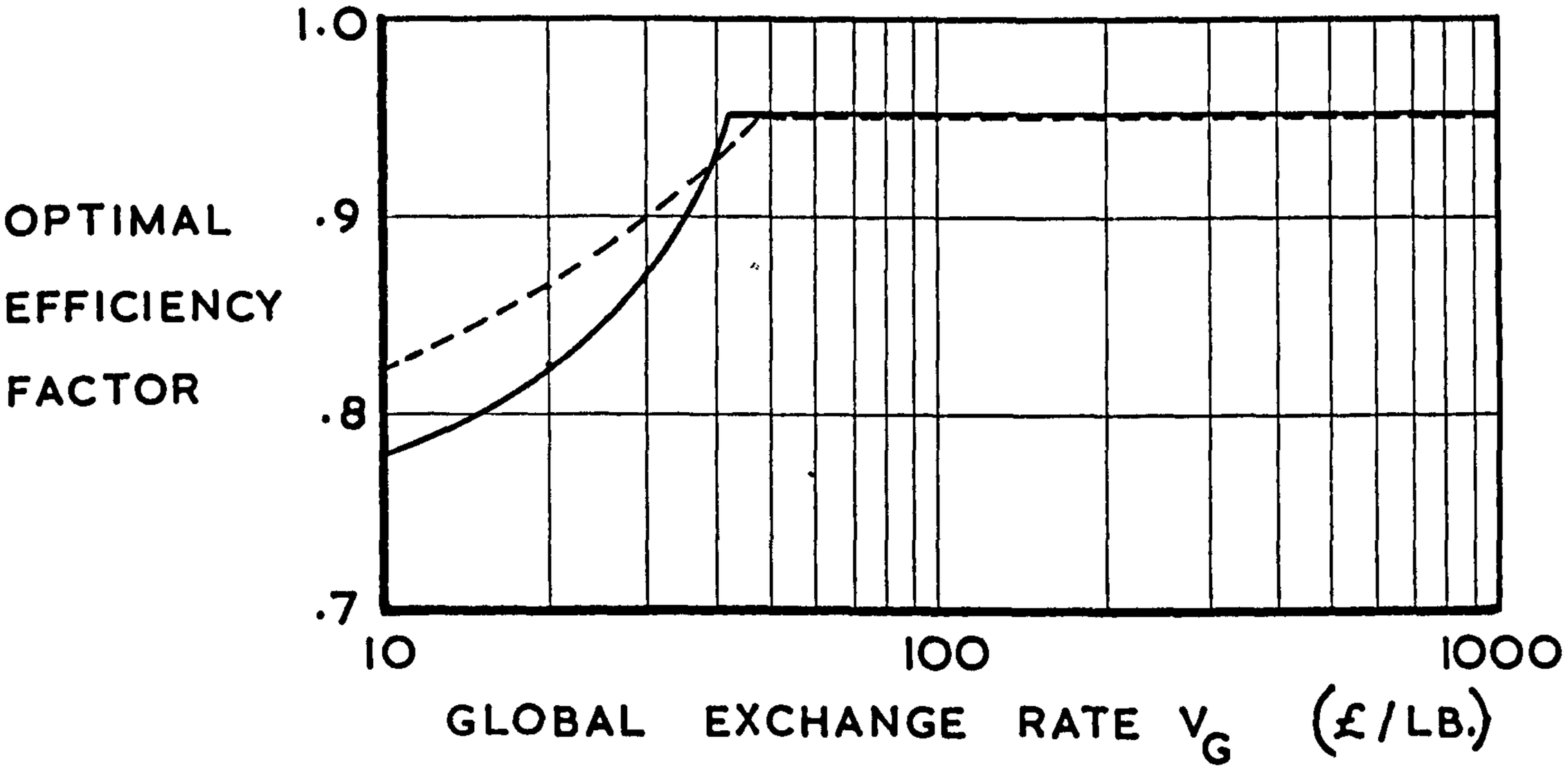


FIG. 10.8 THE LOAD LEVEL $N_X = 10\,000$ LB./IN.

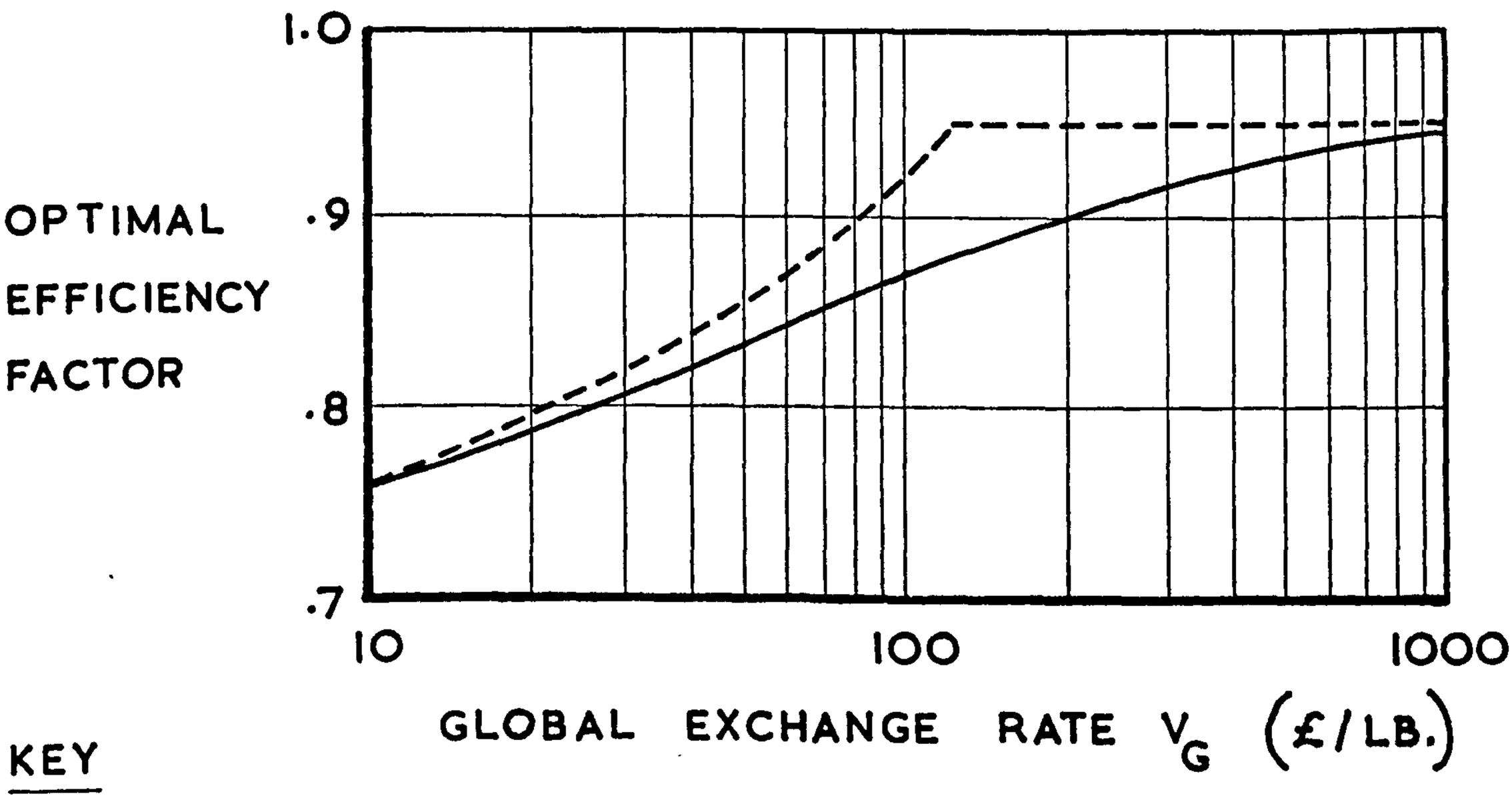


KEY

– – – – COMPONENT STRUCTURE

———— COMPLETE STRUCTURE

THE DIFFERENCES IN THE BOX BEAM COST AND WEIGHT VALUES GIVEN BY THE ANALYSES OF THE COMPONENT AND THE COMPLETE STRUCTURES

FIG. 10.9 THE LOAD LEVEL $N_X$ 1000 LB./IN.

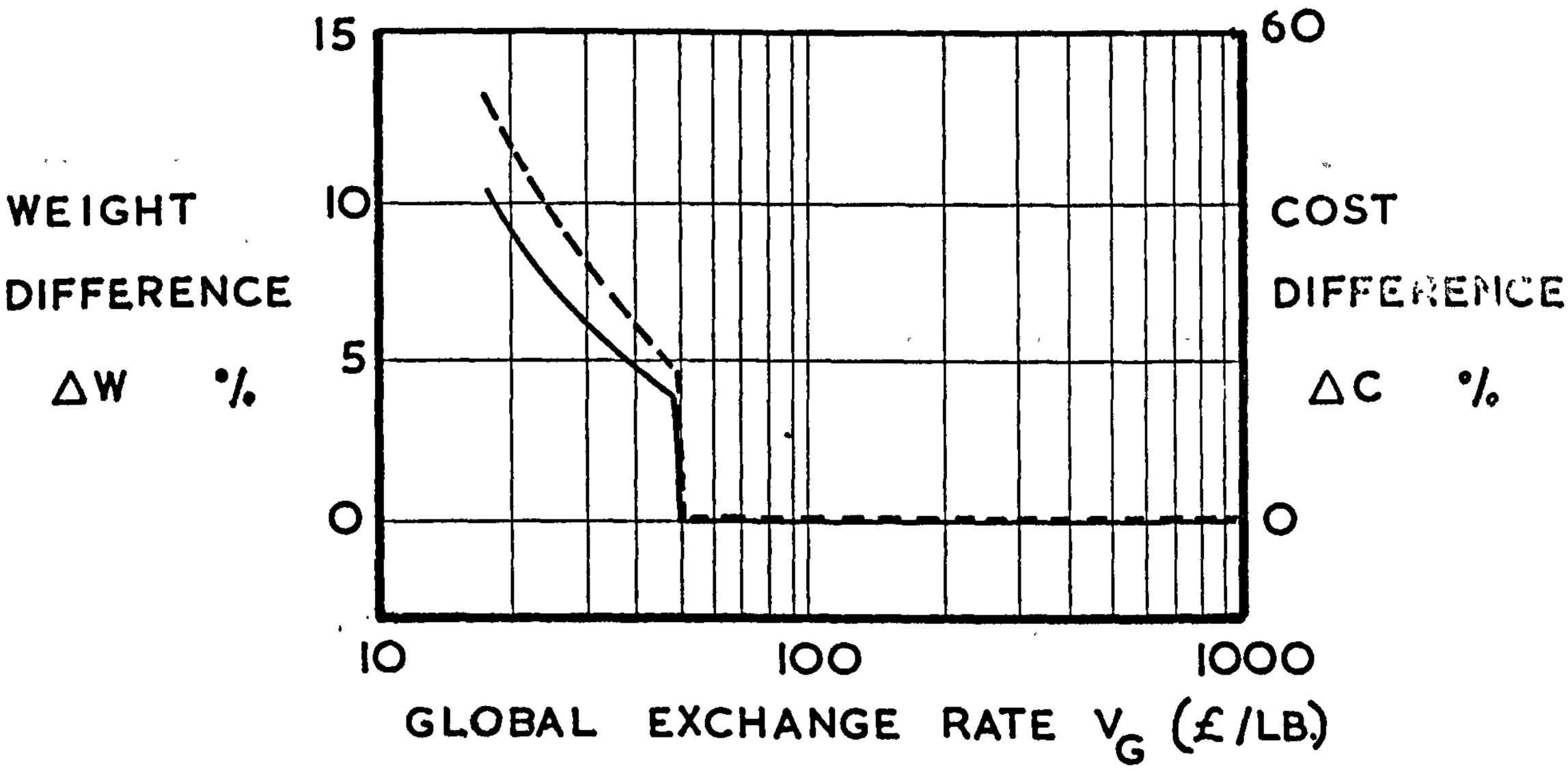


FIG. 10.10 THE LOAD LEVEL $N_X$ 2500 LB./IN.

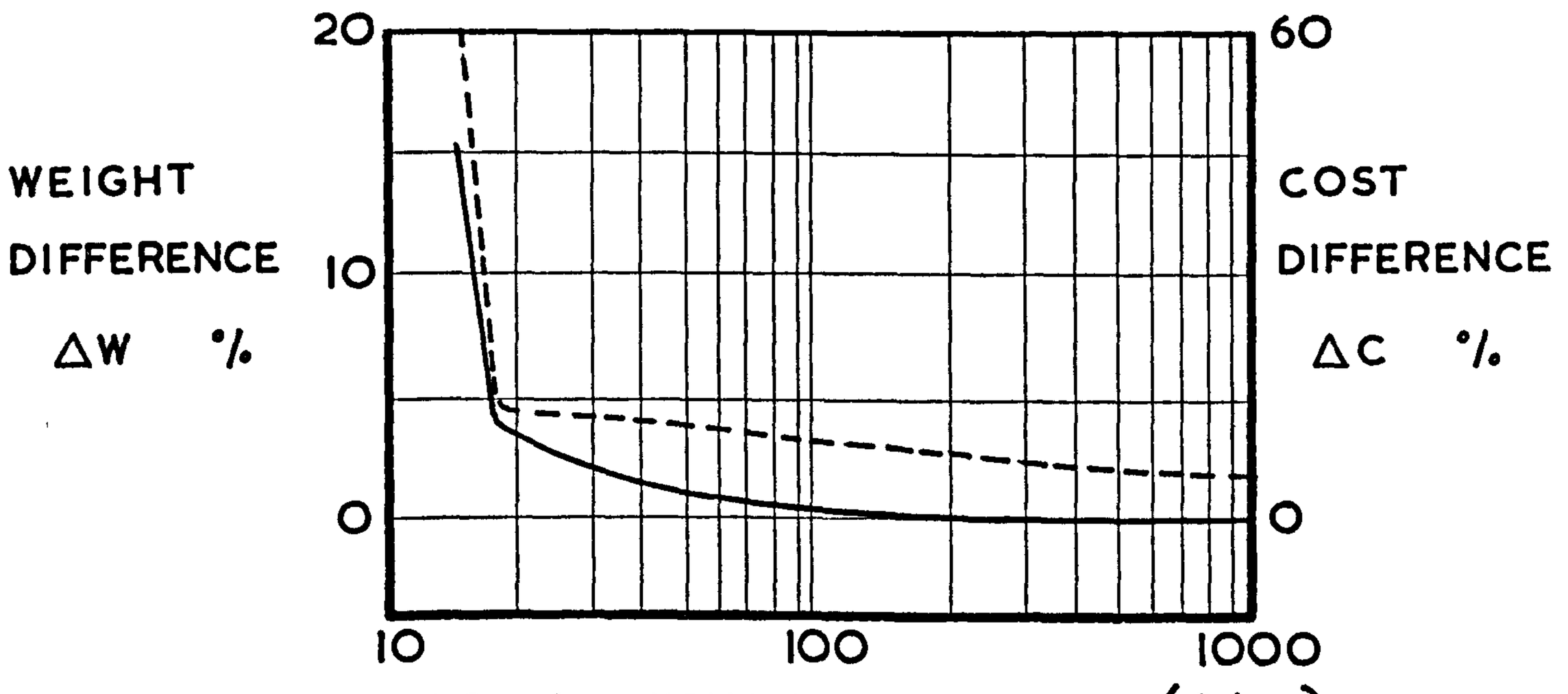


KEY

---- COST DIFFERENCE

—— WEIGHT DIFFERENCE

THE DIFFERENCES IN THE BOX BEAM COST AND WEIGHT VALUES GIVEN BY THE ANALYSES OF THE COMPONENT AND THE COMPLETE STRUCTURES

FIG. 10.11 THE LOAD LEVEL $N_x$ 5000 LB./IN.

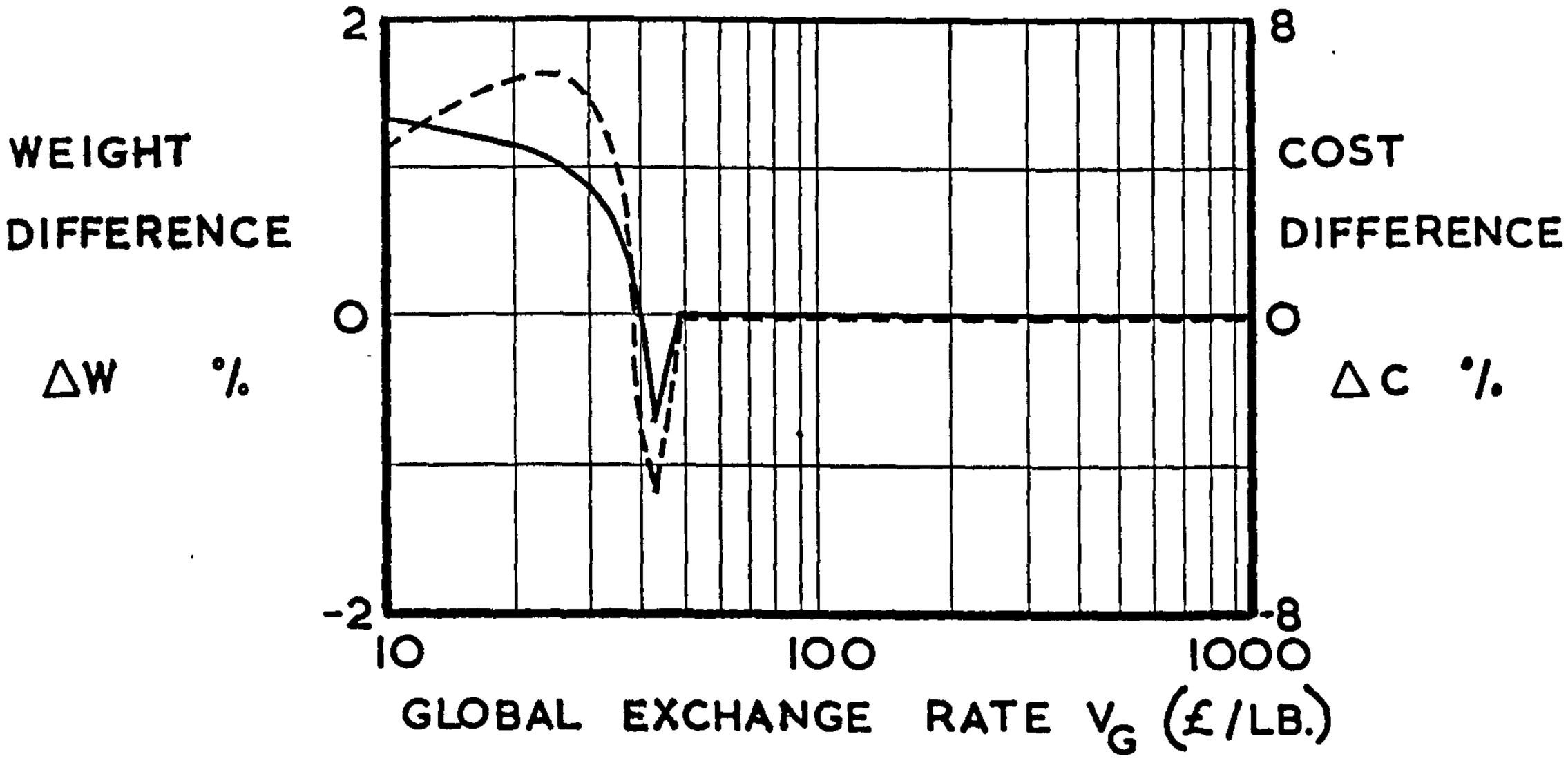


FIG. 10.12 THE LOAD LEVEL $N_x$ 10,000 LB./IN.

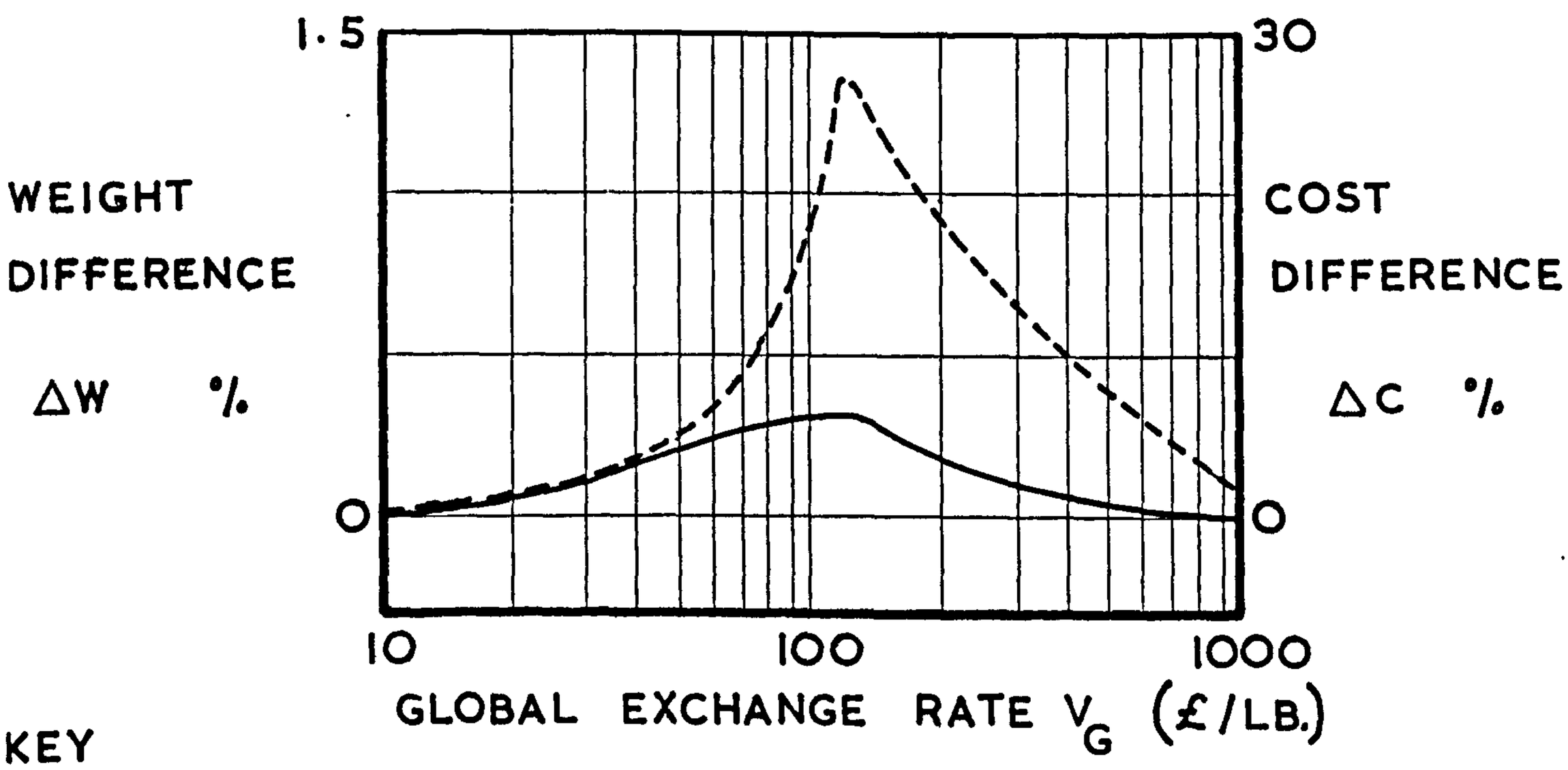


KEY

---- COST DIFFERENCE

——— WEIGHT DIFFERENCE

# P A R T  3 :

# AN ANALYTICAL METHOD FOR PRACTICAL STRUCTURES

# INTRODUCTION

The design process, which is presented in Part 1, is generally applicable to any type of structure. However, the precise treatment of the individual stages of the design process must take into account the circumstances of the structural item under examination.

Several simplifying assumptions were applied to the Specimen structure, which are discussed in Part 2, to ease the task of analysis, since the boundary conditions for practical structures are essentially more complex than was the case for the idealised model.

The adaptation of the process, which was specified for the idealised model, to cater for practical structures is now presented.

# C H A P T E R  1 1

# IMPORTANT CONSIDERATION APPLYING IN THE DESIGN OF PRACTICAL STRUCTURES

## 11.1 Introduction

Although the specimen structure was of an essentially practical nature, many simplifying assumptions were made in order to ease the analysis. The main considerations applying to practical structures are now reviewed and the differences in the boundary conditions for the specimen structure are presented.

## 11.2 The Loading Systems Applied to Practical Structures

The analysis of the specimen structure was mainly intended as an investigation of the performance of the optimal design process, so that a simple loading system was adopted.

The end loading, which was applied to the upper and lower covers of the specimen structure, was assumed to be constant along the box beam span, although a series of end loading values was considered, in order to allow the variation of the optimal configuration with load level to be examined.

It was assumed that there was no torque load applied to the box section, which meant that the shear load was the same in each spar.

The magnitude of the end loading in the covers of a practical wing tends to vary with the spanwise position, in a manner determined by the distribution of the aerodynamic and inertia loads along the span.

The internal geometry of the wing section is designed to carry the torque loading which is experienced in practical wings.

Locally applied loads, such as engine loads, undercarriage loads and control surface loads, form an important element of a practical loading system and have a major influence on the arrangement of the internal geometry of the wing. To cater for these loads local thickening of the skins and specially strengthened ribs may have to be employed, which can cause a considerable divergence from the optimal configuration determined in the absence of these loads.

## 11.3 Some Constraints Imposed on Practical Structures

The arrangement of the internal geometry of the idealised structure was held constant over the box beam span to suit the system of applied loads.

As mentioned in section 11.2, the loading applied to a practical wing varies with the spanwise position, in general. The results derived for the specimen structure, which are presented in Chapter 7, indicate a variation of the optimal configuration with the load level. Hence the optimal design would require a variation of the configuration with the spanwise position to suit the local load level. This implies that a continuous variation of rib pitch, stringer pitch, and rib, stringer and skin thickness along the span would be required. Obviously, such a design would be totally impracticable, since producibility requirements impose contraints on the internal geometry of a practical design.

The following examples are representative of the type of contraint encountered in practice:

i) the provision of alternative load paths in the structure may be required to satisfy fail-safe requirements,

ii) the provision of access panels to allow the inspection of the internal structure influences the structural arrangement of the wing,

iii) producibility requirements determine the minimum allowable pitches for the stringers and the ribs,

iv) producibility problems probably dictate a linear variation of the skin thickness along the span, if taper is to be introduced to cater for variations of the load level with spanwise position. Alternatively the skin can be stepped along the span using several sheets of different uniform thickness,

v) for ease of production, it is usual for a skin panel to have a constant stringer pitch and a constant stringer depth.

# C H A P T E R  1 2

# A PRACTICAL METHOD OF STRUCTURAL DESIGN

## 12.1 Introduction

In spite of the constraints imposed on practical structures, which are discussed in Chapter 11, the design process may still be used to identify the structural arrangement which is superior to the other arrangements examined.

The design process which was used for the optimisation of the specimen structure has been refined to cater for practical structures and is described in this Chapter.

## 12.2 The Structural Model for Practical Structures

The results of the sensitivity analysis, which are presented in Chapter 10, emphasise the importance of including all relevant structural items in the structural model to be analysed. The omission of those structural items from the structural model which, due to the effects of the interactions of the component parts in the complete structure, influence the magnitudes of the cost and weight values of the structure as a whole, can lead to a structural system being selected which does not possess the true optimal characteristics.

## 12.3 The Specification of Practical Structural Systems

As stated in section 11.2, practical wings tend to exhibit a variation of the load level with the spanwise position. If the constraints discussed in section 11.3 were

neglected, the optimal structure defined by the variation of the configuration along the span, to suit the local load level, could be obtained in the following manner:

Using the design process applied to the specimen structure, box beam sections designed to constant load levels may be optimised. The optimal configurations, defined by these constant load level studies, can be matched to the variation of the load level along the span, thus giving the optimal wing structure.

However, the practical constraints described in section 11.3 cannot be ignored. Practical structural systems must be obtained by dividing the wing into discrete sections in a spanwise direction. The variation of the configuration of the individual wing sections can approximate to the optimal variation derived above, within the limits allowed by the practical constraints such as a linear skin taper and a constant stringer pitch.

Alternative structural systems can investigate the effects of having different joint positions, different numbers of joints and different variations of the configuration within the wing sections.

## 12.4 The Evaluation of the System Values

Because of the influence of component interaction effects, the weight and cost values for each practical structure must be carefully specified.

Assume that a structural system has $m$ sections along the span, joined by $m - 1$ joints.

The weight, W (lb.), of the structural system is given by

$$W = \sum_{i=1}^{i=m} (WS)_i + \sum_{i=1}^{i=m-1} (WJ)_i \qquad (12.1)$$

where $(WS)_i$ = the structural weight of the $i^{th}$ wing section sub-assembly (lb.),

and $(WJ)_i$ = the extra weight due to the joint at the $i^{th}$ and $i+1^{th}$ wing section sub-assemblies (lb.).

The cost, C (£), of the structural system is given by

$$C = \sum_{i=1}^{i=m} (CS)_i + \sum_{i=1}^{i=m-1} (CJ)_i \qquad (12.2)$$

where $(CS)_i$ = the unit cost of the $i^{th}$ wing section sub-assembly (£),

and $(CJ)_i$ = the cost of joining the $i^{th}$ and $i+1^{th}$ wing section sub-assemblies (£).

## 12.5 The Practical Selection Process

If n alternative structural systems are proposed, the best system may be located by using the selection process employed in the examination of the specimen structure. Incorporating the system values of a practical structural system in the merit function equation (2.27) gives

$$M_j = W_j + \frac{C_j}{V_G} \qquad (12.3)$$

where $M_j$ = merit function value of the $j^{th}$ structural system (lb.), with j = 1 . . . n,

$W_j$ = weight of the $j^{th}$ structural system (lb.),

$C_j$ = cost of the $j^{th}$ structural system (£),

$V_G$ = value of the global exchange rate (£/lb.).

The structural system having the minimum value of the merit function $M_j$ gives the optimal solution.

## 12.6 The Influence of Errors in the Practical Estimation Methods

If errors are present in the practical methods of cost and weight estimation, the ability to define a unique solution is degraded.

The errors inherent in the practical methods of cost and weight estimation should be assessed in the manner proposed in section 9.2, providing the data is available in a suitable form. The performance of the selection process when comparing alternative structural systems can then be judged by the incorporation of the relevant quantities in the sensitivity equations, which are presented in section 9.2.

# GENERAL CONCLUSIONS

# CONCLUSIONS

A method of structural design has been formulated for the improvement of the economic performance of an aircraft project, by selecting the structural configuration which maximises the airline profit generated by the aircraft over its life span.

The selection of the optimal configuration is accomplished using the global exchange rate parameter, the value of which is dependent on the characteristics of the particular aircraft type. Although exchange rate values are widely used in the aircraft industry, a literature search failed to reveal a comprehensive definition of exchange rate. Thus the definition of three different types of exchange rate and the mathematical derivation of their values represents a significant contribution by this thesis.

The ability to locate a unique solution is degraded in a practical environment by the effects of errors in the methods of cost and weight estimation and by the degree of completeness of the structural component chosen for analysis. A valuable insight into the extent to which the selection process is affected by these factors is provided by the sensitivity analyses described in Chapters 9 and 10.

The optimal analysis of the idealised aircraft wing discloses design trends which may be applied to the specification of the structural arrangements for future projects, providing allowance is made for the simplifying assumptions adopted in the analysis.

The most interesting design trend is the decrease in the value of the detail exchange rate at which the optimal structure changes from an aluminium alloy to a titanium alloy design as the design load level is increased. Indeed, at a load level of 10,000 lb./in., the value of the global exchange rate for an aircraft project need only be greater than £61/lb. for the optimal design to use titanium alloy material, a value which is well within the range of global exchange rate values in use at the present time for civil subsonic aircraft.

The results indicate that titanium alloy represents a practical proposition for airframe applications, providing the load level is high enough to enable the weight saving potential of the material, relative to aluminium alloy, to be fully exploited.

## Suggestions for Further Work

The following courses of investigation could be profitably pursued to develop the findings of the research work reported in this thesis:

i) The design process may be applied to other structural components, an aircraft's fuselage forming an ideal subject for further analysis.

ii) Alternative types of construction, different materials and different production methods may be considered to widen the scope of the possible solutions.

iii) When dealing with a specific aircraft project the assumptions made in the mathematical derivation of the

break-even exchange rate value should be modified, if necessary, to accommodate the particular characteristics of the aircraft type under examination.

iv) An assessment, using statistical techniques, should be made of the magnitude of the errors in the methods of cost and weight estimation employed in past aircraft programs. The influence of these errors on the selection process may then be determined using the sensitivity equations. If possible, improvements should be sought in the estimating methods to reduce the error levels.

# A P P E N D I X 1

# THE COMPUTER PROGRAMS FOR THE EVALUATION OF THE STRUCTURAL WEIGHT

Complex equations had to be solved in the weight analysis area of the design process. A computer program was written to undertake the solution of these equations in order to ensure accuracy and to expedite the process.

An existing computer program was used for the evaluation of the spar weight of the specimen structure.

All programs, excepting the Diagonal Tension Analysis program, satisfied the requirements of the Egdon Algol operating system of the English Electic-Leo K.D.F.9 computing facility at the University of Salford.

## A1.1 A Computer Program Solution of the Structural Design Equations

The main constraints imposed on the internal dimensions of the box beam were applied by the structural design equations, which are presented in section 3.3.

The following computer program solves the structural design equations and presents the results in a non-dimensionalised form. The program output gives the values of the tension cover, compression cover and rib thicknesses and the rib pitch, required for structural integrity, over a range of values of the end loading and the structural efficiency factor.

The sequence of the data input is as follows:

d = box beam depth (in.),

e = material modulus of elasticity (lb./in.$^2$),

b = number of non-dimensional loading coefficients under examination,

p = material density (lb./in.$^3$),

x = lowest structural efficiency factor value,

y = structural efficiency factor step length,

z = highest structural efficiency factor value,

fc = material 0.1% proof stress (lb./in.$^2$),

ft = material ultimate tensile stress (lb./in.$^2$),

tcmin = minimum gauge constraints on the covers (in.),

palum = density of aluminium alloy material (lb./in.$^3$),

fcalum = 0.1% proof stress of aluminium alloy material (lb./in.$^2$),

fr = Farrar efficiency factor applied to the ribs,

tcalum = minimum gauge constraint applied to the aluminium alloy covers (in.),

xx[1] = lowest value of the non-dimensional loading coefficient,

xx[b] = highest value of the non-dimensional loading coefficient.

The program listing is as follows:

```
SOLUTION OF THE STRUCTURAL DESIGN EQUATIONS

begin integer i,f1,f2,b;

real f,fr,d,e,p,x,y,z,fc,ft,tcmin,trmin,palum,fcalum,pratio,

fcratio,tcalum,tcratio;

f1:=layout([2s-d.ddd₁₀+nd]); f2:=layout([2s-d.ddd₁₀+ndc]);
```

```
open(20);open(30);
d:=read(20); e:=read(20);b:=read(20);p:=read(20);
x:=read(20);y:=read(20);z:=read(20);
fc:=read(20);ft:=read(20);tcmin:=read(20);
palum:=read(20);fcalum:=read(20);fr:=read(20);
tcalum:=read(20);
write(30,f1,d); write(30,f1,e); write(30,f1,b);
write(30,f1,p);write(30,f1,x);write(30,f2,y);
write(30,f1,z);write(30,f1,fc);
write(30,f1,ft);write(30,f2,tcmin);write(30,f1,palum);
write(30,f1,fcalum);write(30,f1,fr);
newline(30,3);
writetext(30,[WING*DEPTH*=*]);write(30,f2,d);
trmin:=tcmin;
fcratio:=fcalum/fc;
tcratio:=tcalum/tcmin;
pratio:=palum/p;
begin real array aa,ab,ac,ad,ae,af,ag,ah,aj,aopt,wca,wcb,
wcc,wcd,wce,wcf,wcg,wch,wcj,wcomp,wten,wtot,wcra,wcrb,
wcrc,wcrd,wcre,wcrf,wcrg,wcrh,wcrj,wta,wtb,wtc,tra,trb,
trc,trd,tre,trf,trg,trh,trj,nn,xx,zz[1:b];
xx[1]:=read(20);
xx[b]:=read(20);
close(20);
write(30,f2,xx[1]);write(30,f2,xx[b]);
for f:=x step y until z do
begin writet(30,[EFFICIENCY*FACTOR*=*]);
write(30,f2,f);
```

```
newline(30,2);
for i:=1 step 1 until b do
begin xx[i]:=xx[1]+(i-1)×(xx[b]-xx[1])/(b-1);
zz[i]:=xx[i]×fcratio;
nn[i]:=zz[i]×fc×tcmin×tcratio;
tra[i]:=1/tcratio;
wca[i]:=1/(pratio×tcratio);
wcra[i]:=(1+(nn[i]×trmin×d)/(f↑2×ext cmin↑3))/(pratio×tcratio);
aa[i]:=tcmin×f↑2×e/(nn[i]×tcratio);
aopt[i]:=aa[i];
wcomp[i]:=wcra[i];
trb[i]:=f×(2×tcmin×nn[i]/e)↑.5/(fr×trmin×tcratio);
ab[i]:=aa[i];
wcb[i]:=1/(pratio×tcratio);
wcrb[i]:=(1/tcratio+(d×trb[i]×trmin)/(ab[i]×tcalum↑2))/pratio;
if trb[i]>tra[i] then
begin aopt[i]:=ab[i];
wcomp[i]:=wcrb[i];
end;
ac[i]:=aa[i];
wcc[i]:=1/(pratio×tcratio);
trc[i]:=2×nn[i]×tcmin×f↑2/(d×fc×trmin×tcratio);
wcrc[i]:=(1/tcratio+(d×trc[i]×trmin)/(ac[i]×tcalum↑2))/pratio;
if trc[i]>trb[i] and trc[i]>tra[i] then
begin aopt[i]:=ac[i];
wcomp[i]:=wcrc[i];
end;
ad[i]:=((4×f↑2×d↑2×trmin↑2×e)/(nn[i]×tcalum↑3))↑(1/3);
```

```
trd[i]:=1/tcratio;
wcd[i]:=((2×nn[i]×d×trmin)/(ex f↑2×tcalum↑3))↑(1/3)/pratio;
wcrd[i]:=1.5×wcd[i];
if wcd[i]>wca[i] and trd[i]>trc[i] and trd[i]>trb[i] then
begin aopt[i]:=ad[i];
wcomp[i]:=wcrd[i];
end;
ae[i]:=(4.5×d↑2×f↑3×nn[i]↑.5/(fr↑2×e↑.5))↑.4/tcalum;
tre[i]:=(12×nn[i]↑4×f↑4×d/(fr↑6×e↑4))↑.2/(trmin×tcratio);
wce[i]:=(ae[i]×tcalum)↑.5×nn[i]↑.5/(e↑.5×f×pratio×tcalum);
wcre[i]:=wce[i]+d×tre[i]×trmin/(ae[i]×tcalum↑2×pratio);
if wce[i]>wcd[i] and wce[i]>wca[i] and tre[i]>trd[i] and
tre[i]>trc[i] and tre[i]>trb[i] then
begin aopt[i]:=ae[i];
wcomp[i]:=wcre[i];
end;
af[i]:=2×nn[i]×f↑2/(fc×tcalum);
trf[i]:=2↑1.5×nn[i]↑2×f↑2/(e↑.5×d×fc↑1.5×trmin×tcratio);
wcf[i]:=af[i]↑.5×nn[i]↑.5/(e↑.5×f×pratio×tcalum↑.5);
wcrf[i]:=wcf[i]+d×trf[i]×trmin/(af[i]×tcalum↑2×pratio);
if wcf[i]>wce[i] andwcf[i]>wcd[i] andwcf[i]>wca[i] and
trf[i]>tre[i] and trf[i]>trd[i] andtrf[i]>trc[i] and
 trf[i]>trb[i] then
begin aopt[i]:=af[i];
wcomp[i]:=wcrf[i];
end;
ag[i]:=nn[i]×ex f↑2/(fc↑2×tcalum);
trg[i]:=1/tcratio;
```

```
wcg[i]:=zz[i]/pratio;
wcrg[i]:=(zz[i]+d×trmin/(ag[i]×tcalum↑2))/pratio;
if wcg[i]>wcf[i] and wcg[i]>wce[i] andwcg[i]>wcd[i] and
wcg[i]>wca[i] and trg[i]>trf[i] and trg[i]>tre[i] and
 trg[i]>trc[i] and trg[i]>trb[i] then
begin aopt[i]:=ag[i];
wcomp[i]:=wcrg[i];
end;
ah[i]:=ag[i];
trh[i]:=nn[i]×f×2↑.5/(fr×e↑.5×fc↑.5×trmin×tcratio);
wch[i]:=zz[i]/pratio;
wcrh[i]:=(zz[i]+d×trh[i]×trmin/(ah[i]×tcalum↑2))/pratio;
if wch[i]>wcf[i] and wch[i]>wce[i] and wch[i]>wcd[i] and
wch[i]>wca[i] and trh[i]>trg[i] and trh[i]>trf[i] and
trh[i]>tre[i] and trh[i]>trc[i] and trh[i]>trb[i] then
begin aopt[i]:=ah[i];
wcomp[i]:=wcrh[i];
end;
aj[i]:=ag[i];
trj[i]:=2×nn[i]↑2×f↑2/(d×fc↑2×trmin×tcratio);
wcj[i]:=zz[i]/pratio;
wcrj[i]:=(zz[i]+d×trj[i]×trmin/(aj[i]×tcalum↑2))/pratio;
if wcj[i]>wcf[i] and wcj[i]>wce[i] and wcj[i]>wcd[i] and
wcj[i]>wca[i] and trj[i]>trh[i] and trj[i]>trg[i] and
trj[i]>trf[i] and trj[i]>tre[i] and trj[i]>trc[i] and
trj[i]>trb[i] then
begin aopt[i]:=aj[i];
wcomp[i]:=wcrj[i];
```

```
end;
wta[i]:=1/(pratioxtcratio);
wten[i]:=wta[i];
wtb[i]:=nn[i]/(ftxtcminxpratioxtcratio);
if wtb[i]>wta[i] thenwten[i]:=wtb[i];
wtc[i]:=((aopt[i]xnn[i]/2)/(extcalumxf↑2))↑(1/2)/pratio;
if wtc[i]>wtb[i] and wtc[i]>wta[i] then
wten[i]:=wtc[i];
wtot[i]:=wcomp[i]+wten[i];
end;
writet(30,[MINIMUM*TOTAL*WEIGHT[2c3s]W/(tcminxP)
[6s]N/(Fxtcmin)[2c]]);
for i:= 1 step 1 until b do
begin write(30,f1,wtot[i]);
write(30,f2,xx[i]);
end;
writet(30,[[2c]MINIMUM*COMPRESSION*COVER*PLUS*RIB*WEIGHT
[2c3s]W/(tcminxP)[6s]N/(Fxtcmin)[2c]]);
for i:= 1 step 1 until b do
beginwrite(30,f1,wcomp[i]);
write(30,f2,xx[i]);
end;
writet(30,[[2c]MINIMUM*TENSION*COVER*WEIGHT[2c3s]W/(tcminxP)
[6s]N/(Fxtcmin)[2c]]);
for i:= 1 step 1 until b do
begin write(30,f1,wten[i]);
write(30,f2,xx[i]);
end;
```

```
writet(30,[COMPRESSION*COVER*WEIGHT[2c44s]W/(tcminxP)[47s]
N/(Fxtcmin)[c6s]a[12s]b[12s]c[12s]d[12s]e[12s]f[12s]g[12s]
h[12s]j[2c]]);
for i:=1 step 1 until b do
begin write(30,f1,wca[i]);write(30,f1,wcb[i]);
write(30,f1,wcc[i]);write(30,f1,wcd[i]);
write(30,f1,wce[i]);write(30,f1,wcf[i]);
write(30,f1,wcg[i]);write(30,f1,wch[i]);
write(30,f1,wcj[i]);write(30,f2,xx[i]);
end;
writet(30,[COMPRESSION*COVER*PLUS*RIB*WEIGHT[2c44s]W/(tcminxP)
[47s]N/(Fxtcmin)[c6s]a[12s]b[12s]c[12s]d[12s]e[12s]f[12s]g[12s]
h[12s]j[2c]]);
for i:=1 step 1 until b do
begin write(30,f1,wcra[i]);write(30,f1,wcrb[i]);
write(30,f1,wcrc[i]);write(30,f1,wcrd[i]);
write(30,f1,wcre[i]);write(30,f1,wcrf[i]);
write(30,f1,wcrg[i]);write(30,f1,wcrh[i]);
write(30,f1,wcrj[i]);write(30,f2,xx[i]);
end;
writet(30,[TENSION*COVER*WEIGHT[2c15s]W/(tcminxP)[13s]
N/(Fxtcmin)[c6s]a[12s]b[12s]c[2c]]);
for i:=1 step 1 until b do
begin write(30,f1,wta[i]);write(30,f1,wtb[i]);
write(30,f1,wtc[i]);write(30,f2,xx[i]);
end;
writet(30,[RIB*SPACING[2c44s]A/(tcmin)[47s]N/(Fxtcmin)[c6s]
a[12s]b[12s]c[12s]d[12s]e[12s]f[12s]g[12s]h[12s]j[2c]]);
```

```
for i:=1 step 1 until b do
begin write(30,f1,aa[i]);write(30,f1,ab[i]);
write(30,f1,ac[i]);write(30,f1,ad[i]);
write(30,f1,ae[i]);write(30,f1,af[i]);
write(30,f1,ag[i]);write(30,f1,ah[i]);
write(30,f1,aj[i]);write(30,f2,xx[i]);
end;
writet(30,[[3c]RIB*THICKNESS[2c44s]tr/trmin[47s]N/(Fxtcmin)
[c6s]a[12s]b[12s]c[12s]d[12s]e[12s]f[12s]g[12s]h[12s]j[2c]]);
for i:=1 step 1 until b do
begin write(30,f1,tra[i]);write(30,f1,trb[i]);
write(30,f1,trc[i]);write(30,f1,trd[i]);
write(30,f1,tre[i]);write(30,f1,trf[i]);
write(30,f1,trg[i]);write(30,f1,trh[i]);
write(30,f1,trj[i]);write(30,f2,xx[i]);
end;
newline(30,3);
end;
end;
close(30);
end
```

## A1.2 The Diagonal Tension Analysis Program

This program, which was written by Robinson[15] for the diagonal tension analysis of flat panels in shear, has been used to evaluate the spar weight of the specimen structure.

An iterative approach had to be adopted in the selection of a spar which was capable of carrying the applied shear load, since the program output gave the stresses in the various members of a shear panel.

A constraint was applied to the main spar dimension, namely the spar stiffener pitch, by the operative rib pitch. In practice, the rib pitch is a multiple of the spar stiffener pitch. Hence the rib pitch was determined using the computer program described in section A1.1 before the diagonal tension analysis was undertaken.

Details of the input data required and the form of program output are given in ref. 15.

# A P P E N D I X  2

## THE PRODUCTION COST EQUATIONS AND THE ASSOCIATED PRODUCTION COST ANALYSIS COMPUTER PROGRAMS

As mentioned in section 4.3.2, production cost equations were evolved to expedite the process of calculating the direct labour time required to produce each structural system.

The production method for each structural system was separated into three stages, as follows:

i) the detail manufacture stage,

ii) the sub-assembly stage,

iii) the final assembly stage.

The dominant operations in each production stage were determined. Each operation was expressed in the form of an equation giving the direct labour time expended on the process. A summation procedure was employed to determine the total labour time required to produce the structure; this value being increased by a suitable scale factor to take account of those operations omitted from the production cost equations. The relevant cost factor, stated in Chapter 4, was applied to convert the direct labour time into a total production cost, including the overhead allowance and the cost due to the production learning effect.

To facilitate the evaluation of the production cost equations for each structural system, computerised solutions were adopted, since many calculations were involved in these analyses.

## A2.1 The Production Cost Equations for the Chemically Etched and the Basic Aluminium Alloy Structural Systems

Using the following production cost equations, the production costs of the chemically etched and the basic aluminium alloy designs were evaluated, since the only extra process required for the production of the chemically etched design was the etching of lands on panels 1 and 2. The cost of the chemical etch process was evaluated separately.

The production cost equations were based on the production method description given in section 5.2.2. The main operations involved in the production method were manual drilling, the insertion and removal of pegs, deburring, countersinking, application of protective treatment, manual and automatic riveting and handling.

The Drivmatic automatic riveting machine was used for the attachment of the stiffeners to panels 1, 2, 3 and to the ribs, requiring the manual tack riveting of 10% of the holes to locate the items. The time taken for the automatic riveting process was based on the following operation times:

i) The drilling time taken per hole, which is dependent on drill diameter and stock thickness. The values used are presented in fig. A2.1.

ii) The automatic cycle time taken by the machine to feed and squeeze the rivet, which is a constant for a specific machine type. The value used is presented in Table A2.3.

iii) The time taken, tx, to mark hole postions and to

align the machine between rivets along a row, and the time taken, ty, to traverse the machine between rows. The length of time involved in these operations depends on the handling and positioning system in use. The values used are presented in Table A2.3.

The total production time was given by the summation of the detail manufacture, the sub-assembly and the final assembly times. The individual production cost equations, for each of these stages, are as follows:

The equation giving the detail manufacture time, dtime, in minutes is

$$\begin{aligned} dtime = x \cdot \{ & tc \cdot (cla + clb) + td \cdot nr \\ & + ts \cdot (sa + sb + 2 \cdot (sc + sd)) + aa/(10 \cdot dt) \\ & + ba/(10 \cdot dt) + 1.1 \cdot {}^{ab}/dt + 2 \cdot bb/dt \\ & + 2 \cdot db/dt \} \end{aligned} \qquad (A2.1)$$

The equation giving the sub-assembly time, stime, in minutes is

$$\begin{aligned} stime = y \cdot \{ & m \cdot (sa + sb) + 2 \cdot n \cdot sc \\ & + ({}^{2}/pu + {}^{2}/po + {}^{3}/deb + {}^{1}/dt) \\ & \cdot (aa + ab/2 + ba + {}^{bb}/2 + ca + cb)/10 + \\ & ({}^{1}/csk + {}^{1}/cskr) \cdot (aa + {}^{ab}/2 + ba + {}^{bb}/2) \\ & + {}^{1}/snpr \cdot (ca + cb)/10 + (dma + tx) \cdot 0.9 \\ & \cdot (aa + {}^{ab}/2) + (dmb + tx) \cdot 0.9 \cdot (ba + {}^{bb}/2) \\ & + (dmc + tx) \cdot 0.9 \cdot (cb + ca) + ty \\ & \cdot (sa + sb + sc) \} \end{aligned} \qquad (A2.2)$$

The equation giving the final assembly time, ftime, in minutes is

$$\begin{aligned}\text{ftime} = z \cdot \{ & (ab + bb) \cdot (1/(2 \cdot dt) + 1/(2 \cdot csk) \\ & + 0.2 \cdot (1/pu + 1/po) + 1.5/deb + 1/(2 \cdot cskr)) \\ & + (ac + bc) \cdot (1/dt + 1/csk + 0.4 \\ & \cdot (1/pu + 1/po) + 3/deb + 1/cskr) + (da + db) \\ & \cdot (1/dt + 1/av + 0.4 \cdot (1/pu + 1/po) + 4/deb) \\ & + ea \cdot (1/dt + 1/pu + 1/po + 4/deb + 1/snpr) \\ & + fa \cdot (1/dt + 0.4 \cdot (1/pu + 1/po) + 4/deb \\ & + 1/snpr) + con \}\end{aligned} \qquad \text{(A2.3}$$

The total production time, ttime, in minutes is

$$\text{ttime} = \text{dtime} + \text{stime} + \text{ftime} \qquad \text{(A2.4)}$$

Most of the variable used in the above production cost equations are defined in the computer program description given in section A2.1.1, the remainder being defined as follows:

ea = number of cleat holes,

sd = number, per panel, of panel 3 and 4 extrustion angles,

tc = production time per cleat (mins.),

td = production time per rib (mins.),

ts = production time per stringer (mins.),

tx = indexing time for the automatic riveting machine (mins.),

ty = traverse time for the automatic riveting machine (mins.).

A2.1.1 Computer program description

The following computer program was used to solve the above production cost equations. The sequence of data input required by the program is as follows:

sa = number of panel 1 stringers,

sb = number of panel 2 stringers,

sc = number, per panel, of panel 3 and 4 stiffeners,

nr = number of ribs,

cla = number of panel 1 cleats,

clb = number of panel 2 cleats,

aa = number of panel 1 Z stringer rivets,

ab = number of panel 1 extrusion angle rivets,

ac = number of panel 1 rib flange rivets,

ba = number of panel 2 Z stringer rivets,

bb = number of panel 2 extrusion angle rivets,

bc = number of panel 2 rib flange rivets,

ca = number of panel 3 extrusion angle rivets,

cb = number of panel 3 stiffener rivets,

da = number of panel 4 extrusion angle rivets,

db = number of panel 4 stiffener rivets,

fa = number of rib stiffener rivets,

ta = panel 1 skin thickness (s.w.g.),

tsa = panel 1 stringer thickness (s.w.g.),

tb = panel 2 skin thickness (s.w.g.),

tsb = panel 2 stringer thickness (s.w.g.),

tc = panel 3 and 4 skin thickness (s.w.g.),

tcb = panel 3 and 4 stiffener thickness (s.w.g.),

tab = panel 3 and 4 extrusion angle thickness (s.w.g.),

tr = rib thickness (s.w.g.),

daa → dfa = rivet diameters (in.) corresponding to rivets listed aa → fa,

av = blind rivet rate (n°./min.),

pu = rate of peg insertion (n°./min.),

po = rate of peg removal (n°./min.),

deb = deburring rate (n°./min.),

k = upper limit of drill diameter array,

l = upper limit of material gauge array,

x = detail manufacture scale factor,

y = sub-assembly scale factor,

z = final assembly scale factor,

m = cost factor related to the number of stringers (mins./stringer),

n = cost factor related to the number of web stiffeners (mins./stringer),

dma, dmb, dmc = automatic rivet time comprising the automatic cycle time plus the drill time related to the stock thickness of panels 1, 2 and 3 respectively (mins.),

con = time allowance for handling and application of treatment (mins.),

dd [1:k] = drill diameter array (in.),

csk [1:k] = countersink rate (n°./min.) corresponding to diameters dd,

cskr [1:k] = countersink rivet rate (n°./min.) corresponding to diameters dd,

snpr [1:k] = snaphead rivet rate (n°./min.) corresponding to diameters dd,

g [1:l] = material gauge array (s.w.g.),

dt [1:k, 1:l] = manual drill rate array (n°./min.).

The program listing is as follows:

```
EVALUATION OF THE PRODUCTION COST OF THE BASIC
ALUMINIUM ALLOY DESIGN
begin procedure drilltime(a,b,c,d,e,f,g,h);
value g,h;
real d,e,f;
integer g,h;
real array a,b,c;
begin integer i,u,v;
for i:=1 step 1 until g do
if d-a[i]<.001 then begin u:=i;
goto ha;
end;
ha:     for i:= 1 step 1 until h do
if e-b[i]<.001 then begin v:=i;
goto hb;
end;
hb:     f:=c[u,v];
enddrilltime;
procedure selection(a,b,c,d,e);
value e;
real c,d;
integer e;
real array a,b;
```

```
begin integer i,u;
for i:= 1 step 1 until e do
if c-a[i]<.001 then begin u:=i;
goto hc;
end;
hc:     d:=b[u];
end selection;
begin integer i,j,k,l,s,f1,f2;
real sa,sb,sc,nr,cla,clb,aa,ab,ac,ba,bb,bc,ca,cb,da,db,
ea,fa,ta,tsa,tb,tsb,tc,tcb,tab,tr,daa,dab,dac,dba,dbb,dbc,
dca,dcb,dda,ddb,dea,dfa,av,pu,po,deb,x,y,z,m,n,dma,dmb,dmc,
dtime,stime,ftime,ttime,p,r,con;
f1:=layout([2s-d.dddd10+nd]);f2:=layout([2s-d.dddd10+ndc]);
open(20);
sa:=read(20);sb:=read(20);sc:=read(20);nr:=read(20);
cla:=read(20);clb:=read(20);aa:=read(20);ab:=read(20);
ac:=read(20);ba:=read(20);bb:=read(20);bc:=read(20);
ca:=read(20);cb:=read(20);da:=read(20);db:=read(20);
fa:=read(20);ta:=read(20);tsa:=read(20);tb:=read(20);
tsb:=read(20);tc:=read(20);tcb:=read(20);tab:=read(20);
tr:=read(20);daa:=read(20);dab:=read(20);dac:=read(20);
dba:=read(20);dbb:=read(20);dbc:=read(20);dca:=read(20);
dcb:=read(20);dda:=read(20);ddb:=read(20);dea:=read(20);
dfa:=read(20);av:=read(20);pu:=read(20);po:=read(20);
deb:=read(20);k:=read(20);l:=read(20);x:=read(20);
y:=read(20);z:=read(20);m:=read(20);n:=read(20);
dma:=read(20);dmb:=read(20);dmc:=read(20);con:=read(20);
close(20);
```

```
ea:=4×(cla + clb);
open(30);
write(30,f1,sa);write(30,f1,sb);write(30,f2,sc);
write(30,f1,nr);write(30,f1,cla);write(30,f2,clb);
write(30,f1,aa);write(30,f1,ab);write(30,f2,ac);
write(30,f1,ba);write(30,f1,bb);write(30,f2,bc);
write(30,f1,ca);write(30,f1,cb);write(30,f2,da);
write(30,f1,db);write(30,f1,ea);write(30,f2,fa);
write(30,f1,ta);write(30,f1,tsa);write(30,f2,tb);
write(30,f1,tsb);write(30,f1,tc);write(30,f2,tcb);
write(30,f1,tab);write(30,f1,tr);write(30,f2,daa);
write(30,f1,dab);write(30,f1,dac);write(30,f2,dba);
write(30,f1,dbb);write(30,f1,dbc);write(30,f2,dea);
write(30,f1,dca);write(30,f1,dcb);write(30,f2,dda);
write(30,f1,ddb);write(30,f1,dfa);write(30,f2,av);
write(30,f1,pu);write(30,f1,po);write(30,f2,deb);
write(30,f1,k);write(30,f1,l);write(30,f2,x);
write(30,f1,y);write(30,f1,z);write(30,f2,m);
write(30,f1,n);write(30,f1,dma);write(30,f2,dmb);
write(30,f1,dmc);write(30,f2,con);
close(30);
begin real array dd,csk,cskr,snpr[1:k],g[1:l],dt[1:k,1:l];
open(20);
for i:= 1 step 1 until k do dd[i]:=read(20);
for i:= 1 step 1 until k do csk[i]:=read(20);
for i:=1 step 1 until k do cskr[i]:=read(20);
for i:= 1 step 1 until k do snpr[i]:=read(20);
for i:= 1 step 1 until l do g[i]:=read(20);
```

```
for i:= 1 step 1 until k do
for j:= 1 step 1 until l dodt[i,j]:=read(20);
close(20);
comment In the next block the detail assembly time
is evaluated;
dtime:=cla + clb + 5xnr;
drilltime(dd,g,dt,daa,tsa,r,k,l);
dtime:=dtime + (4+aa/(10xsaxr))xsa;
drilltime(dd,g,dt,dba,tsb,r,k,l);
dtime:=dtime + (4+ba/(10xsbxr))xsb;
drilltime(dd,g,dt,dab,tab,r,k,l);
dtime:=dtime + (4+.55xab/(2xr))x4;
drilltime(dd,g,dt,dca,tab,r,k,l);
dtime:=dtime +(4+bb/(2xr))x4;
drilltime(dd,g,dt,dcb,tcb,r,k,l);
dtime:=dtime + (4+db/(scxr))x2xsc;
dtime:=xxdtime;
comment In the next block the sub assembly time
is evaluated;
stime:=mx(sa+sb)+nx2xsc;
drilltime(dd,g,dt,daa,ta,r,k,l);
p:=(aa+ab/2)/10;
stime:=stime + (p/pu+p/po)x2+p/r+3xp/deb;
selection(dd,csk,daa,r,k);
stime:=stime+p/r;
selection(dd,cskr,daa,r,k);
stime:=stime+p/r;
p:=px9;
```

```
stime:=stime+px.055+sax.15+pxdma;
drilltime(dd,g,dt,dba,tb,r,k,l);
p:=(ba+bb/2)/10;
stime:=stime+(p/pu+p/po)x2+p/r+3xp/deb;
selection(dd,csk,dba,r,k);
stime:=stime+p/r;
selection(dd,cskr,dba,r,k);
stime:=stime+p/r;
p:=px9;
stime:=stime+px.055+sbx.15+pxdmb;
drilltime(dd,g,dt,dcb,tc,r,k,l);
p:=(cb+ca)/10;
stime:=stime+(p/pu+p/po)x2+p/r+3xp/deb;
selection(dd,csk,dcb,r,k);
stime:=stime+p/r;
selection(dd,snpr,dcb,r,k);
stime:=stime+p/r;
p:=px9;
stime:=stime+px.055+scx.15+pxdmc;
stime:=stimexy;
comment In the next  block the final assembly time
is evaluated;
ftime:=con;
drilltime(dd,g,dt,dea,tsa,r,k,l);
ftime:=ftime+ea/r;
selection(dd,snpr,dea,r,k);
ftime:=ftime+ea/r+ea/pu+ea/po+4xea/deb;
drilltime(dd,g,dt,dac,ta,r,k,l);
```

```
ftime:=ftime+ac/r;
selection(dd,csk,dac,r,k);
ftime:=ftime+ac/r+(ac/pu+ac/po)x.4+3xac/deb;
selection(dd,cskr,dac,r,k);
ftime:=ftime+ac/r;
drilltime(dd,g,dt,dbc,tb,r,k,l);
ftime:=ftime+bc/r;
selection(dd,csk,dbc,r,k);
ftime:=ftime+bc/r+(bc/pu+bc/po)x.4+3xbc/deb;
selection(dd,cskr,dbc,r,k);
ftime:=ftime+bc/r;
s:=0;
hd:     drilltime(dd,g,dt,dab,ta,r,k,l);
ftime:=ftime+ab/(2xr);
selection(dd,csk,dab,r,k);
ftime:=ftime+ab/(2xr)+(ab/pu+ab/po)x.2+1.5xab/deb;
selection(dd,cskr,dab,r,k);
ftime:=ftime+ab/(2xr);
s:=s+1;
if s>1 then goto he else begin ab:=bb;
dab:=dbb;
ta:=tb;
goto hd;
end;
he:     drilltime(dd,g,dt,dfa,tr,r,k,l);
ftime:=ftime+fa/r;
selection(dd,snpr,dfa,r,k);
ftime:=ftime+fa/r+(fa/pu+fa/po)/2.5+4xfa/deb;
```

```
drilltime(dd,g,dt,ddb,tc,r,k,l);
ftime:=ftime+db/r+db/av+(db/pu+db/po)/2.5+4xdb/deb;
drilltime(dd,g,dt,dda,tc,r,k,l);
ftime:=ftime+da/r+da/av+(da/pu+da/po)/2.5+4xda/deb;
ftime:=ftimexz;
ttime:=dtime+stime+ftime;
open(30);
writet(30,[[3c]TORSION*BOX*PRODUCTION*COST*ANALYSIS[2c]
DETAIL*MANUFACTURE*COST[c]]);
write(30,f2,dtime);
writet(30,[MINUTES[2c]SUB*ASSEMBLY*COST[c]]);
write(30,f2,stime);
writet(30,[MINUTES[2c]FINAL*ASSEMBLY*COST[c]]);
write(30,f2,ftime);
writet(30,[MINUTES[2c]TOTAL*PRODUCTION*COST[c]]);
write(30,f2,ttime);
writet(30,[MINUTES]);
close(30);
end;
end;
end
```

Two useful procedures were employed extensively throughout both aluminium alloy production cost programs.

Procedure "drilltime" is essentially a method of selecting the correct drill rate for the operative combination of drill diameter and material thickness. Information on the drill rates required for combinations

of drill diameter and stock thickness was held in a data file, and the correct value was selected using a comparative procedure. The values used are presented on Table A2.1.

Procedure "selection" functioned in a similar manner to "drilltime", allowing the correct counter-sinking rate or riveting rate to be selected for a given hole diameter. The values used are presented on Table A2.2.

The values used in the computer programs for the other production processes are presented on Table A2.3.

## A2.2 The Production Cost Equations for the Spin Dimpled Aluminium Alloy Structural System

The production cost equations were based on the production method description given in section 5.2.4. The basic difference between the production methods of the spin dimpled design and the basic design was the use of spin dimpling, rather than cut-countersinking, to produce a flush finish for panels 1 and 2.

The time taken to produce a completed joint was allowed for in the cost equations by applying a production rate based on the combined time of drilling, peg insertion and removal, application of treatment, spin dimpling and riveting for one fastener. The value used is given on Table A2.3.

The equation giving the detail manufacture time, dtime, in minutes is

$$\text{dtime} = x \cdot \{tc \cdot (cla + clb) + td \cdot nr + 2 \cdot ts \cdot (sc + sd) + 1.1 \cdot ab/dt + 2 \cdot (bb/dt + db/dt)\} \quad \text{(A2.5)}$$

The equation giving the sub-assembly time, stime, in minutes is

$$\text{stime} = y \cdot \{ (^2/pu + {}^2/po + {}^1/dt + {}^3/deb + {}^1/snpr) \cdot (ca + cb)/10 + 0.9 \cdot (ca + cb) \cdot (dmc + tx) + ty \cdot sc \} \quad \text{(A2.6)}$$

The equation giving the final assembly time, ftime, in minutes is

$$\text{ftime} = z \cdot \{ {}^1/spind \cdot (aa + ab + ac + ba + bb + bc) + (da + db) \cdot ({}^1/dt + {}^1/av + 0.4 \cdot ({}^1/pu + {}^1/po) + {}^4/deb) + ea \cdot ({}^1/dt + {}^1/snpr + {}^1/pu + {}^1/po + {}^4/deb) + fa \cdot ({}^1/dt + {}^1/snpr + 0.4 \cdot ({}^1/pu + {}^1/po) + {}^4/deb) + con \} \quad \text{(A2.7)}$$

The total production time, ttime, in minutes is

$$\text{ttime} = \text{dtime} + \text{stime} + \text{ftime} \quad \text{(A2.8)}$$

### A2.2.1 Computer program description

The following computer program was used to solve the above production cost equations. The sequence of data input required by the program is the same as for the preceding program up to, and including the variable n. After this the sequence of data input becomes:

dmc = automatic rivet time comprising the automatic
cycle time plus the drill time related to the
stock thickness of panel 3 (mins.),
con = time allowance for handling and application of
treatment (mins.),
spind = production rate for a completed fastening (no./min.),
From dd [1:k] the sequence remains the same as for the
above program.

The program listing is as follows:

```
EVALUATION OF THE PRODUCTION COST OF THE SPIN
DIMPLED ALUMINIUM ALLOY DESIGN

begin procedure drilltime(a,b,c,d,e,f,g,h);

value g,h;

real d,e,f;

integer g,h;

real array a,b,c;

begin integer i,u,v;

for i:=1 step 1 until g do

if d-a[i]<.001 then begin u:=i;

goto ha;

end;

ha:     for i:= 1 step 1 until h do

if e-b[i]<.001 then begin v:=i;

goto hb;

end;

hb:     f:=c[u,v];

enddrilltime;

procedure selection(a,b,c,d,e);
```

```
value e;
real c,d;
integer e;
real array a,b;
begin integer i,u;
for i:= 1 step 1 until e do
if c-a[i]<.001 then begin u:=i;
goto hc;
end;
hc:     d:=b[u];
end selection;
begin integer i,j,k,l,s,f1,f2;
real sa,sb,sc,nr,cla,clb,aa,ab,ac,ba,bb,bc,ca,cb,da,db,
ea,fa,ta,tsa,tb,tsb,tc,tcb,tab,tr,daa,dab,dac,dba,dbb,dbc,
dca,dcb,dda,ddb,dea,dfa,av,pu,po,deb,x,y,z,m,n,dmc,spind,
dtime,stime,ftime,ttime,p,r,con;
f1:=layout([2s-d.dddd10+nd]);f2:=layout([2s-d.dddd10+ndc]);
open(20);
sa:=read(20);sb:=read(20);sc:=read(20);nr:=read(20);
cla:=read(20);clb:=read(20);aa:=read(20);ab:=read(20);
ac:=read(20);ba:=read(20);bb:=read(20);bc:=read(20);
ca:=read(20);cb:=read(20);da:=read(20);db:=read(20);
fa:=read(20);ta:=read(20);tsa:=read(20);tb:=read(20);
tsb:=read(20);tc:=read(20);tcb:=read(20);tab:=read(20);
tr:=read(20);daa:=read(20);dab:=read(20);dac:=read(20);
dba:=read(20);dbb:=read(20);dbc:=read(20);dca:=read(20);
dcb:=read(20);dda:=read(20);ddb:=read(20);dea:=read(20);
```

```
dfa:=read(20);av:=read(20);pu:=read(20);po:=read(20);
deb:=read(20);k:=read(20);l:=read(20);x:=read(20);
y:=read(20);z:=read(20);m:=read(20);n:=read(20);
dmc:=read(20);con:=read(20);spind:=read(20);
close(20);
ea:=4×(cla + clb);
open(30);
write(30,f1,sa);write(30,f1,sb);write(30,f2,sc);
write(30,f1,nr);write(30,f1,cla);write(30,f2,clb);
write(30,f1,aa);write(30,f1,ab);write(30,f2,ac);
write(30,f1,ba);write(30,f1,bb);write(30,f2,bc);
write(30,f1,ca);write(30,f1,cb);write(30,f2,da);
write(30,f1,db);write(30,f1,ea);write(30,f2,fa);
write(30,f1,ta);write(30,f1,tsa);write(30,f2,tb);
write(30,f1,tsb);write(30,f1,tc);write(30,f2,tcb);
write(30,f1,tab);write(30,f1,tr);write(30,f2,daa);
write(30,f1,dab);write(30,f1,dac);write(30,f2,dba);
write(30,f1,dbb);write(30,f1,dbc);write(30,f2,dea);
write(30,f1,dca);write(30,f1,dcb);write(30,f2,dda);
write(30,f1,ddb);write(30,f1,dfa);write(30,f2,av);
write(30,f1,pu);write(30,f1,po);write(30,f2,deb);
write(30,f1,k);write(30,f1,l);write(30,f2,x);
write(30,f1,y);write(30,f1,z);write(30,f2,m);
write(30,f1,n);
write(30,f1,dmc);write(30,f2,con);write(30,f2,spind);
close(30);
begin real array dd,csk,cskr,snpr[1:k],g[1:l],dt[1:k,1:l];
```

```
open(20);
for i:= 1 step 1 until k do dd[i]:=read(20);
for i:= 1 step 1 until k do csk[i]:=read(20);
for i:=1 step 1 until k do cskr[i]:=read(20);
for i:= 1 step 1 until k do snpr[i]:=read(20);
for i:= 1 step 1 until l do g[i]:=read(20);
for i:= 1 step 1 until k do
for j:= 1 step 1 until l dodt[i,j]:=read(20);
close(20);
comment In the next block the detail assembly time
is evaluated;
dtime:=cla + clb + 5xnr;
drilltime(dd,g,dt,dab,tab,r,k,l);
dtime:=dtime + (4+.55xab/(2xr))x4;
drilltime(dd,g,dt,dca,tab,r,k,l);
dtime:=dtime +(4+bb/(2xr))x4;
drilltime(dd,g,dt,dcb,tcb,r,k,l);
dtime:=dtime + (4+db/(scxr))x2xsc;
dtime:=xxdtime;
comment In the next block the sub assembly time
is evaluated;
drilltime(dd,g,dt,dcb,tc,r,k,l);
p:=(cb+ca)/10;
stime:=(p/pu+p/po)x2+p/r+3xp/deb;
selection(dd,csk,dcb,r,k);
stime:=stime+p/r;
selection(dd,snpr,dcb,r,k);
```

```
stime:=stime+p/r;
p:=p×9;
stime:=stime+p×.055+sc×.15+p×dmc;
stime:=stime×y;
comment In the next  block the final assembly time
is evaluated;
ftime:=con;
drilltime(dd,g,dt,dea,tsa,r,k,l);
ftime:=ftime+ea/r;
selection(dd,snpr,dea,r,k);
ftime:=ftime+ea/r+ea/pu+ea/po+4×ea/deb;
ftime:=ftime+(aa+ab+ac+ba+bb+bc)/spind;
drilltime(dd,g,dt,dfa,tr,r,k,l);
ftime:=ftime+fa/r;
selection(dd,snpr,dfa,r,k);
ftime:=ftime+fa/r+(fa/pu+fa/po)/2.5+4×fa/deb;
drilltime(dd,g,dt,ddb,tc,r,k,l);
ftime:=ftime+db/r+db/av+(db/pu+db/po)/2.5+4×db/deb;
drilltime(dd,g,dt,dda,tc,r,k,l);
ftime:=ftime+da/r+da/av+(da/pu+da/po)/2.5+4×da/deb;
ftime:=ftime×z;
ttime:=dtime+stime+ftime;
open(30);
writet(30,[[3c]TORSION*BOX*PRODUCTION*COST ANALYSIS[2c]
DETAIL*MANUFACTURE*COST[c]]);
write(30,f2,dtime);
writet(30,[MINUTES[2c]SUB*ASSEMBLY*COST[c]]);
```

```
write(30,f2,stime);
writet(30,[MINUTES[2c]FINAL ASSEMBLY*COST[c]]);
write(30,f2,ftime);
writet(30,[MINUTES[2c]TOTAL*PRODUCTION*COST[c]]);
write(30,f2,ttime);
writet(30,[MINUTES]);
close(30);
    end;
    end;
    end
```

## A2.3 The Production Cost Equations for the Titanium Alloy Structural System

At the present time little use has been made of welded titanium structures in aircraft applications, so that information on practical production rates tends to be somewhat limited. Production rates are influenced to a great extent by the complexity of the welding apparatus and by the welding technique it employs.

In the production method described in section 5.3.1 two types of welding were employed, plasma arc welding and tungsten inert gas welding. For each welding method the production rate, used in the cost equations, was based on the total time required to clean the area to be welded and to complete the welding operation. The values used are given in Table A2.3, however, they may be subject to considerable variation in a practical application.

The equation giving the detail manufacture time, dtime, in minutes is

$$\begin{aligned} dtime = x \cdot \{ & (a + b + 2 \cdot c + d \cdot e) \cdot r \\ & + ((a + b) \cdot l + 2 \cdot c \cdot n + d \cdot e \cdot n) \cdot s \\ & + (nb + 2 \cdot ns) \cdot ({}^{1}/_{dm} + {}^{2}/_{deb}) + dcon \} \end{aligned} \qquad (A2.9)$$

The equation giving the sub-assembly time, stime, in minutes is

$$\begin{aligned} stime = y \cdot \{ & (2 \cdot (a + b) \cdot l + 2 \cdot c \cdot n + d \cdot e \cdot n) \cdot t \\ & + scon \} \end{aligned} \qquad (A2.10)$$

The equation giving the final assembly time, ftime, is

$$\begin{aligned} ftime = z \cdot \{ & (2 \cdot d \cdot m + 2 \cdot f \cdot l + c \cdot n + 4 \cdot g \cdot l) \cdot u \\ & + (nb + 2 \cdot ns) \cdot ({}^{1}/_{dh} + {}^{4}/_{deb} + 0.2 \cdot ({}^{1}/_{pu} + {}^{1}/_{po}) \\ & + {}^{1}/_{riv}) + fcon \} \end{aligned} \qquad (A2.11)$$

The total production time, ttime, in minutes is

$$ttime = dtime + stime + ftime \qquad (A2.12)$$

Most of the variables used in the above production cost equations are defined in the computer program description given in section A2.3.1, the remainder being defined as follows:

f = number of panel 3 booms,

g = number of panel 4 booms,

l = box length (in.),

m = box chord (in.),

n = box depth (in.),

r = production time per stiffener (min.),

s = treatment time (min./in.),

t = electron beam welding rate (min./in.),

u = tungsten inert gas welding rate (min./in.).

## A2.3.1 Computer program description

The following computer program was used to solve the above production cost equations. The sequence of data input required by the program is as follows:

a = number of panel 1 stringers,

b = number of panel 2 stringers,

c = number, per panel, of panel 3 and 4 stringers,

d = number of ribs,

e = number of stiffeners per rib,

x = detail manufacture cost factor,

y = sub-assembly cost factor,

z = final assembly cost factor,

nb = number of spar boom rivets per spar,

ns = number of spar stiffener rivets per spar,

dm = bench drill rate (no./min.),

dh = hand drill rate (no./min.),

po = rate of peg removal (no./min.),

pu = rate of peg insertion (no./min.),

deb = deburring rate (no./min.),

riv = blind rivet rate (no./min.),

dcon = time allowance for handling in the detail stage (min.),

scon = time allowance for handling and heat treatment in the sub-assembly stage (mins.),

fcon = time allowance for handling, heat treatment and application of protective treatment in the final assembly stage (mins.)

The program listing is as follows:

EVALUATION OF THE PRODUCTION COST OF THE

TITANIUM ALLOY DESIGN

```
begin integer f1,f2;
real a,b,c,d,e,r,s,t,u,v,x,y,z,
nb,ns,dm,dh,po,pu,deb,riv,
dcon,scon,fcon,dtime,stime,
ftime,ttime;
f1:=layout([2s-d.ddddm+nd]);
f2:=layout([2s-d.ddddm+ndc]);
open(20);
a:=read(20);b:=read(20);c:=read(20);
d:=read(20);e:=read(20);x:=read(20);
y:=read(20);z:=read(20);nb:=read(20);
ns:=read(20);dm:=read(20);dh:=read(20);
po:=read(20);pu:=read(20);deb:=read(20);
riv:=read(20);dcon:=read(20);scon:=read(20);
fcon:=read(20);
close(20);
open(30);
write(30,f1,a);write(30,f1,b);
write(30,f1,c);write(30,f2,d);
write(30,f1,e);write(30,f1,x);
write(30,f1,y);write(30,f2,z);
write(30,f1,nb);write(30,f1,ns);
write(30,f1,dm);write(30,f2,dh);
write(30,f1,po);write(30,f1,pu);
write(30,f1,deb);write(30,f2,riv);
write(30,f1,dcon);write(30,f1,scon);
```

```
write(30,f2,fcon);
r:=5;s:=10;t:=1.5;u:=2;v:=4;
comment In the next block the detail
manufacture time is calculated;
dtime:=(a+b+2xc+dxe)xr
+(a+b+.3xc+.15xdxe)xs
+(nb+2xns)x(1/dm+2/deb)
+dcon;
dtime:=xxdtime;
comment In the next block the sub
assembly time is calculated;
stime:=(2x(a+b)+.3xc+2+.15xdxe)x100xt+scon;
stime:=stimexy;
comment In the next block the final
assembly time is calculated;
ftime:=(dx100+200+cx15)xu
+200xv+(nb+2xns)x(1/dh+4/deb
+2/(10xpu)+2/(10xpo)+1/riv)
+fcon;
ftime:=zxftime;
ttime:=dtime+stime+ftime;
writet(30,[[3c]TITANIUM*TORSION*BOX*
PRODUCTION*COST*ANALYSIS[2c]DETAIL*
MANUFACTURE*COST[c]]);
write(30,f2,dtime);
writet(30,[MINUTES[2c]SUB*ASSEMBLY*
COST[c]]);
write(30,f2,stime);
```

```
writet(30,[MINUTES[2c]FINAL* ASSEMBLY*
COST[c]]);
write(30,f2,ftime);
writet(30,[MINUTES[2c]TOTAL* PRODUCTION*
COST[c]]);
write(30,f2,ttime);
writet(30,[MINUTES]);
close(30);
end
```

TABLE A2.1 Manual drilling rates (No. of holes per minute) for aluminium alloy material.

| Stock thickness (S.W.G.) | Hole diameter (in.) | | |
|---|---|---|---|
| | 1/8 | 3/16 | 1/4 |
| 22 | 10 | 9 | 8 |
| 20 | 9 | 8 | 7 |
| 18 | 8 | 7 | 6 |
| 16 | 7 | 6 | 5 |
| 14 | 6 | 5 | 4.5 |
| 12 | 5 | 4.5 | 4 |
| 10 | 4.5 | 4 | 3.5 |
| 8 | 4 | 3.5 | 3 |
| 6 | 3.5 | 3 | 2.5 |

TABLE A2.2 Countersinking and riveting rates (no. of holes per minute) for aluminium alloy material.

| | Hole diameter (in.) | | |
|---|---|---|---|
| | 1/8 | 3/16 | 1/4 |
| Countersinking rate | 10 | 6 | 2 |
| Snaphead riveting rate | 8 | 5 | 3 |
| Countersink riveting rate | 7 | 4 | 2.5 |

TABLE A2.3 The production rate values used in the cost equations

| | Aluminium alloy | Titanium alloy |
|---|---|---|
| Rate of peg insertion (no./min.) | 6 | 6 |
| Rate of peg removal (no./min.) | 8 | 8 |
| Deburring rate (no./min.) | 20 | 15 |
| Automatic riveting cycle time (min.) | 0.042 | - |
| Automatic riveting positioning time (min.) | 0.055 | - |
| Automatic riveting row traverse time (min.) | 0.15 | - |
| Rate of blind riveting for $\frac{1}{8}$" dia. rivets (no./min.) | 3 | 3 |
| Spin dimple operation time (min.) | 1.25 | - |
| Plasma arc welding rate (in./min.) | - | 0.67 |
| T.I.G. welding rate (in./min.) | - | 0.5 |
| Detail manufacture cost factor | 1.25 | 1.25 |
| Sub-assembly cost factor | 1.25 | 1.25 |
| Final assembly cost factor | 1.25 | 1.25 |

FIG. A2.1 THE DRILL TIME FOR THE DRIVMATIC RIVETING MACHINE IN ALUMINIUM ALLOY MATERIAL

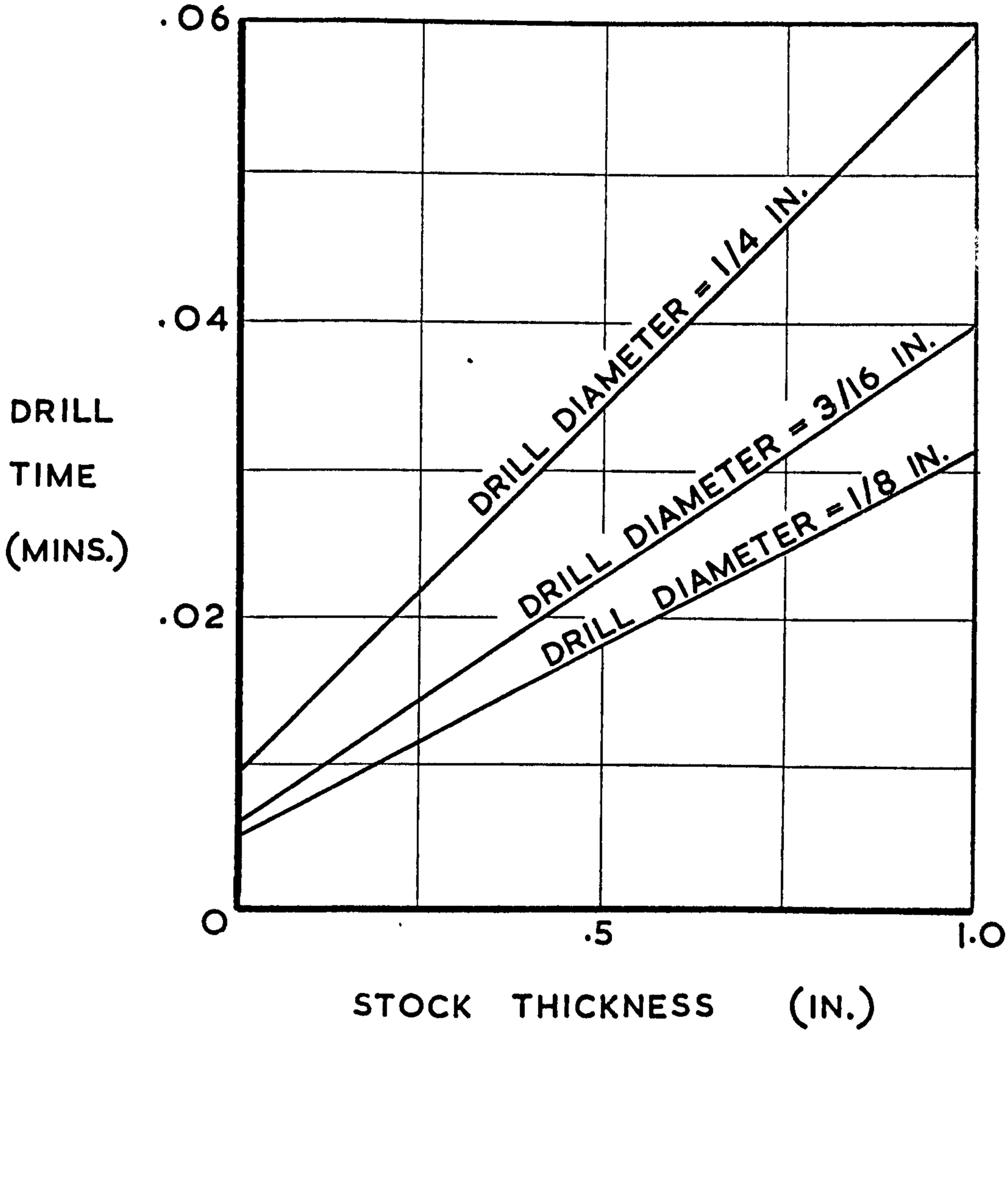

# A P P E N D I X  3

## A DESCRIPTION OF THE COMPUTER PROGRAM FOR THE LOCATION OF THE OPTIMAL STRUCTURAL CONFIGURATION

Using this computer program the optimal structural configuration, expressed in terms of a structural efficiency factor value, may be located at any value of the global exchange rate.

The program functions in the following manner:

Values of unit cost and structural weight, corresponding to structural configurations having different efficiency factor values, form the basic input data.

The procedure "Lagrange" uses the Lagrange interpolation method, described in section 7.2, to fit curves to the cost and the weight data, with efficiency factor as the independent variable in each case. For a series of global exchange rate values, the cost and the weight values are incorporated in equation (7.4) to generate merit function values. A step-wise comparative procedure is used to locate the minimum merit function value, which, by definition, gives the optimal structural configuration.

The program output lists the optimal efficiency factor and the minimum merit function values which define the optimal configuration at each global exchange rate value.

The sequence of data input required by the program is as follows:

m = number of efficiency factor values at which the cost and weight values are evaluated,

n = number of global exchange rate values under examination,

p = the efficiency factor interval used in the Lagrange procedure,

ws = standard weight value (lb.),

cs = standard cost value (£),

v [1] = lowest global exchange rate value,

v [n] = highest global exchange rate value,

f [1], w [1] → f [m], w [m] = efficiency factor, weight combinations for the m configurations examined,

far [1] = lowest efficiency factor value used in the Lagrange procedure,

far [p] = highest efficiency factor value used in the Lagrange procedure,

f [1], c [1] → f [m], c [m] = efficiency factor, cost combinations for the m configurations examined.

The program listing is as follows:

```
LOCATION OF THE OPTIMAL STRUCTURAL CONFIGURATION
begin procedure lagrange(x,y,z,d,e,k);
value k,z;
integer k,z;
real array x,y,d,e;
begin integer h,s,t;
real l;
real array a,b[1:z];
for h:=1 step 1 until k do
```

```
begin d[h]:=d[1]+(h-1)x(d[k]-d[1])/(k-1);
e[h]:=0;
for t:=1 step 1 until z do
begin a[t]:=1;
for s:=1 step 1 until z do
begin l:=d[h]-x[s];
if s=t then l:=1;
a[t]:=a[t]xl;
end;
b[t]:=1;
for s:=1 step 1 until z do
begin l:=x[t]-x[s];
if s=t then l:=1;
b[t]:=b[t]xl;
end;
e[h]:=e[h]+y[t]xa[t]/b[t];
end;
end;
end lagrange;
begin integer i,j,m,n,p,jopt,f1,f2;
real mopt,ws,cs;
f1:=layout([2s-d.dddd10+nd]);
f2:=layout([2s-d.dddd10+ndc]);
open(20);
m:=read(20);n:=read(20);p:=read(20);
ws:=read(20);cs:=read(20);
open(30);
write(30,f1,m);write(30,f1,n);
```

```
write(30,f2p);write(30,f1,ws);
write(30,f2,cs);
begin real array c,f,w[1:m],far,cost,wt[1:p],
merit[1:n,1:p],v[1:n];
v[1]:=read(20);v[n]:=read(20);
write(30,f1,v[1]);write(30,f2,v[n]);
for i:=1 step 1 until n do
v[i]:=v[1]+(i-1)×(v[n]-v[1])/(n-1);
for i:=1 step 1 until m do
begin f[i]:=read(20);w[i]:=read(20);
write(30,f1,f[i]);
write(30,f2,w[i]);
end;
far[1]:=read(20);far[p]:=read(20);
write(30,f1,far[1]);write(30,f2,far[p]);
lagrange(f,w,m,far,wt,p);
m:=read(20);p:=read(20);
write(30,f1,m);write(30,f2,p);
for i:=1 step 1 until m do
begin f[i]:=read(20);c[i]:=read(20);
write(30,f1,f[i]);
write(30,f2,c[i]);
end;
far[1]:=read(20);far[p]:=read(20);
write(30,f1,far[1]);
write(30,f2,far[p]);
lagrange(f,c,m,far,cost,p);
close(20);
```

```
writet(30,[[3c]FITTED*CURVES[c]EFFICIENCY
[5s]WEIGHT[9s]COST[c]]);
for i:=1 step 1 until p do
begin write(30,f1,far[i]);write(30,f1,wt[i]);
write(30,f2,cost[i]);
end;
writet(30,[[3c]EXC*RATE[7s]OPT*EFF[9s]
OPT*MER*FUN[2c]]);
for i:=1 step 1 until n do
begin write(30,f1,v[i]);
merit[1,1]:=wt[1]+cost[1]/v[i];
mopt:=merit[1,1];
jopt:=1;
for j:=2 step 1 until p do
begin
merit[i,j]:=wt[j]+cost[j]/v[i];
if mopt-merit[i,j]>0 then
begin mopt:=merit[i,j];
jopt:=j;
end;
end;
write(30,f1,far[jopt]);
write(30,f2,mopt);
end;
writet(30,[[3c]STANDARDISED*CURVES[c]EFFICIENCY
[5s]WEIGHT[9s]COST[c]]);
for i:=1 step 1 until p do
begin wt[i]:=wt[i]/ws;
```

```
cost[i]:=cost[i]/cs;
write(30,f1,far[i]);write(30,f1,wt[i]);
write(30,f2,cost[i]);
end;
writet(30,[[3c]STANDARDISED*VALUES[c]EXC*RATE
[7s]OPT*EFF[9s]OPT*MER*FUN[2c]]);
for i:=1 step 1 until n do
begin write(30,f1,v[i]);
merit[i,1]:=merit[i,1]/ws;
mopt:=merit[i,1];
jopt:=1;
for j:=2 step 1 until p do
begin merit[i,j]:=merit[i,j]/ws;
if mopt-merit[i,j]>0 then
begin mopt:=merit[i,j];
jopt:=j;
end;
end;
write(30,f1,far[jopt]);
write(30,f2,mopt);
end;
close(30);
end;
end
```

# A P P E N D I X  4

## THE SOLUTION OF THE LEARNING CURVE INTEGRAL

In the evaluation of the learning cost $C_L$ per item undertaken in section 4.3.3, the following integral I, forming part of equation (4.3), had to be solved:

$$I = \int_1^{n_1} C_1 \cdot r^{\frac{\log_e n}{\log_e 2}} \cdot dn \qquad \text{(A4.1)}$$

The solution is obtained using the following method:

Let $k = \frac{1}{\log_e 2}$

and $y = \log_e n$

$\therefore dy = \frac{1}{n} \cdot dn$

and $dn = e^y \cdot dy.$

Since $C_1$ is a constant, the integral becomes

$$I = C_1 \cdot \int_1^{n_1} r^{k.y} \cdot e^y \cdot dy$$

$$= C_1 \cdot \int_1^{n_1} e^{k.y \cdot (\log_e r)} \cdot e^y \cdot dy$$

$$= C_1 \cdot \int_1^{n_1} e^{y\,(k \cdot \log_e r + 1)} \cdot dy$$

$$= C_1 \cdot \left[ \frac{e^{y\,(k \cdot \log_e r + 1)}}{k \cdot \log_e r + 1} \right]_1^{n_1}$$

$$= C_1 \cdot \left[ \frac{n \cdot r^k \cdot \log_e n}{k \cdot \log_e r + 1} \right]_1^{n_1}$$

$$I = C_1 \cdot \left[ \frac{n \cdot r^{\frac{\log_e n}{\log_e 2}}}{\frac{\log_e r}{\log_e 2} + 1} \right]_1^{n_1} \qquad \text{(A4.2)}$$

# REFERENCES


1. Middleton, P., 'Concorde for the Airlines', Flight International, Vol. 99, No. 3240, pp. i-xiv, 15 April 1971.

2. Alvey, V. W. and Emero, D. H., 'Structures Cost Effectiveness', J. Aircraft, Vol. 4, No. 3, pp. 218-23, May - June 1967.

3. Levenson, G. S. and Barro, S. M., 'Cost Estimating Relationships for Aircraft Airframes', Memo. No. RM-4845-PR, The Rand Corporation, May 1966.

4. Carrier, J. M. and Smith, R. W., 'Aircraft Airframe Cost Estimating Techniques', Memo. No. RM-3375-PR, The Rand Corporation, November 1962.

5. Yates, E. H., 'Cost Analyses as an Aid to Aircraft Design', J. Aircraft, Vol. 2, No. 2, pp. 100-7, March - April 1965.

6. Sanchez, L., 'Methods of Estimating Fixed-Wing Airframe Costs', Memo. No. P.R.C. R-547, Planning Research Corporation, 1965.

7. Dykes, J. C., 'The Economic Value of Weight Saving', The Aeroplane, Vol. 94, No. 2426, pp. 294-8, 28 February 1958.

8. Gerard, G., 'Structural Guidelines for Materials Development : Some Vehicle Performance and Design Generalisations', J. Aircraft, Vol. 5, No. 6, pp. 564-9, November - December 1968.

9. Civil Aeronautics Board, 'Aircraft Operating Cost and Performance Report 1966-7', Vol. 2, p. 33.

10. Troughton, A. J. and Major, E. R., 'The Influence of the Designer and the Operator on Total Aircraft Operating Costs', The Proceedings of the Convention on Economic Factors in Aviation, The Royal Aeronautical Society, 13-14 May 1970.

11. Unpublished report, 'The Use of Titanium Alloy in Airframes', Value Engineering Department, Hawker Siddeley Aviation Ltd., Manchester, January 1969.

12. Kolom, A. L., 'Titanium Diffusion Bonded Honeycomb', J. Aircraft, Vol. 6, No. 5, pp. 410-5, September - October 1969.

13. Farrar, D. J., 'The Design of Compression Structures for Minium Weight', J. R. Ae. S, Vol. 53, No. 467, pp. 1041-52, November 1949.

14. Emero, D. H. and Spunt, L., 'Wing Box Optimisation under Combined Shear and Bending', J. Aircraft, Vol. 3, No. 2, pp. 130-41, March - April 1966.

15. Robinson, J., 'Computerised Diagonal Tension Analysis', J. R. Ae. S., Vol. 69, No. 657, pp. 638-42, September 1965.

16. Engineering Sciences Data Unit, 'Structures Data Sheets', Vol. 2, section 3.

17. Howarth, F., 'The Application of Value Engineering to Tooling', A paper presented at the Tooling Conference, Cranfield, 1969.

18. Owler, L. W. J., and Brown, J. L., 'Wheldons Cost Accounting and Costing Methods', Macdonald and Evans, 1965.

19. Legg, K. L. C., 'Integral Construction : A Survey and an Experiment', J. R. Ae. S., Vol. 58, No. 523, pp. 485-504, July 1954.

20. Wright, T. P., 'Factors affecting the cost of air-planes', J. Ae. Sc., pp. 122-8, February 1936.

21. Noah, J. W. and Smith, R. W., 'Cost Quantity Calculator', Memo. No. RM-2786-PR, The Rand Corporation, January 1962.

22. Meikle, G., 'The Effect of Temperatures up to 450°C on Metals', A lecture presented at the Institution of Metallurgists Refresher Course, 1956.

23. Buckingham, R. A., 'Numerical Methods', Sir Isaac Pitman and Sons Ltd., London, 1957.

24. International Civil Aviation Organisation, 'Digest of Statistics No. 145 : Financial Data', p. 254, 1968.

25. Air Transport Association, 'Standard Method of Estimating Comparative Direct Operating Costs of Transport Airplanes', pp. 16-9, June 1960.